

Universidad de Valladolid

DOCTORAL PROGRAM OF
INFORMATION AND TELECOMMUNICATION TECHNOLOGIES

DOCTORAL THESIS

CHARACTERIZATION OF NEURAL ACTIVITY USING
COMPLEX NETWORK THEORY. APPLICATION TO
THE IDENTIFICATION OF THE ALTERED NEURAL
SUBSTRATES IN SCHIZOPHRENIA

THESIS PRESENTED BY **D. JAVIER GÓMEZ PILAR**
TO APPLY FOR THE *Ph.D. degree*
FROM THE *University of Valladolid*

DIRECTED BY:
DR. ROBERTO HORNERO SÁNCHEZ
DR. JESÚS POZA CRESPO

2018
VALLADOLID, SPAIN

TITLE: Characterization of Neural Activity using
 Complex Network Theory. Application to
 the Identification of the Altered Neural Sub-
 strates in Schizophrenia

AUTHOR: D. Javier Gómez Pilar

ADVISORS: Dr. Roberto Hornero Sánchez
 Dr. Jesús Poza Crespo

DEPT.: Teoría de la Señal y Comunicaciones e Inge-
 nería Telemática

Thesis committee:

PRESIDENTE: Dr.

VOCAL: Dr.

SECRETARIA: Dra.

agree to grant the qualification of

At Valladolid,



Universidad de Valladolid

Escuela Técnica Superior de Ingenieros de Telecomunicación
Dpto. de Teoría de la Señal y Comunicaciones e Ingeniería Telemática

RESEARCH STAY FOR THE INTERNATIONAL MENTION

City: Ottawa (Canada)

Institution: Institute of Mental Health Research

Research group: Mind, Brain Imaging and Neuroethics Research Unit

Dates: 02/08/2017-02/12/2017

Duration: 123 Days (4 Months)

Tutor of the research stay: Prof. Georg Northoff

Agradecimientos

Me gustaría empezar expresando mi más sincera gratitud a mis directores de Tesis, el Dr. Roberto Hornero y el Dr. Jesús Poza, cuyo continuo apoyo e implicación han sido factores cruciales para concluir esta Tesis. Espero que los largos debates sobre modelos cerebrales y nuevas medidas de grafos hayan servido para ablandar mi rígida plasticidad neuronal. Ambos son un referente en el ámbito académico, pero el nivel humano que me han demostrado estos años no se queda a la zaga.

Quiero extender mi gratitud a todos los miembros del Grupo de Ingeniería Biomédica (los que son y los que fueron): María, Carlos, Dani, Gonzalo, Rebeca, Luis Fernando, Víctor M., Pablo, Fer, Vero, Rober, Saúl, Celia, Edu, Adrián, Víctor R., Aarón y Jorge. Si ya de por sí me gusta la investigación, con los cafés, las cervezas y los *'happy meals'* se crea un ambiente estupendo en el que trabajar se hace fácil. No me puedo olvidar de Alejandro, mi maestro particular de ERPs. Perdón por mis continuas preguntas y gracias por tu incorruptible paciencia.

También quiero dar las gracias al excelente equipo dirigido por el Dr. Vicente Molina. Su predisposición y colaboración han sido claves para llevar a buen término esta Tesis. Gracias también a Alba, compañera de andanzas, sobresaliente profesional y, si cabe, mejor persona. Gracias al Dr. Rodrigo de Luis del Laboratorio de Procesado de Imagen. Algunos resultados de esta Tesis no habrían sido posibles sin él, pero además, su mirada crítica me han ayudado enormemente.

Without the inspiring experience in Ottawa, several ideas of this Tesis would be different. The research stay with the members of the group led by Dr. Northoff, 'Mind, Brain Imaging and Neuroethics Research Group', was an unforgettable experience, where I have grown both professionally and personally. Thanks Georg for introducing me in the world of the nonadditivity and the spatio-temporal structure of the brain. I greatly appreciate your way of working, humor and friendliness. I am also very grateful to all the nice people in Ottawa who shared their time with me: Annemarie, Shankar, Mehrshad, Samira, Benedetta, Stefano, Steven, Diana and everyone.

Finalmente, quiero dar las gracias a mi familia por su constante apoyo, no solo estos años de Tesis, sino toda mi vida. Su cara de orgullo con cualquiera de mis pequeños logros me han dado fuerzas para hacer lo que me gusta. Gracias Carlos, por animarme en su día a hacer el doctorado. Mi hermano pequeño me seguirá dando lecciones toda la vida.

Para terminar, Vero, mi más cercano apoyo, gracias de corazón. Solo tú y yo sabemos cuánta de esta Tesis te debo a ti. Durante años has compartido, y a veces aguantado, mis alegrías y mis preocupaciones. Gracias por escucharme y aconsejarme en todo momento. Pero sobre todo, gracias por compartir tu vida conmigo y hacerme tan feliz. Te quiero.

*When you make the finding yourself,
even if you're the last person on Earth to see the light,
you'll never forget it.*

Carl Sagan

*Todo ser humano puede ser,
si se lo propone,
escultor de su propio cerebro.*

Santiago Ramón y Cajal

Abstract

Neuroscience is a field in constant evolution. From Ramon y Cajal's works, we recognize neuronal synapses as the basis for brain communication and coordination. These electric connections make up a tangle of pathways of extraordinary density. Until recently, the sophisticated techniques needed for acquiring these complex interactions, mapping their sources and analyzing them with advanced mathematical tools were out of our reach. It is now the right moment in which the technology and the state of the research provide us an opportunity to disentangle the underpinnings of the brain.

In this context, this Doctoral Thesis is focused on the study, development and assessment of a specific framework to investigate neural interactions from the perspective of Complex Network Theory. Particularly, the new measures and the novel models provided in this Thesis are aimed at improving our current knowledge of schizophrenia disorder. Schizophrenia is a disabling mental disorder characterized by disintegration of the process of thinking, contact with reality and emotional responsiveness. People with a large variety of symptoms can currently be considered patients with schizophrenia. It is not clear that they all share a common physiological substrate though. The heterogeneity of this illness could be the problem to find the adequate treatment for each one. This problem is accentuated since its prevalence is around 0.5% and patients have a 20% decrease in life expectancy compared with the general population. Genetics, child abuse or cannabis consumption are some of the risk factors of schizophrenia. Nevertheless, not much is known about brain coordination and communication in this disorder compared to general population. As seen throughout this Thesis, Complex Network Theory can significantly contribute in this regard.

Neural oscillations can be considered as the main contributing mechanism for enabling coordinated activity during normal brain functioning. Alterations in neural oscillations have been observed in schizophrenia using electroencephalographic

(EEG) recordings. Aberrant relevance assignment to stimulus is a common finding in several studies, which could be assessed using event-related potentials (ERPs). Schizophrenia has been also identified as a *dysconnectivity* syndrome; a concept related to the reduced capacity to integrate information among different brain regions. The concept of *connectome* and the use of graph theory to model, estimate and simulate the topology and dynamics of the brain network reduce the complexity of this problem with a remarkably flexible representation. Despite the growing use of graph theory in neuroscience in the last decade, only a handful of studies focused on brain dynamics using graphs (*chronnectomic*) and, to the best of our knowledge, the studies presented here are among the first ones in using this approach for assessing brain dynamics in schizophrenia.

All the studies that comprise this Doctoral Dissertation use the neuroelectrical signal from EEG recordings during an auditory oddball task to assess the schizophrenia underpinnings. In particular, a 3-stimulus auditory-oddball paradigm was used for examining cognitive processing as response to both relevant and irrelevant stimuli. Two incremental databases were used in the studies: the former reaching a total of 48 patients with schizophrenia and 87 healthy controls with 16 electrodes; the latter including 39 patients and 78 healthy controls with 32 electrodes.

Using local and network measures, changes of the brain activation from pre-stimulus to cognitive response were characterized. The main findings in this Thesis include: (i) a hyper-segregated state in schizophrenia during the expectation of stimulation; (ii) a deficit in the change from pre-stimulus to response activity in local and network features linked to the previously mentioned hyper-segregated state; (iii) a non-remarkable correlation between structural connectivity (obtained by diffusion magnetic resonance imaging, dMRI) and functional connectivity (EEG-based); and (iv) a noticeable reinforcement in the secondary pathways, i.e., pathways weakly connected during pre-stimulus, followed by most of the controls, but the patients's behavior is split between primary and secondary pathways reinforcement. Additionally, two genuine novelties were introduced: (i) a new measure of graph complexity based on the balance of the edge weights that does not need surrogate data, and (ii) a dynamical network model for the assessment of changes in the synchronization of brain regions during cognition, useful both for healthy and diseased brain interactions.

Our findings are consistent with previous reports in schizophrenia, revealing an abnormal salience assignment and disorganized internal representation, as well as desynchronized coupling in long-range brain interactions. On the other hand,

the studies of this compendium of publications show a hyper-activation of the pre-stimulus interval accompanied by reduced entropy followed by a deficit of change during cognition. This highlights that the higher the range of the available frequencies during pre-stimulus (spectral entropy), the higher flexibility or capability to change during the subsequent stimulus, providing a novel link between local and network features, in which patients with schizophrenia show abnormalities. The lack of findings related to the association between structural and functional connectivity, as well as the mentioned division in the behavior of the network dynamics during cognition in schizophrenia, supports the likely heterogeneity in schizophrenia disorder. Further studies must be addressed to corroborate this hypothesis, which could involve a breakthrough in this field. In summary, this Doctoral Thesis evaluates dynamical network features in schizophrenia during an auditory cognitive task, resulting in a reliable characterization of dynamical neural patterns. For this purpose, local measures based on the spectral distribution from the EEG, as well as network characteristics were estimated. Novel network measures and a new network modeling during cognition were presented. The findings of this Thesis reinforce previous works, whereas open the door to new frameworks to study the heterogeneity of schizophrenia.

Acronyms

APA	American Psychiatry Association
BACS	Brief Assessment of Cognition in Schizophrenia
CH	Chronic
CIC	Clustering Coefficient
CPL	Characteristic Path Length
COI	Cone of Influence
CWT	Continuous Wavelet Transform
CS	Connectivity Strength
D	Density
dMRI	Difusion Magnetic Resonance Imaging
DNA	Deoxyribonucleic Acid
DSM-V	Diagnostic and Statistical Manual of Mental Disorders, Fifth Edition
DTI	Diffusion Tensor Imaging
EEG	Electroencephalography
ECoG	Electrocorticography
ERP	Event-Related Potential
FA	Fractional Anisotropy
FE	First Episode
FIR	Finite Impulse Response
fMRI	Functional Magnetic Resonance Imaging
GABA	Gamma-Aminobutyric Acid
GD	Graph Density

ICA	Independent Component Analysis
IQ	Intelligence Quotient
IPR	Intellectual Property Rights
ISI	Inter-Stimulus Interval
JCR	Journal Citation Reports
LFP	Local Field Potentials
MEG	Magnetoencephalography
MRI	Magnetic Resonance Imaging
MSE	Mean Square Error
NMDA	N-methyl-Daspartate
PANSS	Positive and Negative Syndrome Scale
PL	Path Length
PLV	Phase-Locking Value
RP	Relative Power
SA	Synchronized-Averaging
SD	Standard Deviation
SE	Shannon Entropy
sEEG	Stereoencephalography
SGE	Shannon Graph Entropy
SGC	Shannon Graph Complexity
ST	Single-Trial
SW	Small-World
WAIS-III	Wechsler Adult Intelligence Scale, Third Edition
WE	Wavelet Entropy
WC	Wavelet Coherence
WCS	Wavelet Cross-Spectrum
WOS	Web Of Science

Contents

Abstract	I
Acronyms	V
1 Introduction	1
1.1 Compendium of publications: Thematic consistency	2
1.2 Context: Biomedical Engineering and neural signal processing	10
1.3 Schizophrenia	11
1.3.1 Aetiology	12
1.3.2 Diagnosis	13
1.3.3 Treatment	14
1.4 Electroencephalogram	15
1.5 Neural oscillations	17
1.6 Event-related potentials	18
1.6.1 Synchronized-averaging (SA) approach	19
1.6.2 Single-trial (ST) approach	22
1.7 Complex Network Theory in neuroscience	22
1.7.1 Brain network structures	23
1.7.2 Network measures	25
1.7.3 Brain networks on cognition	26
2 Hypotheses and objectives	29
2.1 Hypotheses	30
2.2 Objectives	31
3 Materials and methods	33
3.1 Subjects' databases	33
3.2 Acquisition protocol	35
3.3 Signal preprocessing	36

3.4	Continuous Wavelet Transform	37
3.5	Connectivity matrices	38
3.5.1	Coherence	38
3.5.2	Phase-locking value	39
3.5.3	Adjacency matrices	39
3.6	Graph parameters	40
3.7	Network modeling	43
3.8	Statistical analyses	45
3.8.1	Statistical hypothesis tests	45
3.8.2	Correlation analyses	47
3.8.3	Surrogate data	47
4	Results	49
4.1	Regularity patterns at sensor-level in controls and patients with schizophrenia	49
4.2	Network abnormalities in schizophrenia and relationship with regularity	50
4.3	Functional and structural relationship	53
4.4	Brain complexity	54
4.5	Functional network model during cognition	55
5	Discussion	63
5.1	Confirming the well-established hypotheses in schizophrenia	64
5.2	Determining possible causes of dysconnectivity in schizophrenia	64
5.3	A novel measure for characterizing network complexity	65
5.4	Towards a model of cognition	66
5.5	Limitations of the study	67
6	Conclusions	69
6.1	Original contributions	70
6.2	Main conclusions	71
6.3	Future research lines	72
A	Papers included in this Doctoral Thesis	75
B	Scientific achievements	175
B.1	Scientific production	175
B.1.1	Papers included in this Doctoral Thesis	175

B.1.2	Papers indexed in the Journal Citation Reports	176
B.1.3	Book Chapters	178
B.1.4	International Conferences	179
B.1.5	National Conferences	182
B.2	International research stay during the Doctoral Thesis	186
B.3	Intellectual property protection for computer software	188
B.4	Awards and honors	189
C	Resumen en castellano	191
C.1	Antecedentes	191
C.1.1	Introducción a la esquizofrenia	191
C.1.2	Teoría de Redes Complejas en neurociencia	193
C.2	Hipótesis y objetivos	193
C.3	Materiales	195
C.4	Métodos	196
C.5	Resultados y discusión	198
C.6	Conclusiones	199

List of Figures

1.1	Schematic diagram illustrating the relationship of the papers included in the compendium of publications. The spatial distribution of the papers represents the level of abstraction (vertical axis) and the type of connectivity studied (horizontal axis). Acronyms of the journals: Entropy, Entropy; PN&BP, Progress in Neuro-Psychopharmacology & Biological Psychiatry; HBM, Human Brain Mapping; NIC, Neuroimage: Clinical; IJNS, International Journal of Neural Systems; SR, Schizophrenia Research	3
1.2	International 10-10 EEG electrode location system. Picture adapted from (Chatrian et al., 1985).	15
1.3	Schematic representation of the source effect and field spread, which are inherent phenomena of EEG recordings.	16
1.4	Schematic overview of the processing steps in synchronized-averaging and single-trial approaches. This process must be followed for each of the electrodes in order to obtain the connectivity among all of them	20
1.5	ERP waves at parieto-central region (Pz channel) for controls (blue) and patients with schizophrenia (red). Mean (bold line) and standard error (transparent area) are depicted (left panel). ERP amplitude for pre-stimulus and P3b response for both groups (right panel). Parieto-occipital brain regions are mainly activated during P3b for both groups. However, patients with schizophrenia show a reduced activation (right panel).	21
1.6	Example of four typical networks for 50 nodes (top) and their node degree distribution (bottom). k represents the node degree of the network.	24

3.1	Example of the normalized wavelet coefficients at Pz electrode averaged across trials in a control subject from the database of 32 electrodes. The transparency outline represents the limits of the COI in the baseline and response windows, where the spectral content is not affected by edge effects. Figure from Gomez-Pilar et al. (2018c)	38
3.2	Averaged connectivity matrices from 35 controls and 51 patients with schizophrenia. The connectivity matrices are shown for controls and patients with schizophrenia from the database of 32 electrodes before (from -300 to 0 ms) and after (from 150 to 450 ms) stimulus onset. Figure from Gomez-Pilar et al. (2018d).	40
3.3	Examples of simple graphs with 4 nodes ($N = 4$) and their values of graph irregularity (SGE), graph complexity (SGC) and connectivity strength (D). For a completely weight-balanced network (left), SGE is maximum and SGC is minimum. A high weight-unbalanced network (right) yields low SGE and SGC values. On the opposite, neither a very weighted-balanced nor weighed-unbalanced network (center) reach higher SCG values.	43
3.4	Overview of the network modeling procedure. After the EEG acquisition, the pre-stimulus window and the response window were segmented. During the signal processing step, graph parameters in each window were computed from the connectivity matrix. In the modeling step, the pre-stimulus connectivity matrix was modified by applying the six different cognitive models under study. Finally, in the model selection step, the cognitive model and the iteration that obtained the minimum Mean Square Error (MSE) with respect to the network parameters in the response window were selected. (Gomez-Pilar et al., 2018d)	46
4.1	Sensor-level topographic maps of the statistics computed for the Wavelet Entropy using synchronized-averaging approach between controls and patients with schizophrenia. Right column shows within-group differences from pre-stimulus to response windows (Wilcoxon signed-rank test), whereas bottom row shows between-group differences for each window (Mann–Whitney U -test). The corrected p -values are obtained controlling false discovery rate (FDR). Figure from Gomez-Pilar et al. (2015).	50

4.2	Sensor-level topographic maps of the statistics computed for the Wavelet Entropy using single trial approach between controls and patients with schizophrenia. Right column shows within-group differences from pre-stimulus to response windows (Wilcoxon signed-rank test), whereas bottom row shows between-group differences for each window (Mann–Whitney U -test). The corrected p -values are obtained controlling false discovery rate (FDR). Figure from Gomez-Pilar et al. (2015).	51
4.3	Nodal clustering maps depicting the spatial distribution of within-group (comparison between pre-stimulus and response) and between-group differences in CIC (C: Controls; SP: patients with schizophrenia; FEP: First episode patients; CP: Chronic patients). Figure from Gomez-Pilar et al. (2017).	52
4.4	Scatterplots showing the association between modulation of functional connectivity strength and first factor (principal component analysis) of WE change for patients (top) and between modulation of functional connectivity strength and first factor of WE change for controls (bottom). Open circles: First episode patients; solid circles: Chronic patients; stars: Healthy controls). Figure from Gomez-Pilar et al. (2018b).	53
4.5	Scatterplots showing the association in the patients between pre-stimulus theta density and first factor (principal component analysis) of WE change (top) and between structural clustering coefficient and first factor of WE change (bottom). Open circles: First episode patients; solid circles: Chronic patients. Figure from Gomez-Pilar et al. (2018b).	54
4.6	Schematic overview for the network analyses from the structural and functional data. Figure from Gomez-Pilar et al. (2018b).	55
4.7	Error bars corresponding to the graph properties with statistically significant differences between patients and controls. Circles represent the mean value, while bars indicate the confidence interval (95%). Figure from Gomez-Pilar et al. (2018a).	56
4.8	Shannon Graph Complexity (left) and connectivity strength (right) values for each group, window and frequency band. Values are depicted as mean and standard error. * indicates $p < 0.01$, while ** indicates $p < 0.001$ (Mann-Whitney U -test). Figure from Gomez-Pilar et al. (2018c).	57

- 4.9 Detailed plot of the complexity dynamics from pre-stimulus to response in the theta frequency band for controls (blue arrow) and patients with schizophrenia (red arrow). The small figure represents the total range of SGC values for this network size (30 nodes/electrodes). The square in the small figure corresponds to the zoomed area in the large figure. SGE increases and SGC decreases for both groups, but the behavior is more remarkable for controls than for patients with schizophrenia. Figure from Gomez-Pilar et al. (2018c). 58
- 4.10 Prediction capability of the network modeling from the pre-stimulus window. Grand-average normalized network parameters for the pre-stimulus window (yellow) and the real response window (dark orange). The network measures prediction obtained by the model from the phase information of the pre-stimulus window is also shown (light orange). The model fitting for both the controls and the patient groups is computed by minimizing the mean square error (MSE). Figure from Gomez-Pilar et al. (2018d). 59
- 4.11 Histogram of the selected models. Percentage of subjects that best fit each model for controls and patients with schizophrenia. The reinforcement of the secondary connections is the most frequently selected model for both groups; however, statistically significant differences between the histograms of controls and patients were found and marked with an asterisk ($\chi^2 = 6.6874$, $p < 0.05$; Chi-square test). Figure from Gomez-Pilar et al. (2018d). 60
- 4.12 Averaged brain networks for controls and patients with schizophrenia before and after stimulus onset. Both groups show an increase in the edge weight values from the pre-stimulus (from -300 ms to the stimulus onset) to the response window (from 150 ms to 450 ms after the stimulus), though this increase is more noticeable for controls. To facilitate the visualization of the networks, a threshold was applied: only those connections with phase-locking values higher than 0.5 were depicted. The brain networks were visualized using the BrainNet Viewer Xia et al. (2013). Figure from Gomez-Pilar et al. (2018d). 61

4.13	Time evolution of the network parameters. At the left panel, mean and standard error of the network parameters for controls (blue) and patients (red). Control subjects exhibit higher changes from pre-stimulus (yellow) to cognitive response (orange) compared to patients. Statistically significant differences between the network parameter evolution across time of both groups are highlighted by a black rectangle. At the right panel, distribution of the averaged change of the network parameters from pre-stimulus (yellow transparency in the left panel) to cognitive response (orange transparency in the left panel) for both groups. The degree of statistically significant differences between groups is indicated with one asterisk ($p < 0.05$, Mann-Whitney U -test) or two asterisks ($p < 0.01$, Mann-Whitney U -test). Figure from Gomez-Pilar et al. (2018d).	62
A.1	(A) P300 waveforms in the middle line of the brain scalp (Fz, Cz and Pz electrodes) for controls (blue) and patients (red). (B) Scalp map depicting the P300 peak amplitude at Pz for controls and patients around the latency of both groups (450 ms).	131
A.2	Upper row: Lateral and superior views of the regions from which the structural connectivity matrix was built. Lower row: Lateral and superior views of hypothetical dMRI network based on segmented regions.	132
A.3	(A) P300 waveforms at Pz electrode for controls (blue) and patients (red). (B) Scalp maps depicting the P3b peak amplitude (from 300 ms to 550 ms) for controls and patients.	167
A.4	Averaged connectivity matrices. The connectivity matrices are shown for controls and schizophrenia patients before (from -300 to 0 ms) and after (from 150 to 450 ms) stimulus onset.	168
A.5	Histogram of the selected models and mean square error (MSE) distribution for each model. Only the subjects that follow a model based on weakening the network connections were depicted in this histogram.	168

List of Tables

3.1	Number of subjects for each group and number of electrodes used in each study included in the Thesis.	34
3.2	Socio-demographic, clinical and cognitive characteristics of the database of 16 active electrodes. Values are expressed as: mean (SD). The significant statistical differences between both groups were marked with an asterisk ($p < 0.05$, Student t -test).	34
3.3	Socio-demographic, clinical and cognitive characteristics of the database of 32 active electrodes. Values are expressed as: mean (SD). The significant statistical differences between both groups were marked with an asterisk ($p < 0.05$, Student t -test).	35
A.1	Comparison between chronic and first episode (FE) patients of the values with significant differences between patients and healthy controls. Values are shown as mean (SD). Statistical significance was assessed using Mann-Whitney U -tests. Entropy modulation factor scores were significantly higher in both chronic and FE patients as compared to healthy controls (see main text).	113
A.2	Factor structure of connectivity networks and cognitive scores. Results of the principal components analyses performed to obtain factor scores for structural and functional (global band and theta band) networks and cognitive performance. The variables included in each component are boldfaced.	129
A.3	P300 latency and amplitude at Pz electrode.	130
A.4	Mean values and comparison between first episode (FE) and chronic (CH) schizophrenia patients for the network variables with significant differences between patients and healthy controls. * Significantly higher in chronic patients (Mann-Whitney U -test, $p = 0.009$)	131

A.5	Correlation coefficient and p -values for all the possible comparisons between cognition and network parameters. Three correlations remain statistically significant after Bonferroni correction ($p < 0.001$, highlighted in bold).	169
A.6	Correlation coefficient and p -values for all the possible comparisons between cognition and symptoms. Two correlations are statistically significant ($p < 0.01$, highlighted in bold).	170
A.7	Correlation coefficient and p -values for all the possible comparisons between symptoms and network parameters. Four correlations are statistically significant ($p < 0.01$, highlighted in bold).	170
C.1	Características socio-demográficas, clínicas y cognitivas de la base de datos completa de 16 electrodos activos. Valores expresados como media(desviación típica). Las diferencias estadísticas significativas entre ambos grupos están marcadas con un asterisco ($p < 0.05$, test t de Student).	196
C.2	Características socio-demográficas, clínicas y cognitivas de la base de datos completa de 32 electrodos activos. Valores expresados como media(desviación típica). Las diferencias estadísticas significativas entre ambos grupos están marcadas con un asterisco ($p < 0.05$, test t de Student).	197

Chapter 1

Introduction

The current Doctoral Thesis focuses on characterizing brain network dynamics by means of Complex Network Theory to elucidate neural substrates in schizophrenia disorder. Electroencephalographic (EEG) signals, acquired during a cognitive task, were used to obtain connectivity matrices that describe the functional brain network. Graph measures were computed from these matrices using coherence and phase-based measures. These investigations have led to results which have been published, or accepted for publication, in journals indexed in the Journal Citation Reports from Thomson Reuters Web of ScienceTM (JCR-WOS). Specifically, up to five papers were published between July 2015 and August 2018. Additionally, one more paper was accepted for publication (April 2018). This scientific productivity has allowed writing this work as a compendium of publications. The thematic consistency of the papers included in the Thesis is justified in this introductory chapter (Subsection 1.1). The general context of Biomedical Engineering and neural signal processing is briefly described in Subsection 1.2. Subsection 1.3 is devoted to schizophrenia disorder. Subsection 1.4 is oriented to explain physiological underpinnings of the EEG recordings. In Subsection 1.5, the basis of neural oscillations and their generation is explained. Subsection 1.6 is focused on Event-Related Potential (ERP) and its usefulness in research. Finally, Subsection 1.7 provides the basis for understanding the current tendency to model brain interactions as a graph. The latter, indeed, motivates the research problem and, subsequently, the research questions.

Of note, this document is not intended to provide an exhaustive description of the studies carried out. That description is already provided by the papers, which passed a peer review process in high impact indexed journals. Therefore,

this document, according to the normative of the University of Valladolid, provides the framework of this Doctoral Thesis, summarizes the most relevant results and offers joint discussion. In this way, the conclusions of this document would not necessarily have been obtained by each paper separately.

1.1 Compendium of publications: Thematic consistency

For over a century, the notion that connections among neurons are the basis for the coordination of nearby and distant brain regions has been the cornerstone of neuroscience. One of the most influential contribution supporting this insight comes from Ramon y Cajal's work. He provided clear evidence of intricate neural circuits in the brain, which exchange information via electrical signals. However, even today, it is not well-known how these neural circuits interact among them. The necessary sophisticated tools for recording and mapping functional brain networks, as well as the advanced and novel mathematical methods for analyzing the resulting networks, have been slow to emerge. All this has changed in recent years. Improved technologies for accurately acquiring electric interactions among large-scale neural systems have led us to develop new reliable techniques for answering the question for several years kept in our mind: How can we get the fundamentals of brain functioning and its dynamical organization?

Beyond the knowledge of brain functioning, which is important itself, the answer to previous questions will provide a framework for improving the understanding and, consequently, the treatment of psychiatric disorders. In this context, the present Doctoral Thesis focuses on analyzing the physiological underpinnings in schizophrenia during a cognitive task performing. This is the common thread shared by the papers included in the compendium of publications. A scheme depicting the thematic consistency and the relationship among the studies of this Thesis is shown in Figure 1.1.

Given that previous studies have reported a disconnection syndrome in schizophrenia (Friston, 1998) – later renamed as *disconnectivity* syndrome (Whalley, 2005) – the first paper in chronological order (Gomez-Pilar et al., 2015) aims at characterizing neural network organization in healthy subjects and patients with schizophrenia using wavelet entropy to check the validity of this hypothesis. After proving new insights that support the findings of previous studies by using two complementary techniques, the two following papers investigate the possible causes of

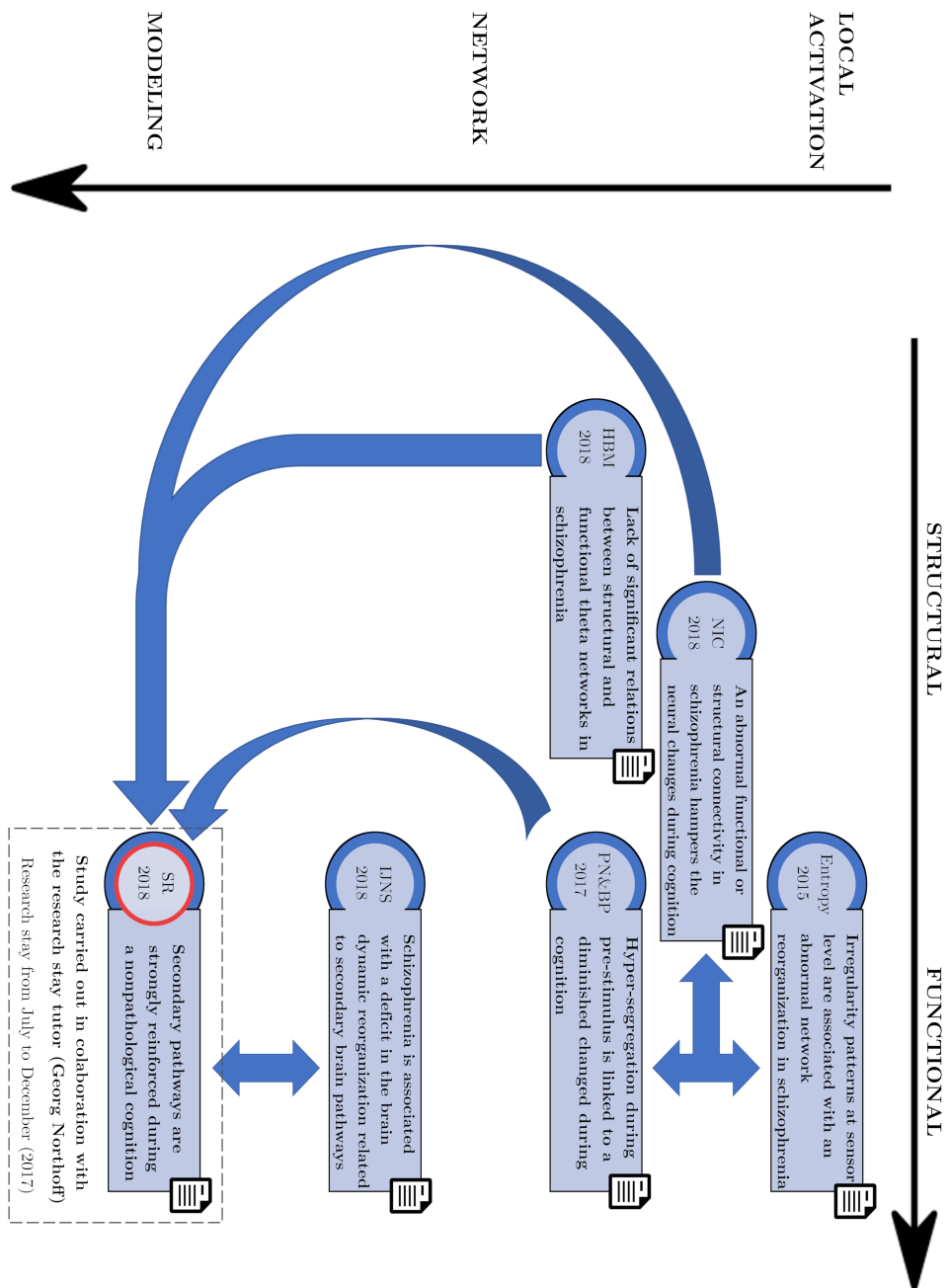


Figure 1.1: Schematic diagram illustrating the relationship of the papers included in the compendium of publications. The spatial distribution of the papers represents the level of abstraction (vertical axis) and the type of connectivity studied (horizontal axis). Acronyms of the journals: Entropy, Entropy; PN&BP, Progress in Neuro-Psychopharmacology & Biological Psychiatry; HBM, Human Brain Mapping; NIC, Neuroimage: Clinical; IJNS, International Journal of Neural Systems; SR, Schizophrenia Research

such *disconnectivity*. In one of them, we look for abnormalities in the changes of functional brain network during cognition using graph measures from Complex Network Theory (Gomez-Pilar et al., 2017). In the other paper, the relationship between EEG functional connectivity and structural connectivity measured by diffusion magnetic resonance imaging (dMRI) is assessed (Gomez-Pilar et al., 2018a). This association is compared between healthy controls and patients with schizophrenia to look for abnormalities in the disease. In the fourth paper (Gomez-Pilar et al., 2018b), we propose that functional and structural graph-derived network measurements would predict task-related entropy changes found in the first paper. As we will see, this provides direct evidence about the important effect of local features on the whole brain network. The aim of the fifth paper is to present a novel and reliable measure of network complexity (Gomez-Pilar et al., 2018c). It helps us in characterizing the neural dynamics of healthy and pathological brain networks during a cognitive task. This measure, based on the edge weight distribution balance, can be used not only in brain networks, but also in any enough large network (typically over 30 nodes). Thanks to this measure, we find abnormalities in the secondary functional neural pathways in patients with schizophrenia during a cognitive task. Finally, in the sixth paper (Gomez-Pilar et al., 2018c), the predictive capability of a proposed brain network modeling based on the pre-stimulus neural activity (e.g., prior to stimulus perception) provides the basis to present the brain as a complex system, which reinforces particular connections during a cognitive task. This paper also supports the hypothesis of abnormal connectivity in schizophrenia associated with weak connections and shows evidence of the schizophrenia heterogeneity.

Another of the connections among the papers is the strategy conducted to study brain dynamics, which is also one of the novelties of the study. While most of the state-of-the-art researches focus on a static approach (Rubinov et al., 2009; Stam et al., 2009; Uhlhaas and Singer, 2006), we studied the variation (or modulation) between the pre-stimulus EEG activity and the activity during cognitive response. The pre-stimulus serves as an objective baseline or reference to infer the importance of the change between brain states. This could be one of the first attempts in the literature to converge in the *chronnectome* approach (Dimitriadis and Salis, 2017; Nomi et al., 2017). Thus, although this specific term was not used in the Thesis' papers, the study of the neural coupling was assessed not only using a static approach, usually called *connectome*, but also from a dynamic perspective, recently called *chronnectome*.

In summary, neural network dynamics in healthy and diseased brain were as-

sessed along these studies. In addition, a novel brain complexity measure graph-theory-based was developed, as well as a new model of brain network dynamics for enabling a better understanding of the neural processes in the healthy brain and the abnormalities in schizophrenia.

Due to the nature of the present Doctoral Thesis, the Appendix A, in which the papers comprised in the compendium are included, is of crucial importance for a comprehensive understanding of this manuscript as a whole.

Titles, authors, and abstracts of the papers encompassed in Appendix A, as well as the scientific journals where these were published, are shown below, sorted as previously mentioned:

- **Neural network reorganization analysis during an auditory oddball task in schizophrenia using wavelet entropy. (Gomez-Pilar et al., 2015)**

Javier Gomez-Pilar, Jesús Poza, Alejandro Bachiller, Carlos Gómez, Vicente Molina, and Roberto Hornero. *Entropy*, 2015, 17, 5241-5256. Impact factor: 1.743 (reference year: 2015). Q2 in “Physics, Multidisciplinary” (25/79), (JCR-WOS).

Abstract: The aim of the present study was to characterize the neural network reorganization during a cognitive task in schizophrenia (SCH) by means of wavelet entropy (WE). Previous studies suggest that the cognitive impairment in patients with SCH could be related to the disrupted integrative functions of neural circuits. Nevertheless, further characterization of this effect is needed, especially in the time-frequency domain. This characterization is sensitive to fast neuronal dynamics and their synchronization that may be an important component of distributed neuronal interactions; especially in light of the disconnection hypothesis for SCH and its electrophysiological correlates. In this work, the irregularity dynamics elicited by an auditory oddball paradigm were analyzed through synchronized-averaging (SA) and single-trial (ST) analyses. They provide complementary information on the spatial patterns involved in the neural network reorganization. Our results from 20 healthy controls and 20 SCH patients showed a WE decrease from baseline to response both in controls and SCH subjects. These changes were significantly more pronounced for healthy controls after ST analysis, mainly in central and frontopolar areas. On the other hand, SA analysis showed more widespread spatial differences than ST results. These findings suggest that the activation response is weakly phase-locked to stimulus onset in SCH

and related to the default mode and salience networks. Furthermore, the less pronounced changes in WE from baseline to response for SCH patients suggest an impaired ability to reorganize neural dynamics during an oddball task.

- **Functional EEG network analysis in schizophrenia: Evidence of larger segregation and deficit of modulation (Gomez-Pilar et al., 2017)**

Javier Gomez-Pilar, Alba Lubeiro, Jesús Poza, Roberto Hornero, Marta Ayuso, César Valcárcel, Karim Haidar, José A. Blanco, Vicente Molina. *Progress in Neuropsychopharmacology & Biological Psychiatry*, 2017, 76, 116-123. Impact factor: 4.185 (reference year: 2017). Q1 in “Clinical Neurology” (39/197), “Pharmacology & Pharmacy” (38/261), and “Psychiatry” (28/142), (JCR-WOS).

Objective: Higher mental functions depend on global cerebral functional coordination. Our aim was to study fast modulation of functional networks in schizophrenia that has not been previously assessed.

Methods: Graph-theory was used to analyze the electroencephalographic (EEG) activity during an odd-ball task in 57 patients with schizophrenia (18 first episode patients, FEPs) and 59 healthy controls. Clustering coefficient (CIC), characteristic path length (PL) and small-worldness (SW) were computed at baseline ([-300 0] ms prior to stimulus delivery) and response ([150 450] ms post-stimulus) windows. Clinical and cognitive assessments were performed.

Results: CIC, PL and SW showed a significant modulation between baseline and response in controls but not in patients. Patients obtained higher CIC and SW at baseline, lower CIC and higher PL at response, and diminished modulation of CIC and SW as compared to controls. In patients, CIC and SW modulation were inversely associated to cognitive performance in executive tasks and directly associated to working memory. Similar patterns were observed in FEPs. CIC and SW during the baseline were inversely associated to their respective modulation magnitudes.

Conclusions: Our results are coherent with a hyper-segregated network at baseline (higher CIC) and a decreased modulation of the functional connectivity during cognition in schizophrenia.

- **Relations between structural and EEG-based graph metrics in healthy controls and schizophrenia patients (Gomez-Pilar et al., 2018a)**

Javier Gomez-Pilar, Rodrigo de Luis-García, Alba Lubeiro, Henar de la Red, Jesús Poza, Pablo Núñez, Roberto Hornero, Vicente Molina. *Human Brain Mapping*, 2017, *in press*. Impact factor: 4.927 (reference year: 2017). Q1 in ‘Neurosciences’ (48/261), ‘Neuroimaging’ (2/14), and ‘Radiology, Nuclear Medicine & Medical Imaging’ (16/128), (JCRWOS).

Our aim was to assess structural and functional networks in schizophrenia patients; and the possible prediction of the latter based on the former. The possible dependence of functional network properties on structural alterations has not been analyzed in schizophrenia. We applied averaged path-length (PL), clustering coefficient, and density (D) measurements to data from diffusion magnetic resonance and electroencephalography in 39 schizophrenia patients and 79 controls. Functional data were collected for the global and theta frequency bands during an odd-ball task, prior to stimulus delivery and at the corresponding processing window. Connectivity matrices were constructed from tractography and registered cortical segmentations (structural) and phase-locking values (functional). Both groups showed a significant electroencephalographic task-related modulation (change between prestimulus and response windows) in the global and theta bands. Patients showed larger structural PL and prestimulus density in the global and theta bands, and lower PL task-related modulation in the theta band. Structural network values predicted prestimulus global band values in controls and global band task-related modulation in patients. Abnormal functional values found in patients (prestimulus density in the global and theta bands and task-related modulation in the theta band) were not predicted by structural data in this group. Structural and functional network abnormalities respectively predicted cognitive performance and positive symptoms in patients. Taken together, the alterations in the structural and functional theta networks in the patients and the lack of significant relations between these alterations, suggest that these types of network abnormalities exist in different groups of schizophrenia patients.

- **Deficits of entropy modulation in schizophrenia are predicted by functional connectivity strength in the theta band and structural clustering (Gomez-Pilar et al., 2018b)**

Javier Gomez-Pilar, Rodrigo de Luis-García, Alba Lubeiro, Nieves de Uribe, Jesús Poza, Pablo Núñez, Marta Ayuso, Roberto Hornero, Vicente Molina. *Neuroimage-Clinical*, 2018, 18, 382-389. Impact factor: 4.242 (reference year: 2017). Q1 in “Neuroimaging” (3/14), (JCRWOS)

Spectral entropy (SE) allows comparing task-related modulation of electroencephalogram (EEG) between patients and controls, i.e. spectral changes of the EEG associated to task performance. A SE modulation deficit has been replicated in different schizophrenia samples. To investigate the underpinnings of SE modulation deficits in schizophrenia, we applied graph-theory to EEG recordings during a P300 task and fractional anisotropy (FA) data from diffusion tensor imaging in 48 patients (23 first episodes) and 87 healthy controls. Functional connectivity was assessed from phase-locking values among sensors in the theta band, and structural connectivity was based on FA values for the tracts connecting pairs of regions. From those data, averaged clustering coefficient (CIC), characteristic path-length (PL) and connectivity strength (CS, also known as density) were calculated for both functional and structural networks. The corresponding functional modulation values were calculated as the difference in SE and CIC, PL and CS between the pre-stimulus and response windows during the task. The results revealed a higher functional CS in the pre-stimulus window in patients, predictive of smaller modulation of SE in this group. The amount of increase in theta CS from pre-stimulus to response related to SE modulation in patients and controls. Structural CIC was associated with SE modulation in the patients. SE modulation was predictive of negative symptoms, whereas CIC and PL modulation was associated with cognitive performance in the patients. These results support that a hyperactive functional connectivity and/or structural connective deficits in the patients hamper the dynamical modulation of connectivity underlying cognition.

- **Quantification of graph complexity based on the edge weight distribution balance: Application to brain networks (Gomez-Pilar et al., 2018c)**

Javier Gomez-Pilar, Jesús Poza, Alejandro Bachiller, Carlos Gómez, Pablo Núñez, Alba Lubeiro, Vicente Molina, Roberto Hornero. *International Journal of Neural Systems*, 2018, 28(1), 1750032. Impact factor: 4.580 (reference year: 2017). Q1 in “Computer Science, Artificial Intelligence” (13/132), (JCR-WOS).

The aim of this study was to introduce a novel global measure of graph complexity: Shannon graph complexity (SGC). This measure was specifically developed for weighted graphs, but it can also be applied to binary graphs. The proposed complexity measure was designed to capture the interplay between two properties of a system: the 'information' (calculated by means of Shannon entropy) and the 'order' of the system (estimated by means of a disequilibrium measure). SGC is based on the concept that complex graphs should maintain an equilibrium between the aforementioned two properties, which can be measured by means of the edge weight distribution. In this study, SGC was assessed using four synthetic graph datasets and a real dataset, formed by electroencephalographic (EEG) recordings from controls and schizophrenia patients. SGC was compared with graph density (GD), a classical measure used to evaluate graph complexity. Our results showed that SGC is invariant with respect to GD and independent of node degree distribution. Furthermore, its variation with graph size (N) is close to zero for $N > 30$. Results from the real dataset showed an increment in the weight distribution balance during the cognitive processing for both controls and schizophrenia patients, although these changes are more relevant for controls. Our findings revealed that SGC does not need a comparison with null-hypothesis networks constructed by a surrogate process. In addition, SGC results on the real dataset suggest that schizophrenia is associated with a deficit in the brain dynamic reorganization related to secondary pathways of the brain network.

- **Altered predictive capability of the brain network EEG model in schizophrenia during cognition (Gomez-Pilar et al., 2018d)**

Javier Gomez-Pilar, Jesús Poza, Carlos Gómez, Georg Northoff, Alba Lubeiro, Benjamín B. Cea-Cañas, Vicente Molina, Roberto Hornero. *Schizophrenia Research*, 2017, *in press*. Impact factor: 3.958 (reference year: 2017). Q1 in "Psychiatry" (33/142), (JCR-WOS).

The study of the mechanisms involved in cognition is of paramount importance for the understanding of the neurobiological substrates in psychiatric disorders. Hence, this research is aimed at exploring the brain network dynamics during a cognitive task. Specifically, we analyze the predictive capability of the pre-stimulus theta activity to ascertain the functional brain dynamics during cognition in both healthy and schizophrenia subjects. Firstly, EEG recordings were acquired during a three-tone oddball task from

fifty-one healthy subjects and thirty-five schizophrenia patients. Secondly, phase-based coupling measures were used to generate the time-varying functional network for each subject. Finally, pre-stimulus network connections were iteratively modified according to different models of network reorganization. This adjustment was applied by minimizing the prediction error through recurrent iterations, following the predictive coding approach. Both controls and schizophrenia patients follow a reinforcement of the secondary neural pathways (i.e., pathways between cortical brain regions weakly connected during pre-stimulus) for most of the subjects, though the ratio of controls that exhibited this behavior was statistically significant higher than for patients. These findings suggest that schizophrenia is associated with an impaired ability to modify brain network configuration during cognition. Furthermore, we provide direct evidence that the changes in phase-based brain network parameters from pre-stimulus to cognitive response in the theta band are closely related to the performance in important cognitive domains. Our findings not only contribute to the understanding of healthy brain dynamics, but also shed light on the altered predictive neuronal substrates in schizophrenia.

1.2 Context: Biomedical Engineering and neural signal processing

This Doctoral Thesis arises in the context of Biomedical Engineering, which is defined as an interdisciplinary field that focuses on altering, controlling, or understanding biological systems by applying engineering principles (Bronzino, 1999). This covers a wide range of activities, including theoretical and experimental research. Given the growth of the computational branch in the last decades, biomedical signal processing is becoming one of the most relevant activities in this field. Human body produces a large number of physiological signals, which reflect its physiological underpinnings. The study of these signals, let us to identify a wide range of pathological conditions (Bronzino, 1999). Unfortunately, the information contained in biomedical signals is usually not directly interpretable. Therefore, a processing step is needed to attribute meaning to the biomedical raw signals. Particularly, neural signal processing is getting an astonishing development in recent years, especially since the concept of *connectome* is being used to refer to the neural interactions in the human brain (Sporns et al., 2005). Consequently, neural

signal processing has become an essential tool for extracting the hidden basis of brain behavior.

This Thesis is mainly focused on the bioelectric signals of the brain. Electroencephalography (EEG) is a useful tool to acquire the oscillatory electrical waves produced by the firing of synchronized neural bunches in the brain cortex. In order to help in the characterization of dynamical neural activity associated with schizophrenia, EEG signals recorded during the performance of an auditory cognitive task have been analyzed. Similarly, novel time-frequency signal techniques followed by complex-network-theory-based measures have been applied and studied. Hence, all the aforementioned background reflects the framework in which this Doctoral Thesis is encompassed.

1.3 Schizophrenia

Schizophrenia is a chronic mental disorder characterized by an array of symptoms, including disintegration with the process of thinking, contact with reality and emotional responsiveness (American Psychiatric Association 2013). The chronic course of this disease along with its early onset make schizophrenia a disabling disorder for the patients and their relatives.

Prior to the fifth edition of the Diagnostic and Statistical Manual of Mental Disorders (DSM-V) in 2013 (American Psychiatric Association, 2013), schizophrenia diagnosis was categorized into five different subtypes: (i) paranoid schizophrenia, (ii) disorganized, or hebephrenic schizophrenia, (iii) catatonic schizophrenia, (iv) childhood schizophrenia, and (v) schizoaffective disorder. However, according to the American Psychiatric Association (APA), due to the limited diagnostic stability, low reliability, and poor validity, the method of classification was modified to bring all these categories under a single heading: schizophrenia.

With the DSM-V (American Psychiatric Association, 2013), a new way of schizophrenia diagnosis also arises. Nowadays, a person with schizophrenia must have at least two of the following symptoms¹:

- **Delusions.**
- **Hallucinations.**
- **Disorganized speech (e.g., frequent derailment or incoherence).**

¹Only one of these symptoms is required if delusions are bizarre or hallucinations consist of a voice keeping up a running commentary on the person's behavior or thoughts, or two or more voices conversing with each other (American Psychiatric Association, 2013).

- **Grossly disorganized or catatonic behavior.**
- **Negative symptoms, i.e. affective flattening, avolition, or alogia.**

Note that with the previous protocol of diagnosis, two people may have schizophrenia but not share any symptoms. This makes rather difficult to find common neural substrates in this disorder, which in part gives rise to the justification of this Thesis. In fact, increasing tendency to consider schizophrenia as a hodgepodge of different diseases is growing up (Lubeiro et al., 2016; Barch and Sheffield, 2014).

Epidemiologically, the prevalence rates of schizophrenia depend upon a whole range of factors, including the availability of a response to treatment (Bhugra, 2005) and low socio-economic status (Lewis and Lieberman, 2000). Depending on the study, the global life span prevalence of this disorder ranges from 0.26% to 0.51% (Simeone et al., 2015). Schizophrenia patients have a 20% decrease in life expectancy compared with the general population (Laursen et al., 2014). Nevertheless, the gender is a non-differentiating feature of schizophrenia (Bhugra, 2005). This suggests that schizophrenia has an important relationship to the environment and it is not only associated with genetic factors.

1.3.1 Aetiology

The causes of the schizophrenia remain unknown. Although it is clear that the genetic predisposition is an important risk factor (Harrison and Owen, 2003), other aspects have demonstrated to be involved in the disorder. Among them, viral infections (Brown, 2008), childhood antecedents (Welham et al., 2009) and substance abuse (Swartz et al., 2006) have proven to play an important role in the development of the illness.

Different hypotheses have been proposed to find the underlying cause of this psychiatric disorder: genetic/epigenetic hypothesis, executive function failure hypothesis, environmental hypothesis, among others (Orellana and Slachevsky, 2013). However, this Thesis is focused on the neurotransmitter dysfunction hypothesis, since it provides the basis for understanding the synaptic abnormalities in the brain (Javitt and Sweet, 2015). This hypothesis involves three aspects about three different neurotransmitters: (i) glutamate, (ii) GABA, and (iii) dopamine. The excess concentration of these neurotransmitters (glutamate), the deficit (GABA), or the dysregulation (dopamine) produces dysconnectivity, impaired inhibitory process and aberrant salience attributions, respectively (Javitt and Sweet, 2015). These abnormalities have a direct influence in the electric signal of the brain.

Thus, the use of the EEG is appropriate for characterizing and assessing the neural coupling and its abnormalities in schizophrenia.

Neurotransmitter model, therefore, involves three neurochemical models: (i) glutamatergic (ii) GABAergic and (iii) dopaminergic. All of them are focused on prefrontal cortex, hippocampus and temporal lobes (Javitt and Sweet, 2015):

- i) Glutamate receptors could link schizophrenia symptoms to neurocognitive deficits. It is known the role of glutamate blocking neurotransmission at N-methyl-D-aspartate (NMDA) receptors (Stone et al., 2007), which is associated with poorer global performance and a possible disconnection syndrome in the prefrontal cortex (Friston, 1998).
- ii) By reducing neuronal excitability throughout the nervous system, GABA is the main inhibitory neurotransmitter in mammals. GABAergic dysfunctions are linked to abnormal brain activity in high frequencies (Javitt and Sweet, 2015). Since cognitive memory has been linked to fast oscillations, GABA reductions may be linked to the deficits in schizophrenia related to task with cognitive memory demands (Lewis and Lieberman, 2000).
- iii) Dopamine model suggests that a dysregulation of this neurotransmitter could generate hallucinations and delusions in schizophrenia, through the aberrant attribution of abnormal salience to normal internal and external events (Kapur, 2003). This is the basis of antipsychotic drug action. Thus, to reduce psychotic symptoms, antipsychotic drugs are prescribed, which block dopamine receptors, preventing from hallucinations (Carlsson et al., 2004).

1.3.2 Diagnosis

To date, schizophrenia diagnosis is based on the fifth version of DSM (DSM-V). The criterion A for its diagnosis includes the presence of different symptoms (at least one), as previously mentioned. However, other factors must be considered before the final diagnosis. One of them is the duration of the illness, since a duration of less than one month must be diagnosed as schizophreniform disorder. Other criteria describe complementary considerations in diagnosis, such as the impact in the daily live, duration of the prodromal phase, differential diagnosis to discriminate schizophrenia from bipolar or schizoaffective disorders, disturbance not attributable to substance abuse and additional considerations for people with autism (American Psychiatric Association, 2013).

During prodromal phase, schizophrenia exhibits specific behavioral and cognitive characteristics that are considered precursors to an episode of psychosis (Klosterkotter and Schultze-Lutter, 1998). Symptoms during the prodromal phase include reduced concentration and attention, depressed mood, brief psychotic symptoms and sleep disturbance (Yung and McGorry, 1996). After that, symptoms are diverse resulting on a variety of manifestations for the same illness. It is thought that these differences in symptom manifestations could be related to different underpinnings of the disorder, which could be studied by the EEG or other biological signals (Gomez-Pilar et al., 2018a,b). Although schizophrenia patients could have a remission of their symptoms with no further relapse, periods of relapse or no remission at all are also usually showed (American Psychiatric Association, 2013).

1.3.3 Treatment

The most common treatment in schizophrenia is the use of antipsychotic medication (Buckley, 2008). The typical (or traditional) antipsychotic drugs are chlorpromazine and haloperidol. They are usually based on dopamine antagonism, which interacts with the neurotransmitter (dopamine) receptors (Edwards and Smith, 2009).

The effectiveness of these drugs mainly affects to positive symptoms, but the usefulness in the treatment of negative and cognitive symptoms is more reduced (Buckley, 2008). Another concern on the use of antipsychotic medication is tolerability problem. While the tolerance of some patients to the drugs is very high, others can show problems with tardive dyskinesia and extrapyramidal motor side-effects (Patterson and Leeuwenkamp, 2008). Due to these problems, a new generation of antipsychotics are being contemplated for the treatment. Among them, risperidone, olanzapine, clozapine and quetiapine have demonstrated to be at least as effective as traditional antipsychotic drugs, but with a lower propensity for inducing some types of adverse events (Patterson and Leeuwenkamp, 2008). On the other hand, the tendency of increasing triglycerides and cholesterol due to the use of these medication must be followed and controlled (Kapur and Remington, 2001).

Given the different responses by the patients to medication, physicians and patients must work together in order to fit the right doses and type of medication for controlling the symptoms and improving the quality of live (Buckley, 2008). For that purpose, EEG studies can be the basis for future advances in this field.

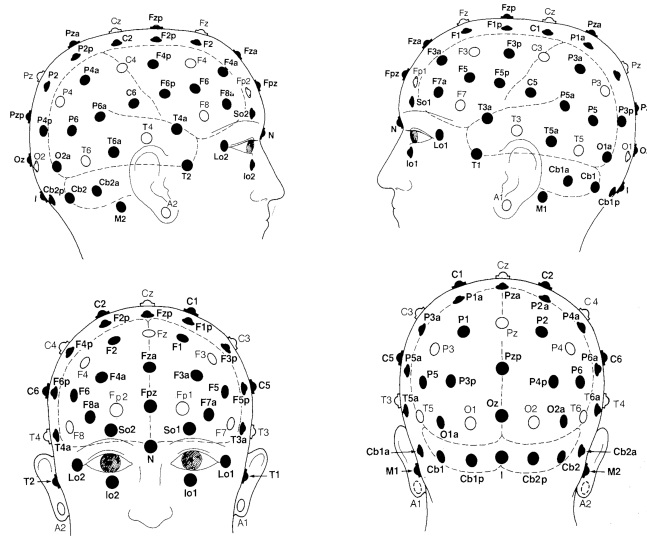


Figure 1.2: International 10-10 EEG electrode location system. Picture adapted from (Chatrian et al., 1985).

1.4 Electroencephalogram

In 1929, Hans Berger developed the EEG as a neurophysiological exploration system based on the recording of bioelectrical activity of the brain cortex. EEG acquires electrical signals of the pyramidal neurons of the brain working together in large and synchronized assemblies. These coordinated firing produces an electric field strong enough to be measurable by scalp electrodes. Therefore, EEG is the electrical signal or time-varying voltages produced by the brain and recorded over the human scalp (Nunez and Srinivasan, 2006a). As all the voltage-based measurements, each channel of the EEG measures electric potential differences between two sensors or electrodes, usually placed in an elastic cap following 10-20 or 10-10 international system (Chatrian et al., 1985). These systems provide the location of up to 21 electrodes in the case of 10-20 system, or up to 81 electrodes for 10-10 system (see Figure 1.2). Both of them maximize the covered area of the scalp, whereas equispaced electrodes are placed. Since 1929, EEG has been thoroughly used as a clinical tool. However, it is not until the eighties/nineties that improved technologies for accurately acquiring electric interactions among large-scale neural systems have clearly emerged.

EEG has become a suitable tool for assessing brain processing, since cognitive

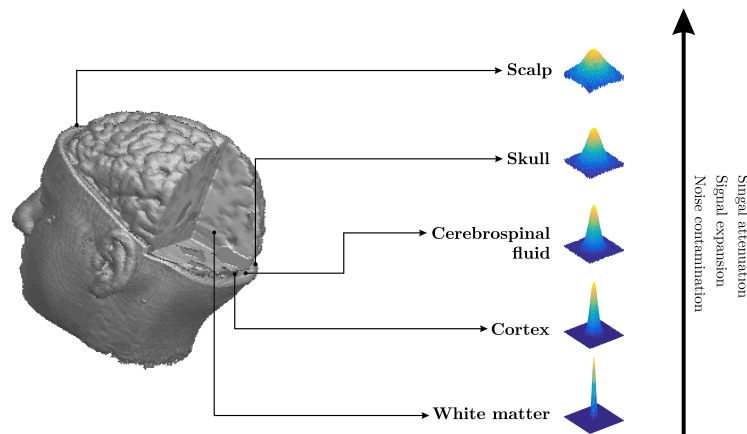


Figure 1.3: Schematic representation of the source effect and field spread, which are inherent phenomena of EEG recordings.

changes produce electric changes in the cortex in the range of milliseconds (Cohen, 2014). Therefore, the high temporal resolution of the EEG allows to capture the direct electric consequences of the neurological processes. Besides the temporal resolution, the low cost and the portability, the widespread use in clinical assessment confers the EEG the category of being one of the most important tools to measure brain activity. Despite these important advantages, EEG recordings have two main drawbacks that merit special attention. The first one is the source effect. The electrical activity generated by the cortex was partially distorted and attenuated when it passes through the cortex, meninges and skull. It produces that EEG signal has small amplitudes and spatially poorly localization (Wang, 2010). The second disadvantage is the volume conduction or field spread effect. When the bioelectrical signal of the brain arrives at any surface, such as the scalp, it spreads out the surface, producing a linear mixture of multiple brain sources recorded by the same electrode. Therefore, signals are affected by three effects: attenuation, expansion and noise contamination (Nunez and Srinivasan, 2006b) (see Figure 1.3).

More accurate measurements could be obtained invasively using subdural electrocorticogram (ECoG) with the electrodes directly placed on the cortical surface. Other technique to directly measure brain activity is the stereoelectroencephalography (sEEG), which records EEG signals via electrodes surgically implanted into the brain tissue. Despite the quality of the EEG signals using these techniques, both of them are invasive and/or require surgery. For that reason, EEG using

scalp electrodes is becoming a growing technique in the clinical practice. In comparison to other brain-imaging tools, EEG allows to directly assess neurocognitive processes (Cohen, 2014). The EEG oscillations reflect electric neural oscillations in the cortex, whereas brain-imaging techniques do not directly measure neural events. That is the case of functional MRI (fMRI), which measures the blood-oxygen-level-dependent signal. However, these techniques are usually suited for studies in which precise spatial localization is important (Cohen, 2014).

1.5 Neural oscillations

EEG signals can be divided into ongoing activity and task-related activity. Ongoing or spontaneous activity is brain activity in the absence of an explicit task, and hence also referred to as resting-state activity. Ongoing activity is not usually considered for the study about the stimulus processing. However, it is known that plays an important role during brain development, such as in network formation and synaptogenesis (Buckner et al., 2008). On the other hand, task-related activity can modulate neural synchronization. During many years, the relationship between ongoing and task-related activity was believed as completely linear, i.e. neural activity during a task is a simple superposition of spontaneous and task-related activity (Arieli et al., 1996). However, important and recent evidences have demonstrated that evoked and spontaneous brain activities are not independent but rather interact nonadditively and, further, the interaction can be characterized as a negative interaction (Huang et al., 2017). These findings show that the study of the task-related activity must also consider the activity during the spontaneous fluctuations (e.g., taking into account the brain activity prior to a task).

The oscillations that characterize both spontaneous and task-related brain activity have different frequency ranges and spatial distributions. EEG oscillations can be further subdivided into five different rhythms according to the frequency band of the signal (Cohen, 2014):

- Delta band (δ , 1-4 Hz): High-amplitude waves typically found in deep slow wave sleep, mainly observed in the frontal regions in adults. In pathological brain, delta waves are involved with epileptic seizures.
- Theta band (θ , 4-8 Hz): It is associated with drowsiness and is increased during sleep. Theta rhythms are found in the frontal midline region and they have been associated with inhibition of elicited responses.

- Alpha band (α , 8-13 Hz): It is the predominant rhythm in awaked subjects in a relaxed or reflected state with eyes closed condition. They are most pronounced in parietal and occipital regions. They have been usually related to the EEG activity that reflects gating by inhibition (Jensen and Mazaheri, 2010).
- Beta band (β , 13-30 Hz): With reduced amplitudes as compared to alpha waves, beta rhythms are associated with states of active concentration, anxiety or tension. Beta band is commonly divided into β_1 and β_2 sub-bands, which include the frequency ranges (13-19 Hz) and (19-30 Hz), respectively.
- Gamma band ($\gamma > 30$ Hz): It is associated with both basic sensory and higher cognitive processing. It has been suggested that the neurochemical basis of gamma-band oscillatory activity is related to interactions between excitatory and inhibitory neurotransmitter concentrations (Fuchs et al., 2007).

Note that all these frequencies simultaneously co-occur during a regular EEG recording of the brain activity, but usually only one of them predominates among the others. Although the research community has paid special attention to the different frequencies of the brain oscillations for a long time, it has recently gained popularity the study of how these oscillations relate to cognition and behavior (Lopes da Silva, 2013). In this regard, ERPs are presented as an alternative to the classic studies of resting-state activity, since they link brain activity with a cognitive response.

1.6 Event-related potentials

ERPs provide a suitable method for exploring the psychophysiological processes during a mental task. ERPs are the brain response, averaged across trials, to a specific somatosensory, cognitive or motor event. They emerge as a series of peaks and troughs that interact to ongoing EEG activity in a nonadditive way (Huang et al., 2017). ERPs are classically considered as an indicator of the degree of involvement of the cortical areas to the event of the task (Niedermeyer and da Silva, 2005).

An ERP signal is comprised by different signals that can be classified as phase-locked and non-phase-locked, as well as time-locked and non-time-locked. Phase- and time-locked signals are usually named evoked activity, whereas non-phase-locked but time-locked signals are named induced activity. A third case is a signal

whose activity are neither phase-locked nor time-locked, i.e. the background activity also existing during resting but unrelated to the task. This can be removed using a baseline normalization, thus allowing to focus on task-related dynamics (Cohen, 2014). The three types of brain activity can be analyzed in the time-frequency domain. However, induced and background activity cannot be examined using time-domain averaging, since they are not phase-locked. Therefore, they have no representation in the ERP.

The relation between these three kinds of activity remains unresolved. The classic model about how ERPs can emerge from ongoing activity is the additive model. This model proposes that ERP reflects a signal that is elicited by an external stimulus (externally-guided activity) or by an internal event (internally-guided activity). In this model, the task-related activity is linearly added to ongoing background oscillations (Cohen, 2014). However, recent studies pose the idea that there is a nonadditive interaction between spontaneous and task-related activity (Huang et al., 2017). Ultimately, this debate may be never resolved due to the variety of neural origins of the ERPs, which complicates the understanding of their neurophysiological mechanisms (Cohen, 2014).

Different methods can be used to compute phase-locked and non-phase-locked activity. Among them, two are highlighted in the literature due to their widespread usage: (i) Synchronized-averaging (SA) approach (also named time-averaging approach) and (ii) single-trial (ST) approach. Figure 1.4 summarizes the two approaches, later described. Other methods, such as non-phase-locked-power, involve subtraction of the ERP from the total signal (Cohen, 2014). This only could be right if the interaction between the different brain activities was nonadditive, which remains under debate as previously mentioned.

1.6.1 Synchronized-averaging (SA) approach

SA approach obtains the ERP wave as the average of a set of trials acquired in the same electrode and time-locked to an event (internally- or externally-guided). The non-phase-locked activity is canceled out and, thus, evoked ERPs are the voltage deflections that survive this averaging process (Roach and Mathalon, 2008).

With a simple experimental design, auditory oddball task is one of the most extended approaches to evaluate the different ERP components. After time-averaging, ERPs show well defined deflections (see Figure 1.5). Among them, P300 component is the most extensively ERP component explored. P300 wave includes two components (Polich, 2007):

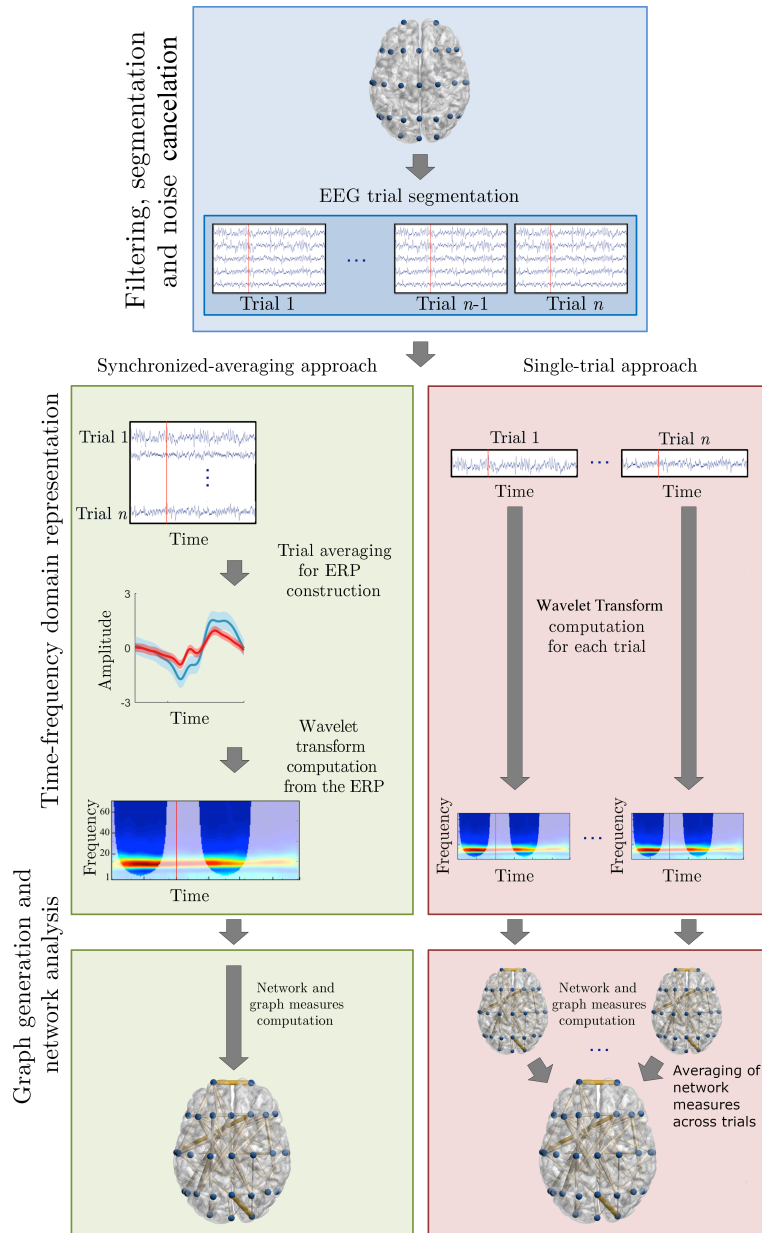


Figure 1.4: Schematic overview of the processing steps in synchronized-averaging and single-trial approaches. This process must be followed for each of the electrodes in order to obtain the connectivity among all of them

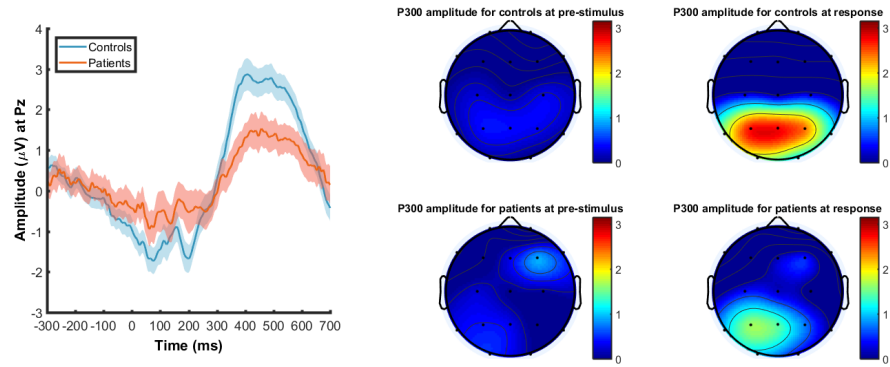


Figure 1.5: ERP waves at parieto-central region (Pz channel) for controls (blue) and patients with schizophrenia (red). Mean (bold line) and standard error (transparent area) are depicted (left panel). ERP amplitude for pre-stimulus and P3b response for both groups (right panel). Parieto-occipital brain regions are mainly activated during P3b for both groups. However, patients with schizophrenia show a reduced activation (right panel).

- i) P3a represents the response to unexpected deviant stimuli or distractor associated with a shift of the attention (novelty). It is associated with frontal-dopaminergic neurotransmitters; therefore, the usual activity is a negative deflection in frontal regions.
- ii) P3b is a component associated with the parietal-norepinephrine neurotransmitter action and, therefore, observable as a positive deflection mainly in parieto-occipital brain regions (see right panel of the Figure 1.5). It is usually linked to the neural processing of a novel and relevant stimuli during a task of sustained attention, such as the auditory oddball task.

Traditionally, ERPs have been studied in the temporal domain by assessing the amplitude or latency of different components (Polich, 2007). In this regard, schizophrenia disorder shows a significant reduction in the P300 amplitude and, sometimes, an increase in the P300 latency compared to healthy controls (Jeon and Polich, 2003; Mathalon et al., 2000; O'Donnell et al., 2004). However, further studies are needed in order to localize the neural origins of the P300, as well as the networks and hierarchical frequency-related organization involved in the P300 during cognition.

1.6.2 Single-trial (ST) approach

Although SA approach provides useful insights about the neural dynamics during cognitive processes, this method only examines the phase-locked activity, leaving out induced activity that could play an important role in cognition (Cohen, 2014). In addition, temporal approaches could not be enough for a complete description of the neural processes, which involve changes in the range of milliseconds. For that reason, time-frequency analyses applied to the whole ERP (phase-locked and non-phase locked components) are needed (Makeig et al., 2004). Additional information about the true nature of the neural dynamics in healthy and underlying pathological processes, such as schizophrenia, can be obtained using ST analyses together with time-frequency representations (Roach and Mathalon, 2008).

The study of the ERP in a ST way allows decomposing neural oscillations into magnitude and phase information in the time-frequency plane (Makeig et al., 2004). As a result of these studies, oscillations at low frequency ranges (delta, theta and alpha) have been associated with long-range coordination of neural assemblies (Gomez-Pilar et al., 2015; Uhlhaas and Singer, 2010; Von Stein and Sarnthein, 2000). On the contrary, frequencies related to faster oscillations (beta and gamma) reflect synchronization in both local (Womelsdorf et al., 2007) and large-scale networks (Roux et al. 2013). Impairments in any of these oscillations (both low or high frequencies) may contribute to generalized network dysfunction in schizophrenia (Uhlhaas and Singer, 2010), causing functional disconnectivity between brain regions (Friston, 1998; Gomez-Pilar et al., 2017). However, the underlying neural mechanisms of these alterations remain hidden; for that reason, novel proposals using Complex Network Theory approaches for modelling network brain dynamics may be appreciated in this field (Gomez-Pilar et al., 2018d).

1.7 Complex Network Theory in neuroscience

In 1735, Euler resolved the “Königsberg walk” problem using graphs. He proved that it was impossible to find any route around the city that crossed each and every bridge only one. Since then, we have seen how the graph theory plays an integral role in recent efforts to characterize network structure and function of the brain. Indeed, the Complex Network Theory has been applied to micro-, meso- and macro-scale brain models (Bullmore and Sporns, 2009). Graphs provide us a simple way to represent complex connectivity patterns from entangled brain connections. However, as a quote attributed to Albert Einstein claims, “*everything*

must be as simple as possible, but not simpler". Therefore, models must be as simple as possible, but not so simplistic that they lose sight of the underlying physiological bases. The answer to this question can be addressed by the apparently ubiquitous macroscopic behavior in the brain despite the significant differences in microscopic details. These findings have been replicated in the neural structure of a worm (Watts and Strogatz, 1998), a cat (Scannell et al., 1991), a macaque (Felleman and Van Essen, 1991) and several times in humans (Sporns, 2013). All of them discovered that the networks of the neural structure are "small-world" networks (also named Watts-Strogatz structure), following the theoretical principle of Cajal's conservation law (Ramón y Cajal, 1995). This law can be stated in terms of a balance between minimization of path length and maximization of integrative topology. In Cajal's words: "*the various conformations of the neuron are simple morphological adaptations governed by laws of conservation for time, space and material*" (Ramón y Cajal, 1995).

This finding is only the first step towards a comprehensive understanding of these networks, as well as how other complex structures, such as Albert-Barabási (Barabási and Albert, 1999) or Erdős-Rényi networks (Erdős and Rényi, 1959), are involved in the brain *connectome*. Efforts should be also carried out to model the dynamics of complex networks and quantify complementary topological features of brain systems as complexity, regularity, integration, segregation, strength or centrality, among others.

1.7.1 Brain network structures

Network structures can be classified in several ways, being the one based on node degree distribution the most widespread. Following this kind of classification, the following networks have been related to brain functioning (see also Figure 1.6):

- i) Lattice networks (or mesh graphs). This kind of networks corresponds with a graph whose drawing forms a regular tiling. Although these networks have not been directly related to brain interactions, they are the starting point for further and more complex comparisons, as those related to the "small-world" concept (see point iv). Figure 1.6 shows an example of lattice network with 50 nodes and its typical degree distribution. Note that all nodes have the same degree in a lattice network.
- ii) Random networks (or Erdős-Rényi networks). They are networks in which any two independent nodes have the same probability to be connected to

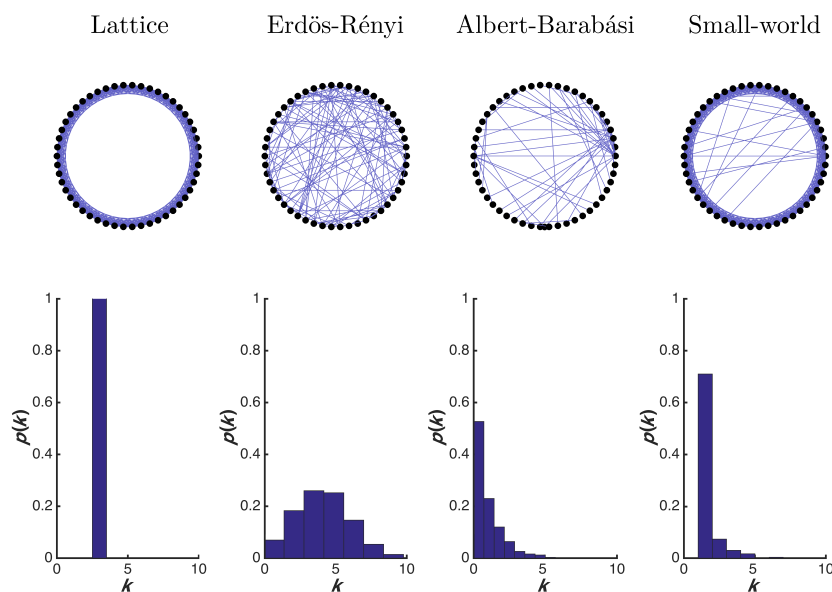


Figure 1.6: Example of four typical networks for 50 nodes (top) and their node degree distribution (bottom). k represents the node degree of the network.

a third node. The node degree (number of connections incident to a node) distribution of this kind of graphs follows a gaussian distribution (Erdős and Rényi 1959). Figure 1.6 shows an example of random network with 50 nodes and its typical degree distribution. Note that node degree distribution is gaussian for an enough large number of nodes.

- iii) Scale-free networks (or Albert-Barabási networks). These networks follow a power-law distribution (Barabási and Albert, 1999). They do not completely fit the brain topology, since their node degree distributions are usually truncated (Bullmore and Sporns, 2009). However, the similarities of the brain with this kind of networks have been reported (Eguíluz et al. 2005). Figure 1.6 shows an example of scale-free network with 50 nodes and its typical degree distribution. Note that node degree distribution is an exponentially decreasing function for an enough large number of nodes.
- iv) “Small-world” networks. These networks combine a high level of segregation (local clustering among neural assemblies) and a short characteristic path length (paths that globally link all nodes of the network) (Watts and Strogatz, 1998). Currently, brain networks cannot be described without

the concept of the “small-world” property. Being small-world the network with more similarities with human brain, functional interaction cannot be explained using only this model (van den Heuvel et al., 2010). Figure 1.6 shows an example of small-world network with 50 nodes and its typical degree distribution. Note that node degree distribution is midway between the distribution of a lattice and a random network.

“Small-world” property is not incompatible with scale-free property, so much so that a large evidence of small-world attributes and scale-free features have been reported in a wide range of fMRI studies (Eguíluz et al., 2005). In this manner, scale-free distributions of functional connections have been found in different human brain regions (Eguíluz et al., 2005). In addition, characteristic path length showed to be small (Gomez-Pilar et al., 2017) and comparable with those of equivalent random networks (Watts and Strogatz, 1998), whereas clustering coefficient is usually larger than its equivalent Erdős-Rényi networks (Watts and Strogatz, 1998). Therefore, these properties characterize human brain as a scale-free small-world network, in which a “rich-club”, i.e., well-connected nodes also connected to each other, usually appears (van den Heuvel et al., 2010).

1.7.2 Network measures

There is large variety of network measures (Bullmore and Bassett, 2011; Rubinov and Sporns, 2010). Despite this large diversity, most of them has a high correlation among each other, since they usually serve to characterize the same network feature. In other words, there exist several measures to characterize the same (or very similar) feature of a network, such as: (i) integration (e.g. path length, global efficiency, eccentricity, network radius or network diameter); (ii) segregation (e.g. clustering coefficient, local efficiency or transitivity); or (iii) centrality (e.g. degree, closeness, betweenness or eigenvector centrality), among others. It is needed, therefore, to develop graph measures that summarize complementary network characteristics (Gomez-Pilar et al., 2017). In the context of the current Thesis, some steps have been done to provide novel graph measures, such as regularity or complexity (Gomez-Pilar et al., 2018c), and to characterize brain network dynamics in a comprehensive way (Gomez-Pilar et al., 2018d).

Graph measures can also be classified as nodal and global measures. On the one hand, nodal measures refer to a node or edge features based on the links to adjacent nodes. On the other hand, global measures describe the network as a whole, i.e., consider the characteristics of the nodes in the entire network. In this

Doctoral Thesis, we mostly consider global measures, since EEG provides a non-high spatial resolution and therefore limits the ability to precisely localize hubs or important links in the brain space.

Finally, graphs measures can also be categorized as weighted, semi-weighted or binary, depending on the type of links between the nodes of the network. Most brain graph studies use binary connections between nodes, i.e. a threshold is applied to dichotomize the edge weights (Bullmore and Bassett, 2011). Although, binary graphs are an apparently simple model, these graphs are interpretable in relation to general principles of complex system organization (Bullmore and Bassett, 2011). On the other hand, weighted networks introduce the concept of connection strength between nodes. It can be considered a more realistic approach of the physiological properties of brain networks (Ansmann and Lehnertz, 2012). Unfortunately, the use of weighted graphs is not exempt from methodological concerns, which have not been completely solved yet (Ansmann and Lehnertz, 2012). Other possible approach is to remove those links with nonsignificant connections (but maintaining the links with their weights in the rest of the nodes). In the present Thesis, we used weighted graphs, since we consider it a more reliable and realistic approach, but knowing the limitations about the existence of possible spurious connections.

1.7.3 Brain networks on cognition

A comprehensive understanding of the neuropsychological mechanisms of the cognition ultimately depends on knowledge of brain organization. During many years, it was assumed that cognitive tasks depend on a specific and isolated brain region. However, a large evidence supports nowadays the notion that cognitive functions are based on the dynamic interaction of large and distributed brain areas operating as a coordinate large-scale network.

Underlying “cognitive networks”, functional networks have been postulated as the central core of the communication and coordination of large neuron assemblies (Petersen and Sporns, 2015). Functional networks are, in turn, based on the anatomical linkage of their neurons, i.e., the structural networks underlie functional ones. Communication is only possible when two regions (let we name it ‘nodes’) have a real link. On the contrary, a link between regions can exist without being necessary a communication between them. Similarly, the existence of structural connectivity is a necessary but not sufficient condition for the existence of functional connectivity. As shown, the relationship between them occurs, but

it is not obvious. Nevertheless, only a small amount of studies is focused on this issue. To the best of our knowledge, one of the papers of this Doctoral Thesis is the first attempt to relate them in the schizophrenia disorder using a combination of EEG and dMRI techniques (Gomez-Pilar et al., 2018a). Further efforts should be done in future studies to precisely disentangle the basis of cognition.

Chapter 2

Hypotheses and objectives

The neural mechanisms of the brain and, particularly, the neural networks involved in pathological behavior as in the schizophrenia disorder, have become a relevant research topic. Hence, the proposal developed in this Doctoral Thesis is focused on analyzing EEG recordings to characterize the underlying neural mechanisms of the brain aimed at finding altered neural substrates in schizophrenia.

In order to obtain a comprehensive characterization of human neural networks, EEG data were examined using a three-level analysis: (i) local-activation; (ii) functional interactions, and (iii) network organization. Local-level activation was assessed using an information-theory-derived measure, Spectral Entropy (SE), which applied to the wavelet transform is usually named Wavelet Entropy (WE). Functional integration was analyzed by means of magnitude-squared coherence (MSCH) and phase-locking value (PLV). Finally, network organization was studied using graph-derived measures, such as clustering coefficient (CIC), characteristic path length (CPL), connectivity strength or graph density (D), as well as two novel measures proposed in this Thesis: Shannon Graph Entropy (SGE) and Shannon Graph Complexity (SGC).

The following schedule was conducted in the studies of this compendium of publications:

- i) EEG acquisition.
- ii) EEG segmentation and preprocessing.
- iii) Time-frequency decomposition using wavelet transform.
- iv) Local activation analyses.
- v) Brain interactions/coupling analyses.
- vi) Brain graph analyses.

- vii) Statistical analyses.
- viii) Assessment of how these measures translate into behavior and/or cognition.

This research proposal is substantiated by the hypotheses and objectives described below.

2.1 Hypotheses

Schizophrenia has been associated with a failure in the information integration in long-range scales of the brain during cognition (Friston, 1998). Complex Network Theory provides an adequate framework to characterize this functional disruption among brain regions. Therefore, *graph analyses of the neural activity could be useful for understanding the brain processes underlying the altered cognitive functions in schizophrenia*. Cognitive tasks elicit rapid responses in the brain in the range of milliseconds. Furthermore, previous studies showed that schizophrenia is accompanied by an aberrant salience attribution of relevant stimulus (Kapur, 2003; Bachiller et al., 2014), which could affect the neural coupling among brain areas during cognition (Bachiller et al., 2015). Hence, *high temporal resolution techniques, such as the EEG, acquired during an auditory oddball task, can be used to characterize brain dynamics at network level in schizophrenia*.

Cognitive tasks depend on global dynamics of cerebral networks that involve changes in the coupling balance among regions, which is likely disrupted in mental disorders. It is therefore reasonable to hypothesize that *the analysis of the connection weight balance can provide the basis for revealing relevant information of the neural substrates affecting the pathological brain*. Although the abnormalities in schizophrenia are ultimately related to disrupted brain network, local activation irregularities could influence on interrelations among functional regions. Therefore, *sensor-level activation may be related to long-range interactions in which particular brain regions are involved*. These interactions may not only be related to functional connectivity, but also to structural connectivity or ‘physical’ pathways of the brain. Indeed, functional network alterations might be secondary to structural abnormalities. Therefore, *the assessment of the relationship between functional and structural networks in schizophrenia may help characterizing the neural substrates of the cortical dysfunction in this disorder*.

Because of the amount of factors involved in brain coordination, the difficulty to characterize the brain network in a comprehensive way makes difficult to model the brain dynamical behavior. In addition, several network measures are strongly

related between them, which ultimately does not provide a global view of how the neural networks are reorganized during a cognitive task. Hence, *the use of complementary network measures to assess brain dynamics during a cognitive task can shed light to develop new models of cognition.*

In order to validate these hypotheses, this Doctoral Thesis proposes the use of *the Complex Network Theory applied to the EEG and to other structural techniques to obtain a meaningful framework for assessing and, eventually, modeling the dynamic brain interactions presumably altered in schizophrenia.*

2.2 Objectives

The general goal of this Doctoral Thesis is *to study, to design and to apply biomedical signal processing methodologies to explore and characterize the neural substrates altered in schizophrenia using EEG.* This functional data were examined using Complex Network Theory with the aim of achieving a reliable characterization of dynamical dysfunctions of the neural network interactions in schizophrenia. In order to achieve the main objective, the following specific objectives arise:

- 1) To review the bibliography and state-of-the-art related to biomedical signal processing methodologies, useful to characterize EEG data. Particularly, this objective is focused on identifying appropriate graph theory methods to comprehensively characterize neural dynamics.
- 2) To build a database, including EEG recordings, socio-demographic data and clinical variables from adult patients with schizophrenia and healthy controls.
- 3) To select and implement the more suitable methods to reduce the noise of the ERP signals, to obtain local and network measures of the brain dynamics (from the literature or new ones) and to characterize the brain network behavior during cognition using EEG.
- 4) To conduct statistical analyses of the results to explore the brain dynamics, the relationship between local and network measures and the association between functional and structural connectivity, as well as to identify the pathophysiological patterns in schizophrenia. This objective also includes the construction of a novel dynamical network probabilistic-based model during cognition to explain the neural network changes at individual level.
- 5) To compare and discuss the results to extract appropriate conclusions. This objective includes the comparison with the state-of-the-art ERP studies and the comparison of our findings with the results obtained using other tech-

niques, such as magnetoencephalography (MEG) or fMRI.

- 6) To disseminate the main results and conclusions of the research in high-impact journals, as well as in international and national conferences.

Chapter 3

Materials and methods

In this compendium of publications, different methods and databases were used. To avoid redundancy, a brief summary of the methods followed and the databases used is provided in this chapter. However, a detailed explanation of them is described in the papers of the compendium of publications (see Appendix A).

3.1 Subjects' databases

Different databases were used as the number of subjects was growing throughout this Thesis. This is clearly shown in Table 3.1, which summarizes the number of subjects in each study, as well as the number of electrodes of EEG recordings. In order to increase the spatial resolution of the analyses, the EEG acquisition system was replaced during the development of the Thesis by a new one with the double number of electrodes (from 16 to 32). Having improved the spatial resolution, the number of subjects of the database decreases though. Thus, two databases were analyzed after completing the Thesis: (i) the former one with 16 electrodes consists of 87 controls and 48 patients with schizophrenia, and (ii) the latter one with 32 electrodes comprises 78 controls and 39 patients with schizophrenia. See Table 3.2 and Table 3.3 for a detailed description of the clinical and socio-demographic data of the participants of each dataset.

Table 3.1: Number of subjects for each group and number of electrodes used in each study included in the Thesis.

Study	Schizophrenia	Controls	EEG electrodes
Gomez-Pilar et al. (2015)	20	12	16
Gomez-Pilar et al. (2017)	57 (FE: 18; CH: 39)	59	16
Gomez-Pilar et al. (2018d)	48	87	16
Gomez-Pilar et al. (2018b)	28 (FE: 23; CH: 25)	51	32
Gomez-Pilar et al. (2018c)	35	51	32
Gomez-Pilar et al. (2018a)	39 (FE: 20; CH: 19)	78	32

CH: Chronic patients;

FE: First episode patients

Table 3.2: Socio-demographic, clinical and cognitive characteristics of the database of 16 active electrodes. Values are expressed as: mean (SD). The significant statistical differences between both groups were marked with an asterisk ($p < 0.05$, Student t -test).

	Schizophrenia	Controls
N	48	87
Age (years)	33.58 (9.27)	30.51 (10.77)
Gender (Male:Female)	25:23	44:43
Dose of CPZ (mg/d)	377.92 (196.94)	NA
Illness duration (months)	97.84 (116.94)	NA
Education (years)	14.19 (3.60)	16.56 (2.25)
PANSS Positive symptoms	11.63 (3.39)	NA
PANSS Negative symptoms	18.03 (7.52)	NA
PANSS Total symptoms	54.35 (18.56)	NA
IQ *	91.22 (14.19)	111.83 (11.87)
Verbal memory *	33.92 (12.74)	51.65 (8.26)
Working memory *	15.81 (5.01)	21.46 (3.90)
Motor speed *	58.14 (14.41)	68.59 (17.84)
Verbal fluently *	17.99 (5.70)	27.13 (5.33)
Processing speed *	42.83 (15.78)	68.79 (13.25)
Problem resolution capacity *	15.40 (4.64)	17.54 (2.72)
WCST perseverative errors *	27.31 (47.43)	10.17 (5.81)
WCST completed categories *	4.39 (1.87)	5.79 (0.72)

Table 3.3: Socio-demographic, clinical and cognitive characteristics of the database of 32 active electrodes. Values are expressed as: mean (SD). The significant statistical differences between both groups were marked with an asterisk ($p < 0.05$, Student t -test).

	Schizophrenia	Controls
<i>N</i>	39	78
Age (years)	33.05 (8.80)	30.95 (10.84)
Gender (Male:Females)	23:16	46:32
Dose of CPZ (mg/d)	377.90 (196.93)	NA
Illness duration (months)	95.17 (117.39)	NA
Education (years)	14.19 (3.60)	16.56 (2.25)
PANSS Positive symptoms	11.70 (3.43)	NA
PANSS Negative symptoms	17.571 (7.31)	NA
PANSS Total symptoms	53.810 (18.89)	NA
IQ *	91.061 (14.53)	113.21 (11.09)
Verbal memory *	34.262 (12.89)	51.11 (8.19)
Working memory *	16.151 (5.01)	21.63 (3.62)
Motor speed *	58.879 (13.78)	72.61 (16.58)
Verbal fluently *	18.352 (5.73)	27.86 (5.15)
Processing speed *	43.700 (15.36)	69.59 (14.38)
Problem resolution capacity	15.253 (4.62)	17.52 (2.57)
WCST perseverative errors *	17.92 (10.12)	9.80 (5.14)
WCST completed categories *	4.42 (1.88)	5.85 (0.61)

All controls and patients gave their informed written consent to be included in each of the studies of this Thesis. The study protocols were approved by the research board of the Clinical University Hospital of Valladolid (Spain) and were conducted in accordance with the Declaration of Helsinki guidelines.

3.2 Acquisition protocol

The EEG acquisition protocol was similar across all the studies. It consists in a 13 minutes three-tone P300 oddball task. Recordings were performed while the participants were sat, relaxed and with their eyes closed. The auditory oddball task consisted in random series of 600 tones whose duration was 50 ms, intensity

being 90 dB and inter-stimulus interval (ISI) between tones was randomly jittered between 1.16 s and 1.44 s. Three different tones were presented: target (500 Hz tone), distractor (1000 Hz tone) and standard (2000 Hz tone) with probabilities of 0.20, 0.20 and 0.60, respectively. The participants were asked to press a mouse button with their right hand whenever they detected the target tones. Only target tones followed by the mouse click, i.e. attended target tones, were considered for further analyses.

EEG recordings were acquired at a sampling frequency of 500 Hz in 16/32 electrodes with a BrainVision[®] equipment (Brain Products GmbH; Munich, Germany) while the participants underwent the previously mentioned oddball task. Electrode impedance was always kept under 5 k Ω and each channel was referenced over Cz electrode.

The general methodology starts with an initial preprocessing stage proposed to minimize undesirable noise and artifacts. It is described in the next section.

3.3 Signal preprocessing

In order to remove undesirable artifacts, signals were filtered between 1 and 70 Hz by means of a band-pass Finite Impulse Response (FIR) filter. A 50 Hz notch FIR filter using a Hamming window was also used to remove the power line artifact. Lastly, a three-steps artifact rejection algorithm was applied to minimize, mainly, electrooculographic and electromyographic contamination (Bachiller et al., 2015):

- i) Firstly, Independent Component Analysis (ICA) was carried out. After visual inspection, ICA components associated with artifacts were discarded.
- ii) Secondly, after ICA reconstruction, EEG data were divided into trials of 1 second length ranging from 300 ms before to 700 ms after stimulus onset, which ensures no overlapping with subsequent trials (the minimum ISI is 1.16 s).
- iii) Finally, an automatic and adaptive trial rejection was performed by applying a statistical-based thresholding method in order to remove ERP trials displaying amplitudes that exceeded a statistically based local threshold. The mean and standard deviation of each channel was computed. Then, trials that exceeded mean \pm 4 standard deviation in at least two channels were discarded (Bachiller et al., 2015; Núñez et al., 2017).

3.4 Continuous Wavelet Transform

EEG recordings are non-stationary signals, whose properties may change over time. Hence, methods that require stationary time series, like Fourier Transform, are not suitable to analyze their time-varying properties. For that reason, a time-frequency approach was used. Specifically, the Continuous Wavelet Transform (CWT), with a complex Morlet as mother wavelet, was selected. It provides a suitable alternative to describe the dynamic properties of EEG. Wavelet analysis relies on the introduction of an appropriate basis of functions. A wavelet is a zero mean function characterized by its localization in time (Δt) and frequency (Δf) (Roach and Mathalon, 2008). The complex Morlet wavelet was chosen as ‘mother wavelet’ in all the studies of the compendium, since it provides a biologically plausible fit to ERP data (Roach and Mathalon, 2008). Complex Morlet wavelet is defined as follows (Mallat, 1999):

$$\phi(t) = \frac{1}{\sqrt{\pi \cdot \Omega_b}} e^{j2\Omega_c t} \cdot e^{-\frac{t^2}{\Omega_b}}, \quad (3.1)$$

where Ω_b is the bandwidth parameter and Ω_c represents the wavelet center frequency. In this study, both were set to 1 in order to obtain a balanced relationship between Δt and Δf at low frequencies (Bachiller et al., 2015).

The CWT of each trial is defined as the convolution of the trial, $x(t)$, with a scaled and translated version of the complex Morlet wavelet:

$$CWT(k, s) = \frac{1}{\sqrt{s}} \int_{-\infty}^{\infty} x(t) \cdot \phi^*\left(\frac{t-k}{s}\right) dt, \quad (3.2)$$

where s represents the dilation factor ($s = \{s_i, i = 1, \dots, M\}$), k is the translation factor and * denotes the complex conjugation. The dilation factor was set in order to include frequencies from 1 Hz (s_1) to 70 Hz (s_M) in equally-spaced intervals of 0.5 Hz (Bachiller et al. 2015).

Several previous studies did not consider the effect of edges in the time-frequency plane (very important especially with short length windows, as in those associated with ERPs) (Roach and Mathalon, 2008). In this Thesis, however, a cone of influence (COI) was defined in order to avoid these edge effects. In particular, two windows were always defined: pre-stimulus (also called baseline in the first two studies) from -300 to 0 ms and response from 150 to 450 ms with respect to the stimulus onset. Thus, the spectral content must be only considered into the time-frequency regions delimited by their respective COIs. Figure 3.1 shows the CWT for a single EEG channel averaged across trials from a control subjects. Two

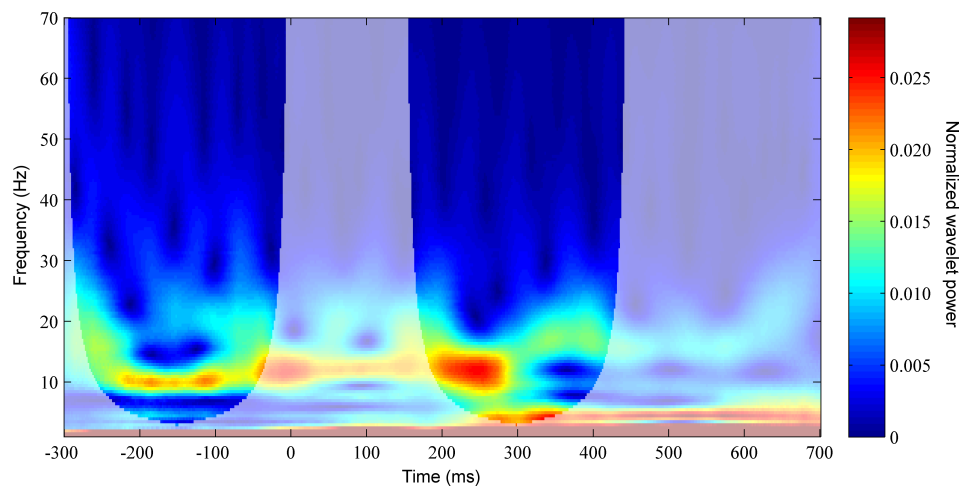


Figure 3.1: Example of the normalized wavelet coefficients at Pz electrode averaged across trials in a control subject from the database of 32 electrodes. The transparency outline represents the limits of the COI in the baseline and response windows, where the spectral content is not affected by edge effects. Figure from Gomez-Pilar et al. (2018c)

COIs related to the time windows are represented.

3.5 Connectivity matrices

After time-frequency decomposition, connectivity matrices were constructed using two different measures of coupling: Coherence and PLV. The choice between them was determined by the specific objective of the study. Both metrics provide a measure of the degree of coupling among brain regions, with values ranging from 0 to 1.

3.5.1 Coherence

From CWT decomposition, Coherence was computed to assess linear functional interactions (Nunez et al., 1997). Coherence is useful to identify coherent activity between cognitive networks (Yener and Başar, 2013), since it is a measure of the degree of coordination between assemblies of neurons triggered by a cognitive task. Coherence was calculated for each pair of electrodes (i and j) to obtain a global similarity measure for each time window:

$$Coh_{ij}(s) = \frac{|WCS_{ij}(s)|^2}{WCS_{ii}(s) \cdot WCS_{jj}(s)}, \quad (3.3)$$

where WCS is the wavelet cross-spectrum between two EEG trials, as follows:

$$WCS_{ij}(k, s) = CWT_i(k, s) \cdot CWT_j^*(k, s), \quad (3.4)$$

Coherence is analogous to the squared Pearson correlation, which reflects the amount of variance of electrode i in each frequency that can be explained by a linear transformation of the wavelet coefficients in electrode j (Roach and Mathalon, 2008).

3.5.2 Phase-locking value

The PLV has become a useful tool to quantify the phase steadiness between pairs of electrodes (Lachaux et al., 1999), given its sensitivity to measure the neural synchronization, even between EEG oscillations with relatively small amplitude (Spencer et al., 2003). Being able to use different approaches for computing the PLV, the CWT was used to extract the phase information from each trial (Bob et al., 2008). First, the extraction of the instantaneous phase of each signal in a narrow bandwidth was performed. The CWT can be used to perform filtering and phase extraction in a single step (Bob et al., 2008). Thus, the instantaneous phases $\varphi_x(k, s, \tau)$ and $\varphi_y(k, s, \tau)$ of two EEG signals, $x(t)$ and $y(t)$, can be used to define the phase difference as follows:

$$\Delta\Phi_{xy}(k, s, \tau) = \Phi_x(k, s, \tau) - \Phi_y(k, s, \tau), \quad (3.5)$$

where τ indexes each artifact-free trial.

After phase extraction, PLV estimates the variability of the phase differences across successive trials, as follows:

$$PLV_{xy}(k, s) = \frac{1}{N_t} \left| \sum_{\tau=1}^{N_t} e^{\Delta\Phi_{xy}(k, s, \tau)} \right|, \quad (3.6)$$

where N_t is the total number of artifact-free trials.

3.5.3 Adjacency matrices

After Coherence or PLV computation, adjacency matrices can be obtained as the coupling or synchronization between all possible pair of channels. These func-

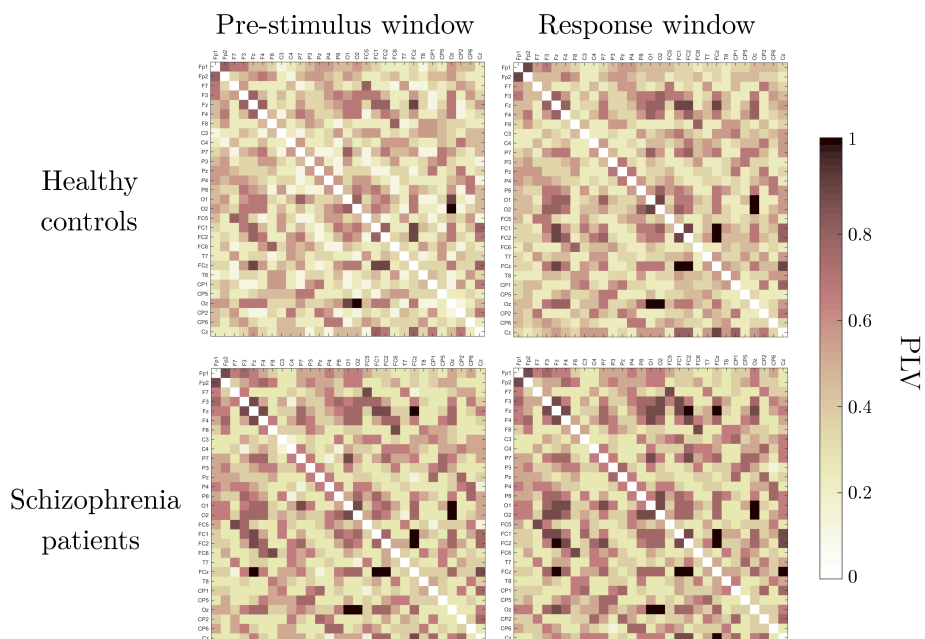


Figure 3.2: Averaged connectivity matrices from 35 controls and 51 patients with schizophrenia. The connectivity matrices are shown for controls and patients with schizophrenia from the database of 32 electrodes before (from -300 to 0 ms) and after (from 150 to 450 ms) stimulus onset. Figure from Gomez-Pilar et al. (2018d).

tional connectivity matrices contain the values of the graph connection weight (w_{ij}), which are ranged between 0 and 1 (weighted network). A value of 1 is obtained with completely synchronized signals and a value of 0 implies an absence of synchronization. Of note no threshold was applied. This has the advantage that all the connections are considered (even the lower ones), but the computational cost increases comparing to a semi-weighted network. We are aware of the limitations of this method, but we consider it a more realistic approach to describe the physiological properties of brain networks. Two examples of connectivity matrices from Gomez-Pilar et al. (2018d) are depicted in Figure 3.2 using PLV in two different temporal windows of the cognitive oddball task.

3.6 Graph parameters

A large variety of graph measures exist in the literature (Rubinov and Sporns, 2010). However, most of them are strongly correlated, since they represent the same network property (Rubinov and Sporns, 2010). For that reason, this Doc-

toral Thesis uses three complementary and well-known graph measures to characterize three key aspects of the network: (i) connectivity strength (using D), (ii) network integration (using CPL) and (iii) network segregation (using CIC). In addition, a widely extended measure named small-world index (SW) was used to compare with previous findings. SW is defined as the ratio between CIC and CPL , when both of them have been corrected by the same measures computed in a random network. Specifically, surrogate data were obtained by means of reshuffling the connections of the network. This procedure is explained in detail in the “3.8.3 Surrogate data” subsection. The conventional graph parameters that were used to quantify the network properties can be formally defined as follows:

- The connectivity strength was computed using the network density as follows (Gomez-Pilar et al., 2018c):

$$D = \frac{\sum_{i=1}^N \sum_{j>i} w_{ij}}{T}, \quad (3.7)$$

where w_{ij} represents the connection weight between nodes i and j , N is the number of nodes in the network and $T = \frac{N(N-1)}{2}$ is the total number of connections in an undirected graph.

- The integration of the network was characterized by means of the CPL . It is defined as the average shortest path length between all pairs of nodes in the network (Rubinov and Sporns, 2010):

$$CPL = \frac{1}{N} \sum_{i \in n} \frac{\sum_{i \in n, j \neq i} d_{ij}}{n-1}, \quad (3.8)$$

where d_{ij} indicates the minimum distance, i.e. the inverse of PLV or the Coherence depending on the study of the compendium, between electrodes i and j .

- The segregation of the network was quantified by the averaged CIC (Rubinov and Sporns, 2010). In the case of weighted networks, the averaged clustering coefficient can be generalized as follows to avoid the influence of the main connection weights:

$$CIC = \binom{N}{3} \sum_{i \in n} \sum_{j, k \in n} (w_{ij} w_{ih} w_{jh})^{\frac{1}{3}}. \quad (3.9)$$

Finally, the present Thesis also aimed at presenting two new graph measures of the network. These measures were applied to characterize the regularity (SGE) and complexity (SGC) of the brain network. Both rely in the concept that, for a fixed topology, the weight distribution of a complex network is directly related to its reliability and amount of information stored. Therefore, these novel graph measures were defined based on the following requirements: (i) they should be able to measure the interplay between reliability and amount of information stored in the system, (ii) they should be independent of the network topology, and (iii) they should not require a comparison with null-hypothesis networks.

Formally, the irregularity and the complexity of the network were defined in (Gomez-Pilar et al., 2018c), as follows:

- The irregularity of the brain network was characterized by the Shannon Graph Entropy, defined in our previous work as follows (Gomez-Pilar et al., 2018c):

$$SGE = \frac{-1}{\log_2 T} \sum_{i=1}^N \sum_{j>i} \frac{w_{ij}}{W} \log_2 \frac{w_{ij}}{W}, \quad (3.10)$$

where W is the sum of all weights of the graph and $\log_2 T$ is a normalization factor introduced to ensure that $0 \leq SGE \leq 1$.

Thus, the more uniform the distribution of the graph weights, the higher the SGE. The opposite situation, a very narrow distribution of the weight values, implies a minimum value of SGE. Both situations are considered simple ones. Therefore, the balance between those situations is considered the point with maximum complexity in terms of SGC. An example of this behavior is shown in Figure 3.3 for a simple graph with 4 nodes.

- The complexity of the brain network was estimated using the Shannon Graph Complexity, defined in our work (Gomez-Pilar et al., 2018c) as follows:

$$SGC = SGE \cdot \sqrt{\frac{1}{T-1}} \cdot \frac{\sigma}{\bar{x}}, \quad (3.11)$$

where \bar{x} is the average of all connection weights of the graph and σ is the standard deviation of those values.

In summary, up to five complementary graph parameters were used depending on the study to further characterize the brain network structure and topology in healthy controls and patients with schizophrenia.

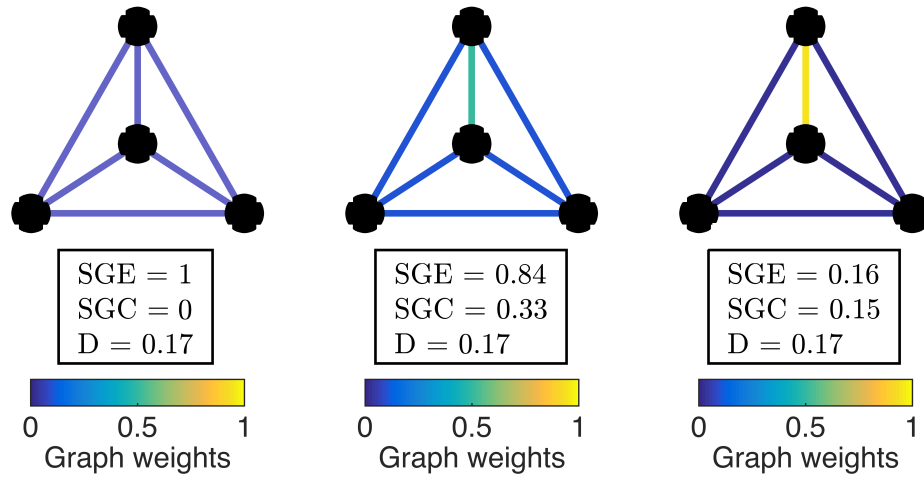


Figure 3.3: Examples of simple graphs with 4 nodes ($N = 4$) and their values of graph irregularity (SGE), graph complexity (SGC) and connectivity strength (D). For a completely weight-balanced network (left), SGE is maximum and SGC is minimum. A high weight-unbalanced network (right) yields low SGE and SGC values. On the opposite, neither a very weighted-balanced nor weighed-unbalanced network (center) reach higher SCG values.

3.7 Network modeling

Network parameters may not be sufficient to properly characterize brain dynamics. For that reason, one of the objectives of this Doctoral Thesis includes the “construction of a novel dynamical network probabilistic-based model during cognition to explain the neural network changes”. Due to the intrinsic neural variability, this model should be individually identified for each subject. For this purpose, six different models of brain dynamics were considered. Being possible to propose a huge number of possible models, these six models were selected for being intuitive and easy to explain in physiological terms. We are aware that changes in the brain network are probably more complex, but a model must be as simpler as possible without losing its generalization capability.

Three of the proposed models consist in iterative reinforcement of the network connections until reaching the minimum error with the graph parameters of the real brain network. These three models are the following:

- i) **Reinforcement of primary connections.** This model assumes that the primary connections of the brain, i.e. connections with higher values of

connectivity during pre-stimulus, will be reinforced during the cognition with higher probability.

- ii) **Reinforcement of secondary connections.** This model assumes that the secondary connections of the brain, i.e. connections with lower values of connectivity during pre-stimulus, will be reinforced during cognition with higher probability.
- iii) **Reinforcement of random connections.** This model assumes that all the brain connections during pre-stimulus will be reinforced with the same probability during cognition.

Three similar models were also studied, but considering a decrease of the edge values:

- iv) **Weakening of primary connections.**
- v) **Weakening of secondary connections.**
- vi) **Weakening of random connections.**

The algorithm to model the network changes during cognition consists in the following steps:

- 1) To compute graph parameters in the pre-stimulus and in the cognitive response windows.
- 2) To select a specific connection, w_{ij} , of the pre-stimulus connectivity matrix.
- 3) To modify the value of the connection with a probability P . The value of P depends on the specific model being considered, as we explain below. In addition, the connection is reinforced or weakened also depends upon the model.
- 4) To compute the network features in the modified connectivity matrix.
- 5) To compute the Mean Square Error (MSE) of the obtained network features with respect to the network parameters in the response window (computed in the first step).
- 6) To repeat the steps 2), 3) 4) and 5) 5000 times¹ and the MSE is stored for each iteration.
- 7) To select the connectivity matrix that minimizes the MSE.

The previous procedure was repeated six times (one for each model). As aforementioned, the value of P and how it was modified depend on the model:

- i) Reinforcement of primary connections: The value of the selected connection

¹The simulations showed that the MSE is a concave function with a minimum that varies for each subject. We checked that the minimum was always achieved before 5000 repetitions. Of note, the number of iterations required for reaching the minimum MSE is different for each subject.

- is increased in 1% with probability $P = w_{ij}$ (w_{ij} ranges from 0 to 1).
- ii) Reinforcement of secondary connections: The value of the selected connection is increased in 1% with probability $P = 1 - w_{ij}$.
 - iii) Reinforcement of random connections: The value of the selected connection is increased a 1% with probability $P = 1$.
 - iv) Weakening of primary connections: The value of the selected connection is decreased a 1% with probability $P = w_{ij}$.
 - v) Weakening of secondary connections: The value of the selected connection is decreased a 1% with probability $P = 1 - w_{ij}$.
 - vi) Weakening of random connections: The value of the selected connection is decreased a 1% with probability $P = 1$.

The percentage of change (1%) was heuristically determined as a compromise between goodness of fit and computational cost. Due to the stochastic nature of the algorithm, all the experiment was repeated 100 times and MSE results were averaged across repetitions. We observed that the variability among experiments for each subject was negligible. A general scheme of the procedure is shown in Figure 3.4.

3.8 Statistical analyses

3.8.1 Statistical hypothesis tests

Statistical analyses of this Thesis were mainly focused on statistical hypothesis tests. First, statistical hypothesis testing was used to assess data normality (Kolmogorov-Smirnov test), as well as to evaluate homoscedasticity (Leneve test). The previous test results can show that data meet (or did not meet) parametric assumptions. When data did not meet the parametric assumptions (the most usual situation in the studies of this Thesis), non-parametric statistical significance tests (Mann-Whitney or Wilcoxon tests) were used to assess the level of statistical significance. Of note that, with multiclass extension, Kruskal-Wallis test was used for comparison among three groups (chronic patients, first episodes and controls) or among the different models of cognition. On the other hand, related-samples t -tests or independent-samples t -tests were used for further analyses in the cases that data met the parametric criteria. Finally, Chi-squared test was used for comparisons when one or more variables were categorical, such as gender or type of reorganization model.

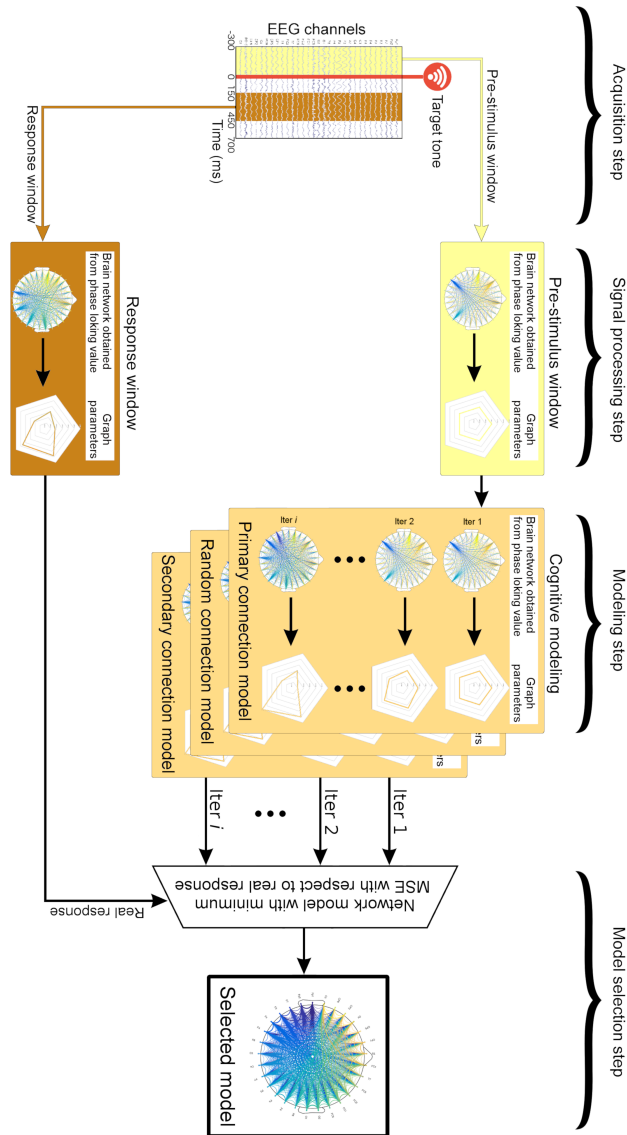


Figure 3.4: Overview of the network modeling procedure. After the EEG acquisition, the pre-stimulus window and the response window were segmented. During the signal processing step, graph parameters in each window were computed from the connectivity matrix. In the modeling step, the pre-stimulus connectivity matrix was modified by applying the six different cognitive models under study. Finally, in the model selection step, the cognitive model and the iteration that obtained the minimum Mean Square Error (MSE) with respect to the network parameters in the response window were selected. (Gomez-Pilar et al., 2018d)

3.8.2 Correlation analyses

Following the same procedure as for statistical hypothesis testing, before any correlation analysis, normality and homoscedasticity of the data were assessed. Pearson correlation coefficient was used for parametric data, whereas Spearman correlation coefficient was used in other case.

3.8.3 Surrogate data

The statistical significance of the network parameters must be considered by comparing them with null-hypothesis networks, i.e. networks constructed by a surrogate process. Null models are often used as a reference point to determine whether a graph displays a topological feature to a greater extent than expected by chance. These null-hypothesis networks are usually modeled as networks with the same basic characteristics as the original network (number of nodes, D , and node degree distribution), but with different topology (Rubinov and Sporns, 2010). However, all of these requirements cannot be met with weighted graphs at the same time. For that reason, different alternatives have been proposed (Ansmann and Lehnertz, 2012).

To date, the two most used weighted null-hypothesis networks are: (i) weight-preserving null-hypothesis that preserve the number of nodes, D , and edge weight distribution by means of a connection reshuffling process (Stam et al., 2009) and (ii) null-hypothesis networks that preserve N , D and the degree of each node (Nakamura et al., 2009). It is important to note that none of the two models preserve node degree distribution for weighted graphs, especially if the weight distribution is nonhomogeneous (Ansmann and Lehnertz, 2012). These two approaches have been previously compared, concluding that weight-preserving approach could segregate the influence of basic parameters more accurately than degree-preserving network model and the model performed without any surrogate process (Ansmann and Lehnertz, 2012).

In view of these findings, this Doctoral Thesis follows the weight-preserving null-hypothesis approach. Thus, surrogate random networks were generated by randomly reshuffling the weights of 50 randomized graphs (de Haan et al., 2009). We are aware that this method is not bias-free, but it provides a rapprochement to the real data.

Chapter 4

Results

This chapter summarizes the most relevant results displayed in the compendium of publications. They have been split according to the different hypotheses of the “2 Hypotheses and Objectives” Section, which has an almost direct correspondence with the papers included in this Thesis (see Appendix A).

4.1 Regularity patterns at sensor-level in controls and patients with schizophrenia

Regularity patterns of the EEG signal at sensor level were assessed by WE using two different approaches: SA and ST analyses (Gomez-Pilar et al., 2015). A reduction in WE was observed during a cognitive task both in healthy and schizophrenia groups. However, that reduction was significantly more noticeable for controls using both SA and ST approaches (see Figures 4.1 and 4.2). This is a finding reiteratively observed in this Thesis: changes in schizophrenia from pre-stimulus (also called baseline in the first two papers of the compendium) to cognitive response are statistically lower compared to controls.

Within-group analyses showed a widespread decrease of WE for controls from pre-stimulus to active response, mainly using SA approach. This reduction affects to more regions than in ST analysis. This decrease can also be observed in patients with schizophrenia, but it was less widespread for both approaches. Regarding between-group analyses, statistically nonsignificant differences were found in the pre-stimulus window for SA or ST. However, statistical differences were found for active response window using SA approach. Although both groups showed a

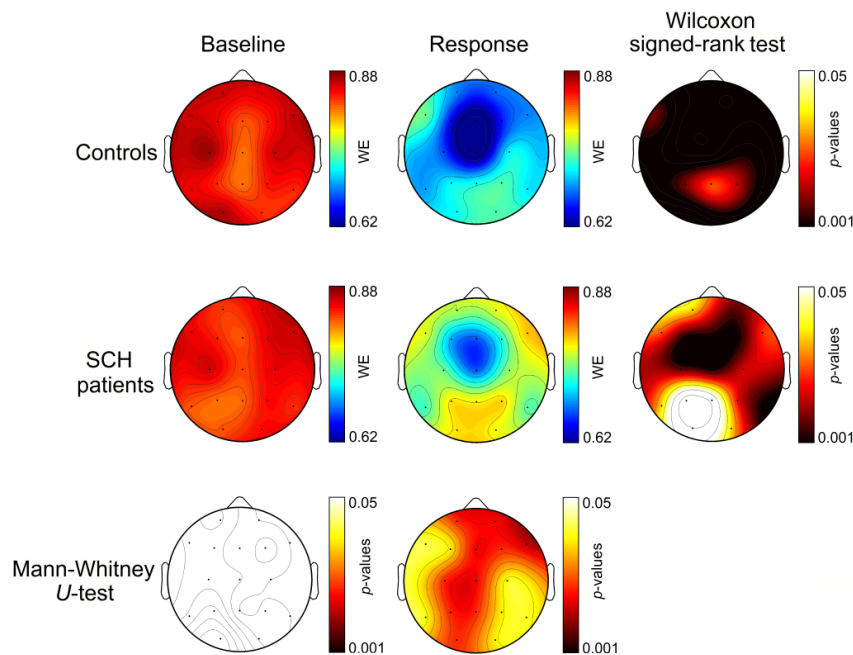


Figure 4.1: Sensor-level topographic maps of the statistics computed for the Wavelet Entropy using synchronized-averaging approach between controls and patients with schizophrenia. Right column shows within-group differences from pre-stimulus to response windows (Wilcoxon signed-rank test), whereas bottom row shows between-group differences for each window (Mann-Whitney U -test). The corrected p -values are obtained controlling false discovery rate (FDR). Figure from Gomez-Pilar et al. (2015).

decrease in WE during the cognitive response, it was more noticeable for controls, mainly in left parieto-occipital regions.

Taken together, differences in the regularity between groups are more marked in central and frontal regions, with a distribution linked to default mode network. The diminished response in schizophrenia is usually manifested in all the frequency bands. Theta band reveals the more prominent differences between groups though.

4.2 Network abnormalities in schizophrenia and relationship with regularity

By analyzing different and incremental databases, robust results revealed statistically significant changes in several network features from pre-stimulus to cog-

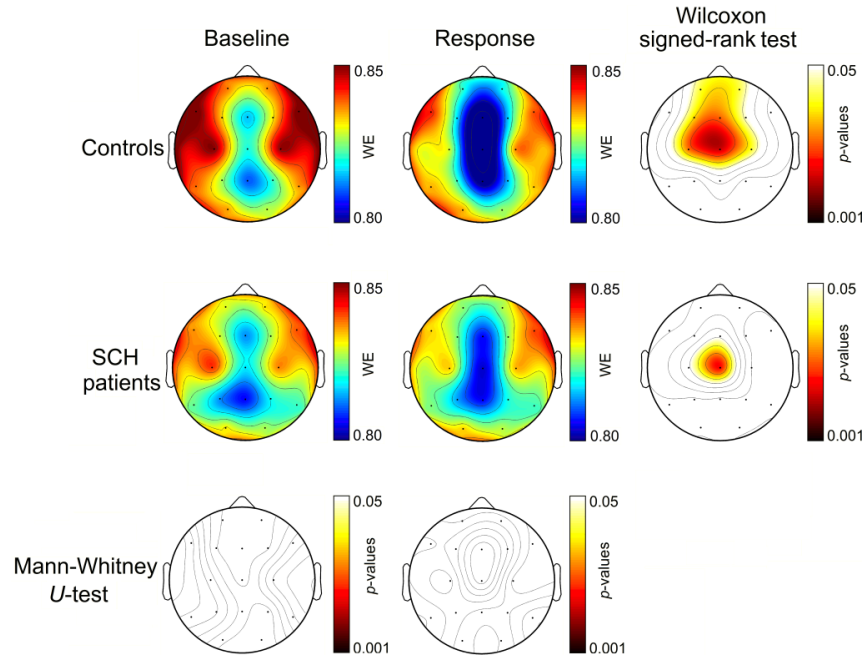


Figure 4.2: Sensor-level topographic maps of the statistics computed for the Wavelet Entropy using single trial approach between controls and patients with schizophrenia. Right column shows within-group differences from pre-stimulus to response windows (Wilcoxon signed-rank test), whereas bottom row shows between-group differences for each window (Mann–Whitney U -test). The corrected p -values are obtained controlling false discovery rate (FDR). Figure from Gomez-Pilar et al. (2015).

nitive response in controls but not in patients (or at least a less noticeable variation) (Gomez-Pilar et al., 2017, 2018a,b,c,d). An example of this is shown in the Figure 4.3, which depicts the clustering coefficient distribution for the different groups under study and the within- and between-group statistical differences. Of note, non-significant differences were found between first episode patients and chronic patients. This supports that the differences between controls and patients are not secondary to medication.

This and the following connectivity findings were analyzed in the theta frequency band. Accordingly with the literature, we observed important differences in the oscillations, frequently related to long-range interactions (Uhlhaas and Singer, 2010).

Several network measures were used in order to characterize brain network behavior, obtaining differences between patients and controls. For example, patients

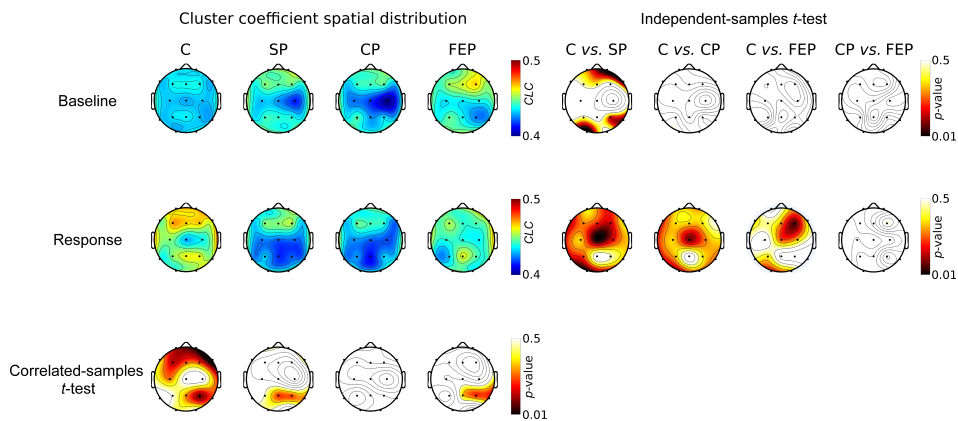


Figure 4.3: Nodal clustering maps depicting the spatial distribution of within-group (comparison between pre-stimulus and response) and between-group differences in ClC (C: Controls; SP: patients with schizophrenia; FEP: First episode patients; CP: Chronic patients). Figure from Gomez-Pilar et al. (2017).

obtained higher ClC and SW at pre-stimulus, lower ClC and higher PL at response, and a diminished variation of ClC and SW as compared to controls (Gomez-Pilar et al., 2017). Changes in these graph measures were inversely correlated to some dimensions of behavior and cognition (as executive tasks and working memory). Importantly, ClC and SW during the pre-stimulus were inversely associated to their respective variations during the cognitive task (Gomez-Pilar et al., 2017).

Established the network abnormalities in schizophrenia, the focus of attention turned to their causes. To investigate the underpinnings of functional and structural abnormalities, WE and graph parameters were computed in the same population formed by chronic and first episode patients, as well as by controls. Results revealed an inversely correlated relationship between WE and the change from pre-stimulus to response windows of functional connectivity strength both for patients and controls (see Figure 4.4). Additionally, WE was positively correlated with functional connectivity strength in the pre-stimulus window for patients (see Figure 4.5) (Gomez-Pilar et al., 2018b). On the contrary, structural ClC was negatively related to WE changes in patients (see Figure 4.5) (Gomez-Pilar et al., 2018b).

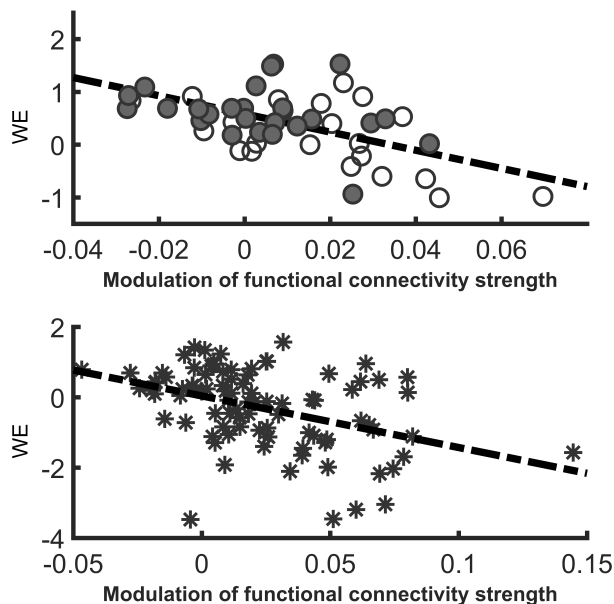


Figure 4.4: Scatterplots showing the association between modulation of functional connectivity strength and first factor (principal component analysis) of WE change for patients (top) and between modulation of functional connectivity strength and first factor of WE change for controls (bottom). Open circles: First episode patients; solid circles: Chronic patients; stars: Healthy controls). Figure from Gomez-Pilar et al. (2018b).

4.3 Functional and structural relationship

The previously mentioned results showed an association between local regularity from the EEG and functional and structural connectivity (Gomez-Pilar et al., 2018a). This association seems to be altered in schizophrenia, but the relation between functional and structural connectivity remained to be unexplored. In fact, we present a completely novel study. To the best of our knowledge, it represents the first attempt to characterize functional and structural relationship in schizophrenia (Gomez-Pilar et al., 2018a). Figure 4.6 depicts a schematic pipeline of the graph measures computation derived from EEG and dMRI data.

Results showed statistically significant differences between controls and schizophrenia patients in several graph properties both in functional and structural networks (see Figure 4.7). Despite of this, the deficit in the dynamical properties in the theta band for schizophrenia patients is independent of the deviation from

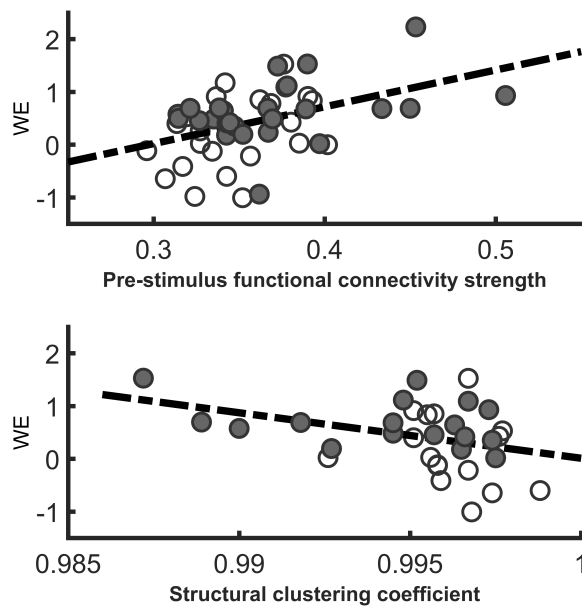


Figure 4.5: Scatterplots showing the association in the patients between pre-stimulus theta density and first factor (principal component analysis) of WE change (top) and between structural clustering coefficient and first factor of WE change (bottom). Open circles: First episode patients; solid circles: Chronic patients. Figure from Gomez-Pilar et al. (2018b).

normal structural network properties (Gomez-Pilar et al., 2018a). This lack of association can be due to several aspects, described in the “5 Discussion” Section.

4.4 Brain complexity

The use conventional graph measures did not provide a comprehensive view of the neural mechanisms. For that reason, a novel measure of graph complexity was proposed. Neural network complexity was computed using SGC, a measure of the balance of the edge weight distribution in a graph (Gomez-Pilar et al., 2018c). Brain graphs were constructed based on the Coherence in the EEG conventional frequency bands. However, only the complexity in the theta band showed statistically significant differences between controls and patients with schizophrenia (see Figure 4.8). In particular, the complexity change from pre-stimulus to cognitive response is lower in schizophrenia compared to controls (Gomez-Pilar et al.,

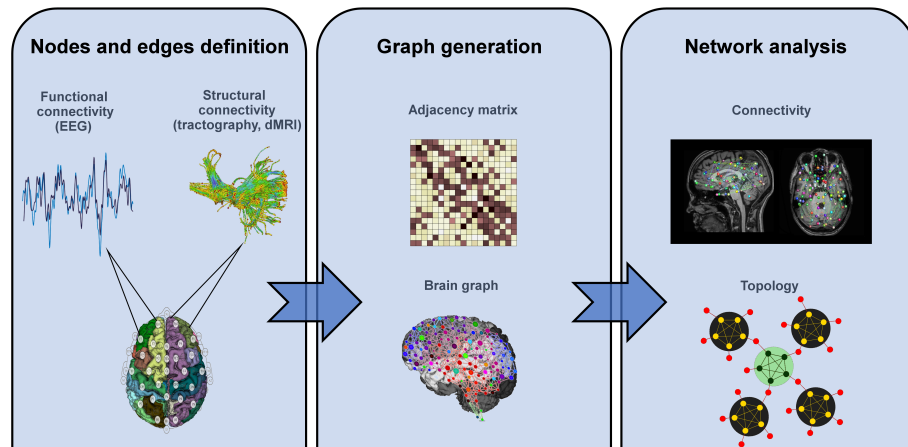


Figure 4.6: Schematic overview for the network analyses from the structural and functional data. Figure from Gomez-Pilar et al. (2018b).

2018c).

The entropy of the brain network was also assessed by measuring the distribution of the graph weights. For that purpose, SGE, a novel graph measure defined in (Gomez-Pilar et al., 2018c), was used. As can be seen in Figure 4.9, both controls and patients with schizophrenia reduced their SGC, whereas SGE was increased during the cognitive task performance. Following our previous studies, these changes from pre-stimulus to cognitive response were statistically reduced in schizophrenia compared to controls.

4.5 Functional network model during cognition

Previous findings, mainly the ones related to complexity, lead us to hypothesize that neural connections strength changes during a cognitive task in a way that depends on the value of that connection during the stimulus expectation (Gomez-Pilar et al., 2018d). This results was the basis for a new study proposal in which different reorganization models during cognition were assessed using graph measures (Gomez-Pilar et al., 2018d).

Depending on the main network behavior during the cognitive task, each subject was assigned to one among three different models: (i) reinforcement of the primary connections, (ii) reinforcement of the secondary connections and (iii) random reinforcement. The prediction capability of the network model is shown in the

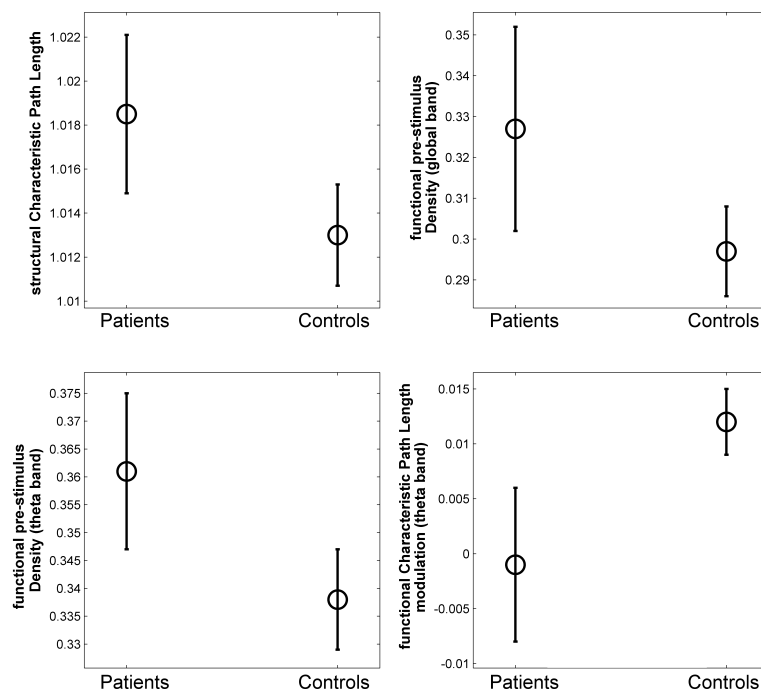


Figure 4.7: Error bars corresponding to the graph properties with statistically significant differences between patients and controls. Circles represent the mean value, while bars indicate the confidence interval (95%). Figure from Gomez-Pilar et al. (2018a).

Figure 4.10. Using only the information of the network during pre-stimulus, the individualized modeling obtains similar values of the five graph measures during the cognitive response. We also took into account three additional models, which are similar to previous models but considering a decrease in the edge values. However, these models were only selected in 15% of the subjects.

From the model of each subject, we inferred that controls showed a marked tendency of reinforcement of secondary connections during cognition. On the other hand, patients were divided in a similar way between reinforcement of primary and secondary connections (see Figure 4.11). This behavior can be also observed in Figure 4.12. On average, both controls and patients reinforce their connections. However, secondary connection are the more reinforced pathways during cognition, mainly for healthy controls.

Finally, the dynamics of the change during cognition detected in our previous studies were evaluated using five complementary graph parameters (see Figure 4.13). In this case, these changes were studied in a more comprehensive way,

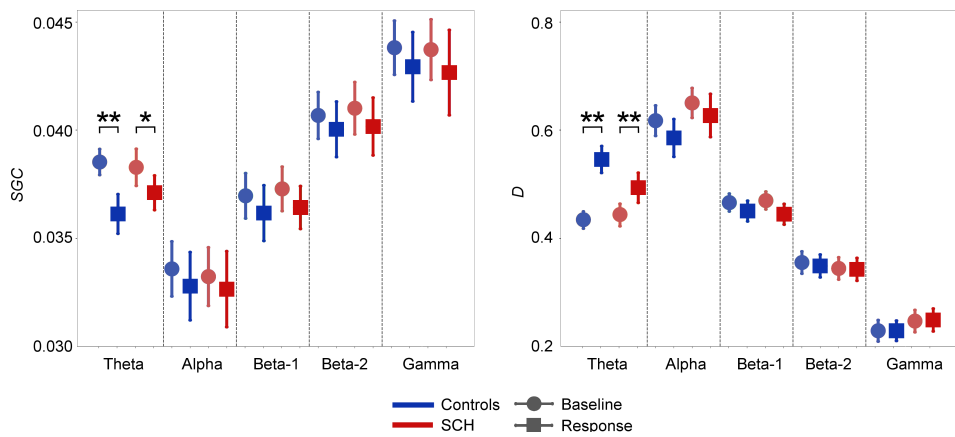


Figure 4.8: Shannon Graph Complexity (left) and connectivity strength (right) values for each group, window and frequency band. Values are depicted as mean and standard error. * indicates $p < 0.01$, while ** indicates $p < 0.001$ (Mann-Whitney U -test). Figure from Gomez-Pilar et al. (2018c).

since dynamical changes were assessed. The brain network dynamics across time (recently named *chronnectomics* in the literature) showed significant differences mainly between 150 ms to 300 ms from the stimulus onset, at the beginning of the response window.

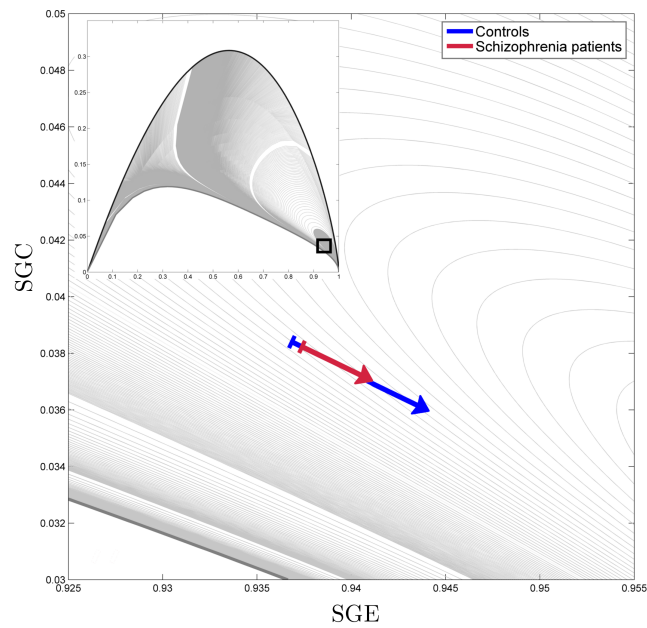


Figure 4.9: Detailed plot of the complexity dynamics from pre-stimulus to response in the theta frequency band for controls (blue arrow) and patients with schizophrenia (red arrow). The small figure represents the total range of SGC values for this network size (30 nodes/electrodes). The square in the small figure corresponds to the zoomed area in the large figure. SGE increases and SGC decreases for both groups, but the behavior is more remarkable for controls than for patients with schizophrenia. Figure from Gomez-Pilar et al. (2018c).

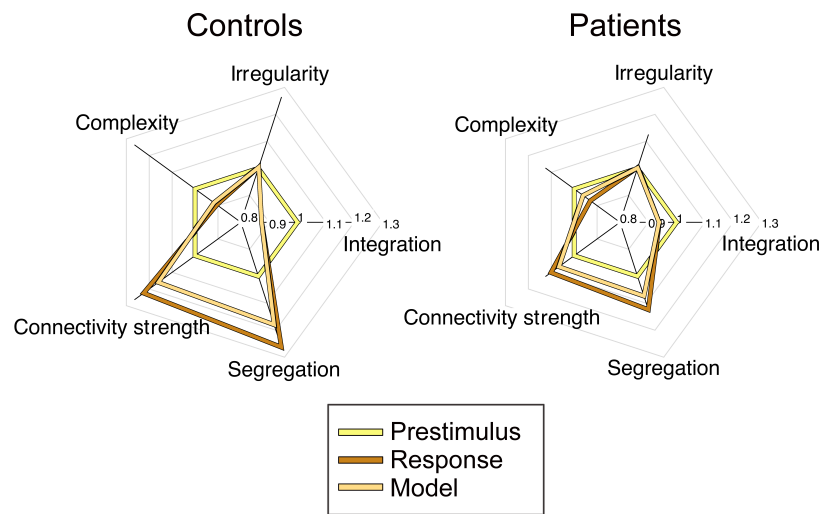


Figure 4.10: Prediction capability of the network modeling from the pre-stimulus window. Grand-average normalized network parameters for the pre-stimulus window (yellow) and the real response window (dark orange). The network measures prediction obtained by the model from the phase information of the pre-stimulus window is also shown (light orange). The model fitting for both the controls and the patient groups is computed by minimizing the mean square error (MSE). Figure from Gomez-Pilar et al. (2018d).

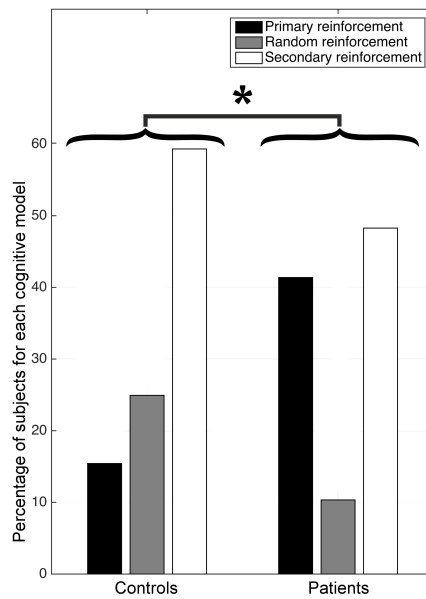


Figure 4.11: Histogram of the selected models. Percentage of subjects that best fit each model for controls and patients with schizophrenia. The reinforcement of the secondary connections is the most frequently selected model for both groups; however, statistically significant differences between the histograms of controls and patients were found and marked with an asterisk ($\chi^2 = 6.6874$, $p < 0.05$; Chi-square test). Figure from Gomez-Pilar et al. (2018d).

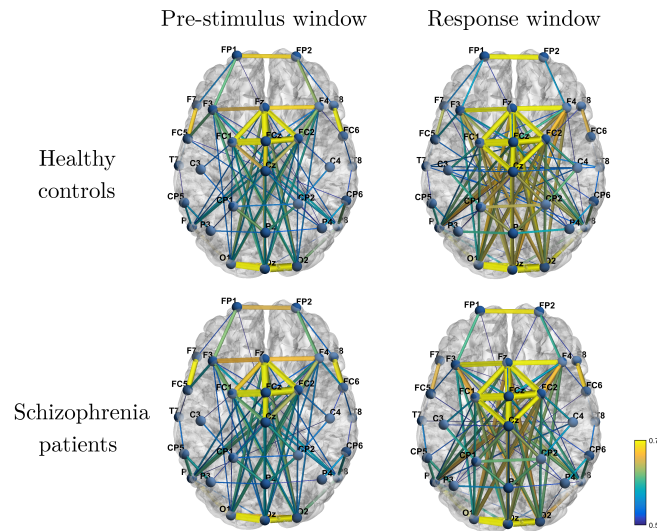


Figure 4.12: Averaged brain networks for controls and patients with schizophrenia before and after stimulus onset. Both groups show an increase in the edge weight values from the pre-stimulus (from -300 ms to the stimulus onset) to the response window (from 150 ms to 450 ms after the stimulus), though this increase is more noticeable for controls. To facilitate the visualization of the networks, a threshold was applied: only those connections with phase-locking values higher than 0.5 were depicted. The brain networks were visualized using the BrainNet Viewer Xia et al. (2013). Figure from Gomez-Pilar et al. (2018d).

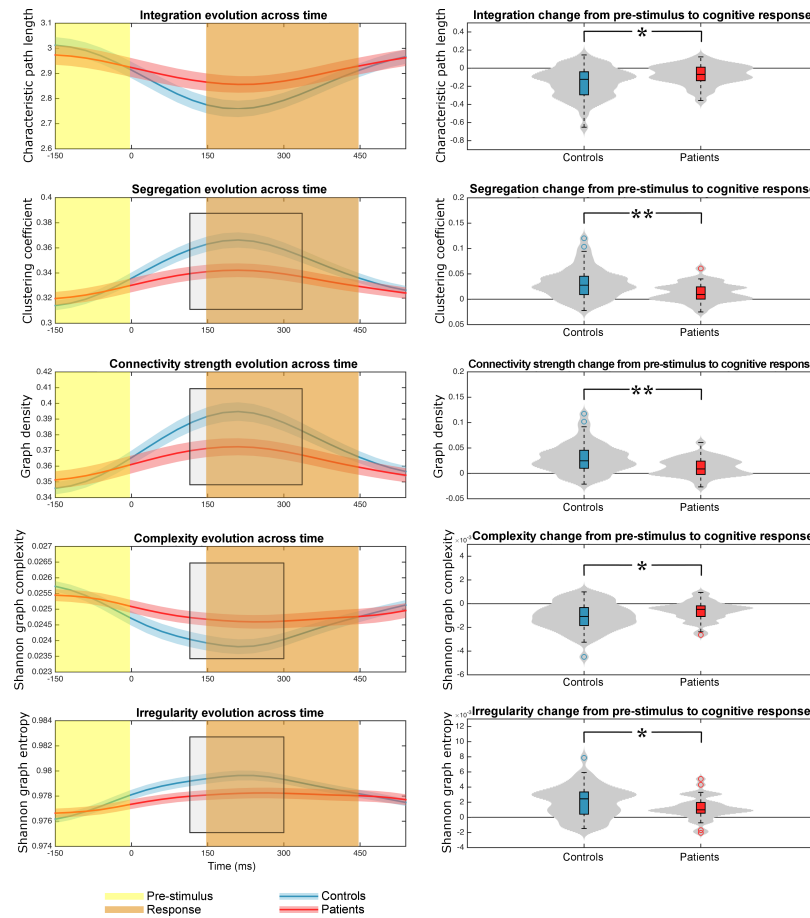


Figure 4.13: Time evolution of the network parameters. At the left panel, mean and standard error of the network parameters for controls (blue) and patients (red). Control subjects exhibit higher changes from pre-stimulus (yellow) to cognitive response (orange) compared to patients. Statistically significant differences between the network parameter evolution across time of both groups are highlighted by a black rectangle. At the right panel, distribution of the averaged change of the network parameters from pre-stimulus (yellow transparency in the left panel) to cognitive response (orange transparency in the left panel) for both groups. The degree of statistically significant differences between groups is indicated with one asterisk ($p < 0.05$, Mann-Whitney U -test) or two asterisks ($p < 0.01$, Mann-Whitney U -test). Figure from Gomez-Pilar et al. (2018d).

Chapter 5

Discussion

In this Doctoral Thesis, the characterization of the altered functional network structure and neural dynamics in schizophrenia during a cognitive task has been addressed. Firstly, new evidences for the *dysconnectivity* hypothesis and the aberrant salience hypothesis in schizophrenia were found. Abnormal response to novel and relevant stimulus (aberrant salience) was recurrently found in patients with schizophrenia in this Thesis. This abnormal response was accompanied by a diminished integration among brain regions connected by long-range interactions. Secondly, novel findings about possible underpinnings of these anomalies were provided by means of the study of the structural network and functional local measures based on regularity. Importantly, a hyperactivation focused on segregated assemblies of neuronal entities during the stimulus expectation can suppose the main difference between the odd response during cognition in schizophrenia. Thirdly, a novel graph measure of network complexity was developed. SCG provides an estimation of the ratio between the order of the network and the amount of information stored in it. The measure is insensitive to changes in connectivity strength and network size for networks large enough ($N > 30$). Having shown its virtues, SCG provides new clues about brain network dynamics in schizophrenia during cognition. Finally, the previously mentioned findings using SGC allow us to propose a novel network modeling to describe the brain network dynamics and the main differences between healthy and schizophrenia subjects. This network modeling identifies different reorganization strategies of the brain network as response to an oddball task for patients with schizophrenia, which could be the basis for new studies focused on the heterogeneity in this disorder.

In this Chapter, the aforementioned findings will be further discussed following

the logical order of this Thesis. Finally, the main limitations of the study are presented.

5.1 Confirming the well-established hypotheses in schizophrenia

With a large number of hypotheses proposed in different schizophrenia studies, two of them are currently accepted by most of the scientific community: the *dysconnectivity* hypothesis (Friston, 1998) and the aberrant salience hypothesis (Kapur, 2003). The first one refers to an abnormal integration of information in schizophrenia, explicitly showed by a diminished connectivity (functional and effective), mainly in long-range interactions. Novel findings on this insight have been provided in the papers of this compendium of publications. The main of them is the statistically significant larger path length of the brain network showed by the patients during the response to an oddball task. Regarding the aberrant salience hypothesis, it states that schizophrenia symptoms may arise out of the aberrant assignment of salience to external objects and internal representations (Kapur, 2003). This altered state in schizophrenia has been proposed to be related to alterations in dopaminergic concentrations. A dysregulation of this neurotransmitter could generate aberrant attributions of abnormal salience, which in turn could be the basis for the hyper-segregation during the pre-stimulus found in this Thesis. An example of this is the reduced change in schizophrenia using WE both for SA and for ST methodologies (Gomez-Pilar et al., 2015). Therefore, the present findings are in line with the previous evidences in the literature, which suppose a control measure for the later results.

5.2 Determining possible causes of dysconnectivity in schizophrenia

To formally analyze the possible causes of dysconnectivity in schizophrenia, two studies were carried out. In the first one, we looked for a relationship between local regularity of the EEG and connectivity strength in the functional network (Gomez-Pilar et al., 2018b). Interestingly, high levels of irregularity change (from pre-stimulus to response activity) of the EEG activity are strongly associated to high change of connectivity during cognition. High values of WE are linked to a more uniform power spectrum. Measured during the pre-stimulus, the higher WE,

the higher flexibility or predisposition to change during the cognitive response, since a wide range of frequencies are available. Measured during the response, a high WE means lower specificity of the task, which leads to an aberrant and diminished relevance assignment to the stimulus, likely related to a disorganized internal representation. In this way, the spectral flexibility can lead to a stronger functional connectivity between regions. Although this is only a hypothesis, it is feasible, and it would explain how the reduced level of entropy in schizophrenia is related to the disconnection hypothesis.

The second paper (Gomez-Pilar et al., 2018a), focused on determining the causes of functional *dysconnectivity*, seeks the answer in the structural abnormalities in schizophrenia. However, despite the statistically significant differences in the graph features of the structural network in schizophrenia compared to controls, no important relationship was found between structural and functional abnormalities. This lack of relationship suggests the existence of different clusters within the schizophrenia syndrome (Gomez-Pilar et al., 2018a).

5.3 A novel measure for characterizing network complexity

A common problem in graph analyses is the bias of many graph measures due to the high dependence with the network size or the average of the connectivity strength. The use of surrogate data and comparisons with null-hypothesis networks become, then, of paramount importance. However, these procedures do not completely remove the bias (Ansmann and Lehnertz, 2012) and the computational cost exponentially increases with the number of comparisons due the high number of permutations needed.

These concerns incited us to design and propose a novel measure of complexity. SGC relies on the concept of the order of the network and the amount of information stored in it, providing a ratio between them (Gomez-Pilar et al., 2018c). Furthermore, the measure is insensitive to changes in connectivity strength and network size for networks large enough ($N > 30$).

SGC can be applied to any kind of graph derived from any network (biological, molecular, logistic or social network), quantifying the system complexity. The application of the measure to the EEG brain network in patients with schizophrenia provided us a new vision of the brain dynamics, showing important differences in the secondary pathways of the brain with respect to control subjects (Gomez-

Pilar et al., 2018d). This study was the starting point for the last study of the Thesis, in which we propose a novel model of brain dynamics during a cognitive task (Gomez-Pilar et al., 2018d).

5.4 Towards a model of cognition

Not many cognitive models have been proposed in the literature to explain the brain behavior and the differences found between healthy controls and patients of any pathology. In addition, the few models proposed suffer from important deficiencies, such as the high computational cost or the complex optimization of several parameters (Gomez-Pilar et al., 2018d). Furthermore, the complexity of these models makes it difficult to draw a direct relationship to brain networks without a strong ‘a priori’ hypotheses. For these reasons, we proposed an intuitive and reliable model focused on explaining the observed neural network dynamics during a cognitive task (Gomez-Pilar et al., 2018d). In this model, the error between the modeled network and the real brain network is recurrently minimized. Thus, the brain network during the pre-stimulus activity determines the brain network during cognition.

In our previous studies, we found a hyper-segregated state in schizophrenia during the stimulus expectation (Gomez-Pilar et al., 2017) and a relationship between local measures during the pre-stimulus and changes in graph measures during the cognitive task (Gomez-Pilar et al., 2018b). Therefore, the association between pre- and post-stimulus exists, but the formal link between them had not been determined before. Now, we can state that the main differences in the functional dynamical changes in a healthy brain during cognition are due to the reinforcement of the secondary pathways, i.e. pathways weakly connected during pre-stimulus window. The fact that only a subgroup of patients with schizophrenia fits this model suggest us the existence of schizophrenia subgroups. This hypothesis has been recently proposed in parallel studies (Lubeiro et al., 2016). However, the concept is not currently widely accepted by the psychiatric community. Further studies in this line should be carried out, which could suppose a breakthrough in the established paradigm of schizophrenia. This could improve patient-care and contribute to achieve better long term outcomes, since specific medication must be provided upon the physiopathological underpinnings of particular schizophrenia subgroups.

5.5 Limitations of the study

This Doctoral Thesis showed the utility of graph theory applied to EEG data for characterizing the neural dynamics underlying cognitive processing in schizophrenia. Several limitations, however, merit additional considerations. First, a larger sample size would enhance the statistical power of the results. As we can observe in Table 3.1, after the mandatory change from 16 to 32 electrodes, the number of subjects under study was progressively increased in each study. The increase of the number of electrodes allow us to improve the accuracy of the spatial resolution. However, the sample collection started from zero, which was reflected in a lower number of subjects under study. Even so, the sample size is comparable with other studies and statistical power analyses indicated that this sample size is large enough for obtaining statistically significant results. Nevertheless, a larger database would be particularly beneficial in the case of future studies focused on identifying clusters of patients with schizophrenia. The second consideration is related to the number of electrodes. Graph analyses are more accurate using as many nodes as possible. In addition, with larger number of electrodes, source analysis could be performed and volume conduction effects would be removed from the results. To address this problem, we rely on the assumption that volume conduction affects the connectivity estimates in a similar way in two different experimental contrasts, such as pre-stimulus and response conditions (Bastos and Schoffelen, 2016). This approach of comparing these two conditions minimizes the bias. For that reason, it was followed in all the studies of this Doctoral Thesis. Nonetheless, the use of higher density EEG recordings could improve the obtained findings. Third, in the papers of this compendium of publications, all EEG connectivity parameters are measures of functional connectivity, i.e. the statistical dependence between electrical brain activations. Although this was compared to structural MRI connectivity, i.e. the physical neural connections, it would be also desirable to assess its relationship with effective connectivity, i.e. the causal inference of one activation to another. Finally, the drugs prescribed to the patients is an important confounding factor. In the studies of the Thesis, this effect was controlled by considering the medication doses or comparing to a third group (first episode patients). However, the best way to discard this effect is by means of the inclusion of a group with the same or similar drug prescription but different disease. Our research group is currently working in this matter by recruiting a new group formed by bipolar patients. Therefore, this procedure will be considered in our future studies.

patients with schizophrenia

Chapter 6

Conclusions

All the studies of this Doctoral Thesis share a common thread: the use of analyses based on graph-theory for enhancing the established knowledge about dynamical connectivity properties of noticeable neural assemblies and their abnormalities in schizophrenia. These studies are intended to be a starting point for a future breakthrough in the study of schizophrenia, in which subgroups inside of this disorder with unique and particular biological characteristics will be identified. The heterogeneity in schizophrenia is a reiterative finding in several studies. This may be a reason for obtaining, sometimes, contradictory results and hindering the replication of results with different databases.

Based on functional connectivity, we found a common and reproducible behavior for most of the patients with schizophrenia. However, specific brain dynamics during a cognitive task differ from one patient to another (Gomez-Pilar et al., 2018d). Therefore, though it is possible that schizophrenia has a shared neurophysiologic underpinning, some peculiarities of specific subgroups could be eliciting specific neuronal patterns with respect to each other. By averaging these features, we would be hiding important aspects of the pathology. This would explain the different response to treatment among patients with ‘the same’ illness. Far from being proven, this hypothesis must be addressed in future studies. Nonetheless, this Thesis is a first step for further and more complex multimodal studies in which EEG, dMRI, fMRI, genetic variables, as well as different neurotransmitter-related factors could be jointly analyzed.

Taken together, the advanced computational techniques used in this Doctoral Thesis endorse the creation of a framework for analyzing EEG data from an auditory oddball paradigm in schizophrenia. In particular, the analysis of time-

frequency dynamics of the brain network between the stimulus expectation and the response to a cognitive task time windows allows improving the understanding of schizophrenia disorder mechanisms. In this chapter, the original contributions of this Doctoral Thesis to the state-of-the-art are highlighted. Then, the main conclusions extracted from this compendium of publications are indicated. Finally, several questions emerged from this investigation and future research lines will be listed.

6.1 Original contributions

Next, the main original contributions provided by this Doctoral Thesis are listed:

- 1) Direct comparison of the regularity brain patterns in healthy control subjects and patients with schizophrenia between synchronized-averaging and single-trial approaches. To the best of our knowledge, this is the first time that phase-locked and non-phase-locked entropies were directly compare (Gomez-Pilar et al., 2015). Although a few studies compared evoked and induced responses, none compared their regularity dynamical patterns during cognition.
- 2) Application of time-varying measures of the brain network for assessing fast network modulation during cognitive activity in schizophrenia. The use of dynamical graph measures provided new clues of the hyper-segregated state during the pre-stimulus in schizophrenia (Gomez-Pilar et al., 2017).
- 3) Application of local regularity measures and graph measures for characterizing schizophrenia brain dynamics at local and network level, respectively. The underpinnings of network phase-based mechanisms were related to the regularity at local level (Gomez-Pilar et al., 2018b).
- 4) Application of functional and structural connectivity measures to the same schizophrenia population to assess the relationship between them. This is the first attempt to look for an association between graph measures derived from EEG and from dMRI in schizophrenia (Gomez-Pilar et al., 2018a). The conducted study provides a better characterization of the neural substrates in schizophrenia.
- 5) Definition, development and application of a new measure of network complexity based on the equilibrium between network order and amount of information stored by the system. SGC was used to estimate the ratio between graph entropy and graph disequilibrium in synthetic and real brain graphs

- derived from patients with schizophrenia (Gomez-Pilar et al., 2018c). It provided new insights to understand network dynamics in schizophrenia.
- 6) Proposal of a novel model of brain network dynamics during cognition. This new network model was assessed in healthy controls and patients with schizophrenia. Importantly, different subgroups of patients with schizophrenia were identified, reinforcing the idea of the schizophrenia heterogeneity (Gomez-Pilar et al., 2018d).
 - 7) Development of a Matlab toolbox to provide a framework for the analysis of different brain signals (EEG, MRI or others) from the graph theory perspective. The software has been registered – Intellectual Property Rights (IPR) for computer software protection – as ‘GABA’, Graph Analysis of Brain Activation.

6.2 Main conclusions

The analysis of the results as a whole leads us to the next main conclusions of this Doctoral Thesis:

- Single trial analyses, as well as the study of ERPs, provide valuable information about the contribution of different cortical areas to the coordinated brain activity. Despite the almost overcome skepticism, the usefulness of EEG recordings in understanding neural dynamics has been reinforced throughout this Thesis.
- The synchronized activity of large neural assemblies can be measured using phase-based connectivity measures. This coordinated response constitutes the main via of information exchange between brain areas. Abnormalities in this coordination imply disrupted network properties.
- Schizophrenia shows abnormalities both in functional and structural network properties. However, these abnormalities seem not to be as linked as one might suppose ‘a priori’. This could be explained due to the possible existence of schizophrenia subgroups, which hamper the relationship between structural and functional features of the brain.
- Local regularity of the brain activity plays an important role in the network characteristics. Therefore, alterations in specific regions, as it has been observed in schizophrenia, could affect to the whole network, producing a disconnection between brain areas and contributing to the abnormal capacity to integrate the neural information.

- Schizophrenia shows a hyper-segregated network prior to the stimulus, i.e., higher clustering coefficient during the pre-stimulus, which is linked to a decreased change of the functional connectivity during cognition. This altered state is likely related to the well-known aberrant assignment of relevant stimuli in schizophrenia (aberrant salience hypothesis).
- Network changes on dynamical brain activity during an auditory oddball task were related to cognitive and behavioral characteristics in schizophrenia. Particularly, higher changes in connectivity strength were related to higher cognitive performance. Network segregation and integration, as well as local entropy, were also related to cognitive characteristics.
- The use of five complementary network measures, in terms of information provided on the topology of the network, contributes to comprehensive characterize EEG functional connectivity. Our findings suggest that graph theory analysis is appropriate for summarizing the properties of long-range interactions and phase-based synchrony of the brain network.
- Subjects with the same disorder, schizophrenia, can reorganize their neural activity during a cognitive task following different strategies. Whereas a subgroup of patients reinforces secondary neural pathways during cognition in a similar way as controls, other subgroup suffers a reinforcement of its primary connections. This brings out the heterogeneity of this disorder and open new lines to further explore this finding.

6.3 Future research lines

Several questions derived from this research can be further studied in the future. These questions are out of the scope of the present Doctoral Thesis, but can complement its findings. Below, a number of suggestions for future research lines are listed:

- The possibility of the existence of different tangled subgroups named under the same concept ‘schizophrenia’ leads us to encourage further efforts to identify such clusters. Conducting new research aimed at sorting out likely schizophrenia subgroups could suppose a breakthrough in this field.
- A large database is always desirable to improve the statistical power. Following the previously mentioned future research line, this is of paramount importance in future studies in which clustering analyses would be the central core.

- Future work must be done to increment the number of electrodes of the EEG. High density EEG recordings with 64 or more electrodes would be desirable to enhance the spatial resolution.
- Volume conduction was listed as one of the limitations of this study. In order to overcome this issue, source analyses would be helpful for localizing the spatial source of electrical abnormalities. In this regard, increasing the number of electrodes would be also required to accurately determine the source of the electric fields acquired by the EEG.
- The assessment of the directionality in connectivity measures is another interesting future line of investigation, which is under development in newer Doctoral Theses of our group. These studies will provide casual inference to determine the information flow in the brain.
- Finally, most of the methodology here described can be applied to other signals, such as MEG or fMRI, and other pathologies. In this regard, patients with bipolar disorder are usually treated with similar drugs, which can serve to discard possible confounding factors due to medication. In three of the studies, first episode patients were used to control for treatment. Nevertheless, the use of a different disorder with similar medication will be even more useful. Currently, efforts in this sense are being made.

In summary, the analysis of the response during a cognitive task was used to gain further insights into the neural mechanisms underlying cognitive dysfunctions in schizophrenia. Graph theory analyses based on synchrony and connectivity among brain regions provide a sensitive framework to describe schizophrenia alterations. Our research supports previous findings, such as aberrant salience and disconnection hypotheses, whereas showed a deficit in the change from pre-stimulus to cognitive response brain activity. The brain dynamics assessed by Complex Network Theory highlight the heterogeneity of the schizophrenia disorder. This provides direct evidence of the possible existence of schizophrenia subgroups. However, further efforts must be addressed to clarify this question. Multivariate methods are likely to play a greater role in the future of the *connectome* and *chronnectome*.

Appendix A

Papers included in this Doctoral Thesis

Article

Neural Network Reorganization Analysis During an Auditory Oddball Task in Schizophrenia Using Wavelet Entropy

Javier Gomez-Pilar ^{1,*}, Jesús Poza ^{1,2,3}, Alejandro Bachiller ¹, Carlos Gómez ¹, Vicente Molina ^{3,4} and Roberto Hornero ^{1,2}

¹ Biomedical Engineering Group, Universidad de Valladolid, Paseo Belén 15, 47011 Valladolid, Spain; E-Mails: jesus.poza@tel.uva.es (J.P.); alejandro.bachiller@uva.es (A.B.); carlos.gomez@tel.uva.es (C.G.); roberto.hornero@tel.uva.es (R.H.)

² IMUVA, Instituto de Investigación en Matemáticas, Universidad de Valladolid, Plaza de la Universidad, 1a, 47002 Valladolid, Spain

³ INCYL, Instituto de Neurociencias de Castilla y León, Universidad de Salamanca, Patio de las Escuelas 1, 37008 Salamanca, Spain; E-Mail: vmolina@med.uva.es

⁴ Facultad de Medicina, Universidad de Valladolid, Avenida Ramón y Cajal 7, 47007 Valladolid, Spain

* Author to whom correspondence should be addressed; E-Mail: javier.gomez@gib.tel.uva.es; Tel.: +34-983-423000 (ext. 4713).

Academic Editor: Raúl Alcaraz Martínez

Received: 27 May 2015 / Accepted: 20 July 2015 / Published: 27 July 2015

Abstract: The aim of the present study was to characterize the neural network reorganization during a cognitive task in schizophrenia (SCH) by means of wavelet entropy (WE). Previous studies suggest that the cognitive impairment in patients with SCH could be related to the disrupted integrative functions of neural circuits. Nevertheless, further characterization of this effect is needed, especially in the time-frequency domain. This characterization is sensitive to fast neuronal dynamics and their synchronization that may be an important component of distributed neuronal interactions; especially in light of the disconnection hypothesis for SCH and its electrophysiological correlates. In this work, the irregularity dynamics elicited by an auditory oddball paradigm were analyzed through synchronized-averaging (SA) and single-trial (ST) analyses. They provide complementary information on the spatial patterns involved in the neural network reorganization. Our results from 20 healthy controls and 20 SCH patients showed a WE decrease from baseline to response both in controls and SCH subjects. These changes were significantly more

pronounced for healthy controls after ST analysis, mainly in central and frontopolar areas. On the other hand, SA analysis showed more widespread spatial differences than ST results. These findings suggest that the activation response is weakly phase-locked to stimulus onset in SCH and related to the default mode and salience networks. Furthermore, the less pronounced changes in WE from baseline to response for SCH patients suggest an impaired ability to reorganize neural dynamics during an oddball task.

Keywords: wavelet entropy; schizophrenia; neural reorganization; physiological signal processing; neuroscience

PACS Codes: 89.70.Cf; 87.19.L; 87.19.le; 87.85.Ng

1. Introduction

Schizophrenia (SCH) is a psychiatric disorder characterized by positive and negative symptoms, frequently accompanied by impaired cognitive processing [1]. An early SCH diagnosis is crucial, since the longer the period of untreated psychosis, the worse the outcome [2]. In this regard, SCH prevalence is estimated around 0.5%–1% [1], although this estimation could be overstated [3]. In addition, life expectancy is 11–20 years shorter in SCH patients compared to general population [4]. Therefore, SCH characterization is of paramount importance.

It has been proposed that cerebral substrates in SCH may be modified, at least in some cases, by a deficit in neural network reorganization during simple and complex tasks [5]. In this context, several studies addressed the characterization of neural disconnectivity abnormalities in SCH [6–11]. Most of these studies assessed brain differences by means of structural magnetic resonance imaging (MRI) [6,9], functional MRI [10] or diffusion tensor imaging [8,11]. It is noteworthy that neural mechanisms underlying cognitive dysfunctions in SCH are related to fast changes in the spatio-temporal patterns of neuronal modulation [12]. Thus, these techniques do not provide enough time resolution to study brain dynamics. On the other hand, electroencephalography (EEG) is a non-invasive technique, which provides high temporal resolution in the time range of milliseconds. Therefore, EEG can be then used to study fast interactions (e.g., changes from baseline to response windows). In this regard, event-related potentials (ERPs) have been used to assess cognitive processing in SCH. A P300 amplitude reduction [13] and an increase of P300 latency [14] have been usually reported in SCH. In addition, several studies showed the robust finding that mismatch negativity (MMN) response is diminished in patients with SCH [15,16]. MMN is an important paradigm for SCH research, because it could be linked to altered dopaminergic neurotransmission [17]. Nevertheless, it is necessary a deep study of the spectral and spatial brain dynamics to further understand the neural substrates underlying this pathology [12,18–21].

Different entropy measures have been used to describe the alterations in neural modulation associated with SCH. Takahashi *et al.* [22] computed the multiscale entropy. They identified abnormal EEG signal complexity patterns in anterior brain areas, which were related to disturbed cortical dynamics in SCH. Taghavi *et al.* [23] analyzed the EEG activity from SCH patients and healthy

subjects using approximate entropy. In a recent study, Shannon's entropy was used to classify controls and SCH patients from functional MRI [24]. The results did not show significant differences between both groups. However, they only studied resting state conditions, but no dynamical changes during a cognitive task. ERPs neural dynamics in SCH were analyzed by Bachiller *et al.* [25,26] by means of spectral entropy. In those studies, a widespread increase of signal regularity was obtained for SCH subjects [25,26].

It is noteworthy that most of the previous studies used an entropy definition based on short-time Fourier transform (STFT). Nevertheless, other time-frequency representations can be also considered. In this regard, continuous wavelet transform (CWT) has demonstrated to be a useful tool to perform the spectral characterization of ERPs [27]. CWT provides a good time resolution for high frequencies, as well as good frequency resolution for short time windows [28]. In addition, CWT is suitable for non-stationary time series, like biological signals [29]. In this study, wavelet entropy (WE) was calculated from CWT. WE is a particularization of Shannon's entropy [30]. Hence, WE is useful to assess the dynamic irregularity patterns of electrophysiological signals, providing a measure of transient features for non-stationary ERP data [31].

The aim of the study was to characterize the neural network reorganization as a response to a cognitive task in SCH by means of WE. For this purpose, we analyzed the spectral changes elicited by an auditory oddball paradigm. Specifically, we assessed the dynamic irregularity patterns through synchronized-averaging (SA) and single-trial (ST) analyses. Few studies addressed the characterization of neural dynamics considering these two approaches jointly [32]. Furthermore, to the best of our knowledge, irregularity patterns using these two approaches have never been studied in SCH.

2. Materials

2.1. Subjects

Twenty chronic SCH patients and 20 healthy controls with normal hearing participated in the study. SCH patients were diagnosed according to the Diagnostic and Statistical Manual of Mental Disorders, 5th edition [1] (DSM-V) criteria. The clinical status of the patients was scored using the Positive and Negative Syndrome Scale (PANSS) [33]. On the other hand, healthy controls (age- and gender-matched) were recruited through newspaper advertisements and remunerated for their cooperation. To discard major psychiatric antecedents (personal or family background) and current symptoms or treatments in the control group, semi-structured psychiatric interviews were performed prior to the study. The exclusion criteria can be summarized as follows: (i) neurologic illness or major head trauma that would result in abnormal EEG; (ii) electroconvulsive therapy; (iii) past or present alcohol or drug abuse, except for nicotine; (iv) for the patients, presence of any other current psychiatric process; and (v) for the controls, any current or past psychiatric diagnosis, or current treatment with drugs known to act on the central nervous system. Socio-demographic and clinical data for both groups are presented in Table 1.

It is noteworthy that all participants gave their informed consent prior to their participation in the study. Moreover, the study protocol was approved by the local Ethics Committee of University

Hospitals from Valladolid and Salamanca (Spain) according to the code of ethics of the World Medical Association (Declaration of Helsinki).

Table 1. Socio-demographic and clinical characteristics. Values are shown as mean \pm standard deviation (SD). NA represents “not applicable”.

Characteristic	SCH Patients	Controls
Age (years)*	35.45 \pm 12.07	33.35 \pm 12.26
Gender (Male:Female)	14:6	14:6
PANSS-Positive	18.87 \pm 4.39	NA
PANSS-Negative	20.93 \pm 5.76	NA
PANSS-Total	74.47 \pm 17.70	NA

* Non-significant differences were found in age (Mann–Whitney *U*-test, $p > 0.05$).

2.2. Recording and Preprocessing of ERP Signals

Data acquisition was carried out using an EEG system (BrainVision, Brain Products GmbH; Munich, Germany). Electrode placement followed the 10/20 system, with 17 electrodes at Fp1, Fp2, F3, F4, F7, F8, C3, C4, P3, P4, O1, O2, T5, T6, Fz, Pz and Cz. Impedances were kept below 5 k Ω during ERP acquisition. ERP recordings were performed while the participants were sat, relaxed and with their eyes closed. The auditory oddball task consisted in random series of 600 tones whose duration was 50 ms, intensity being 90 dB and inter-stimulus interval between tones randomly jittered between 1.16 and 1.44 s. Three different tones were presented: target (500 Hz tone), distractor (1000 Hz tone) and standard (2000 Hz tone) with probabilities of 0.20, 0.20 and 0.60, respectively.

ERP signals and stimulus markers were continuously recorded at a sampling frequency of 250 Hz, during 13 min of auditory oddball task. Data were re-referenced over Cz electrode to the average activity of all active sensors in order to minimize the effect of microsaccadic artifacts [34,35]. Then, signals were filtered using a band-pass finite impulse response filter with a Hamming window between 1 and 70 Hz. In addition, a 50 Hz notch filter was used in order to remove the power line artifact. Finally, a three-steps artifact rejection algorithm was applied to minimize oculographic and myographic artifacts [29]: (i) components related to eyeblinks, according to a visual inspection of the scalp maps and their temporal activations from independent component analysis (ICA), were discarded; (ii) segmentation into 1 s-length trials ranging from -300 ms before stimulus onset to 700 ms after stimulus onset; and (iii) automatic and adaptative trial rejection using a statistical-based thresholding method. Only target tones were considered for further analysis. The average number of selected trials for target condition was 80.85 ± 20.62 for SCH patients and 88.75 ± 10.12 for healthy controls (mean \pm SD).

3. Methods

ERPs can be analyzed using two different approaches: SA analysis and ST analysis [36,37]. SA analysis is based on the averaging of all trials. It provides a measure of the evoked response, which is phase-locked to the stimulus onset. On the other hand, ST analysis is useful to jointly analyze the evoked and the induced response, which is non-phase-locked to the stimulus onset. This different

behavior is related to the phase-resetting hypothesis, which implies an interaction between stimulus-related response and ongoing activity [38]. In summary, SA suppresses induced responses that are not time locked to the stimulus, while ST analyses retain both evoked and induced responses. These two methodologies can be helpful to further understand the neural network reorganization in SCH during an oddball task [36].

In SA analysis, the target trials were firstly averaged over time to obtain the evoked response. Then, WE was computed. In ST analysis, WE was calculated for each artifact-free trial. Then, WE was averaged across trials. A descriptive diagram of data acquisition and processing steps is shown in Figure 1, both for SA (left panel) and ST (right panel) analyses. It is noteworthy that both SA and ST analyses are based on similar processing steps, like time-frequency estimation, WE computation and statistical analysis. These methods are described in the following sections.

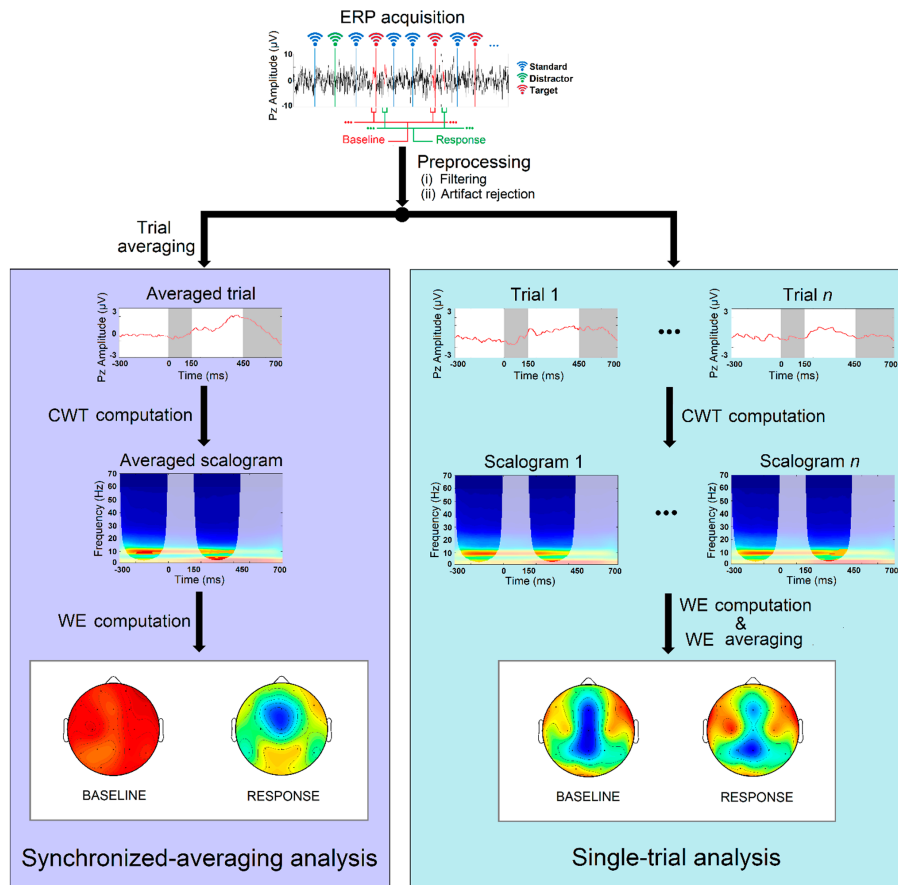


Figure 1. Descriptive diagram corresponding to SA and ST analyses.

3.1. Continuous Wavelet Transform

ERP recordings are non-stationary signals, whose properties may change over time [39]. Hence, methods that require stationary time series, like Fourier transform, are not suitable to analyze their time-varying properties. CWT provides an alternative way to describe the dynamic properties of ERPs. Wavelet analysis relies on the introduction of an appropriate basis of functions. A wavelet is a zero mean function characterized by its localization in time (Δt) and frequency (Δf) [40]. In this study, the complex Morlet wavelet was chosen as “mother wavelet”, since it provides a biologically plausible fit to ERP data [36]. Complex Morlet wavelet is defined as follows [28]:

$$\varphi(t) = \frac{1}{\sqrt{\pi \cdot \Omega_b}} \cdot \exp(j2\pi\Omega_c t) \cdot \exp\left(\frac{-t^2}{\Omega_b}\right), \quad (1)$$

where Ω_b is the bandwidth parameter and Ω_c represents the wavelet center frequency. In this study, both were set to 1, in order to obtain a balanced relationship between Δt and Δf at low frequencies [29].

A wavelet family is a set of elementary functions generated by dilations and translations of the mother wavelet [41]. Thus, the CWT of each trial is defined as the convolution of the trial, $x(t)$, with a scaled and translated version of the complex Morlet wavelet:

$$\text{CWT}(k, s) = \frac{1}{\sqrt{s}} \cdot \int_{-\infty}^{+\infty} x(t) \cdot \varphi^*\left(\frac{t-k}{s}\right) dt, \quad (2)$$

where s represents the dilation factor ($s = \{s_i, i = 1, \dots, M\}$), k is the translation factor and * denotes the complex conjugation. The dilation factor was set to include frequencies from 1 Hz (s_1) to 70 Hz (s_M) in equally-spaced intervals of 0.5 Hz [29].

The wavelet energy is a simple way to represent the magnitude of EEG oscillations at specific scales [41]. The wavelet scalogram (WS) summarizes the distribution of the signal energy in the time-frequency plane. It is obtained as the squared modulus of the wavelet coefficients [28]. In this study, WS was normalized (WS_n) to range from 0 to 1. Thus, it can be interpreted as a probability density function:

$$WS_n(k, s) = \frac{|\text{CWT}(k, s)|^2}{\sum_s |\text{CWT}(k, s)|^2}. \quad (3)$$

Once the WS_n was obtained for each target 1 s-length trial, two windows of interest were considered: (i) the baseline window, [-300, 0] ms before the stimulus onset; and (ii) the response window, [150, 450] ms after stimulus onset [29].

On the contrary to the analyses based on Fourier transform, CWT has a variable time-frequency resolution [28]. Shorter time windows are related to higher frequencies, while longer time windows are associated with lower frequencies [28,42]. It is important to note that ERP signals are finite and short-time recordings. Therefore, edge effects are not negligible [40]. A cone of influence (COI) was defined in order to avoid edge effects [40]. In the present research, two windows were defined: baseline and response (see Figure 1). Thus, the spectral content must be only considered into the time-frequency regions delimited by their respective COIs. Specifically, spectral content between 4 Hz and

70 Hz was considered for further analysis. Thereby, delta band, between 1 and 4 Hz, was not analyzed, since it is associated with a wavelet duration of hundreds of milliseconds [29].

3.2. Wavelet Entropy

Shannon's entropy was defined in 1958 [30]. Similarly, WE provides an estimation of the signal's irregularity. The time-dependent WE can be defined as follows [41]:

$$WE(k) = -\frac{1}{\log(M)} \cdot \sum_s WS_n(k,s) \cdot \log[WS_n(k,s)], \quad (4)$$

In the present study, $WE(k)$ was computed for all subjects from -300 ms to 700 ms from stimulus onset. Then, $WE(k)$ was averaged in the time domain to obtain a single WE value on each window: baseline (*i.e.*, from -300 ms to the stimulus onset) and response (*i.e.*, from 150 ms to 450 ms post-stimulus). The following equation summarizes the averaging of WE for each window of interest:

$$WE_w = \frac{1}{K} \cdot \sum_{k \in w} WE(k), \quad w = \{b, r\} \quad (5)$$

where K represents the number of samples in the analyzed window and w denotes the corresponding window: baseline (b) or response (r). It is important to note that WE computation for SA analysis (WE^{SA}) was directly obtained, because the synchronized trial averaging was previously carried out. However, in the case of WE for ST analysis (WE^{ST}), WE values were averaged across trials (see Figure 1).

Thus, if a signal has few spectral components, there will be few non-zero energy components in the spectrogram. As a consequence, WE will be close to zero. On the other hand, a signal with several spectral components, like white noise, will have the energy distributed over the whole time-frequency plane. Thus, WS_n will be similar for all resolution levels and the WE will yield a maximum value of 1.

3.3. Statistical Analysis

A descriptive analysis was initially performed to explore data distribution (normality and homoscedasticity). Variables did not meet the parametric assumptions. Hence, nonparametric tests were used to analyze the results. Wilcoxon signed-rank test was used to compare baseline and response values for within-group analyses. Mann–Whitney U -test was used for between-group analyses. Finally, in order to deal with the multiple-comparison problem, p -values obtained from both tests were corrected with the false discovery rate (FDR) method [43].

4. Results

4.1. Single-Trial ERP Analysis

Initially, WE_b^{ST} and WE_r^{ST} were averaged over all sensors and trials to obtain a single value per subject. Figure 2 summarizes the global results of WE^{ST} . Pairwise comparisons indicated that controls exhibited a statistically significant decrease of WE_r^{ST} compared to WE_b^{ST} ($p = 7.21 \times 10^{-3}$, Wilcoxon signed-rank test). Non-significant differences were found between baseline and response windows in

SCH patients ($p > 0.05$, Wilcoxon signed-rank test). In addition, non-significant differences were found in WE_b^{ST} and WE_r^{ST} between both groups ($p > 0.05$, Mann–Whitney U -test).

Spatial analyses of the same (un-pooled) data are summarized in Figure 3. It depicts the WE_b^{ST} and WE_r^{ST} spatial distributions for both groups. Statistical analyses showed a widespread decrease of WE^{ST} for controls from baseline to active response. Although this decrease can also be observed in SCH patients, it was less evident. Non-significant differences were found either in the baseline or in the response window between both groups. Nevertheless, between-group analysis showed a more pronounced WE^{ST} decrease for controls than for SCH patients. Controls showed a widespread decrease of WE^{ST} , while SCH patients only exhibit a slight and non-significant decrease. The most significant differences between both groups were found in central regions (Mann–Whitney U -test).

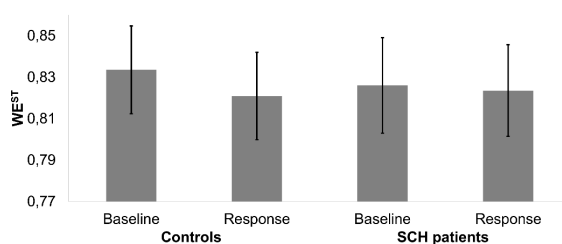


Figure 2. Mean and standard errors corresponding to the grand-average WE^{ST} across subjects for each group (controls and SCH patients) in the baseline and the response windows.

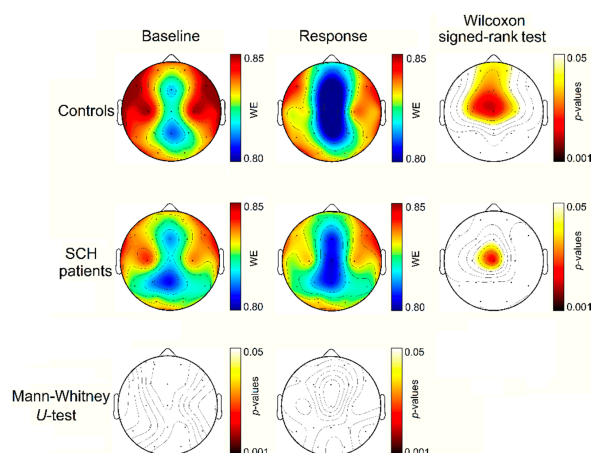


Figure 3. Sensor-level topographic maps of the statistics computed for WE^{ST} between controls and SCH patients. Right column shows within-group differences from baseline to response windows (Wilcoxon signed-rank test), whereas bottom row shows between-group differences for each window (Mann–Whitney U -test). The corrected p -values are obtained controlling FDR.

4.2. Synchronized-Averaging ERP Analysis

In a first step, WE_b^{SA} and WE_r^{SA} were averaged over all sensors to obtain a single value per subject. Figure 4 depicts the boxplots corresponding to the grand-averaged WE^{SA} values for each group. In the case of the controls, WE_r^{SA} was significantly lower than WE_b^{SA} ($p = 8.86 \times 10^{-8}$, Wilcoxon signed-rank test). Significant differences were also found between baseline and response windows in SCH patients ($p = 1.40 \times 10^{-4}$, Wilcoxon signed-rank test). Between-group comparisons showed non-significant differences in WE_b^{SA} ($p > 0.05$, Mann–Whitney U -test). Nevertheless, comparisons for WE_r^{SA} values between both groups showed significant differences ($p = 8.32 \times 10^{-3}$, Mann–Whitney U -test).

Spatial patterns of un-pooled WE^{SA} are summarized in Figure 5. WE_b^{SA} and WE_r^{SA} are depicted for both groups. Within-group analyses showed a widespread decrease of WE^{SA} for controls from baseline to active response. This reduction affects to more regions than in ST analysis. Changes in WE^{SA} were significant in all channels (Wilcoxon signed-rank test). This WE^{SA} decrease can also be observed in SCH patients, but it was less widespread again. Regarding between-group analysis, non-significant differences were found in the baseline window, but these differences were significant in the response window, mainly in central and frontal electrodes (Mann–Whitney U -test). Decrease in WE^{SA} values is more evident for controls group than for SCH patients. However, SCH patients also exhibit a widespread decrease of WE^{SA} , though this reduction is less significant, especially in left parieto-occipital regions.

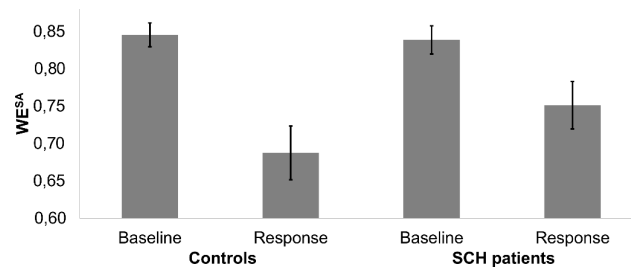


Figure 4. Mean and standard errors corresponding to the grand-average WE^{SA} across subjects for each group (controls and SCH patients) in the baseline and the response windows.

5. Discussion

In this study, we analyzed neural dynamics in SCH during an auditory oddball task by means of WE. We found that SCH patients showed lower changes in their irregularity patterns during the active response compared to controls for the two analyzed approaches: ST and SA. This abnormal spectral modulation suggests that a neural network reorganization deficit can be associated to SCH [44]. ST and SA analyses provided complementary information on the spatial patterns of neural network reorganization. SA approach captures stimulus-evoked processes whose oscillations were phase-synchronized from experimental events [36]. Neurophysiological evidences have linked evoked power to sensory registration procedures, as well as “top-down” cognitive processing during the active perception [36,37].

On the other hand, ST approach obtains event-related changes in ERP activity that are time-locked, but not phase-locked to the stimulus onset. Brain's information processing is characterized by oscillations at various frequencies reflecting multiple neural processes at the same time [36]. Therefore, ST analysis may provide a measure of integrative and dynamically adaptive information processing [36,37].

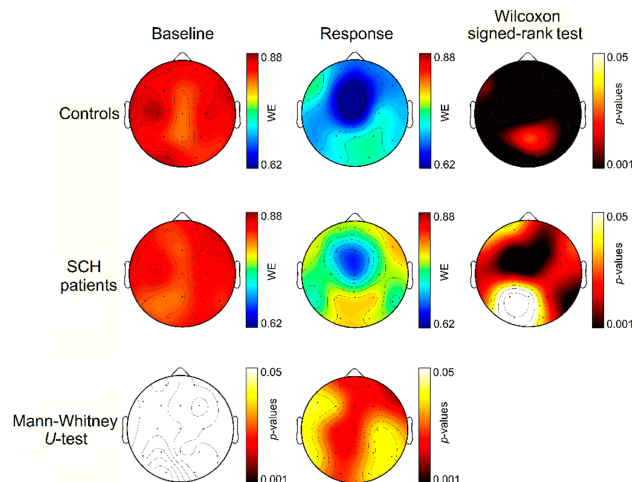


Figure 5. Sensor-level topographic maps of the statistics computed for WE^{SA} between controls and patients. Right column shows within-group differences from baseline to response windows (Wilcoxon signed-rank test), whereas bottom row shows between-group differences for each window (Mann–Whitney U -test). The corrected p -values are obtained controlling FDR.

ST results showed a significant WE decrease from baseline to response window in controls (central and frontopolar areas) and SCH patients (only in central areas). Between-group analyses did not show statistically significant differences during the baseline and the response windows. These findings are consistent with previous studies, which found similar spatial patterns using spectral entropy [25,26] or analyzing the power in different frequency bands [45].

Regarding SA results, WE exhibits a similar behavior to ST analysis: (i) widespread decrease from baseline to response window for both groups; (ii) more pronounced modulation for controls compared to SCH patients; and (iii) non-significant between-group differences in the baseline window. However, SA analysis showed that several brain regions were involved in the neural network reorganization: central, frontal and temporal areas. This result can be due to the fact that only evoked response is considered in SA analysis. If the induced response was similar in baseline and response windows, it could contribute to reduce within-group differences in ST analysis. The oscillatory activity, which was observed in SA analysis, is related to the long-range cortical oscillatory events [46]. On the contrary, the smaller change in irregularity that we observed in ST analysis should correspond to a strong phase-locked variation, partially canceled out by some components non-phase-locked. Likewise, ST

analysis is a useful tool to study phase/synchrony of ERPs [36]; nevertheless, WE is related to the power spectrum distribution. In this regard, phase synchronization was suggested as a key mechanism of dynamical neuronal communication, and can provide a useful measure of neural integration in sensory task-relevant procedures [47]. These findings are consistent with another study that showed greater differences between controls and SCH patients in the assessment of the evoked response than in the evaluation of the total response (induced and evoked) in delta band [32]. Therefore, the significant reduction of the irregularity in the evoked response for controls and the less evident difference in the evoked response for SCH patients reveals that activation response is weakly phase-locked to stimulus in schizophrenia.

It is important to understand the reasons of WE reduction from baseline to active response in ST and SA analyses. Previous studies found a reduction of the P300 amplitude in SCH patients, which was related to a decrease of relative power in alpha frequency band [42,48]. An increase of power in theta band during the P300 window has also been reported [49]. It was associated to the transitory coordination of EEG activity among distant regions [50]. In addition, high frequency bands are more influenced by the induced response than low frequency bands [51]. Thus, following these previous studies, it can be inferred that evoked response produced an increase in the concentration of low-frequency power (mainly around theta band [49]) at the expense of alpha and higher frequencies during the response window [42,48,51]. This result causes a reduction of the WS uniformity, mainly related to a decrease in power in the alpha band [48]. Although, the present study did not focus on spectral changes in specific frequency bands, these previous findings could provide a reasonable explanation for the decrease in WE that we observed. Low frequencies, like alpha band, are related to long-range interactions [20], suggesting that impaired activation response of long-range interactions might contribute to the pathological process. The lower irregularity reduction in the cognitive response of SCH patients seems to be associated with an abnormal information processing, as well as it could be related to the disrupted integrative functions of local and distributed neural circuits [32]. This result suggests that SCH is accompanied by a disrupted network reorganization of neural functions responsible of the P300 generation, mainly in long-range interaction.

Previous studies reported interesting findings regarding tone comparisons in SCH [25,52]. Their conclusions support the notion that bioelectrical responses to both distractor and target tones during an oddball task were attenuated in SCH patients compared to controls. In the present study, similar findings were found using WE. Thus, widespread significant differences were only found in the study of the target tone when comparing between-groups responses. In addition, higher differences between target and standard tones were obtained for controls than for SCH patients when target and standard tones were compared during the response window. Other studies reported similar results [25,36,52]. The standard tone is more likely to occur than the target tone, but lacks the novelty and relevance that characterize the target. Therefore, while the standard tone is similarly processed by SCH patients and controls, the target tone produces a diminished response in SCH patients compared to controls [25]. These outcomes are in line with the disconnection hypothesis in SCH. This hypothesis poses the idea that the SCH pathology is expressed at the modulation level of the associative plasticity for memory, which is more related to target than to non-target tones [5].

The default mode network (DMN) is an important brain network, which is active at rest, but de-activates during the performance of most cognitive tasks [53]. The middle-line of the brain includes

the main cerebral areas associated with DMN [54]. A larger activity in this network is consistent with the spatial patterns at baseline window in both SA and ST approaches (Figures 3 and 5). During the performance of a cognitive task, salience network is active. Some studies suggest that aberrant activity related to salience network can play a cardinal role in psychosis [55]. This network mainly includes insula and anterior cingulate cortex [55,56]. Figures 3 and 5 show that the main differences in a cognitive response appear in these regions. However, this modulation process is more evident in the control group, suggesting that SCH patients show an impaired ability for reconfiguring functional brain networks during a cognitive task. It is noteworthy that our analyses are based on low-density EEG recordings. High-density EEG would be desirable to infer accurate spatial conclusions on neural networks, like DMN or salience networks.

Some limitations of the study merit special attention. It could be appropriate to increase the sample size, including patients with other pathologies different than SCH, like bipolar disorder. The study of the delta band could be interesting to complement the reported results. For that purpose, it would be necessary to change the acquisition protocol in order to increase the window length. Nevertheless, some studies reported the difficulty of including delta band, since the response window must contain a minimum number of oscillation periods to obtain an accurate spectral estimation [47,57,58]. Likewise, other entropy measures, like multiscale entropy, could provide further information on the neural dynamics associated with SCH. Other features related to connectivity or cross-frequency coupling could complement the information obtained from WE. In this regard, ST analysis would merit special attention, since a deeper study of the phase and synchrony of the signals would be required.

6. Conclusions

ST and SA analyses provided complementary information on dynamic patterns of irregularity during a cognitive task. The less pronounced difference in the cognitive response in ST analysis suggests that the active response is weakly phase-locked to stimulus in SCH, mainly in long-range interactions. It is noteworthy that both evoked and induced responses involve the coordinated activity of different brain regions, including dynamic neural networks associated with resting (DMN) and cognitive performance (salience network). In addition, WE proved to be an appropriate measure to characterize ERP dynamics. Hence, WE between-group differences evidenced that irregularity patterns observed in ERP can be associated with an abnormal network reorganization in SCH during an auditory oddball task.

Acknowledgments

This study was supported by “Ministerio de Economía y Competitividad” and FEDER (TEC2014-53196-R), “Consejería de Educación de la Junta de Castilla y León” (VA059U13), “Fondo de Investigaciones Sanitarias del Instituto de Salud Carlos III” (FIS PI1102303) and “Gerencia Regional de Salud de Castilla y León” (GRS 613/A/11; GRS 932/A/14). Finally, J. Gomez-Pilar and A. Bachiller were in receipt of a PIF-UVA grant from University of Valladolid.

Author Contributions

Javier Gomez-Pilar designed the study, analyzed the data, interpreted the results and drafted the manuscript. Alejandro Bachiller took part in the collection of data and analyzed the results. Jesús Poza, Carlos Gómez and Roberto Hornero designed the study and interpreted the results. Vicente Molina took part in the diagnosis of the subjects, the collection of data and the interpretation of the results. All authors have read and approved the final manuscript.

Conflicts of Interest

The authors declare no conflict of interest.

References

1. American Psychiatric Association. *Diagnostic and Statistical Manual of Mental Disorders*, 5th ed.; DSM-5; American Psychiatric Publishing: Arlington, VA, USA, 2013; p. 991.
2. Marshall, M.; Lewis, S.; Lockwood, A.; Drake, R.; Jones, P.; Croudace, T. Association between duration of untreated psychosis and outcome in cohorts of first-episode patients: A systematic review. *Arch. Gen. Psychiatry* **2005**, *62*, 975–983.
3. Saha, S.; Chant, D.; Welham, J.; McGrath, J. A systematic review of the prevalence of schizophrenia. *PLoS Med.* **2005**, *2*, 0413–0433.
4. Laursen, T.M.; Nordentoft, M.; Mortensen, P.B. Excess early mortality in schizophrenia. *Annu. Rev. Clin. Psychol.* **2014**, *10*, 425–448.
5. Friston, K.J. The disconnection hypothesis. *Schizophr. Res.* **1998**, *30*, 115–125.
6. Bogerts, B.; Ashtari, M.; Degreef, G.; Alvir, J.; Bilder, R.M.; Lieberman, J.A. Reduced temporal limbic structure volumes on magnetic resonance images in first episode schizophrenia. *Psychiatry Res. Neuroimaging* **1990**, *35*, 1–13.
7. Uhlhaas, P.J.; Singer, W. Neural Synchrony in Brain Disorders: Relevance for Cognitive Dysfunctions and Pathophysiology. *Neuron* **2006**, *52*, 155–168.
8. Van den Heuvel, M.P.; Mandl, R.C.W.; Stam, C.J.; Kahn, R.S.; Hulshoff Pol, H.E. Aberrant frontal and temporal complex network structure in schizophrenia: a graph theoretical analysis. *J. Neurosci.* **2010**, *30*, 15915–15926.
9. Molina, V.; Hernández, J.A.; Sanz, J.; Paniagua, J.C.; Hernández, A.I.; Martín, C.; Matías, J.; Calama, J.; Bote, B. Subcortical and cortical gray matter differences between Kraepelinian and non-Kraepelinian schizophrenia patients identified using voxel-based morphometry. *Psychiatry Res. Neuroimaging* **2010**, *184*, 16–22.
10. Gur, R.E.; Gur, R.C. Functional magnetic resonance imaging in schizophrenia. *Dialogues Clin. Neurosci.* **2010**, *12*, 333–343.
11. Kubicki, M.; McCarley, R.; Westin, C.-F.; Park, H.-J.; Maier, S.; Kikinis, R.; Jolesz, F.A.; Shenton, M.E. A review of diffusion tensor imaging studies in schizophrenia. *J. Psychiatr. Res.* **2007**, *41*, 15–30.
12. Uhlhaas, P.J.; Singer, W. Abnormal neural oscillations and synchrony in schizophrenia. *Nat. Rev. Neurosci.* **2010**, *11*, 100–113.

13. Mathalon, D.H.; Ford, J.M.; Pfefferbaum, A. Trait and state aspects of P300 amplitude reduction in schizophrenia: A retrospective longitudinal study. *Biol. Psychiatry* **2000**, *47*, 434–449.
14. O'Donnell, B.F.; Faux, S.F.; McCarley, R.W.; Kimble, M.O.; Salisbury, D.F.; Nestor, P.G.; Kikinis, R.; Jolesz, F.A.; Shenton, M.E. Increased rate of P300 latency prolongation with age in schizophrenia. Electrophysiological evidence for a neurodegenerative process. *Arch. Gen. Psychiatry* **1995**, *52*, 544–549.
15. Baldeweg, T.; Klugman, A.; Gruzelier, J.H.; Hirsch, S.R. Impairment in frontal but not temporal components of mismatch negativity in schizophrenia. *Int. J. Psychophysiol.* **2002**, *43*, 111–122.
16. Kircher, T.T.J.; Rapp, A.; Grodd, W.; Buchkremer, G.; Weiskopf, N.; Lutzenberger, W.; Ackermann, H.; Mathiak, K. Mismatch Negativity Responses in Schizophrenia: A Combined fMRI and Whole-Head MEG Study. *Am. J. Psychiatry* **2004**, *161*, 294–304.
17. Friston, K. Disconnection and cognitive dysmetria in schizophrenia. *Am. J. Psychiatry* **2005**, *162*, 429–432.
18. Uhlhaas, P.J.; Haenschel, C.; Nikolić, D.; Singer, W. The role of oscillations and synchrony in cortical networks and their putative relevance for the pathophysiology of schizophrenia. *Schizophr. Bull.* **2008**, *34*, 927–943.
19. Mazaheri, A.; Picton, T.W. EEG spectral dynamics during discrimination of auditory and visual targets. *Cogn. Brain Res.* **2005**, *24*, 81–96.
20. Uhlhaas, P.J.; Roux, F.; Rodriguez, E.; Rotarska-Jagiela, A.; Singer, W. Neural synchrony and the development of cortical networks. *Trends Cogn. Sci.* **2010**, *14*, 72–80.
21. Uhlhaas, P.J. Dysconnectivity, large-scale networks and neuronal dynamics in schizophrenia. *Curr. Opin. Neurobiol.* **2013**, *23*, 283–290.
22. Takahashi, T.; Cho, R.Y.; Mizuno, T.; Kikuchi, M.; Murata, T.; Takahashi, K.; Wada, Y. Antipsychotics reverse abnormal EEG complexity in drug-naïve schizophrenia: A multiscale entropy analysis. *Neuroimage* **2010**, *51*, 173–182.
23. Taghavi, M.; Boostani, R.; Sabeti, M.; Taghavi, S.M.A. Usefulness of approximate entropy in the diagnosis of schizophrenia. *Iran. J. Psychiatry Behav. Sci.* **2011**, *5*, 62–70.
24. Bassett, D.S.; Nelson, B.G.; Mueller, B.A.; Camchong, J.; Lim, K.O. Altered resting state complexity in schizophrenia. *Neuroimage* **2012**, *59*, 2196–2207.
25. Bachiller, A.; Lubeiro, A.; Díez, A.; Suazo, V.; Domínguez, C.; Blanco, J.A.; Ayuso, M.; Hornero, R.; Poza, J.; Molina, V. Decreased entropy modulation of EEG response to novelty and relevance in schizophrenia during a P300 task. *Eur. Arch. Psychiatry Clin. Neurosci.* **2014**, doi:10.1007/s00406-014-0525-5.
26. Bachiller, A.; Díez, A.; Suazo, V.; Domínguez, C.; Ayuso, M.; Hornero, R.; Poza, J.; Molina, V. Decreased spectral entropy modulation in patients with schizophrenia during a P300 task. *Eur. Arch. Psychiatry Clin. Neurosci.* **2014**, *264*, 533–543.
27. Le Van Quyen, M.; Foucher, J.; Lachaux, J.; Rodriguez, E.; Lutz, A.; Martinerie, J.; Varela, F.J. Comparison of Hilbert transform and wavelet methods for the analysis of neuronal synchrony. *J. Neurosci. Methods* **2001**, *111*, 83–98.
28. Mallat, S. *A Wavelet Tour of Signal Processing*; Academic Press: Waltham, MA, USA, 1999; pp. 20–41.

29. Bachiller, A.; Poza, J.; Gómez, C.; Molina, V.; Suazo, V.; Hornero, R. A comparative study of event-related coupling patterns during an auditory oddball task in schizophrenia. *J. Neural Eng.* **2015**, *12*, 016007.
30. Shannon, C.E. A mathematical theory of communication. *Bell Syst. Tech. J.* **1948**, *27*, 379–423.
31. Quiroga, R.Q.; Rosso, O.A.; Başar, E.; Schürmann, M. Wavelet entropy in event-related potentials: A new method shows ordering of EEG oscillations. *Biol. Cybern.* **2001**, *84*, 291–299.
32. Ergen, M.; Marbach, S.; Brand, A.; Başar-Eroğlu, C.; Demiralp, T. P3 and delta band responses in visual oddball paradigm in schizophrenia. *Neurosci. Lett.* **2008**, *440*, 304–308.
33. Kay, S.R.; Opler, L.A.; Lindenmayer, J.P. The Positive and Negative Syndrome Scale (PANSS): Rationale and standardisation. *Br. J. Psychiatry* **1989**, *155*, 59–65.
34. Bledowski, C.; Prvulovic, D.; Hoechstetter, K.; Scherg, M.; Wibrall, M.; Goebel, R.; Linden, D.E. Localizing P300 generators in visual target and distractor processing: A combined event-related potential and functional magnetic resonance imaging study. *J. Neurosci.* **2004**, *24*, 9353–9360.
35. Keren, A.S.; Yuval-Greenberg, S.; Deouell, L.Y. Saccadic spike potentials in gamma-band EEG: Characterization, detection and suppression. *Neuroimage* **2010**, *49*, 2248–2263.
36. Roach, B.J.; Mathalon, D.H. Event-related EEG time-frequency analysis: An overview of measures and an analysis of early gamma band phase locking in schizophrenia. *Schizophr. Bull.* **2008**, *34*, 907–926.
37. Makeig, S.; Debener, S.; Onton, J.; Delorme, A. Mining event-related brain dynamics. *Trends Cogn. Sci.* **2004**, *8*, 204–210.
38. David, O.; Harrison, L.; Friston, K.J. Modelling event-related responses in the brain. *Neuroimage* **2005**, *25*, 756–770.
39. Blanco, S.; Garcia, H.; Quiroga, R.Q.; Romanelli, L.; Rosso, O.A. Stationarity of the EEG series. *IEEE Eng. Med. Biol. Mag.* **1995**, *14*, 395–399.
40. Torrence, C.; Compo, G. A practical guide to wavelet analysis. *Bull. Am. Meteorol. Soc.* **1998**, *79*, 61–78.
41. Rosso, O.A.; Blanco, S.; Yordanova, J.; Kolev, V.; Figliola, A.; Schürmann, M.; Başar, E. Wavelet entropy: A new tool for analysis of short duration brain electrical signals. *J. Neurosci. Methods* **2001**, *105*, 65–75.
42. Ford, J.M.; Roach, B.J.; Faustman, W.O.; Mathalon, D.H. Synch before you speak: Auditory hallucinations in schizophrenia. *Am. J. Psychiatry* **2007**, *164*, 458–466.
43. Lage-Castellanos, A.; Martínez-Montes, E.; Hernández-Cabrera, J.A.; Galán, L. False discovery rate and permutation test: An evaluation in ERP data analysis. *Stat. Med.* **2010**, *29*, 63–74.
44. Kapur, S. Psychosis as a state of aberrant salience: A framework linking biology, phenomenology, and pharmacology in schizophrenia. *Am. J. Psychiatry* **2003**, *160*, 13–23.
45. Ferrarelli, F.; Massimini, M.; Peterson, M.J.; Riedner, B.A.; Lazar, M.; Murphy, M.J.; Huber, R.; Rosanova, M.; Alexander, A.L.; Kalin, N.; Tononi, G. Reduced Evoked Gamma Oscillations in the Frontal Cortex in Schizophrenia Patients a TMS EEG Study. *Am. J. Psychiatry* **2008**, *165*, 996–1005.
46. Tallon-Baudry, C.; Bertrand, O.; Delpuech, C.; Pernier, J. Stimulus specificity of phase-locked and non-phase-locked 40 Hz visual responses in human. *J. Neurosci.* **1996**, *16*, 4240–4249.

47. Stefanics, G.; Hangya, B.; Hernádi, I.; Winkler, I.; Lakatos, P.; Ulbert, I. Phase entrainment of human delta oscillations can mediate the effects of expectation on reaction speed. *J. Neurosci.* **2010**, *30*, 13578–13585.
48. Bramon, E.; Rabe-Hesketh, S.; Sham, P.; Murray, R.M.; Frangou, S. Meta-analysis of the P300 and P50 waveforms in schizophrenia. *Schizophr. Res.* **2004**, *70*, 315–329.
49. Polich, J. Updating P300: An integrative theory of P3a and P3b. *Clin. Neurophysiol.* **2007**, *118*, 2128–2148.
50. Von Stein, A.; Chiang, C.; König, P. Top-down processing mediated by interareal synchronization. *Proc. Natl. Acad. Sci. USA* **2000**, *97*, 14748–14753.
51. Tallon-Baudry, C.; Bertrand, O. Oscillatory gamma activity and its role in object representation. *Trends Cogn. Sci.* **1999**, *3*, 151–162.
52. Potts, G.F.; Hirayasu, Y.; O'Donnell, B.F.; Shenton, M.E.; McCarley, R.W. High-density recording and topographic analysis of the auditory oddball event-related potential in patients with schizophrenia. *Biol. Psychiatry* **1998**, *44*, 982–989.
53. Raichle, M.E.; MacLeod, A.M.; Snyder, A.Z.; Powers, W.J.; Gusnard, D.A.; Shulman, G.L. A default mode of brain function. *Proc. Natl. Acad. Sci. USA* **2001**, *98*, 676–682.
54. Greicius, M.D.; Krasnow, B.; Reiss, A.L.; Menon, V. Functional connectivity in the resting brain: A network analysis of the default mode hypothesis. *Proc. Natl. Acad. Sci. USA* **2003**, *100*, 253–258.
55. Palaniyappan, L.; Doege, K.; Mallikarjun, P.; Liddle, E. Cortical thickness and oscillatory phase resetting: A proposed mechanism of salience network dysfunction in schizophrenia. *Psychiatriki* **2012**, *23*, 117–129.
56. White, T.P.; Joseph, V.; Francis, S.T.; Liddle, P.F. Aberrant salience network (bilateral insula and anterior cingulate cortex) connectivity during information processing in schizophrenia. *Schizophr. Res.* **2010**, *123*, 105–115.
57. Mormann, F.; Fell, J.; Axmacher, N.; Weber, B.; Lehnertz, K.; Elger, C.E.; Fernández, G. Phase/amplitude reset and theta-gamma interaction in the human medial temporal lobe during a continuous word recognition memory task. *Hippocampus* **2005**, *15*, 890–900.
58. Gomez-Ramirez, M.; Kelly, S.P.; Molholm, S.; Sehatpour, P.; Schwartz, T.H.; Foxe, J.J. Oscillatory Sensory Selection Mechanisms during Intersensory Attention to Rhythmic Auditory and Visual Inputs: A Human Electrocorticographic Investigation. *J. Neurosci.* **2011**, *31*, 18556–18567.



Contents lists available at ScienceDirect

Progress in Neuropsychopharmacology & Biological Psychiatry

journal homepage: www.elsevier.com/locate/pnp

Functional EEG network analysis in schizophrenia: Evidence of larger segregation and deficit of modulation



Javier Gomez-Pilar^a, Alba Lubeiro^b, Jesús Poza^{a,c,d}, Roberto Hornero^{a,c,d}, Marta Ayuso^e, César Valcárcel^{f,g}, Karim Haidar^{f,g}, José A. Blanco^h, Vicente Molina^{d,h,*}

^a Biomedical Engineering Group, Department TSCIT, ETS Ingenieros de Telecomunicación, University of Valladolid, Spain

^b Psychiatry Department, School of Medicine, University of Valladolid, Spain

^c Instituto de Investigación en Matemática (IMUVA), University of Valladolid, Spain

^d Neuroscience Institute of Castilla y León (INCYL), University of Salamanca, Spain

^e Clinical Neurophysiology Service, University Hospital of Valladolid, Valladolid, Spain

^f Centro de Investigación Biomédica en Red de Salud Mental (CIBERSAM), Spain

^g Psychiatry Service, University Hospital of Alava, Spain

^h Psychiatry Service, University Hospital of Valladolid, Valladolid, Spain.

ARTICLE INFO

Keywords:

Complex network theory
Schizophrenia
Electroencephalography
Evoked response

ABSTRACT

Objective: Higher mental functions depend on global cerebral functional coordination. Our aim was to study fast modulation of functional networks in schizophrenia that has not been previously assessed.

Methods: Graph-theory was used to analyze the electroencephalographic (EEG) activity during an odd-ball task in 57 schizophrenia patients (18 first episode patients, FEPs) and 59 healthy controls. Clustering coefficient (CLC), characteristic path length (PL) and small-worldness (SW) were computed at baseline ([−300 0] ms prior to stimulus delivery) and response ([150 450] ms post-stimulus) windows. Clinical and cognitive assessments were performed.

Results: CLC, PL and SW showed a significant modulation between baseline and response in controls but not in patients. Patients obtained higher CLC and SW at baseline, lower CLC and higher PL at response, and diminished modulation of CLC and SW as compared to controls. In patients, CLC and SW modulation were inversely associated to cognitive performance in executive tasks and directly associated to working memory. Similar patterns were observed in FEPs. CLC and SW during the baseline were inversely associated to their respective modulation magnitudes.

Conclusions: Our results are coherent with a hyper-segregated network at baseline (higher CLC) and a decreased modulation of the functional connectivity during cognition in schizophrenia.

1. Introduction

Mental functions depend on global dynamic coordination of cerebral networks (Dehaene and Changeux, 2011; Varela et al., 2001), whose characteristics can be assessed using methods derived from graph-theory. Previous studies in the normal brain revealed structural and functional small-world properties as an efficient way to balance local specialization and integration (Latora and Marchiori, 2001; Sporns et al., 2004). These network properties can be jointly summarized in the “small-worldness” parameter (SW), which is defined as the

ratio between the global clustering coefficient (CLC) and the characteristic path length (PL) of the network. In a binary network, local CLC is the ratio between the number of triangles in which a given node participates and the maximum possible number of triangles including that node. This measure, averaged across the nodes of the entire network, can be used as an indicator of the network segregation and of local efficiency of information transfer, probably related to specialization. PL is the average of shortest distances for all possible pairs of nodes. It is usually interpreted as a metric of information integration across areas. Both parameters are of interest in the study of schizo-

Abbreviations: BACS, Brief Assessment in Cognition in Schizophrenia Scale; CLC, clustering coefficient; COI, scores of influence; CWT, Continuous wavelet transform; EEG, electroencephalography; ERC, event-related Coherence; FEP, first episode patients; FIR, finite impulse response; fMR, functional magnetic resonance; ICA, independent component analysis; IQ, intelligence quotient (IQ); MEG, magnetoencephalography; PANSS, Positive and Negative Syndrome Scale; PL, characteristic path length; SW, small-worldness; TMT, Trail-Making Test; WCST, Wisconsin Card Sorting Test

* Corresponding author at: Dept. of Psychiatry, University Hospital of Valladolid, Av. Ramón y Cajal, 7, Valladolid 48005, Spain.

E-mail address: vicente.molina@uva.es (V. Molina).

<http://dx.doi.org/10.1016/j.pnpbp.2017.03.004>

Received 10 October 2016; Received in revised form 17 March 2017; Accepted 17 March 2017

Available online 20 March 2017

0278-5846/© 2017 Elsevier Inc. All rights reserved.

phrenia, given the abnormal integration of cerebral networks observed in this psychiatric disorder (de Jong et al., 2013; Friston, 1998; Kaufmann et al., 2015; Touskova and Bob, 2015).

Quickly evolving patterns of interaction (in the order of hundreds of milliseconds) are likely to underlie cognitive function in real time (Bressler and Tognoli, 2006), (Sporns, 2011b). Considering such rapid modulation of cortical activity (Bressler et al., 1993; Dehaene and Changeux, 2011), the high temporal resolution of electroencephalography (EEG) and magnetoencephalography (MEG), combined with a complex network analysis, can be useful for assessing global connectivity dynamics in normal and altered cognition. In healthy subjects, a MEG study showed that the cognitive effort drives normal brain networks to a less clustered configuration and more long-range synchronization (Kitzbichler et al., 2011). Using the EEG we observed in healthy subjects a significant *SW* increase from baseline (−300 to 0 ms prior to stimulus onset) to response (150 to 450 ms post-stimulus) windows during an odd-ball task (Martin-Santiago et al., 2016).

However, most EEG or MEG network analyses published in schizophrenia did not take into account temporal dynamics or compared parameters during different tasks. Using graph theory analyses from resting EEG signals, lower *CLC* and shorter *PL* were reported in schizophrenia (Rubinov et al., 2009). Also, a lower *SW* index was reported in 20 chronic patients at rest, whereas decreased *CLC* and increased *PL* values were appreciated during a working memory test (Micheloyannis et al., 2006). More recently, globally reduced segregation and integration were described in 34 schizophrenia patients during an odd-ball task (Shim et al., 2014), without discriminating between windows in the task. In a functional magnetic resonance (fMRI) study, a lower *SW* index in schizophrenia patients when compared to controls was reported both at rest and during an odd-ball task (Ma et al., 2012). Shorter *PL* values during task performance were also observed in 20 schizophrenia patients performing a contextual paradigm (Fogelson et al., 2013). These previous studies are in line with an abnormal neural synchrony in schizophrenia, which involves dysfunctional integration among neural systems (Friston, 1998). In this context, graph theory would predict in schizophrenia a smaller modulation of the whole network, observable in the small-world characteristics of the brain.

Thus, deficits in the fast modulation of network properties might be found in schizophrenia. In particular, our working hypotheses were that (i) patients would exhibit altered modulation of functional network properties with cognitive activity across the brain; and (ii) such modulation would correlate with patient's symptoms and/or cognitive performance. We analyzed stimulus-evoked oscillations given its association with “top-down” cognitive processing (Makeig et al., 2004). Due to the fact that the odd-ball task is relatively easy to perform, it was used for the analyses of the dynamical changes in brain network properties. Thus, differences in performance are unlikely to hamper the data interpretation. Furthermore, it is well-known that oddball tasks activate a relatively large neural network (Bledowski et al., 2004; Linden et al., 1999) and an extensive literature supports their relevance in schizophrenia (Bramon et al., 2004).

1.1. Aims of the study

To assess the fast dynamic modulation of brain network properties during a cognitive task in schizophrenia using network parameters summarizing segregation and integration of this network.

2. Materials and methods

2.1. Participants

Fifty-nine healthy controls and 57 schizophrenia patients (39 chronic and 18 first-episode (FE) patients) with normal hearing were included in the study. Exclusion criteria were: (i) any neurological illness; (ii) history of cranial trauma with loss of consciousness longer

Table 1
Demographic and clinical characteristics. Significant differences with respect to controls.

	Schizophrenia patients (n = 57)	First episode patients (n = 18)	Controls (n = 59)
Age (years)	34.1 (8.4)	28.4 (8.5)**	35.0 (11.6)
Sex (male:female)	29:28	12:6	32:27
PANSS-positive	11.6 (4.8)	11.3 (3.7)	NA
PANSS-negative	18.0 (8.5)	21.2 (9.3)	NA
PANSS-total	55.2 (22.6)	59.8 (25.6)	NA
Total IQ	88.1 (16.4)	87.7 (16.6)	104.9 (10.0)
BACS list of words	36.0 (11.7)**	34.3 (12.2)**	55.5 (7.7)
BACS digits	16.5 (5.1)**	15.3 (5.7)**	22.8 (3.2)
BACS motor speed	46.5 (19.3)**	40.0 (17.8)**	57.0 (15.4)
BACS verbal fluency	17.2 (6.0)**	17.5 (5.1)**	25.4 (4.6)
BACS execution speed	36.7 (15.6)**	33.9 (14.1)**	67.7 (10.7)
BACS Tower of London	14.1 (5.4)**	12.7 (5.7)**	18.6 (2.6)
WCST completed categories	3.8 (2.0)**	3.5 (2.2)**	5.8 (0.8)
WCST perseverative errors (%)	20.4 (13.3)**	22.9 (9.8)**	9.6 (4.8)
TMT (time B-A/A)	1.9 (1.4)**	2.4 (1.7)**	0.9 (0.6)
Oddball task accuracy (%)	93.0 (9.0)	94.2 (7.4)	97.9 (4.4)
Oddball task reaction time (ms)	223 (77)	220 (66)	247 (32)
P300 amplitude in Pz (μV)	1.1 (0.5)	1.7 (0.6)	2.2 (0.8)
P300 latency in Pz (ms)	375 (87)	370 (60)	357 (45)

** $p < 0.001$.

than one minute; (iii) past or present substance abuse, except nicotine or caffeine (iv) total intelligence quotient (IQ) smaller than 70; and (v) for patients, presence of any other psychiatric process, and (vi) for controls, any current psychiatric or neurological diagnosis or treatment.

Patients were diagnosed according to the Diagnostic and Statistical Manual of Mental Disorders, 4th edition. They were on antipsychotic monotherapy. Chronic patients received stable doses of atypical antipsychotics. FEP only received antipsychotics for < 72 h prior to EEG acquisition followed by a wash-out period of 24 h. Hence, the possible bias due to the selection of acutely ill patients able to cooperate during EEG acquisition without any prior treatment was avoided. Symptoms were scored using the Positive and Negative Syndrome Scale (PANSS) (Kay et al., 1987). Healthy controls were recruited through newspaper advertisements. Demographic and clinical characteristics are shown in Table 1.

Cognitive data from patients and controls were collected using: the Wechsler Adult Intelligence Scale, WAIS-III (IQ); the Trail-Making Test, TMT ((time part B – time part A)/time part A); the Wisconsin Card Sorting Test (WCST); completed categories and percentage of perseverative errors); and the Spanish version of the Brief Assessment in Cognition in Schizophrenia Scale (BACS) (Segarra et al., 2011).

Written informed consent was obtained from all participants after full printed information. The ethical committees of the participating hospitals approved the study.

2.2. Electroencephalographic recordings

EEG data were recorded using a 17-channel EEG system (BrainVision®, Brain Products GmbH). Active electrodes were placed in an elastic cap at Fp1, Fp2, F3, F4, F7, F8, C3, C4, P3, P4, O1, O2, T5, T6, Pz, Cz and Cz (international 10–20 system). Impedance was kept under 5 kΩ. Thirteen minutes of eyes-closed EEG was obtained during an auditory odd-ball 3-stimulus paradigm, which consisted of 600 random sequences of target (500 Hz-tone, probability 0.2), distractor (1000 Hz-tone, probability 0.2), and standard (2000 Hz-tone, probability 0.6) tones. The tone duration was 50 ms, rise and fall time being 5 ms and intensity being 90 dB. Inter-stimulus interval between tones

randomly jittered between 1.16 and 1.44 s. The participants were asked to press a button whenever they detected the target tones. Target tones were considered ‘attended tones’ when they were followed by a button press. Only ‘attended’ target tones were taken into account for further analysis (Gomez-Pilar et al., 2015). Alertness differences across groups were controlled by comparing accuracy of target responses.

EEG signals were recorded using a sampling frequency of 500 Hz and referenced over Cz electrode. EEG recordings were subsequently re-referenced to the average activity of all sensors in order to minimize the effect of microsaccadic artifacts (Bledowski et al., 2004). Data were filtered using a finite impulse response (FIR) band-pass filter (1–70 Hz, Hamming window) and a notch filter to remove the power line frequency interference (50 Hz, Butterworth filter). Artifact rejection was conducted following a three-step approach (Bachiller et al., 2015, Gomez-Pilar et al., 2015). Firstly, an independent component analysis (ICA) was carried out to decompose each EEG recording into a total of 17 components (Delorme and Makeig, 2004). After a visual inspection of the scalp maps and the temporal activation, components related to eye-blinks and muscle artifacts were discarded. Secondly, continuous EEG data were segmented into 1 s-length trials ranging from –300 ms before target stimulus onset to 700 ms after onset. Thirdly, trials with artifacts were automatically rejected if their amplitude exceeded a statistical-based local adaptive threshold (Bachiller et al., 2015).

2.3. Signal similarity across sensors: event-related coherence

Continuous wavelet transform (CWT) was computed to obtain a time-frequency representation of EEG recordings. Complex Morlet wavelet was used because it provides a biologically plausible fit to the signal being modeled (Roach and Mathalon, 2008). The scaling factor was set to include frequencies from 1 to 70 Hz (Bachiller et al., 2015, Gomez-Pilar et al., 2015, Tallon-Baudry et al., 1996). Thus, 1 s-length evoked responses ([-300–700] ms) were decomposed using CWT into two windows: (i) baseline ([-300 0] ms to stimulus onset); and (ii) response ([150 450] ms after stimulus onset) (Bachiller et al., 2015, Gomez-Pilar et al., 2015). These windows were chosen to summarize the underlying temporal dynamics between resting (inter-stimulus) and the cognitive processing (centered around the usual P300 peak) windows. We previously showed a significant modulation of graph parameters between these windows in healthy subjects (Martin-Santiago et al., 2016). It is noteworthy that edge effects are not negligible, since EEG trials are finite and short-time recordings. Hence, two cones of influence (COIs) were defined around baseline and response windows to avoid border distortion (Torrence and Compo, 1998).

From CWT decomposition, event-related Coherence (ERC) was computed to assess linear functional interactions (Nunez et al., 1997). ERC is useful to identify coherent activity between cognitive networks (Yener and Basar, 2013), since it is a measure of the degree of coordination between assemblies of neurons triggered by a cognitive task (Basar et al., 2016). In this study, ERC was calculated for each pair of electrodes and its values were averaged in the 4–70 Hz frequency band to obtain a global similarity measure for each time window. Changes in ERC between resting and active windows allowed the assessment of task-related modulation in graph parameters for each group. Since we had no a priori hypothesis regarding modulation deficits in any particular band, network analyses were performed in the whole frequency band to avoid an inflation of the number of comparisons.

Further description of CWT and ERC is detailed in the Supplementary material.

2.4. Graph parameters

In order to model a system as a graph, nodes should represent the dynamical units and their links should be the interactions between

them (Boccaletti et al., 2006). Thereby, the brain can be assimilated to a complex network with functional connectivity units that can be altered due to a pathological process (Stam and van Straaten, 2012). The linear interaction between the neural activity in different cerebral regions can be used to represent the brain as a graph. Each electrode would correspond to a vertex (or node) and the relationships between electrodes would be the links (or edges) between them. In the present study, we used ERC to set the weights of the links. ERC could be useful in patients with cognitive impairment, such as schizophrenia, to study whether sensory and cognitive networks are manifested in topologically different places and in different frequency windows (Yener and Basar, 2013). Completely filled ERC matrices were then used as adjacency matrices. Hence, the generated fully connected network was composed of $N = 17$ nodes, corresponding to the electrodes, and network weights set by the ERC values between electrodes.

Networks can be described by several parameters. The present study focused on two complementary features of the brain network: segregation and integration, together with their fast modulation during a cognitive task. In order to characterize the segregation of the network, we computed CLC (Rubinov and Sporns, 2010). In the case of weighted networks, CLC has been generalized as follows in order to avoid the influence of the mean edge weight:

$$CLC = \left(\frac{N}{3} \right) \sum_{i \in n} \sum_{j, k \in n} (w_{ij}^b w_{ik}^b w_{jk}^b)^{1/3}, \quad (1)$$

where w_{xy} denotes the edge weight between electrodes i and j .

To quantify the integration of the network, we computed PL. It is defined as the average shortest path length between all pairs of nodes in the network (Rubinov and Sporns, 2010):

$$PL = \frac{1}{N} \sum_{i \in n} \frac{\sum_{j \in n, j \neq i} d_{ij}}{n-1}, \quad (2)$$

where d_{ij} indicates the minimum distance (i.e. the inverse of ERC) between electrodes i and j . It is noteworthy that the previous definition takes into account that some of the paths with minimum distance can be formed of multiple edges.

To facilitate the comparison with previous research, the balance between CLC and PL was computed. This ratio (known as SW) is useful to assess the small-world properties of the network. Small-world networks are defined as those significantly more clustered than random networks, yet have approximately the same PL as random networks (Rubinov and Sporns, 2010). SW index is defined as the ratio between segregation and integration, where CLC and PL have been normalized in order to eliminate the dependence on basic parameters of the network, such as network size, or density (Stam et al., 2009):

$$\gamma = \frac{CLC}{\langle CLC \rangle_{\text{random}}}, \quad (3)$$

$$\lambda = \frac{PL}{\langle PL \rangle_{\text{random}}}, \quad (4)$$

$$SW = \frac{\gamma}{\lambda}, \quad (5)$$

where $\langle CLC \rangle_{\text{random}}$ and $\langle PL \rangle_{\text{random}}$ denote CLC and PL averaged over an ensemble of 50 surrogate networks, which were computed from a randomization of the original network by reshuffling its connections (Stam et al., 2009).

2.5. Parameter baseline correction (modulation)

The baseline correction process was applied to achieve a stimulus-independent characterization (Bachiller et al., 2015) and to quantify the dynamical changes during the evoked response (i.e. modulation). Network parameters were computed for each temporal window (baseline and response), providing meaningful information about the

temporal evolution of network properties (Bachiller et al., 2015). Modulation in each parameter (P^C) was assessed as the result of the following baseline correction procedure:

$$P^C = P^{RES} - P^{BL}, P = \{\gamma, \lambda, SW\}, \quad (6)$$

where P^{BL} and P^{RES} represent the parameter averaged for the baseline and the response windows. Negative or positive values indicate decreases or increases from baseline to response, respectively.

2.6. Statistical analyses

After testing normality and homoscedasticity of the distribution of network parameters (using Kolmogorov-Smirnov and Levene's tests, respectively), the following analyses were performed:

- i. Network parameters at baseline and response windows were compared between groups using a multivariate analysis of covariance ('group' as fixed factor, and 'sex' and 'age' as covariates) with Bonferroni correction. Using a similar multivariate analysis of covariance, modulation of network parameters (γ , λ and SW changes between baseline and response windows) was compared between groups. Effect sizes were assessed using Cohen's d when statistically significant differences were found. This was followed by univariate within-group analyses of network parameters using paired t -tests (significance level: $\alpha = 0.009$).
- ii. The statistical significance of possible associations between baseline network parameters and the corresponding modulation values in patients, (only where significant between-group differences in modulation were detected) was assessed using Pearson correlation. In order to discard a major role for long-term treatment and chronicity, these and the previous analyses were repeated only for FEP.
- iii. We also assessed the significance of the association between modulation of network parameters (only those that showed significant between-group differences) and clinical and cognitive data. Spearman's correlation was used, since cognitive data distribution did not meet parametric assumptions.
- iv. Finally, spatial analyses of the network changes were performed using nodal CLC , paired and independent t -test for within and between group comparison respectively.

3. Results

3.1. Between- and within group differences in network parameters

3.1.1. Between-groups differences at baseline and response windows

There was a significant multivariate effect for 'group' (Wilk's

lambda = 0.87; $F = 2.24$; $df = 6109$; $p = 0.045$) but not for 'age' or 'sex'. The inter-subject effects tests (Table 2) revealed statistically significant differences in SW , normalized clustering coefficient (γ) and normalized path length (λ). During the baseline, SW^{BL} and γ^{BL} were higher for patients than for controls. In the case of the response, patients obtained smaller γ^{RES} values and larger λ^{RES} values than controls. There were no statistically significant differences between FEP and chronic patients in mean network parameters.

3.1.2. Between- and within-group differences in network modulation

There was a significant multivariate effect for 'group' but not for 'age' or 'sex' on mean network modulation (Wilk's lambda = 0.98; $F = 3.64$; $df = 3112$; $p = 0.040$). The inter-subject effects tests revealed statistically significant differences with moderate effect sizes for modulation (values at response minus baseline windows) in path length, clustering coefficient and small-worldness (γ^c , λ^c and SW^c , respectively) with smaller values in patients (see Table 2).

Controls showed statistically significantly positive changes for γ^c (i.e. a statistically significant increase from baseline to response windows) ($t = 3.38$, $df = 58$, $p = 0.001$), λ^c ($t = 2.84$, $df = 58$, $p = 0.006$) and SW^c ($t = 3.27$, $df = 58$, $p = 0.002$). In patients, non-significant changes were observed for γ^c ($t = -0.96$, $df = 56$, $p = 0.340$), λ^c ($t = 0.74$, $df = 56$, $p = 0.460$) and SW^c ($t = -0.34$, $df = 56$, $p = 0.700$). FEP showed similar deficits of modulation in γ^c ($t = -0.85$, $df = 17$, $p = 0.410$), λ^c ($t = -1.07$, $df = 17$, $p = 0.30$) and SW^c ($t = 0.37$, $df = 17$, $p = 0.720$) (Table 2).

3.2. Association between baseline parameters and modulation

In patients, baseline parameters (γ^{BL} , λ^{BL} and SW^{BL}) were negatively associated with the corresponding modulation values, i.e. γ^c (all patients $r = -0.569$, $p < 0.0001$; FEP $r = -0.535$, $p = 0.022$), λ^c (all patients $r = -0.602$, $p < 0.0001$; FEP $r = -0.821$, $p < 0.001$) and SW^c (all patients $r = -0.525$, $p < 0.0001$; FEP $r = -0.647$, $p = 0.004$). Therefore, higher values at baseline were associated with smaller task-related modulation of the corresponding network parameter (Fig. 1).

3.3. Association between network modulation and cognitive performance

In patients, modulation in path-length values (λ^c) was inversely associated to completed categories (all patients: $r = -0.348$, $p = 0.015$; FEP $r = -0.325$, $p = 0.219$) and directly to the percent of perseverative errors in WCST (all patients: $r = 0.316$, $p = 0.029$; FE: $r = 0.022$, $p > 0.05$). Modulation in small-worldness values (SW^c) was inversely associated to performance in the Tower of London test (all patients: $r = -0.338$, $p = 0.004$; FEP $r = -0.382$, $p = 0.118$) and

Table 2
Mean network parameters for each group and summary of the statistical results obtained after comparing schizophrenia patients and controls. Effect sizes for within- and between-group significant differences are shown (Cohen's d).

	Controls	Schizophrenia patients (n = 57)	Type III square sum; F, p	Effect-size (patients vs controls)	First episodes (n = 18)
SW baseline (SW^{BL}) [*]	1.021 (0.015)	1.027 (0.013)	0.001; 6.627; 0.011	0.427	1.024 (0.014)
SW response (SW^{RES}) [*]	1.030 (0.019)	1.027 (0.160)	0.000; 1.340; 0.249		1.027 (0.016)
SW modulation (SW^c) ^{**}	0.010 (0.020)	0.000 (0.018)	0.003; 7.484; 0.007	0.525	0.003 (0.021)
Effect size (within-group)	0.525	0.000			0.199
CLC baseline (λ^{BL}) [*]	1.050 (0.022)	1.059 (0.020)	0.003; 5.733; 0.018	0.428	1.048 (0.019)
CLC response (λ^{RES}) [*]	1.065 (0.030)	1.056 (0.023)	0.002; 3.025; 0.085	0.336	1.056 (0.026)
CLC modulation (λ^c) ^{**}	0.015 (0.034)	-0.003 (0.027)	0.009; 10.155; 0.002	0.586	0.009 (0.031)
Effect size (within-group)	0.587	0.139			0.351
PL baseline (γ^{BL}) [*]	1.033 (0.013)	1.030 (0.011)	0.000; 2.432; 0.122		1.033 (0.013)
PL response (γ^{RES}) [*]	1.028 (0.009)	1.031 (0.011)	0.000; 3.758; 0.055	0.298	1.027 (0.009)
PL modulation (γ^c) [*]	-0.005 (0.016)	0.002 (0.014)	0.001; 4.635; 0.033	0.456	-0.006 (0.016)
Effect size (within-group)	0.447	0.090			0.536

^{*} $p < 0.05$.

^{**} $p < 0.01$.

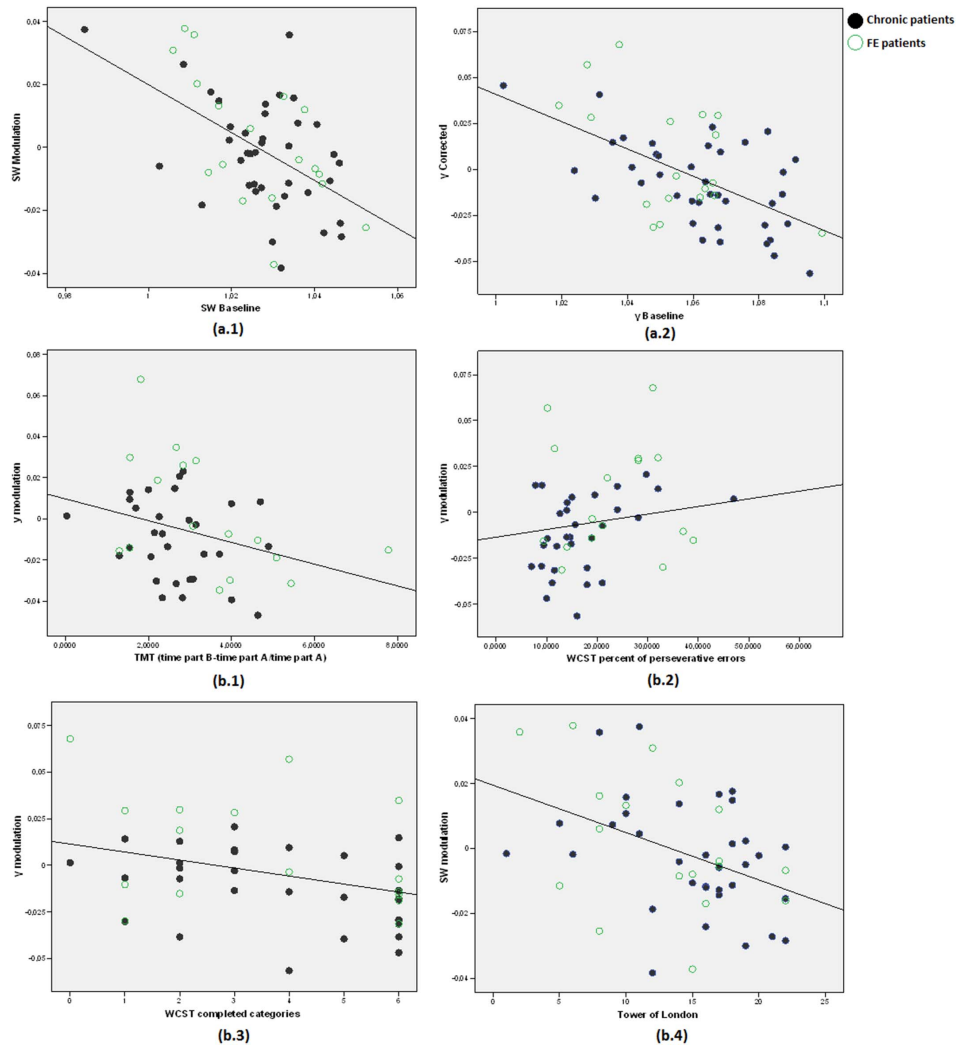


Fig. 1. A) Association between baseline and modulation values in schizophrenia patients for: (a1) SW, and (a2) normalized CLC. B) Significant relationships between cognitive performance and modulation of network parameters for patients: b1, b2 and b3 depict associations with modulation of CLC; b4 depicts an association with SW modulation: larger values in Tower of London, completed categories in WCST and less perseverative errors in WCST indicate better executive function. Lower values in adjusted TMT indicate better working memory. Filled circles: chronic patients; empty circles: FEP.

completed categories in WCST (all patients: $r = -0.373, p = 0.009$; FE: $r = -0.389, p = 0.0136$). Consequently, higher increases in SW and γ^c from baseline to response can be related to a poorer performance in schizophrenia patients, although this was not confirmed in the FEP subgroup (Fig. 1). γ^c was inversely related to normalized scores in TMT (all patients;

$r = -0.298, p = 0.044$; FE: $r = -0.512, p = 0.043$), suggesting a direct association with working memory performance (Fig. 1).

In controls, no significant associations were found for network modulation or cognitive performance.

There was no association between symptom scores and network modulation.

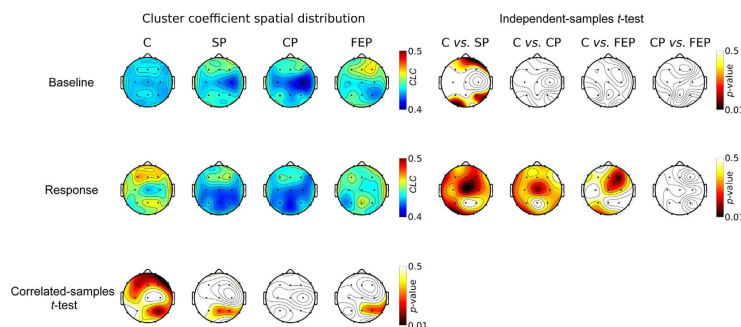


Fig. 2. Nodal clustering maps depicting the spatial distribution of intra- (comparison between baseline and response) and inter-group differences in *CLC* (C: controls; SP: schizophrenia patients; FEP: first episode patients; CP: chronic patients).

3.4. Spatial analyses

Controls showed bilateral frontal and right temporoparietal increases from baseline to the response window, γ not found in patients. Patients showed a statistically significantly lower widespread γ value during the response window (Fig. 2).

4. Discussion

In our study, a modulation deficit in all network parameters was found in schizophrenia patients during a P300 task. Moreover, *CLC* and *SW* values were higher at baseline and lower in response windows, whereas *PL* was higher in the response window for patients during the task. In this group, an inverse relationship between positive modulation of *CLC* and *SW* and performance in executive function tests was found. This relationship likely indicates that the larger increases of clustering between baseline and response hamper executive functions in schizophrenia patients, which might be related to higher baseline clustering values (γ^{BL}) for patients.

Previous evidences in humans (Varela et al., 2001) and animals (Bressler et al., 1993) showed that rapid and transient modulation of coherence and functional integration play a role in cognition, which may be hampered in schizophrenia patients according to the present data. Our analyses support the notion that schizophrenia can be associated with a deficit to reconfigure the brain network during a cognitive task. The particular brain sources driving such deficit may be further explored.

The larger baseline *CLC* in patients may reflect more segregated cortical activity in comparison to controls prior to stimulus onset. Previous results on clustering in schizophrenia using graph analyses are discrepant. In the resting state, a larger clustering was observed with fMRI in 19 schizophrenia patients (Yu et al., 2011), as well as non-significant differences in clustering using MEG (Rutter et al., 2013). By means of EEG, a reduced clustering was seen in 34 schizophrenia patients performing an odd-ball task (Shim et al., 2014) and in 40 patients looking at a stationary dot (Rubinov et al., 2009). Ma et al. (2012) reported with fMRI a reduced clustering in schizophrenia both at rest and during an odd-ball task, with shorter path length at rest but longer during the task. Our findings support the notion that both increased (larger *CLC* values during the baseline) and reduced (smaller *CLC* values during the response) clustering may be found in schizophrenia patients at different temporal points depending on the time of cognitive processing. This result could correspond to respectively increased and decreased functional segregation in patients during baseline and response windows.

The temporal resolution of fMRI would not allow discriminating

between resting and active windows as defined in the present study. This may contribute to the discrepancies with previous reports of reduced clustering in schizophrenia using fMRI (Lynall et al., 2010). However, information from fMRI studies may help to explain the reconfiguration deficit observed in our study. Fewer hubs (i.e. highly connected nodes) have been reported with fMRI in schizophrenia in the resting state (Lo et al., 2015) and during an odd-ball task (Ma et al., 2012), along with a significant randomization of global network metrics (Lo et al., 2015). Such reduction in the number of highly connected nodes may explain the network reconfiguration deficit and the larger *PL* in the response window in our patients. Likewise, it would be also coherent with the less globally coordinated mode of brain connectivity in schizophrenia, reported with fMRI (Lynall et al., 2010).

Baseline clustering was higher for patients, and its positive modulation (i.e., its increase from baseline to response windows) was associated to poorer performance in executive function. Thus, additional increases of *CLC* over baseline levels predicted worse performance on executive tasks in patients but not in controls. This result indicates that a larger basal (i.e. pre-stimulus) segregation hinders cognition in schizophrenia. Thus, larger increases in clustering above a hyper-segregated basal state could hamper the more complex cognitive capacities, for which a larger integration of cortical activity among distant brain regions is needed (Dehaene and Changeux, 2011; Varela et al., 2001). Hypothetically, this might be related to the fewer number or strength of hubs, which could hamper cortical integration. Cognitive demands of the P300 task are low, but more demanding tasks drive the transitory formation of long-range integrative networks (Kitzbichler et al., 2011). However, *CLC* modulation was directly related to working memory. Therefore, larger segregation could provide some advantage for working memory performance when network modularity was more important than integration. In a previous fMRI study modularity, but not *SW*, predicted working memory performance (Stevens et al., 2012).

Patients also showed larger *PL* values in the response window, which might result from the structural long-range connectivity deficits reported in schizophrenia (Zalesky et al., 2011). Such deficits in network integration might also conceivably contribute to the deficit of modulation in functional clustering.

The investigation of baseline hyper-clustering in patients is beyond our research, but speculatively might be related to inhibitory deficits in schizophrenia (Gonzalez-Burgos and Lewis, 2012; Lewis et al., 2012). *CLC* quantifies the linear similarity degree between the neighbors of each node and most short-range cortico-cortical (Hellwig, 2000) and recurrent (Douglas et al., 1995) connections are excitatory. As a consequence, inhibitory cortical deficits might drive a basal hyper-synchronization secondary to mutual excitation among pyramidal neurons, which could be reflected in larger local phase and power

coupling (and therefore in larger *CLC* values). This possibility seems consistent with previous EEG studies in schizophrenia that showed an increased neural noise (i.e. the amount of spontaneous, non-task evoked EEG power) (Diez et al., 2013; Diez et al., 2014; Winterer et al., 2004; Winterer et al., 2000). In this context, spontaneous neural activity is not stochastic noise, but rather exhibits patterns largely conditioning by evoked responses (Sporns, 2011a).

Husserl's phenomenology (and Aristotle's "koine aesthesis" *κοινή αἴσθησις*) proposes the "synthesis" of multiple mental processes as the basis of conscious experience. Conscious and subliminal perception seem to be different by a larger extension of synchronization in the former (Dehaene and Changeux, 2011). Therefore, a dysfunction in that integrative process (suggested in our cases by the larger basal *CLC* and the modulation deficits in *CLC* and *PL*) may disturb the conscious experience in patients with schizophrenia. The neural representation of internal and external events may be based on the transitory conformation of distributed synaptic assemblies (Buzsáki, 2006). Thus, network deficits, such as those found in our study, might contribute to schizophrenia. This possibility seems to be in line with phenomenological accounts, such as "disturbed ipseity", one of whose facets is hyper-reflexivity. It is defined as "exaggerated self-consciousness, a tendency to objectifying attention towards processes and phenomena that would normally be 'inhabited' or experienced as part of oneself" (Saas and Parnas, 2007). An excess of functional segregation accompanied by a deficit in network modulation might be compatible with increased consciousness of these phenomena. Cortical hyper-segregation may hamper an adequate phenomenological integration of elements of mental life, leading to misinterpretation or hindered cognition.

We did not find any significant correlation between symptoms scores and network properties. We speculate that these properties could be closer to more elementary phenomena than symptoms, such as those described in the former paragraph (i.e., disturbed ipseity), while PANSS scores may be influenced by other factors that may obscure their possible association to cerebral networks (such as environmental characteristics or cooperativeness of the patients). Moreover, other kinds of biological factors, such as dopaminergic activity, may have a more direct association to some kind of symptoms than to network properties.

Our study has strengths and limitations. The sample size is larger than previous network studies. Furthermore, this is the first study that assesses fast network modulation during cognitive activity in schizophrenia. However, EEG recordings are hampered by the shared variance among contiguous sensors, though the comparison of different conditions may help to overcome this problem. In addition, our analyses are based on low-density EEG recordings; nonetheless, functional characteristics of dynamic brain networks can be explored using low-density EEG recordings (Qin et al., 2010). Larger *CLC* at baseline in patients may reflect a more segregated brain or a more regular pattern of connections (i.e. diffuse hyperconnectivity). Measures of network segregation may help to elucidate these possibilities by balancing the density between intra- and inter-module connections (Newman, 2006). EEG activity was recorded with eyes closed. Thereby, a larger contribution of alpha rhythms can be expected, but this should not have influenced the results on modulation between windows. Finally, it is uncertain whether the present results, obtained in narrow experimental setting, can be generalized to a network modulation deficit in more complex and/or real-life situations.

In conclusion, our findings support a relevant decrease in the ability to integrate cortical networks in schizophrenia, which may be based on a hyper-segregated basal state and a deficit of network modulation during cognitive activity.

Declaration of interest

None.

Acknowledgements

This work was supported by the Instituto Carlos III (PI11/02708, PI11/02203 and PI15/00299) and the Gerencia Regional de Salud de Castilla y León (GRS 1134/A/15 and GRS 1263/A/16) grants; the 'MINECO and FEDER (TEC2014-53196-R), 'Consejería de Educación de la Junta de Castilla y León' (VA037U16); and predoctoral fellowships to A. Lubeiro ('Consejería de Educación Junta de Castilla y León') and to J. Gomez-Pilar (University of Valladolid).

Appendix A. Supplementary data

Supplementary data to this article can be found online at <http://dx.doi.org/10.1016/j.pnpbp.2017.03.004>.

References

- Bachiller, A., Poza, J., Gomez, C., Molina, V., Suazo, V., Hornero, R., 2015. A comparative study of event-related coupling patterns during an auditory oddball task in schizophrenia. *J. Neural Eng.* 12, 016007.
- Basar, E., Golbasi, B.T., Tulay, E., Aydin, S., Basar-Eroglu, C., 2016. Best method for analysis of brain oscillations in healthy subjects and neuropsychiatric diseases. *Int. J. Psychophysiol.* 103, 22–42.
- Bledowski, C., Prvulovic, D., Hoehstetter, K., Scherg, M., Wibrall, M., Goebel, R., et al., 2004. Localizing P300 generators in visual target and distractor processing: a combined event-related potential and functional magnetic resonance imaging study. *J. Neurosci.* 24, 9353–9360.
- Boccaletti, S., Latora, V., Moreno, Y., Chavez, M., Hwang, D.U., 2006. Complex networks: structure and dynamics. *Phys. Rep.* 424, 175–308.
- Bressler, S.L., Tognoli, E., 2006. Operational principles of neurocognitive networks. *Int. J. Psychophysiol.* 60, 139–148.
- Bramon, E., Rabe-Hesketh, S., Sham, P., Murray, R.M., Frangou, S., 2004. Meta-analysis of the P300 and P50 waveforms in schizophrenia. *Schizophr. Res.* 70, 315–329.
- Bressler, S.L., Coppola, R., Nakamura, R., 1993. Episodic multiregional cortical coherence at multiple frequencies during visual task performance. *Nature* 366, 153–156.
- Buzsáki, G., 2006. Diversity of cortical functions: inhibition. In: *Rhythms of the Brain*. Oxford University Press, New York, pp. 61–79.
- Dehaene, S., Changeux, J.P., 2011. Experimental and theoretical approaches to conscious processing. *Neuron* 70, 200–227.
- Delorme, A., Makeig, S., 2004. EEGLAB: an open source toolbox for analysis of single-trial EEG dynamics including independent component analysis. *J. Neurosci. Methods* 134, 9–21.
- Diez, A., Suazo, V., Casado, P., Martin-Loeches, M., Molina, V., 2013. Spatial distribution and cognitive correlates of gamma noise power in schizophrenia. *Psychol. Med.* 43, 1175–1185.
- Diez, A., Suazo, V., Casado, P., Martin-Loeches, M., Perea, M.V., Molina, V., 2014. Frontal gamma noise power and cognitive domains in schizophrenia. *Psychiatry Res.* 221, 104–113.
- Douglas, R.J., Koch, C., Mahowald, M., Martin, K.A., Suarez, H.H., 1995. Recurrent excitation in neocortical circuits. *Science* 269, 981–985.
- Fogelson, N., Li, L., Li, Y., Fernandez-Del-Olmo, M., Santos-Garcia, D., Peled, A., 2013. Functional connectivity abnormalities during contextual processing in schizophrenia and in Parkinson's disease. *Brain Cogn.* 82, 243–253.
- Friston, K.J., 1998. The disconnection hypothesis. *Schizophr. Res.* 30, 115–125.
- Gomez-Pilar, J., Poza, J., Bachiller, A., Gómez, C., Molina, V., Hornero, R., 2015. Neural network reorganization analysis during an auditory oddball task in schizophrenia using wavelet entropy. *Entropy* 17, 5241–5256.
- Gonzalez-Burgos, G., Lewis, D.A., 2012. NMDA receptor hypofunction, parvalbumin-positive neurons, and cortical gamma oscillations in schizophrenia. *Schizophr. Bull.* 38, 950–957.
- Hellwig, B., 2000. A quantitative analysis of the local connectivity between pyramidal neurons in layers 2/3 of the rat visual cortex. *Biol. Cybern.* 82, 111–121.
- de Jong, J.J., de Gelder, B., Hodiamont, P.P., 2013. Sensory processing, neurocognition, and social cognition in schizophrenia: towards a cohesive cognitive model. *Schizophr. Res.* 146, 209–216.
- Kaufmann, T., Skatun, K.C., Alnaes, D., Doan, N.T., Duff, E.P., Tonnesen, S., et al., 2015. Disintegration of sensorimotor brain networks in schizophrenia. *Schizophr. Bull.* 41, 1326–1335.
- Kay, S.R., Fiszbein, A., Opler, L.A., 1987. The positive and negative syndrome scale (PANSS) for schizophrenia. *Schizophr. Bull.* 13, 261–276.
- Kitzbichler, M.G., Henson, R.N., Smith, M.L., Nathan, P.J., Bullmore, E.T., 2011. Cognitive effort drives workspace configuration of human brain functional networks. *J. Neurosci.* 31, 8259–8270.
- Latora, V., Marchiori, M., 2001. Efficient behavior of small-world networks. *Phys. Rev. Lett.* 87, 198701.
- Lewis, D.A., Curley, A.A., Glausier, J.R., Volk, D.W., 2012. Cortical parvalbumin interneurons and cognitive dysfunction in schizophrenia. *Trends Neurosci.* 35, 57–67.
- Linden, D.E., Prvulovic, D., Formisano, E., Vollinger, M., Zanella, F.E., Goebel, R., Dierks, T., 1999. The functional neuroanatomy of target detection: an fMRI study of visual and auditory oddball tasks. *Cereb. Cortex* 9, 815–823.

J. Gomez-Pilar et al.

- Lo, C.Y., Su, T.W., Huang, C.C., Hung, C.C., Chen, W.L., Lan, T.H., et al., 2015. Randomization and resilience of brain functional networks as systems-level endophenotypes of schizophrenia. *Proc. Natl. Acad. Sci. U. S. A.* 112, 9123–9128.
- Lynall, M.E., Bassett, D.S., Kerwin, R., McKenna, P.J., Kitzbichler, M., Muller, U., et al., 2010. Functional connectivity and brain networks in schizophrenia. *J. Neurosci.* 30, 9477–9487.
- Ma, S., Calhoun, V.D., Eichele, T., Du, W., Adali, T., 2012. Modulations of functional connectivity in the healthy and schizophrenia groups during task and rest. *NeuroImage* 62, 1694–1704.
- Makeig, S., Debener, S., Onton, J., Delorme, A., 2004. Mining event-related brain dynamics. *Trends Cogn. Sci.* 8, 204–210.
- Martin-Santiago, O., Gomez-Pilar, J., Lubeiro, A., Ayuso, M., Poza, J., Hornero, R., Fernandez, M., Ruiz, S., Valcarcel, C., Molina, V., 2016. Modulation of brain network parameters associated with subclinical psychotic symptoms. *Prog. Neuro-Psychopharmacol. Biol. Psychiatry* 66, 54–62.
- Micheloyannis, S., Pachou, E., Stam, C.J., Breakspear, M., Bitsios, P., Vourkas, M., et al., 2006. Small-world networks and disturbed functional connectivity in schizophrenia. *Schizophr. Res.* 87, 60–66.
- Newman, M.E., 2006. Modularity and community structure in networks. *Proc. Natl. Acad. Sci. U. S. A.* 103, 8577–8582.
- Nunez, P.L., Srinivasan, R., Westdorp, A.F., Wijesinghe, R.S., Tucker, D.M., Silberstein, R.B., et al., 1997. EEG coherence. I: statistics, reference electrode, volume conduction, Laplacians, cortical imaging, and interpretation at multiple scales. *Electroencephalogr. Clin. Neurophysiol.* 103, 499–515.
- Qin, Y., Xu, P., Yao, D., 2010. A comparative study of different references for EEG default mode network: the use of the infinity reference. *Clin. Neurophysiol.* 121, 1981–1991.
- Roach, B.J., Mathalon, D.H., 2008. Event-related EEG time-frequency analysis: an overview of measures and an analysis of early gamma band phase locking in schizophrenia. *Schizophr. Bull.* 34, 907–926.
- Rubinov, M., Sporns, O., 2010. Complex network measures of brain connectivity: uses and interpretations. *NeuroImage* 52, 1059–1069.
- Rubinov, M., Knock, S.A., Stam, C.J., Micheloyannis, S., Harris, A.W., Williams, L.M., et al., 2009. Small-world properties of nonlinear brain activity in schizophrenia. *Hum. Brain Mapp.* 30, 403–416.
- Rutter, L., Nadar, S.R., Holroyd, T., Carver, F.W., Apud, J., Weinberger, D.R., et al., 2013. Graph theoretical analysis of resting magnetoencephalographic functional connectivity networks. *Front. Comput. Neurosci.* 7, 93.
- Saas, L.A., Parnas, J., 2007. Explaining schizophrenia: the relevance of phenomenology. In: Cheung Chung, M., F. K.M.M., Graham, G. (Eds.), *Reconceiving Schizophrenia*. Oxford Univ Press, New York, pp. 63–92.
- Segarra, N., Bernardo, M., Gutierrez, F., Justicia, A., Fernandez-Egea, E., Allas, M., et al., 2011. Spanish validation of the Brief Assessment in Cognition in Schizophrenia

Progress in Neuropsychopharmacology & Biological Psychiatry 76 (2017) 116–123

- (BACS) in patients with schizophrenia and healthy controls. *Eur. Psychol.* 26, 69–73.
- Shim, M., Kim, D.W., Lee, S.H., Im, C.H., 2014. Disruptions in small-world cortical functional connectivity network during an auditory oddball paradigm task in patients with schizophrenia. *Schizophr. Res.* 156, 197–203.
- Sporns, O., 2011a. Dynamic patterns in spontaneous neural activity. In: *Networks of the Brain*. The MIT Press, London, pp. 149–178.
- Sporns, O., 2011b. *Networks for cognition*. In: *Networks of the Brain*. MIT Press, Cambridge, Massachusetts, pp. 182.
- Sporns, O., Chialvo, D.R., Kaiser, M., Hilgetag, C.C., 2004. Organization, development and function of complex brain networks. *Trends Cogn. Sci.* 8, 418–425.
- Stam, C.J., van Straaten, E.C., 2012. The organization of physiological brain networks. *Clin. Neurophysiol.* 123, 1067–1087.
- Stam, C.J., de Haan, W., Daffertshofer, A., Jones, B.F., Manshanden, I., van Cappellen van Walsum, A.M., et al., 2009. Graph theoretical analysis of magnetoencephalographic functional connectivity in Alzheimer's disease. *Brain* 132, 213–224.
- Stevens, A.A., Tappan, S.C., Garg, A., Fair, D.A., 2012. Functional brain network modularity captures inter- and intra-individual variation in working memory capacity. *PLoS One* 7, e30468.
- Tallon-Baudry, C., Bertrand, O., Delpuech, C., Pernier, J., 1996. Stimulus specificity of phase-locked and non-phase-locked 40 Hz visual responses in human. *J. Neurosci.* 16, 4240–4249.
- Torrence, C., Compo, G., 1998. A practical guide to wavelet analysis. *Bull. Am. Meteorol. Soc.* 79, 61–78.
- Toukova, T., Bob, P., 2015. Consciousness, awareness of insight and neural mechanisms of schizophrenia. *Rev. Neurosci.* 26, 295–304.
- Varela, F., Lachaux, J.P., Rodriguez, E., Martinerie, J., 2001. The brainweb: phase synchronization and large-scale integration. *Nat. Rev. Neurosci.* 2, 229–239.
- Winterer, G., Ziller, M., Dorn, H., Frick, K., Mulert, C., Wuebben, Y., et al., 2000. Schizophrenia: reduced signal-to-noise ratio and impaired phase-locking during information processing. *Clin. Neurophysiol.* 111, 837–849.
- Winterer, G., Coppola, R., Goldberg, T.E., Egan, M.F., Jones, D.W., Sanchez, C.E., et al., 2004. Prefrontal broadband noise, working memory, and genetic risk for schizophrenia. *Am. J. Psychiatry* 161, 490–500.
- Yener, G.G., Basar, E., 2013. Brain oscillations as biomarkers in neuropsychiatric disorders: following an interactive panel discussion and synopsis. *Suppl. Clin. Neurophysiol.* 62, 343–363.
- Yu, Q., Sui, J., Rachakonda, S., He, H., Gruner, W., Pearson, G., et al., 2011. Altered topological properties of functional network connectivity in schizophrenia during resting state: a small-world brain network study. *PLoS One* 6, e25423.
- Zalesky, A., Fornito, A., Seal, M.L., Cocchi, L., Westin, C.F., Bullmore, E.T., et al., 2011. Disrupted axonal fiber connectivity in schizophrenia. *Biol. Psychiatry* 69, 80–89.

Supplementary material of the paper: “Functional EEG network analysis in schizophrenia: Evidence of larger segregation and deficit of modulation”

Time-frequency representation using wavelet transform

Electroencephalographic (EEG) recordings are non-stationary signals. Accordingly, their properties change over time. This issue can be clearly seen during a sensory-cognitive task, in which different neural networks are involved. In order to accurately assess spectral dynamics, methods that do not require stationarity are recommended. In this regard, wavelet transform is a suitable time-frequency (or time-scale) representation to carry out a time-varying spectral analysis.

In this study, the complex Morlet wavelet was used as basis function, since it provides a plausible biological fit to EEG data (Roach and Mathalon, 2008). It is characterized by its location in time (Δt) and frequency (Δf). Complex Morlet function is defined in the time domain as follows:

$$\phi(t) = \frac{1}{\sqrt{\pi \cdot \Omega_b}} e^{j2\Omega_c t} \cdot e^{-\frac{t^2}{\Omega_b}}, \quad (\text{A.1})$$

where Ω_b and Ω_c represent the bandwidth and wavelet center frequency parameters, respectively. They were set to 1 to obtain an adequate balance between (Δt) and (Δf) (Bachiller et al., 2015).

Wavelet coefficients are calculated as the convolution of each EEG trial of 1 s, $x(t)$, and the complex Morlet function:

$$CWT(k, s) = \frac{1}{\sqrt{s}} \int_{-\infty}^{\infty} x(t) \cdot \phi^*\left(\frac{t-k}{s}\right) dt, \quad (\text{A.2})$$

where s and k denote the dilation and translation factors and $*$ represents the complex conjugation. Finally, the wavelet cross-spectrum (WCS) between two EEG trials of 1 s was computed as follows:

$$WCS_{ij}(k, s) = CWT_i(k, s) \cdot CWT_j^*(k, s), \quad (\text{A.3})$$

where subscripts i and j identify two electrodes. Once WCS was obtained for all pairwise electrode combinations, WCS was averaged across trials in two windows of interest: (i) the baseline window ([300, 0] ms before the stimulus onset); and (ii) the response window, ([150, 450] ms after the stimulus onset). It is noteworthy

that in order to avoid edge effects, the spectral content was only considered into the time-frequency regions delimited by their respective cones of influence (COIs) (Torrence and Compo, 1998). Thus, delta band was not analyzed because it is associated with a wavelet duration higher than the length of the baseline and response windows (i.e. 300 ms) (Bachiller, Poza, 2015, Roach and Mathalon, 2008). In this regard, it is recommended the use of 6 cycles to estimate the wavelet coefficients, but fewer cycles have been also used at the expense of frequency resolution (Roach and Mathalon, 2008). In this study, we used 2 cycles taken into account that the wavelet coefficients corresponding to the frequencies close to 4 Hz could have a small bias due to the frequency resolution (i.e., edge effects) (Roach and Mathalon, 2008).

Assignment of weights to brain graphs

In this study, graph weights were obtained by the event-related Coherence (*ERC*). *ERC* is used to represent the similarity between the spectral content of two electrodes i and j (Bachiller, Poza, 2015, Basar et al. , 2016):

$$ERC_{ij}(s) = \frac{|WCS_{ij}(s)|^2}{WCS_{ii}(s) \cdot WCS_{jj}(s)}, \quad (\text{A.4})$$

ERC is analogous to the squared Pearson correlation, which reflects the amount of variance of electrode i in each frequency that can be explained by a linear transformation of the wavelet coefficients in the electrode j (Roach and Mathalon, 2008). Hence, *ERC* represents the linear relationship between the amplitude of two signals in the spectral domain (Basar, Golbasi, 2016, van Diessen et al. , 2015).

ERC was chosen because it is a straightforward method, commonly used in previous EEG studies. Nonetheless, some concerns merit special attention (van Diessen, Numan, 2015). Firstly, nonlinear relationships are not considered. Secondly, *ERC* does not evaluate the causality, making impossible to make a distinction between direct and indirect relations. Finally, it is sensitive to volume conduction.

ERC was obtained for each time sample and each frequency (or scale). To assess the global behavior of network dynamics, *ERC* was averaged over all frequency range under study (4-70 Hz). Two adjacency matrices, which contain all connections between nodes, were obtained for each subject: one for the baseline window and other one for the response window. Thus, modulation of network

dynamics from baseline to response can be evaluated.

It is noteworthy that for subsequent analyses related to distance measures, such as path length, a distance matrix was computed as the inverse of the adjacency matrix. The adjacency matrix did not contain zero-valued edge weights, but for the diagonal. Therefore, there were not any infinite distances between nodes.

References

Bachiller A, Poza J, Gomez C, Molina V, Suazo V, Hornero R. A comparative study of event-related coupling patterns during an auditory oddball task in schizophrenia. *Journal of Neural Engineering*. 2015;12:016007.

Basar E, Golbasi BT, Tulay E, Aydin S, Basar-Eroglu C. Best method for analysis of brain oscillations in healthy subjects and neuropsychiatric diseases. *International Journal of Psychophysiology: Official Journal of the International Organization of Psychophysiology*. 2016;103:22-42.

Roach BJ, Mathalon DH. Event-related EEG time-frequency analysis: an overview of measures and an analysis of early gamma band phase locking in schizophrenia. *Schizophrenia Bulletin*. 2008;34:907-26.

Torrence C, Compo GP. A Practical Guide to Wavelet Analysis. *Bulletin of the American Meteorological Society*. 1998;79:61-78.

van Diessen E, Numan T, van Dellen E, van der Kooi AW, Boersma M, Hofman D, et al. Opportunities and methodological challenges in EEG and MEG resting state functional brain network research. *Clinical neurophysiology : official journal of the International Federation of Clinical Neurophysiology*. 2015;126:1468-81.



Contents lists available at ScienceDirect

NeuroImage: Clinical

journal homepage: www.elsevier.com/locate/ynicl

Deficits of entropy modulation in schizophrenia are predicted by functional connectivity strength in the theta band and structural clustering

Javier Gomez-Pilar^{a,1}, Rodrigo de Luis-García^{b,1}, Alba Lubeiro^c, Nieves de Uribe^d, Jesús Poza^{a,e,f}, Pablo Núñez^a, Marta Ayuso^g, Roberto Hornero^{a,e,f}, Vicente Molina^{c,d,e,*}

^a Biomedical Engineering Group, University of Valladolid, Paseo de Belén, 15, 47011 Valladolid, Spain

^b Imaging Processing Laboratory, University of Valladolid, Paseo de Belén, 15, 47011 Valladolid, Spain

^c Psychiatry Department, School of Medicine, University of Valladolid, Av. Ramón y Cajal, 7, 47005 Valladolid, Spain

^d Psychiatry Service, Clinical Hospital of Valladolid, Ramón y Cajal, 3, 47003 Valladolid, Spain.

^e Neurosciences Institute of Castilla y León (INCYL), Pintor Fernando Gallego, 1, 37007, University of Salamanca, Spain

^f IMUVA, Mathematics Research Institute, University of Valladolid, Valladolid, Spain

^g Neurophysiology Service, Clinical Hospital of Valladolid, Ramón y Cajal, 3, 47003 Valladolid, Spain

ARTICLE INFO

Keywords:

Schizophrenia
Entropy
Graph-theory
Connectivity
Fractional anisotropy
Negative symptoms

ABSTRACT

Spectral entropy (SE) allows comparing task-related modulation of electroencephalogram (EEG) between patients and controls, i.e. spectral changes of the EEG associated to task performance. A SE modulation deficit has been replicated in different schizophrenia samples. To investigate the underpinnings of SE modulation deficits in schizophrenia, we applied graph-theory to EEG recordings during a P300 task and fractional anisotropy (FA) data from diffusion tensor imaging in 48 patients (23 first episodes) and 87 healthy controls. Functional connectivity was assessed from phase-locking values among sensors in the theta band, and structural connectivity was based on FA values for the tracts connecting pairs of regions. From those data, averaged clustering coefficient (CLC), characteristic path-length (PL) and connectivity strength (CS, also known as density) were calculated for both functional and structural networks. The corresponding functional modulation values were calculated as the difference in SE and CLC, PL and CS between the pre-stimulus and response windows during the task. The results revealed a higher functional CS in the pre-stimulus window in patients, predictive of smaller modulation of SE in this group. The amount of increase in theta CS from pre-stimulus to response related to SE modulation in patients and controls. Structural CLC was associated with SE modulation in the patients. SE modulation was predictive of negative symptoms, whereas CLC and PL modulation was associated with cognitive performance in the patients. These results support that a hyperactive functional connectivity and/or structural connective deficits in the patients hamper the dynamical modulation of connectivity underlying cognition.

1. Introduction

Mental functions are partially based on the dynamic coordination of cerebral networks (Dehaene and Changeux, 2011; Tanaka, 1996; Varela et al., 2001) whose interactions evolve in hundreds of milliseconds (Bressler and Tognoli, 2006; Sporns, 2011). The temporal resolution of electroencephalography (EEG) allows the assessment of this dynamic coordination, which can be applied to the study of functional underpinnings of mental disorders. Measurements summarizing the EEG properties and their modulation with cognition can be useful for that purpose. One of these measurements is Spectral Entropy (SE), a parameter derived from information theory that estimates regularity by

quantifying the degree of uncertainty in a signal (Duff et al., 2013). Larger SE values correspond to more uniform spectra whose frequency content is broader (i.e., more random), and low SE values to spectra with only a few frequency components (i.e., more regular).

In schizophrenia, we have described a SE modulation deficit during a P300 task in response to relevant tones (Bachiller et al., 2014). SE decreased in healthy controls secondarily to task-related increased theta power, and both SE decrease and theta power increase were of smaller magnitude in patients (Bachiller et al., 2014), which seems coherent with the expected increase in theta band power during P300 (Mazaheri and Picton, 2005). Later, we replicated the same SE modulation deficit in schizophrenia in a larger and completely different

* Corresponding author.

E-mail address: vicente.molina@uva.es (V. Molina).

¹ Javier Gomez-Pilar and Rodrigo de Luis are co-first authors.

<https://doi.org/10.1016/j.nicl.2018.02.005>

Received 18 November 2017; Received in revised form 10 January 2018; Accepted 4 February 2018

Available online 06 February 2018

2213-1582/ © 2018 The Author(s). Published by Elsevier Inc. This is an open access article under the CC BY-NC-ND license (<http://creativecommons.org/licenses/by-nc-nd/4.0/>).

sample (Molina et al., 2017a), showing its relation to cognition and symptoms. In these reports we defined modulation as the difference in SE values between the pre-stimulus and the response windows of the P300 task being performed by the subjects. Neither treatment dose nor illness duration were associated to the SE deficit, also found in first episode patients.

Given the apparent robustness of the SE modulation deficit, we considered it worthy to attempt to characterize it. This could help describing a reliable functional alteration in schizophrenia. Since cognition during P300 involves a global network rather than focal engagement (Bledowski et al., 2004), we hypothesized that the analysis of global properties of the functional network would help to identify underpinnings of the SE modulation deficit in schizophrenia. Global network properties can be assessed at system level using graph theory. Thus, parameters derived from graph-theory can help assessing both basal network properties predictive of SE modulation and properties of global network dynamics associated to SE modulation deficits.

Among the graph parameters of interest to this purpose, local clustering coefficient (*CLC*) is related to the degree of local connectivity. Specifically, clustering coefficient is the ratio between the number of triangles in which a node is included and the total number of possible triangles that include the node. This measure, when averaged across the network, indicates the segregation and local efficiency for information transfer. In turn, characteristic path length (*PL*) is the average of shortest distances for all possible pairs of nodes. Thus, *PL* is related to information integration across areas. Mean connectivity strength (*CS*, sometimes also known as density) in a weighted graph can be interpreted as the average of connections among nodes in a network. The application of these parameters to functional connectivity analyses is based on the degree of similarity of signals, based in turn on phase-locking values (*PLV*) of the signals between regions or (for the EEG) sensors. These parameters can be also applied to structural connectivity measurements derived from diffusion magnetic resonance imaging (dMRI), such as fractional anisotropy (*FA*), which may allow a description of the dependence of functional connectivity modulation on structural connectivity. Although a direct relation between both connectivity dimensions could seem intuitive, functional connections are found between regions without direct anatomical connections (Honey et al., 2009).

Our hypotheses are that functional (prior to cognitive activity) and structural graph-derived network measurements would predict task-related SE modulation and that the dynamics of functional network parameters would be associated to SE modulation. As in previous reports (Bachiller et al., 2014; Mazaheri and Picton, 2005) modulation will be defined and the corresponding EEG change (for SE and functional network parameters) associated to task performance. These ideas could reveal relevant insights on the functional deficits in schizophrenia. Based on previous findings supporting a smaller increase of theta power in patients in the response to target (Bachiller et al., 2014) and the relevance of theta power for the task used, the P300 (Mazaheri and Picton, 2005), we focused our analyses on the theta EEG band.

2. Subjects and methods

We included 48 schizophrenia subjects (of them, 23 first episodes (FE) and 87 healthy subjects with normal hearing. Patients were diagnosed according to the Diagnostic and Statistical Manual of Mental Disorders, 5th edition. They were receiving stable doses of antipsychotic monotherapy. Of them, MRI data were also collected in 33 patients (20 males) and 24 controls (15 males). Out of the sample, 42 patients and 65 controls were included in a previous report on SE modulation deficit in schizophrenia (Molina et al., 2017a).

First episode patients were treated with antipsychotics for less than 72 h. prior to MRI and EEG data acquisition, with a wash-out period of 24 h prior to the acquisitions to avoid possible bias due to the selection of patients able to cooperate during EEG acquisition without prior

Table 1

Demographic, clinical and cognitive characteristics of patients and controls, as well as latency and amplitude of the P300 (P3b) potential. Between-group statistically significant differences were marked with asterisks: ****p* < 0.001.

	Controls	Patients
Age (years)	30.51 (10.77)	33.58 (9.27)
Antipsychotic dose (CPZ equivalents)	N/A	377.92 (196.94)
Duration (months)	N/A	97.84 (116.94)
Sex	44/43	25/23
Positive symptoms	N/A	11.63 (3.39)
Negative symptoms	N/A	18.03 (7.52)
Total PANSS score	N/A	54.35 (18.56)
Verbal memory***	51.65 (8.26)	33.92 (12.74)
Working memory***	21.46 (3.90)	15.81 (5.01)
Motor speed***	68.59 (17.84)	58.14 (14.41)
Verbal fluency***	27.13 (5.33)	17.99 (5.70)
Performance speed***	68.79 (13.25)	42.83 (15.78)
Problem solving***	17.54 (2.72)	15.40 (4.64)
Total IQ***	111.83 (11.87)	91.22 (14.19)
WCST (perseverative errors)***	10.17 (5.81)	27.31 (47.43)
WCST (completed categories)***	5.79 (0.72)	4.39 (1.87)
P3b amplitude (microvolts)***	3.20 (1.76)	1.92 (1.21)
P3b latency (milliseconds)	472.28 (67.54)	461.53 (87.57)

treatment.

Exclusion criteria were: (i) any neurological illness; (ii) history of cranial trauma with loss of consciousness; (iii) past or present substance abuse, except nicotine or caffeine (iv) intelligence quotient (IQ) smaller than 70; and (v) for patients, any other psychiatric process, and (vi) for controls, any psychiatric or neurological diagnosis or treatment.

Schizophrenia symptoms were scored using the Positive and Negative Syndrome Scale (PANSS) (Kay et al., 1987). Healthy controls were recruited through advertisements. Demographic and clinical data are shown in Table 1.

Cognitive data for both groups were collected using: the Wechsler Adult Intelligence Scale, WAIS-III (IQ), the Wisconsin Card Sorting Test (WCST; completed categories and percentage of perseverative errors), and the Spanish version of the Brief Assessment in Cognition in Schizophrenia Scale (BACS)(Segarra et al., 2011).

After receiving full printed information, subjects gave their written informed consent. The ethical committees of the Hospital Clínico de Valladolid endorsed the study.

2.1. EEG processing

2.1.1. EEG acquisition and preprocessing

EEG recordings were obtained following MRI scans, after a resting period of 30 minutes. Data were recorded using a 17-channel EEG system (BrainVision®, Brain Products GmbH). Active electrodes were placed in an elastic cap at Fp1, Fp2, F3, F4, F7, F8, C3, C4, P3, P4, O1, O2, T5, T6, Fz, Pz and Cz (international 10–20 system). Impedance was kept under 5 kΩ. Sampling frequency was 500 Hz. During EEG acquisition, each channel was referenced over Cz electrode and re-referenced to the average activity of all active sensors (Bledowski et al., 2004; Gomez-Pilar et al., 2018). Thirteen minutes of eyes-closed EEG was obtained during an auditory odd-ball 3-stimulus paradigm, which consisted of 600 random sequences of target (500 Hz-tone, probability 0.2), distractor (1000 Hz-tone, probability 0.2), and standard (2000 Hz-tone, probability 0.6) tones. The tone duration was 50 ms, rise and fall time being 5 ms and intensity being 90 dB. Inter-stimulus interval between tones randomly jittered between 1.16 and 1.44 s. The participants were asked to press a button whenever they detected the target tones. Target tones were considered 'attended tones' when they were followed by a button press. Only 'attended' target tones were taken into account for further analysis (Gomez-Pilar et al., 2015). Alertness differences across groups were controlled by comparing accuracy of target responses.

A three-step artifact rejection algorithm was applied to minimize electrooculographic and electromyographic contamination (Bachiller et al., 2015a): (i) an Independent Component Analysis (ICA) was carried out to discard noisy ICA components; (ii) after ICA reconstruction, EEG signals were divided into trials of 1 s length (ranging from 300 ms before stimulus onset to 700 ms after stimulus onset); and (iii) an automatic method was applied to reject trials whose amplitude exceeded an adaptive statistical-based threshold (Nunez et al., 2017). In this last method, the mean and standard deviation of each channel and for each stimulus was computed. Then, trials that exceeded mean $\pm 4 \times$ standard deviation in at least two channels were discarded. This ensures to obtain artifact-free trials for all channels.

Signals were band-pass filtered between 1 and 70 Hz. In addition, a 50 Hz notch filter was used to remove the power line artifact.

2.1.2. EEG entropy

Entropy is a thermodynamic function adapted from information theory. Entropy can be seen as a measure of the irregularity of a signal, estimating the degree of disorder by assessing the distribution of its spectral components. In this study, the continuous wavelet transform was used to compute the entropy of the signals. The spectral entropy (SE) can be defined as follows:

$$SE(k) = \frac{1}{\log(M)} \cdot \sum_s WS_n(k, s) \cdot \log[WS_n(k, s)], \quad (1)$$

where WS_n is the normalized wavelet scalogram, k is the time interval, and s the scaling factor of the mother wavelet. In order to avoid edge effects in continuous wavelet transform (CWT), the cone of influence (COI) for pre-stimulus and response time windows was computed. The SE was computed in the broadband, i.e. between 1 Hz and 70 Hz, since we want to describe the overall SE dynamics.

2.1.3. EEG brain graphs

EEG brain graphs provide a useful tool to characterize the functional brain network. Using this approach, network nodes are represented by electrodes, whereas network edges are set by computing the neural coupling between pairs of electrodes. Different methods can be used to estimate the neural coupling. In this study, we selected the PLV across successive trials (Lachaux et al., 1999), since it is sensitive to both low-amplitude oscillatory EEG components (Spencer et al., 2003) and nonlinearities (van Diessen et al., 2015). PLV can be computed using different methodologies. We used the CWT to compute the phase information from each trial (Bob et al., 2008). As in the SE computation, cones of influence were also considered.

Functional connectivity matrices were constructed using PLV values to characterize the neural coupling between each pair of electrodes. With no thresholding applied, these matrices ranged between 0 and 1, thereby, functional connectivity matrices were also constrained based on PLV ranged between 0 and 1: a value of 0 is obtained when signals do not show any synchronization and a value of 1 is observed when two signals are perfectly synchronized.

2.1.3.1. Graph parameters. After using CWT approach to perform filtering and phase extraction in one operation, the PLV between two signals $x(t)$ and $y(t)$ can be obtained evaluating the variability of the phase difference across successive trials:

$$PLV_{xy}(k, s) = \frac{1}{N_t} \left| \sum_{n=1}^{N_t} e^{i\Delta\varphi_{xy}(k, s, n)} \right|, \quad (2)$$

where N_t is the number of trials, $\Delta\varphi_{xy}$ is the instantaneous phase difference between x and y signals, k is the time interval, and s the scaling factor of the mother wavelet.

Firstly, the event-related wave was computed for each subject by the synchronized averaging of all the trials corresponding to attended target tones. Secondly, a low-pass finite impulse response filter with

cut-off frequency of 8 Hz was applied to the evoked wave in order to obtain only the components related to delta and theta frequency bands. Thirdly, the maximum amplitude of the low-pass filtered evoked wave in the Pz channel was located into a window ranging from 250 to 550 ms from the stimulus onset (Bachiller et al., 2015b). The corresponding sample to the maximum amplitude was used as a central time sample of the response window. Finally, the response window was set on ± 150 ms around the central time sample.

Normalized *CLC* and *PL* can be defined as:

$$CLC = \frac{C}{C_{random}}, \quad (3)$$

$$PL = \frac{L}{L_{random}}, \quad (4)$$

where C and L can be defined as:

$$C = \frac{1}{N} \sum_{i=1}^N \frac{\sum_{j \neq i} w_{ij} w_{ji}}{\sum_{j \neq i} w_{ij} w_{ji}}, \quad (5)$$

$$L = \frac{N(N-1)}{\sum_{i=1}^N \sum_{j \neq i} \frac{1}{L_{ij}}}, \quad (6)$$

Finally, the connectivity strength was computed using the network density as:

$$D = \frac{\sum_{i=1}^N \sum_{j > i} w_{ij}}{T}. \quad (7)$$

In the previous equations, w_{ij} refers to PLV between nodes i and j (for functional analyses) or to the structural connectivity between two regions using the streamlines from MRI (for structural analyses). N is the total number of nodes of the network (17 in EEG analyses, 84 in MRI). L_{ij} is defined as the inverse of the network edge weight w_{ij} (Stam et al., 2009). Finally, in Eq. (7), $T = N(N-1)/2$, which is the total number of connections in an undirected graph.

2.1.4. Segmentation of the EEG response

The modulation of the graph parameters along the odd-ball task was assessed by considering two windows: (i) the pre-stimulus window, which is a period of expectation before the stimulus onset, ranging from -300 ms to the stimulus onset; and (ii) the response window, chosen to capture the P3b response (150 to 450 ms after stimulus onset).

2.2. MRI acquisition and processing

A Philips Achieva 3 Tesla Unit (Philips Healthcare, Best, The Netherlands) at the MRI facility from Valladolid University was employed. Acquisitions consisted of a T1-weighted (anatomical) image and diffusion weighted images. A pipeline processing was carried out in order to obtain structural connectivity matrices (structural connectomes), as described in (Molina et al., 2017b).

For the T1 images, a turbo field echo (TFE) sequence was employed, and parameters included the following: 256×256 matrix size, $1 \times 1 \times 1 \text{ mm}^3$ of spatial resolution and 160 slices covering the whole brain.

With regard to the diffusion weighted images (DWIs), a single shot EPI (echo planar imaging) spin echo sequence was employed. 61 gradient directions and one baseline volume were acquired, with $b\text{-value} = 1000 \text{ s/mm}^2$, $2 \times 2 \times 2 \text{ mm}^3$ of voxel size, 128×128 matrix and 66 axial slices covering the entire brain.

From the acquired images, a processing pipeline was designed in order to employ both the T1-weighted and the diffusion images for the construction of structural connectivity matrices. This pipeline is composed of several steps and uses different freely available software tools (FSL, Freesurfer, MRTRIX).

The processing pipeline of the acquired MRI volumes is designed to

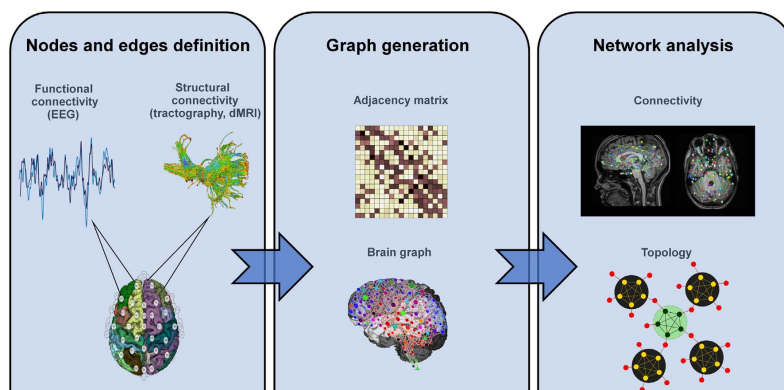


Fig. 1. Schematic overview for the network analyses from the structural and functional data.

obtain structural connectivity matrices by using both the anatomical (T1-weighted) and diffusion images.

Firstly, non-brain structures were removed from the T1 images by means of BET, a brain extraction tool from the FSL software (<http://fsl.fmrib.ox.ac.uk>) (Smith, 2002). Next, 84 cortical structures were segmented using Freesurfer (<https://surfer.nmr.mgh.harvard.edu>) (Fischl et al., 2004; Desikan et al., 2006). Also starting from the same T1 images, gray matter, white matter and cerebrospinal fluid (CSF) were also segmented, and subcortical gray matter structures were delineated using FAST and FIRST utilities from FSL, respectively (Patenaude et al., 2011; Zhang et al., 2001), and combined into a volume called 5tt (5-tissue-type) image.

At the same time, and starting from the diffusion weighted images (DWI), the brain was extracted using DWI2MASK tool from MRtrix (www.mrtrix.org) (Dhollander and Connelly, n.d.). Afterwards, orientation distribution functions were estimated from the diffusion data using spherical deconvolution, employing DWI2RESPONSE and DWI2FOD tools from MRtrix (Tournier et al., 2007). This method allows the use of diffusion information beyond the tensor model, thus overcoming traditional problems of tensor-based tractography such as its bad behavior in fiber crossings and crossings, which are abundant in the white matter. The method of choice for fiber tracking (anatomically-constrained tractography, using TCKGEN -ACT) uses both the diffusion data and the 5tt image (after registration) in order to discard streamlines that are anatomically unfeasible. Two million streamlines were generated for each subject.

In order to describe the diffusion at each voxel, diffusion tensors were estimated using a least squares method (Salvador et al., 2005), and Fractional Anisotropy (FA) volumes were computed from the diffusion tensors using DTIFIT tool from FSL. FA quantifies the amount of anisotropy in the diffusion tensor or, equivalently, how much it deviates from a totally isotropic diffusion. FA is usually interpreted as a descriptor of white matter integrity, and decreases in FA have been related to alterations in the white matter due to several factors (demyelination and axonal destruction, among others).

Finally, connectivity matrices were constructed from the tractography results and the (registered) cortical segmentations using TCK2CONNECTOME tool from MRtrix. When streamlines (tractography output) connecting two cortical regions were found, this tool computes the average FA for that specific connection. Thus, 84×84 connectivity matrices were obtained using FA as connectome metrics. A threshold was not applied to the connectivity matrices; however, some matrix coefficients can be equal to zero when streamlines are not found for that

particular connection.

Similar dMRI analyses have been reported in schizophrenia (Di Biase et al., 2017) and other neurocognitive conditions (Jones et al., 2015).

2.3. Graph-theory parameters

From both the structural and functional connectivity matrices, we calculated three graph-theory parameters to characterize global properties of the brain network: (i) connectivity strength by means of network density (CS), (ii) network segregation using *CLC*, and (iii) network integration by means of *PL* (Rubinov and Sporns, 2010). *CLC* and *PL* were computed over an ensemble of 50 surrogate random networks, which were used to normalize *CLC* and *PL* values obtained from the original networks (Stam et al., 2009). This widespread method is useful to obtain graph parameters independent of the network edge weights and the network size.

As opposed to the broadband approach used to compute de SE, functional parameters were computed into the theta frequency range during pre-stimulus and task-related modulation (i.e. difference between the response and the pre-stimulus windows) and will be referred to as *EEG-PL_{PRE}*, *EEG-CS_{PRE}* and *EEG-CLC_{PRE}*, for the pre-stimulus parameters, and as *EEG-PL_{MOD}*, *EEG-CS_{MOD}* and *EEG-CLC_{MOD}*, for the modulation-related parameters. On the other hand, structural parameters will be referred to as *dMRI-PL*, *dMRI-CS* and *dMRI-CLC*.

The present data do not duplicate our published EEG network analyses in schizophrenia (Gomez-Pilar et al., 2017), since those were performed in a different sample using evoked response instead of single-trial analyses.

A schematic overview for the network analyses both for functional and for structural data is shown in Fig. 1.

3. Statistics

After testing parametric test assumptions, demographic, cognitive and P300 latency and amplitude values were compared between patients and controls using Chi-square and *t* tests.

Network measurements were also compared between patients and controls using *t* tests. When significant differences were found between groups, the corresponding values were compared between chronic and FE patients.

To test the main study hypothesis, in a first step we applied a principal component analysis (PCA) with varimax rotation to individual

SE modulation values, thus reducing the number of SE modulation measurements (one per electrode) to one or few factors capturing most of the corresponding variance for each case. The resulting individual factor scores were saved for further analyses. We compared these SE modulation factor scores between patients and controls using *t* tests. Nodal SE values were compared between patients and controls in previous reports (Bachiller et al., 2014; Molina et al., 2017a) and therefore not shown here.

Then, after testing for normality and homoscedasticity in the distribution of graph parameters, we applied two stepwise multivariate regression models to assess: (i) the baseline predictors of entropy modulation, and (ii) the correlates of entropy modulation. In both cases, the dependent variables were the SE modulation factor scores. For all the analyses, the level of significance was set to 0.05.

In the first analysis, we introduced the pre-stimulus graph parameters with significant between-group differences as independent (predictive) variables. For the second analysis, independent variables were modulation values in these parameters, showing significant differences between patients and controls. These analyses were separately performed in patients and controls, since previous analyses showed a statistically significant difference between groups for both entropy and graph-parameters (Bachiller et al., 2014; Molina et al., 2017a; Gomez-Pilar et al., 2017) and we hypothesized different associations in both groups. We discarded relevant collinearity effects with tolerance values.

When significant between-groups differences were found we repeated the comparisons including only FE patients and controls to discard that differences were merely an effect of chronicity and/or treatment.

In the group with dMRI data, we studied the associations between structural graph parameters and SE modulation. Since the distribution of structural graph parameters differed from normality in the patients, their association with SE modulation was assessed by means of Spearman correlations.

Clinical and cognitive correlates of graph parameters were assessed using multivariate stepwise regression models, where predictive variables were graph parameters with significant differences between groups. We also calculated the possible relationships between treatment doses, illness duration and functional parameters.

A database with the main data supporting the present results is available (Mendeley Data doi:10.17632/g9crh5b6bz.2).

4. Results

There were no significant differences in age or sex distribution between patients and controls. Patients showed a significant generalized cognitive deficit and reduced P300 amplitude (table 1).

Factor analysis for SE modulation yielded a two-factor solution factor (Table 2) that explained 67.11 % of total variance. The first factor was positively contributed by frontal anterior and medial (Fp1, Fp2, F3, F4, Fz), central (C3, C4, Cz) temporal (T5, T6), occipital (O1, O2), sensors (eigenvalue 10.10, 59.44% of variance), while the second factor was contributed by frontal lateral (F7, F8) and parietal (P3, P4, Pz) sensors (eigenvalue 1.41, 8.33% of variance). Scores for the first factor were significantly higher for the patients ($t = 4.20$, $df = 133$, $p < 0.001$), reflecting a smaller modulation at the sensors included in this factor (since SE values decreased at the response window and thus the difference should be negative). FE patients alone also showed more positive values for the first factor (i.e., smaller SE modulation) than controls (mean 0.206, sd 0.695, $t = 2.03$, $df = 108$, $p = 0.04$)

4.1. Comparison of functional network parameters

Patients showed larger connectivity strength values at the pre-stimulus window (EEG-CS_{PRE}) for the theta band ($t = 3.03$, $df = 133$, $p = 0.003$), and smaller modulation values: EEG-CLC_{MOD} ($t = -2.42$, $df = 133$, $p = 0.017$), EEG-PL_{MOD} ($t = -2.77$, $df = 133$, $p = 0.006$)

Table 2

Factor structure resulting from the principal components analysis of SE modulation values for each sensor. Factor loads are shown.

	Component	
	1	2
FP1	0.604	0.551
FP2	0.602	0.527
F3	0.841	0.276
F4	0.739	0.345
C3	0.576	0.492
C4	0.542	0.529
P3	0.282	0.853
P4	0.267	0.764
O1	0.720	0.375
O2	0.704	0.372
F7	0.377	0.705
F8	0.324	0.751
T5	0.666	0.420
T6	0.629	0.378
Fz	0.918	0.098
Cz	0.715	0.374
Pz	0.268	0.844

and EEG-CS_{MOD} ($t = -2.89$, $df = 133$, $p = 0.004$) in that band (Table 3). Those values were used as predictors in further analyses. Chronic patients showed significantly larger EEG-CSPRE values than FE patients, but not significant differences for EEG-CLC_{MOD}, EEG-PL_{MOD} and EEG-CS_{MOD} were found between chronic and FE patients (Table S1, see Supplementary material).

4.2. Prediction of SE modulation

4.2.1. Functional predictors

In controls, pre-stimulus graph parameters were not predictive of factor scores summarizing SE modulation. In patients, theta band EEG-CS_{PRE} directly predicted scores of the first factor for SE modulation ($R^2 = 0.188$, $df = 1,46$; $F = 10.65$; $\beta = 0.43$; $p = 0.01$; Fig. 2). Thus, a larger average strength of pre-stimulus functional connections in this band was associated with smaller SE modulation (since SE decreased from pre-stimulus to response).

In the FE patients considered alone, pre-stimulus EEG-CS_{PRE} did not predict SE modulation.

4.2.2. Structural predictors

In controls, no significant associations were found between structural brain network parameters and SE modulation ($-0.10 < R < 0.20$). In patients, first factor scores for SE modulation were negatively associated to structural dMRI-CLC ($R^2 = 0.144$, $p = 0.03$). Thus, larger structural clustering was associated to better task-related SE modulation (Fig. 3).

Table 3

Spectral entropy (factor scores) and graph parameters (pre-stimulus and modulation) in patients and controls. Statistically significant differences are marked using asterisks: * $p < 0.05$; ** $p < 0.01$; *** $p < 0.005$.

	Controls	Patients
Entropy modulation factor scores (Factor 1)***	-0.31 (1.13)	0.44 (0.66)
Entropy modulation factor scores (Factor 2)	0.06 (1.12)	-0.13 (0.53)
EEG-CLC _{PRE}	1.01 (0.00)	1.01 (0.01)
EEG-PL _{PRE}	1.10 (0.02)	1.10 (0.03)
EEG-CS _{PRE} **	0.34 (0.04)	0.36 (0.04)
EEG-CLC _{MOD} *	0.00 (0.01)	0.00 (0.01)
EEG-PL _{MOD} **	0.01 (0.02)	0.00 (0.02)
EEG-CS _{MOD} ***	0.02 (0.03)	0.01 (0.02)

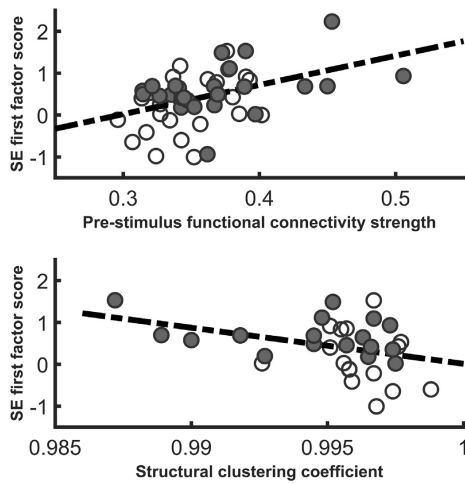


Fig. 2. Scatterplot showing the association in the patients between A) pre-stimulus theta density and SE modulation for the sensors included in the first factor from the principal components analysis and B) between structural clustering coefficient and SE modulation (first factor).

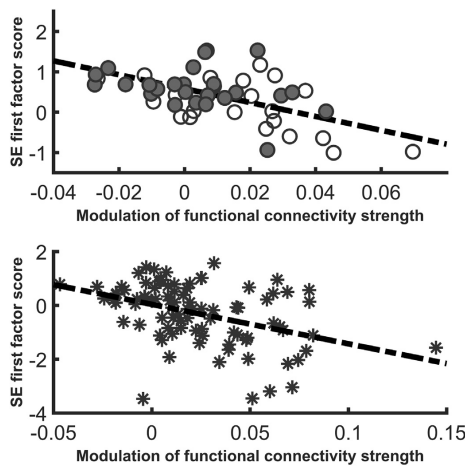


Fig. 3. Scatterplot showing the association of theta band density modulation and SE modulation (first factor) in patients (A) and controls (B). Open circles: FE patients; solid circles: chronic patients; stars: healthy controls. In both groups, the modulation of connectivity strength was inversely associated with SE modulation, but pre-stimulus connectivity strength was associated with SE modulation only for patients (see text).

4.3. Underpinnings of entropy modulation

In controls, first factor scores for SE modulation were inversely associated to $EEG-CS_{MOD}$ ($R^2 = 0.171$, $df = 1,85$; $F = 17.58$; $\beta = -0.414$, $p < 0.0001$; Fig. 3). Therefore, larger increases of $EEG-CS_{MOD}$ (i.e., larger global connectivity increases in the theta band from pre-stimulus

to response) were associated with more negative values of SE modulation. In other words, larger increases of theta connectivity strength were associated to a higher task related SE modulation, since an SE decrease from pre-stimulus to response is the expected task-related response. SE modulation scores for the sensors included in the second factor were not predicted by network modulation properties in controls.

In patients, SE modulation for the electrodes included in the first factor was similarly inversely associated to $EEG-CS_{MOD}$ in the theta band ($R^2 = 0.380$, $df = 1,46$; $F = 28.21$; $\beta = -0.617$ $p < 0.0001$; Fig. 3). Therefore, larger increases of theta band $EEG-CS_{MOD}$ were also associated with higher SE modulation in patients.

In the FE patients considered alone, SE modulation for the first factor was also inversely associated to theta band $EEG-CS_{MOD}$ ($R^2 = 0.318$, $df = 1,21$; $F = 9.32$; $\beta = -0.564$; $p = 0.006$; Fig. 3).

As in controls, SE modulation scores for the sensors included in the second factor were not predicted by network modulation properties.

4.4. Clinical and cognitive correlates

In the patients, $EEG-CS_{MOD}$ was inversely associated with negative symptoms ($R^2 = 0.117$, $df = 1,46$; $F = 5.58$; $\beta = -0.343$ $p = 0.023$). In this group, $EEG-CLC_{MOD}$ predicted verbal memory ($R^2 = 0.102$, $df = 1,46$; $F = 4.54$; $\beta = 0.319$, $p = 0.039$), working memory ($R^2 = 0.208$, $df = 1,46$; $F = 10.25$; $\beta = 0.456$ $p = 0.003$) and verbal fluency ($R^2 = 0.121$, $df = 1,46$; $F = 4.85$; $\beta = 0.348$, $p = 0.035$) performance, and $EEG-PL_{MOD}$ predicted problem solving performance ($R^2 = 0.190$, $df = 1,46$; $F = 8.92$; $\beta = 0.507$ $p = 0.005$).

In controls, modulation of theta network properties was unrelated to cognitive performance.

There were no significant associations between treatment doses or duration and, on the other hand, SE modulation and network parameters.

5. Discussion

In this study, SE modulation at frontal anterior, central, temporal and occipital electrodes (contributing to most of SE variance) was inversely associated with the pre-stimulus functional connectivity strength ($EEG-CS_{PRE}$) in patients. Moreover, a larger theta CS increase from pre-stimulus to response windows ($EEG-CS_{MOD}$) leads to higher SE modulation.

Our data also reveal a large pre-stimulus theta $EEG-CS_{PRE}$ in patients. This result, considered together with the smaller change of theta $EEG-CS$ modulation (i.e., in the patients, this parameter increased from pre-stimulus to response windows to a smaller degree than in controls), suggests that a hyperactive baseline contributes to a smaller capacity for modulation.

It worth mentioning that the first factor in the PCA included the sensors where significant entropy modulation differences were found in our previous SE comparison between patients and controls (F3, C3, C4, Fz and Cz) (Molina et al., 2017a). Thus, the first factor summarized the modulation in the sensors with significant between-group differences. This would imply that theta $EEG-CS$ (both at baseline and its task-related modulation) is relevant to explain the modulation deficits found in schizophrenia.

Connectivity strength represents an average of the graph functional connections. The direct association in the patients between $EEG-CS_{PRE}$ and SE modulation suggests that a larger number of global functional connections in the pre-stimulus period (in the theta band of the functional network) is associated with a smaller task-related change in SE. This seems coherent with a previous finding at the sensor-level: larger values of noise power (likely reflecting induced activity) were associated to smaller entropy modulation in a different sample (Molina et al., 2016). Larger broadband (Winterer et al., 2004) and gamma (Diez et al., 2013) noise power was earlier reported in schizophrenia. Taken together, these results support a functional hyper-connectivity

state in schizophrenia patients that may hamper modulation in the functional network, which also seems coherent with previous data with functional magnetic resonance (Manoach, 2003).

Our functional network analysis is based on connectivity derived from PLV between sensors. Since phase synchrony likely reflects the coordinated activation of neural ensembles between regions (Roach and Mathalon, 2008), the larger density values at baseline in the patients might reflect an over-activation of neural ensembles, which, according to their inverse association with SE modulation, hampers the flexibility of neural assemblies with task demands. One possible reason behind these findings might be related to the described inhibitory hypofunction of the cortex in schizophrenia (Lewis et al., 2012), given the role of GABA cells in the appropriate building of transitory neural assemblies underlying cognition (Buzsáki, 2006). Values of $EEG-CS_{MOD}$ were associated to entropy modulation in both control and schizophrenia groups, whereas in the case of patients, $EEG-CS$ was higher at pre-stimulus and its pre-post stimulus modulation was smaller. Therefore, a quantitative difference seems more likely than a qualitative, categorical difference in the underpinnings of such modulation between patients and controls.

It is interesting that negative symptoms were predicted by $EEG-CS_{MOD}$, but cognitive performance was instead predicted by modulation in $EEG-CLC_{MOD}$ and $EEG-PL_{MOD}$. This may imply that cognitive abilities are underpinned by a reorganization of network properties more readily reflected in graph parameters. For instance, local and inter-regional changes in connectivity may be more easily captured by CLC than by SE modulation, even if the latter was previously reduced to two factors and thus likely reflects a more global effect.

The association found in the patients between SE modulation and structural network properties ($dMRI-CLC$) suggests that density and integrity of short-distance structural connections (clustering reflects the connections among regions connected to a given node) facilitates the modulation of functional connectivity. Structural properties (FA) of interregional connections may thus facilitate the formation of neural assemblies underlying task response. Widespread alterations of white matter integrity (which likely produce structural connectivity deficits) have been reported in schizophrenia using dMRI (Ellison-Wright and Bullmore, 2009).

Our work has limitations, most notably the absence of a treatment-naïve group. However, FE patients showed similar patterns of functional connectivity differences and treatment doses did not relate to entropy or graph parameters. Also, since both entropy and density modulation were obtained from the same dataset, it might be considered that their relation would result from data redundancy. However, both parameters reflect completely different properties of EEG dynamics and connectivity strength measurements help characterizing SE deficit in the patients. In addition, EEG is not completely free of volume conduction, even using a reference average approach as in the present study. Nevertheless, dMRI data can be used as control for the field spread effect. Finally, the number of EEG sensors was low, but this may be a relatively minor problem since we did not attempt to localize sources.

In conclusion, our findings suggest that an excess of pre-stimulus functional connectivity in the theta band and a deficit of structural clustering hamper SE modulation of the EEG, and this deficit might be underpinned by a smaller reorganization of connectivity, with a reduced formation of transitory functional connections.

Supplementary data to this article can be found online at <https://doi.org/10.1016/j.nicl.2018.02.005>.

Acknowledgements

This research project was supported in part by grants from Instituto de Salud Carlos III under project PI15/00299, Consejería de Educación de Castilla y León project VA057P17, “Gerencia Regional de Salud de Castilla y León” under projects GRS 1263/A/16 and GRS 1485/A/17,

and “Ministerio de Economía y Competitividad” and FEDER under grants TEC2014-53196-R and TEC2013-44194-P; by ‘European Commission’ and FEDER under project ‘Análisis y correlación entre el genoma completo y la actividad cerebral para la ayuda en el diagnóstico de la enfermedad de Alzheimer’ (Cooperation Programme Interreg V-A Spain-Portugal POCTEP 2014-2020). J. Gomez-Pilar was in receipt of a grant from University of Valladolid and A. Lubeiro was in receipt of a grant from Consejería de Educación de la Junta de Castilla y León.

Role of funding sources

The funding sources had no role in the study design; collection, analysis or interpretation of data; in the writing of the report or the decision to submit the manuscript for publication.

Declaration of interests

The authors have no conflicts of interest to declare.

References

- Bachiller, A., Diez, A., Suazo, V., Dominguez, C., Ayuso, M., Hornero, R., et al., 2014. Decreased spectral entropy modulation in patients with schizophrenia during a P300 task. *Eur Arch Psychiatry Clin Neurosci*. 264 (6), 533–543 (Sep, PubMed PMID: 24496581). Epub 2014/02/06. eng.
- Bachiller, A., Poza, J., Gomez, C., Molina, V., Suazo, V., Hornero, R., 2015a. A comparative study of event-related coupling patterns during an auditory oddball task in schizophrenia. *J Neural Eng*. 12 (1), 016007 (Feb, PubMed PMID: 25474418). Epub 2014/12/05. eng.
- Bachiller, A., Romero, S., Molina, V., Alonso, J.F., Mananas, M.A., Poza, J., et al., 2015b. Auditory P3a and P3b neural generators in schizophrenia: an adaptive sLORETA P300 localization approach. *Schizophr Res*. 169 (1–3), 318–325 (Dec, PubMed PMID: 26481687). Epub 2015/10/21. eng.
- Bledowski, C., Prvulovic, D., Hoehstetter, K., Scherg, M., Wibrall, M., Goebel, R., et al., 2004. Localizing P300 generators in visual target and distractor processing: a combined event-related potential and functional magnetic resonance imaging study. *J Neurosci*. 24 (42), 9353–60 (Oct 20, PubMed PMID: 15496671). eng.
- Bob, P., Palus, M., Susta, M., Glaslova, K., 2008. EEG phase synchronization in patients with paranoid schizophrenia. *Neurosci Lett*. 447 (1), 73–77 (Dec 05, PubMed PMID: 18835328). Epub 2008/10/07. eng.
- Bressler, S.L., Tognoli, E., 2006. Operational principles of neurocognitive networks. *Int J Psychophysiol*. 60 (2), 139–148 (May, PubMed PMID: 16490271). Epub 2006/02/24. eng.
- Buzsáki, G., 2006. Diversity of Cortical Functions: Inhibition. *Rhythms of the Brain*. Oxford University Press, New York, pp. 61–79.
- Dehaene, S., Changeux, J.P., 2011. Experimental and theoretical approaches to conscious processing. *Neuron*. 70 (2), 200–227 (Apr 28, PubMed PMID: 21521609). Epub 2011/04/28. eng.
- Desikan, R.S., Segonne, F., Fischl, B., Quinn, B.T., Dickerson, B.C., Blacker, D., et al., 2006. An automated labeling system for subdividing the human cerebral cortex on MRI scans into gyral based regions of interest. *Neuroimage*. 31 (3), 968–980 (Jul 01, PubMed PMID: 16530430). Epub 2006/03/15. eng.
- Dholanier T, Connelly A. Unsupervised 3-tissue response function estimation from single-shell or multi-shell diffusion mr data without a co-registered t1 image. ISMRM Workshop on Breaking the Barriers of Diffusion MRI2016.
- Di Biase, M.A., Cropley, V.L., Baune, B.T., Olver, J., Amminger, G.P., Phassouliotis, C., et al., 2017. White matter connectivity disruptions in early and chronic schizophrenia. *Psychol Med*. 22, 1–14 (May, PubMed PMID: 28528586). Epub 2017/05/23. eng.
- van Diessen, E., Numan, T., van Dellen, E., van der Kooij, A.W., Boersma, M., Hofman, D., et al., 2015. Opportunities and methodological challenges in EEG and MEG resting state functional brain network research. *Clin Neurophysiol*. 126, 1468–1481.
- Diez, A., Suazo, V., Casado, P., Martin-Loeches, M., Molina, V., 2013. Spatial distribution and cognitive correlates of gamma noise power in schizophrenia. *Psychol Med*. 43 (6), 1175–1186 (Sep 11, PubMed PMID: 22963867). Epub 2012/09/12. Eng.
- Duff, B.J., Macritchie, K.A., Moorhead, T.W., Lawrie, S.M., Blackwood, D.H., 2013. Human brain imaging studies of DISC1 in schizophrenia, bipolar disorder and depression: a systematic review. *Schizophr Res*. 147 (1), 1–13 (Jun, PubMed PMID: 23602339). Epub 2013/04/23. eng.
- Ellison-Wright, I., Bullmore, E., 2009. Meta-analysis of diffusion tensor imaging studies in schizophrenia. *Schizophr Res*. 108 (1–3), 3–10 (Mar, PubMed PMID: 19128945). Epub 2009/01/09. eng.
- Fischl, B., van der Kouwe, A., Destrieux, C., Halgren, E., Segonne, F., Salat, D.H., et al., 2004. Automatically parcellating the human cerebral cortex. *Cereb Cortex*. 14 (1), 11–22 (Jan, PubMed PMID: 14654453). Epub 2003/12/05. eng.
- Gomez-Pilar, J., Poza, J., Bachiller, A., Gómez, C., Molina, V., Hornero, R., 2015. Neural network reorganization analysis during an auditory oddball task in schizophrenia using wavelet entropy. *Entropy*. 17, 5241–5256.

J. Gomez-Pilar et al.

NeuroImage: Clinical 18 (2018) 382–389

- Gomez-Pilar, J., Lubeiro, A., Poza, J., Hornero, R., Ayuso, M., Valcarcel, C., et al., 2017. Functional EEG network analysis in schizophrenia: evidence of larger segregation and deficit of modulation. *Prog Neuropsychopharmacol Biol Psychiatry*. 20 (Mar, PubMed PMID: 28336496). Epub 2017/03/25. eng.
- Gomez-Pilar, J., Poza, J., Bachiller, A., Gomez, C., Nuñez, P., Lubeiro, A., et al., 2018. Quantification of graph complexity based on the edge weight distribution balance: application to brain networks. *Int. J. Neural Syst.* 28 (1), 1750032.
- Honey, C.J., Sporns, O., Cammoun, L., Gigandet, X., Thiran, J.P., Meuli, R., et al., 2009. Predicting human resting-state functional connectivity from structural connectivity. *Proc Natl Acad Sci U S A*. 106 (6), 2035–2040 (Feb 10, PubMed PMID: 19188601. Pubmed Central PMCID: 2634800). Epub 2009/02/04. eng.
- Jones, J.T., DiFrancesco, M., Zaal, A.I., Klein-Gitelman, M.S., Gitelman, D., Ying, J., et al., 2015. Childhood-onset lupus with clinical neurocognitive dysfunction shows lower streamline density and pairwise connectivity on diffusion tensor imaging. *Lupus*. 24 (10), 1081–1086 (Sep, PubMed PMID: 25701565. Pubmed Central PMCID: Pmc4529818). Epub 2015/02/24. eng.
- Kay, S.R., Fiszbein, A., Opler, L.A., 1987. The positive and negative syndrome scale (ANSS) for schizophrenia. *Schizophr Bull.* 13 (2), 261–276 (PubMed PMID: 3616518).
- Lachaux, J.P., Rodriguez, E., Martinerie, J., Varela, F.J., 1999. Measuring phase synchrony in brain signals. *Hum Brain Mapp.* 8 (4), 194–208 (PubMed PMID: 10619414). Epub 2000/01/05. eng.
- Lewis, D.A., Curley, A.A., Glusier, J.R., Volk, D.W., 2012. Cortical parvalbumin interneurons and cognitive dysfunction in schizophrenia. *Trends Neurosci.* 35 (1), 57–67 (Jan, PubMed PMID: 22154068. Pubmed Central PMCID: 3253230). Epub 2011/12/14. eng.
- Manoach, D.S., 2003. Prefrontal cortex dysfunction during working memory performance in schizophrenia: reconciling discrepant findings. *Schizophr Res.* 60 (2–3), 285–298 (Apr 1, PubMed PMID: 12591590).
- Mazaheri, A., Picton, T.W., 2005. EEG spectral dynamics during discrimination of auditory and visual targets. *Brain Res Cogn Brain Res.* 24 (1), 81–96 (Jun, PubMed PMID: 15922161). Epub 2005/06/01. eng.
- Molina, V., Bachiller, A., Suazo, V., Lubeiro, A., Poza, J., Hornero, R., 2016. Noise power associated with decreased task-induced variability of brain electrical activity in schizophrenia. *Eur Arch Psychiatry Clin Neurosci.* 266 (1), 55–61 (Feb, PubMed PMID: 25547316). Epub 2014/12/31. eng.
- Molina, V., Bachiller, A., Gomez-Pilar, J., Lubeiro, A., Hornero, R., Cea-Canas, B., et al., 2017a. Deficit of entropy modulation of the EEG in schizophrenia associated to cognitive performance and symptoms. A replication study. *Schizophr. Res.* <http://dx.doi.org/10.1016/j.schres.2017.08.057>. (in press, Sep 5. pii: S0920-9964(17)30533-9, Epub ahead of print).
- Molina, V., Lubeiro, A., Soto, O., Rodriguez, M., Alvarez, A., Hernandez, R., et al., 2017b. Alterations in prefrontal connectivity in schizophrenia assessed using diffusion magnetic resonance imaging. *Prog Neuropsychopharmacol Biol Psychiatry*. 76, 107–115 (Mar 10, PubMed PMID: 28288855). Epub 2017/03/16. eng.
- Nunez, P., Poza, J., Bachiller, A., Gomez-Pilar, J., Lubeiro, A., Molina, V., et al., 2017. Exploring non-stationarity patterns in schizophrenia: neural reorganization abnormalities in the alpha band. *J Neural Eng.* 14 (4), 046001 (Aug, PubMed PMID: 28424430). Epub 2017/04/21. eng.
- Patenaude, B., Smith, S.M., Kennedy, D.N., Jenkinson, M., 2011. A Bayesian model of shape and appearance for subcortical brain segmentation. *Neuroimage*. 56 (3), 907–922 (Jun 01, PubMed PMID: 21352927. Pubmed Central PMCID: 3417233). Epub 2011/03/01. eng.
- Roach, B.J., Mathalon, D.H., 2008. Event-related EEG time-frequency analysis: an overview of measures and an analysis of early gamma band phase locking in schizophrenia. *Schizophr Bull.* 34 (5), 907–926 (Sep, PubMed PMID: 18684772. Pubmed Central PMCID: 2632478). Epub 2008/08/08. eng.
- Rubinov, M., Sporns, O., 2010. Complex network measures of brain connectivity: uses and interpretations. *Neuroimage*. 52 (3), 1059–1069 (Sep, PubMed PMID: 19819337). Epub 2009/10/13. eng.
- Salvador, R., Pena, A., Menon, D.K., Carpenter, T.A., Piekard, J.D., Bullmore, E.T., 2005. Formal characterization and extension of the linearized diffusion tensor model. *Hum Brain Mapp.* 24 (2), 144–155 (Feb, PubMed PMID: 15468122). Epub 2004/10/07. eng.
- Segarra, N., Bernardo, M., Gutierrez, F., Justicia, A., Fernandez-Egea, E., Allas, M., et al., 2011. Spanish validation of the brief assessment in cognition in schizophrenia (BACS) in patients with schizophrenia and healthy controls. *Eur Psychiatry*. 26 (2), 69–73 (Mar, PubMed PMID: 20435446). Epub 2010/05/04. eng.
- Smith, S.M., 2002. Fast robust automated brain extraction. *Hum Brain Mapp.* 17 (3), 143–155 (Nov, PubMed PMID: 12391568). Epub 2002/10/23. eng.
- Spencer, K.M., Nestor, P.G., Niznikiewicz, M.A., Salisbury, D.F., Shenton, M.E., McCarley, R.W., 2003. Abnormal neural synchrony in schizophrenia. *J Neurosci.* 23 (19), 7407–7411 (Aug 13, PubMed PMID: 12917376. Pubmed Central PMCID: 2848257). Epub 2003/08/15. eng.
- Sporns, O., 2011. *Networks for Cognition*. Networks of the Brain. MIT Press, Cambridge, Massachusetts, pp. 182.
- Stam, C.J., de Haan, W., Daffertshofer, A., Jones, B.F., Manshanden, I., van Cappellen van Walsum, A.M., et al., 2009. Graph theoretical analysis of magnetoencephalographic functional connectivity in Alzheimer's disease. *Brain*. 132 (Pt 1), 213–224 (Jan, PubMed PMID: 18952674). Epub 2008/10/28. eng.
- Tanaka, K., 1996. Inferotemporal cortex and object vision. *Annu Rev Neurosci.* 19, 109–139 (PubMed PMID: 8833438). Epub 1996/01/01. eng.
- Tournier, J.D., Calamante, F., Connelly, A., 2007. Robust determination of the fibre orientation distribution in diffusion MRI: non-negativity constrained super-resolved spherical deconvolution. *Neuroimage*. 35 (4), 1459–1472 (May 01, PubMed PMID: 17379540). Epub 2007/03/24. eng.
- Varela, F., Lachaux, J.P., Rodriguez, E., Martinerie, J., 2001. The brainweb: phase synchronization and large-scale integration. *Nat Rev Neurosci.* 2 (4), 229–239 (Apr, PubMed PMID: 11283746). Epub 2001/04/03. eng.
- Winterer, G., Coppola, R., Goldberg, T.E., Egan, M.F., Jones, D.W., Sanchez, C.E., et al., 2004. Prefrontal broadband noise, working memory, and genetic risk for schizophrenia. *Am J Psychiatry*. 161 (3), 490–500 (Mar, PubMed PMID: 14992975).
- Zhang, Y., Brady, M., Smith, S., 2001. Segmentation of brain MR images through a hidden Markov random field model and the expectation-maximization algorithm. *IEEE Trans Med Imaging.* 20 (1), 45–57 (Jan, PubMed PMID: 11293691). Epub 2001/04/11. eng.


Supplementary material of the paper: “Deficits of entropy modulation in schizophrenia are predicted by functional connectivity strength in the theta band and structural clustering”

Table A.1: Comparison between chronic and first episode (FE) patients of the values with significant differences between patients and healthy controls. Values are shown as mean (SD). Statistical significance was assessed using Mann-Whitney *U*-tests. Entropy modulation factor scores were significantly higher in both chronic and FE patients as compared to healthy controls (see main text).

	Chronic patients ($n = 26$)	FE patients ($n = 22$)
EEG-CSPRE*	0.370 (0.046)	0.347 (0.030)
EEG-CLCMOD	-0.001 (0.004)	0.000 (0.004)
EEG-PLMOD	-0.001 (0.018)	0.001 (0.020)
EEG-CSMOD	0.001 (0.023)	0.017 (0.021)
Entropy modulation factor scores (Factor 1)*	0.634 (0.576)	0.206 (0.695)

*Indicates significant difference ($p < 0.05$).

Relations between structural and EEG-based graph metrics in healthy controls and schizophrenia patients

Javier Gomez-Pilar¹ | Rodrigo de Luis-García² | Alba Lubeiro³ | Henar de la Red⁴ |
Jesús Poza^{1,4,5,6} | Pablo Núñez¹ | Roberto Hornero^{1,5,6} | Vicente Molina^{3,4,5} 

¹Biomedical Engineering Group, University of Valladolid, Paseo de Belén, 15, 47011 Valladolid, Spain

²Imaging Processing Laboratory, University of Valladolid, Paseo de Belén, 15, 47011 Valladolid, Spain

³Psychiatry Department, School of Medicine, University of Valladolid, Av. Ramón y Cajal, 7, Valladolid 47005, Spain

⁴Psychiatry Service, Clinical Hospital of Valladolid, Ramón y Cajal, 3, Valladolid 47003, Spain

⁵Neurosciences Institute of Castilla y León (INCYL), Pintor Fernando Gallego, 1, 37007 University of Salamanca, 37007 Salamanca, Spain

⁶IMUVA, Mathematics Research Institute, University of Valladolid, Valladolid, Spain

Correspondence

Vicente Molina, Psychiatry Department,
School of Medicine, University of
Valladolid, Av. Ramón y Cajal, 7, 47005
Valladolid, Spain.
Email: vicente.molina@uva.es

Funding information

Instituto de Salud Carlos III, Grant/Award
Number: PI15/00299; "Gerencia Regional
de Salud de Castilla y León", Grant/Award
Number: GRS 1263/A/16 and GRS 1485/
A/17; "Ministerio de Economía y
Competitividad" and FEDER. Grant/Award
Number: TEC2014-53196-R and TEC2013-
44194-P; "European Commission" and
FEDER under project "Análisis y correlación
entre el genoma completo y la actividad
cerebral para la ayuda en el diagnóstico de
la enfermedad de Alzheimer" ("Cooperation
Program Interreg V-A Spain-Portugal POC-
TEP 2014-2020"), and by "Consejería de
Educación de la Junta de Castilla y León"
and FEDER Grant/Award Number:
VAO37U16; University of Valladolid and
Consejería de Educación de la Junta de
Castilla y León

Abstract

Our aim was to assess structural and functional networks in schizophrenia patients; and the possible prediction of the latter based on the former. The possible dependence of functional network properties on structural alterations has not been analyzed in schizophrenia. We applied averaged path-length (PL), clustering coefficient, and density (D) measurements to data from diffusion magnetic resonance and electroencephalography in 39 schizophrenia patients and 79 controls. Functional data were collected for the global and theta frequency bands during an odd-ball task, prior to stimulus delivery and at the corresponding processing window. Connectivity matrices were constructed from tractography and registered cortical segmentations (structural) and phase-locking values (functional). Both groups showed a significant electroencephalographic task-related modulation (change between prestimulus and response windows) in the global and theta bands. Patients showed larger structural PL and prestimulus density in the global and theta bands, and lower PL task-related modulation in the theta band. Structural network values predicted prestimulus global band values in controls and global band task-related modulation in patients. Abnormal functional values found in patients (prestimulus density in the global and theta bands and task-related modulation in the theta band) were not predicted by structural data in this group. Structural and functional network abnormalities respectively predicted cognitive performance and positive symptoms in patients. Taken together, the alterations in the structural and functional theta networks in the patients and the lack of significant relations between these alterations, suggest that these types of network abnormalities exist in different groups of schizophrenia patients.

KEYWORDS

brain network, diffusion magnetic resonance, dysconnectivity, electroencephalography, graph-theory, schizophrenia

1 | INTRODUCTION

Mental functions depend on global dynamics of cerebral networks (Dehaene & Changeux, 2011; Varela, Lachaux, Rodríguez, & Martinerie, 2001), whose functional and structural characteristics can be assessed

in vivo using methods derived from graph-theory (Bullmore & Sporns, 2009). In this context, underpinnings of syndromes like schizophrenia likely involve distributed networks rather than regional alterations, as supported by studies using functional magnetic resonance imaging (fMRI) that revealed network alterations in the resting state (Lo et al.,

2015; Yu et al., 2011) and during task performance (Ma, Calhoun, Eichele, Du, & Adali, 2012; Shim, Kim, Lee, & Im, 2014) in this syndrome. However, considering the rapid and transient change of functional integration of diverse cerebral regions in cognition in humans (Varela et al., 2001) and animals (Bressler, Coppola, & Nakamura, 1993), assessing fast change of cerebral networks in schizophrenia holds a great interest. Techniques with high temporal resolution are useful to this purpose: change of network properties using electroencephalographic (EEG) during a cognitive task was significantly decreased in schizophrenia patients (Gomez-Pilar et al., 2017). Using relative power analyses, we also reported lower EEG task-related change in theta but not in faster bands during an odd-ball task in schizophrenia (Bachiller et al., 2014).

As mentioned, methods derived from graph-theory are useful to assess the properties of cerebral networks, which can be summarized in parameters such as clustering coefficient (CLC) and characteristic path length (PL). In a binary network, local CLC is the ratio between the number of triangles in which a given node participates and the maximum possible number of triangles including that node. When CLC is averaged across the nodes of a network, it quantifies network segregation and local efficiency of information transfer. In turn, PL is the average of shortest distances for all possible pairs of nodes; it is likely related to information integration across areas. These network parameters provide complementary information about the properties of the whole brain network. Therefore, the use of these parameters instead of their corresponding nodal versions, allows to characterize the global and predominant changes of the network. A recent meta-analysis of functional graph-analytical studies in schizophrenia revealed significant decreases in measures of local organization (CLC) with preservation in short communication paths (PL) (Kambeitz et al., 2016).

Abnormalities in structural connectivity are also prevalent in schizophrenia (Ellison-Wright & Bullmore, 2009). These abnormalities are likely reflected in structural network properties, since longer structural PL values were found in schizophrenia at frontal and temporal regions using dMRI (van den Heuvel, Mandl, Stam, Kahn, & Hulshoff Pol, 2010) and may be associated to genetic liability to this disorder (Bohken et al., 2016). Thus, the possibility exists that functional network alterations might be secondary to structural abnormalities in schizophrenia. Indeed, in this syndrome, a relationship has been reported between a reduction in "rich-club density" (i.e., connections among high-degree hub nodes) and global efficiency of functional connectivity in the resting state using fMRI (van den Heuvel et al., 2013). Similarly, connectivity deficits in rich-club hubs have been described in young offspring of schizophrenia patients associated to disruption of the functional connectome (Collin, Scholtens, Kahn, Hillegers, & van den Heuvel, 2017). However, functional connectivity alterations in schizophrenia are not necessarily determined by structural connectivity, since functional connections in the resting state can be found between regions without direct anatomical connections (Honey et al., 2009).

The application of graph-theory parameters to functional and structural measurements can yield complementary information and help uncovering hidden relationships (Sui, Yu, He, Pearson, & Calhoun, 2012). Using diffusion MRI (dMRI), graph-theory parameters may

inform about structural connectivity differences between anatomical structures, revealing highly connected hubs (Honey, Thivierge, & Sporns, 2010). Graph-theory parameters applied to functional analysis may reveal baseline network characteristics and its dynamic modulation during cognition of signals such as synchrony of the bold-oxygen level dependent signal between regions, or magneto-electrical signals between sensors. Considering the millisecond-scale of modulation of cortical activity during cognition (Bressler et al., 1993; Dehaene & Changeux, 2011), the combination of network analyses with temporal resolution of EEG recordings can be useful to assess this task-related modulation. Indeed, using EEG in healthy subjects, we reported a significant task-related modulation of network parameters from prestimulus (from -300 to 0 ms prior to stimulus onset) to response (from 150 to 450 ms poststimulus) windows (Martin-Santiago et al., 2016) during an odd-ball task.

To our knowledge, no previous study has assessed the relationship between structural and EEG networks in schizophrenia. Such investigation may help identifying the substrate of the cortical dysfunction in schizophrenia. Therefore, this study was aimed at characterizing the properties of structural and EEG-based functional networks in schizophrenia and assessing the relationships between properties of those networks in this syndrome, particularly between structural connectivity and EEG modulation.

2 | SUBJECTS AND METHODS

2.1 | Subjects

A total of 39 schizophrenia (19 stable chronic and 20 first-episode, FE) patients and 78 healthy controls with normal hearing were included. Demographic, clinical, cognitive and EEG data were collected for each participant (Table 1). In addition, dMRI data were also available in 33 patients (16 FE) and 27 controls (Table 1). One of the psychiatrists in the group (VM) diagnosed the patients according to the Diagnostic and Statistical Manual of Mental Disorders, 5th edition. Chronic patients received atypical antipsychotics, 30 of them in monotherapy (12 received antidepressants and 7 benzodiazepines). FE patients were receiving stable doses of antipsychotics for <15 days, with a wash-out period of 24 hr prior to EEG acquisition. This was so done to minimize the possible effects of treatment in this group, given their relatively short exposure to antipsychotics. Symptoms were scored using the Positive and Negative Syndrome Scale (PANSS) (Kay, Fiszbein, & Opler, 1987). Exclusion criteria were: (a) any neurological illness; (b) history of cranial trauma with loss of consciousness longer than 1 min; (c) past or present substance abuse, except nicotine or caffeine; (d) total intelligence quotient (IQ) smaller than 70; (e) for patients, any other psychiatric process; and (f) for controls, any current psychiatric or neurological diagnosis or treatment.

The population here included overlaps in part with that of previous reports of our group in schizophrenia on functional networks based on evoked response (Gomez-Pilar et al., 2017), graph complexity (Gomez-Pilar et al., 2018) and structural connectivity of specific tracts of the prefrontal region (Molina et al., 2017)

TABLE 1 Demographic, clinical and cognitive data in patients and controls

	Schizophrenia		Controls	
	Schizophrenia (EEG, n = 39)	Schizophrenia (EEG + dMR; n = 33)	Controls (EEG; n = 78)	Controls (dMR + EEG; n = 27)
Age	33.053 (8.801)	33.059 (8.951)	30.948 (10.839)	34.668 (11.150)
Sex (M:F)	23:16	19:14	46:32	18:9
CPZ equivalents (mg/d)	377.901 (196.934)	374.802 (193.419)	NA	
Duration(months)	95.169 (117.388)	83.86 (117.456)	NA	
Education years	14.191 (3.600)	14.882 (3.051)	16.561 (2.254)	17.427 (2.866)
PANSS positive symptoms	11.702 (3.427)	11.388 (3.457)	NA	
PANSS negative symptoms	17.571 (7.309)	15.450 (5.057)	NA	
Total symptoms	53.810 (18.892)	53.313 (18.913)	NA	
Total IQ	91.061 (14.528)***	94.701 (11.789)***	113.209 (11.088)	109.458 (12.165)
Verbal memory	34.262 (12.889)***	35.315 (12.345)***	51.115 (8.194)	53.000 (7.274)
Working memory	16.151 (5.010)***	17.074 (4.148)***	21.626 (3.621)	23.140 (2.723)
Motor speed	58.879 (13.781)***	62.538 (12.041)***	72.610 (16.583)	85.503 (8.154)
Verbal fluency	18.352 (5.730)***	19.613 (4.799)***	27.856 (5.155)	28.827 (5.177)
Processing speed	43.700(15.360)***	45.641 (14.672)***	69.588 (14.378)	69.251 (14.841)
Problem solving	15.253 (4.622)	16.317 (3.418)	17.524 (2.571)	17.042 (2.641)
WCST perseverative errors (%)	17.921 (10.123)***	21.152 (17.077)***	9.801 (5.141)	8.221 (3.573)
WCST completed categories	4.419 (1.878)***	4.812 (1.711)**	5.847 (0.610)	5.879 (0.478)

Significant differences with respect to controls are shown for patients * $p < .05$; ** $p < .001$; *** $p < .001$

We obtained written informed consent from all participants after full printed information. The ethical committee of the University Hospital of Valladolid approved the study.

2.2 | Cognitive assessment

Cognitive data from patients and controls were collected using: the Wechsler Adult Intelligence Scale, WAIS-III (IQ); the Wisconsin Card Sorting Test (WCST; completed categories and percentage of perseverative errors); and the Spanish version of the Brief Assessment in Cognition in Schizophrenia Scale (BACS) (Segarra et al., 2011).

2.3 | MRI acquisition and processing

Acquisitions were carried out using a Philips Achieva 3 Tesla MRI unit (Philips Healthcare, Best, The Netherlands) at the MRI facility at Valladolid University, including anatomical T1-weighted and diffusion-weighted images. For the T1-weighted images, acquisition parameters were: turbo field echo sequence, 256×256 matrix size, $1 \times 1 \times 1$ mm³ of spatial resolution and 160 slices covering the whole brain. About the diffusion-weighted images (DWIs), the acquisition protocol parameters were: 61 gradient directions and one baseline volume, b -value = 1,000 s/mm², $2 \times 2 \times 2$ mm³ of voxel size, 128×128 matrix and 66 slices covering the entire brain. Total acquisition time was 18 min.

The processing pipeline of the acquired MRI volumes is designed to obtain structural connectivity matrices by using both the anatomical (T1-weighted) and diffusion images (Figure 1).

First, nonbrain structures were removed from the T1 images, using BET, the brain extraction tool from the FSL software suite (<http://fsl.fmrib.ox.ac.uk>) (Smith, 2002). After that, the segmentation of 84 cortical structures was performed employing Freesurfer (<https://surfer.nmr.mgh.harvard.edu>) (Desikan et al., 2006; Fischl et al., 2004). From the same T1 images, gray matter, white matter, and cerebrospinal fluid were also segmented, and subcortical gray matter structures were obtained using FMRIB's Automated Segmentation Tool (FAST) and FMRIB's Integrated Registration and Segmentation Tool (FIRST) utilities from FSL, respectively (Patenaude, Smith, Kennedy, & Jenkinson, 2011; Zhang, Brady, & Smith, 2001), and combined into a volume called 5tt (5-tissue-type) image.

In parallel, the brain was extracted from the DWIs using DWI2-MASK tool from MRtrix (www.mrtrix.org) (Dhollander & Connolly, 2016). Also employing MRtrix, orientation distribution functions were estimated from the diffusion data using spherical deconvolution (Tournier, Calamante, & Connolly, 2007), which were later employed to generate anatomically constrained tractography using both the diffusion data and the 5tt image (after registration). Two million streamlines were generated for each subject.

In order to characterize diffusion at each voxel, diffusion tensors were estimated using a least squares method (Salvador et al., 2005),

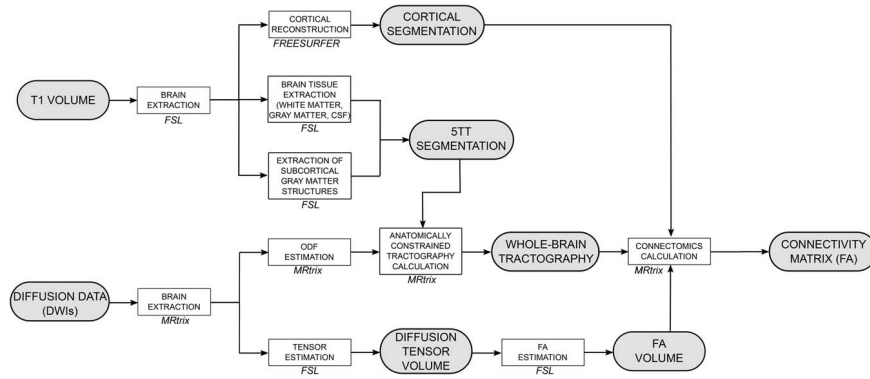


FIGURE 1 Processing pipeline yielding FA values to be used in graph-theory calculations

and scalar fractional anisotropy (FA) volumes were computed from the diffusion tensors. FA quantifies the amount of anisotropy in the diffusion tensor, that is, how much it deviates from a totally isotropic diffusion. FA is usually interpreted as a descriptor of white matter integrity, and decreases in FA have been related to alterations in the white matter due to several factors (demyelination and axonal destruction, among others).

Finally, connectivity matrices were constructed from the tractography results and the (registered) cortical segmentations. When a streamline between two cortical segmentations was found, the averaged FA was computed. Thus, 84×84 connectivity matrices were obtained using FA as connectome metrics (Figure 2). A threshold was not applied

to the obtained matrices; however, some matrix coefficients were equal to zero when a streamline was not found.

Similar connectomics analyses have been reported in schizophrenia (Di Biase et al., 2017) and other neurocognitive conditions (Jones et al., 2015)

2.4 | EEG recordings and processing

2.4.1 | EEG acquisition and preprocessing

EEG recordings were obtained following MRI scans, after a resting period of 30 min. Participants performed a 13 min three-tone P300 oddball task (for a detailed description see (Gomez-Pilar et al., 2017).

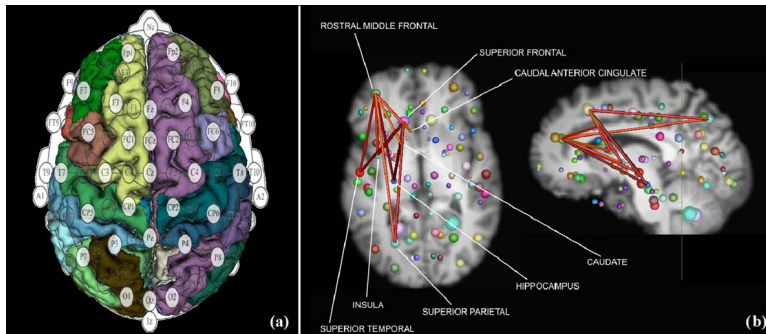


FIGURE 2 (a) The 29 EEG channel labels superposed on the structural ROIs. EEG nodes (filled in white) were used to generate functional connectivity matrices from PLV values between each pair of electrodes. The figure illustrates the approximate placement of the EEG electrodes over the ROIs. The list of the 29 electrodes used in the study according to international 10-10 system is: Fp1, Fp2, F7, F3, Fz, F4, F8, FC5, FC1, FCz, FC2, FC6, T7, C3, Cz, C4, T8, CP5, CP1, CP2, CP6, P7, P3, Pz, P4, P8, O1, Oz and O2. (b) Schematic depiction (axial and sagittal views) of the relevant tracts (streamlines) from which FA was calculated to generate structural connectivity matrices. Streamlines were calculated between each pair of the 84 nodes corresponding to the cortical segmentation are shown as spheres (their sizes are proportional to the actual size of the corresponding ROI). For the sake of clarity, only tracts linking PFC with anterior cingulate, superior temporal, insular, and superior parietal cortices and hippocampus and caudate are drawn [Color figure can be viewed at wileyonlinelibrary.com]

Electrode impedance was always kept under 5 k Ω . Ground was placed at Fpz electrode and each channel was referenced over Cz electrode and re-referenced to the average activity of all active sensors (Bledowski et al., 2004; Gomez-Pilar et al., 2018), yielding a total of 29 channels.

The P300 task has several advantages for assessing functional network modulation in schizophrenia. In addition to its widespread previous use in the field: (a) it is easy to perform, thus decreasing bias related to lack of subject's cooperation; (b) its performance activates a large cerebral network (Bledowski et al., 2004; Linden et al., 1999); and (c) differences in EEG global activation patterns have been reported in schizophrenia using this paradigm (Gomez-Pilar et al., 2017).

Signals were band pass filtered between 1 and 70 Hz. In addition, a zero-phase 50 Hz notch filter was used to remove the power line artifact. A three-step artifact rejection algorithm was applied to minimize electrocuculographic and electromiographic contamination (Bachiller et al., 2015a): (a) an independent component analysis (ICA) was carried out to discard noisy ICA components; (b) after ICA reconstruction, EEG signals were divided into trials of 1 s length (ranging from 300 before to 700 ms after stimulus onset); and (c) an automatic method was applied to reject trials whose amplitude exceeded an adaptive statistical-based threshold, which consists of two stages. First, the mean and standard deviation of each channel was computed. Then, trials that exceeded mean $\pm 4 \times SD$ in at least two channels were discarded (Nunez et al., 2017). After this adaptive artifact rejection, 91.21 \pm 11.28 trials for controls—with a median (interquartile range) of 91 (85–97) trials—and 86.33 \pm 14.13—with a median (interquartile range) of 86 (76.75–94)—were left for further analyses ($p = .051$, Mann-Whitney U -test).

In order to describe the event-related potential (ERP) waveforms, Supporting Information Figure S1 has been included in the Supplementary material. ERPs in the midline electrodes are shown in Supporting Information Figure S1A. Supporting Information Figure S1B shows the channel grand average waveforms. Finally, Supporting Information Figure S1C depicts scalp maps with the P300 peak amplitude for both groups.

2.4.2 | EEG brain graphs

The functional brain network was characterized using EEG graphs. Electrodes were used to represent network nodes, whereas network edges were set by computing the neural coupling between pairs of electrodes. Specifically, neural coupling was established using the phase-locking value (PLV) across successive trials (Lachaux, Rodriguez, Martinerie, & Varela, 1999). PLV is sensible to small oscillations of the EEG (Spencer et al., 2003) and takes into account nonlinearities (van Diessen et al., 2015), which is an intrinsic feature of EEG recordings. PLV can be computed using different approaches. In this study, the continuous wavelet transform (CWT) was used to extract the phase information from each trial (Bob, Palus, Susta, & Glaslova, 2008). Edge effects in CWT were considered by computing the cone of influence (COI) for prestimulus and response time windows. Only wavelet coefficients inside the respective COI were considered for the analyses to avoid edge effects. We refer to our previous studies (Gomez-Pilar

et al., 2018) for detailed explanations about how wavelet coefficient were computed, the wavelet parameters were configured and the COIs were applied to the CWT decomposition in order to minimize edge effects. After using CWT approach to perform filtering and phase extraction in one operation (Bob et al., 2008), the PLV between two signals $x(t)$ and $y(t)$ can be obtained evaluating the variability of the phase difference across successive trials:

$$PLV_{xy}(k, s) = \frac{1}{N_i} \left| \sum_{n=1}^{N_i} e^{i\Delta\phi_{xy}(k, s, n)} \right|, \quad (1)$$

where N_i is the number of trials, $\Delta\phi_{xy}$ is the instantaneous phase difference between x and y signals, k is the time interval, and s the scaling factor of the mother wavelet (see Bachiller et al., 2015a,b for details).

Thus, functional connectivity matrices based on PLV ranged between 0 and 1, where a value of 1 is obtained with completely synchronized signals and a value of 0 implies an absence of synchronization. Following the same methodology as in the structural data, functional connectivity matrices were not thresholded.

2.4.3 | Segmentation of the EEG response

In order to assess the task-related modulation of the graph parameters along the odd-ball task, two-time windows were considered for comparison. On the one hand, the prestimulus window (i.e., a period of expectation before the stimulus onset) ranges from -300 ms to the stimulus onset. On the other hand, the response window was selected to capture the P3b response. In order to take into account, the inter-individual variability of the P3b response, the response window was adaptively set for each participant. First, the event-related wave was computed for each subject by the synchronized averaging of all the trials corresponding to attended target tones. Second, a low-pass finite impulse response filter with cut-off frequency of 8 Hz was applied to the evoked wave in order to obtain only the components related to delta and theta frequency bands. It is noteworthy that this filter was only applied to estimate the time window related to the EEG response. Thirdly, the maximum amplitude of the low-pass filtered evoked wave in the Pz channel was located into a window ranging from 250 to 550 ms from the stimulus onset (Bachiller et al., 2015b). The corresponding sample to the maximum amplitude was used as a central time sample of the response window. Finally, the response window was set on ± 150 ms around the central time sample.

2.5 | Graph-theory parameters

From both the structural and functional connectivity matrices, we calculated three graph-theory parameters to characterize global properties of the brain network: (a) connectivity strength (i.e., mean network degree) by means of network density (D), also named network strength (b) network segregation using CLC, and (c) network integration by means of PL (Rubinov & Sporns, 2010). For the sake of comparability and to obtain results independent of network size and network strength, CLC and PL were computed over an ensemble of 50

surrogate random networks, which were used to normalize CLC and PL values obtained from the original networks (Stam et al., 2009).

Therefore, normalized CLC and PL can be defined:

$$CLC = \frac{C}{C_{\text{random}}}, \quad (2)$$

$$PL = \frac{L}{L_{\text{random}}}, \quad (3)$$

where C and L can be defined as follows:

$$C = \frac{1}{N} \sum_{i=1}^N \sum_{j \neq i}^N \frac{w_{ij} w_{ji}}{\sum_{i=1}^N \sum_{j \neq i}^N w_{ij} w_{ji}}, \quad (4)$$

$$L = \frac{N(N-1)}{\sum_{i=1}^N \sum_{j \neq i}^N L_{ij}}, \quad (5)$$

In Equation 4, w_{ij} can be referred to PLV between nodes i and j (for functional analyses) or the structural connectivity between two regions using the streamlines from MRI. N is the total number of nodes of the network (29 in EEG analyses, 84 in MRI). Finally, L_{ij} is defined as the inverse of the edge weight (Stam et al., 2009).

With regard to the EEG functional network, parameters were computed into two frequency ranges. They were selected based on their relevance for the task-related modulation of the EEG during P300 tasks shown in schizophrenia in previous studies: the global band (from 1 to 70 Hz) (Gomez-Pilar et al., 2017) and the theta band (from 4 to 8 Hz) (Bachiller et al., 2014; Doege et al., 2009). A diminished task-related modulation of theta activity during an oddball task was found in schizophrenia, but not in faster frequency bands (Bachiller et al., 2014). In addition, the assessment of the theta band showed abnormalities in the brain network reconfiguration in the secondary functional pathways in schizophrenia (Gomez-Pilar et al., 2018). On the other hand, the global band could be also useful to assess the specificity of the theta band.

Functional network parameters during prestimulus and its corresponding task-related modulation (i.e., difference between the response and the prestimulus windows) were used for statistics.

Structural connectivity network parameters will be referred to as dMRI-PL, dMRI-D, and dMRI-CC, and functional network parameters as EEG-PL, EEG-D, and EEG-CLC.

2.6 | Statistics

We compared socio-demographic data (age, sex, education years, and parental education) between patients and controls (t or χ^2 tests when appropriate). Each subgroup of patients (i.e., those with only EEG and those with EEG plus dMRI data) was compared with the corresponding controls.

2.6.1 | Comparisons of graph-theory parameters

After testing normality and homoscedasticity of data distribution using Kolmogorov-Smirnov and Levene tests, we compared functional (EEG-based) and structural (dMRI-based) graph-theory parameters between

patients and controls using Student's t -tests. Within-group changes in functional network parameters were assessed using t -tests for related samples. After Bonferroni adjustment, p level was set to $.05/15 = .003$.

For the sake of interpretability, we studied the relationship between structural connectivity parameters (dMRI-PL, dMRI-D, and dMRI-CLC) and the average FA values in identifiable relevant white matter tracts. With this analysis, it could be easier to interpret the results of graph-theory data in terms of integrity of white matter tracts. To do this, we used the methodology employed in a previous study (Molina et al., 2017), in which FA was assessed in tracts connecting prefrontal cortex (PFC) with other relevant regions. Correlation coefficients between structural connectivity network parameters and FA values in these tracts were computed, with Bonferroni adjustment with p set to $.001$.

When statistically significant differences in network parameters were found between patients and controls, we compared the corresponding values between FE and stable chronic patients using Mann-Whitney U-tests for independent samples, to discard a major effect of chronicity in those differences.

2.6.2 | Association between structural and functional networks

The main hypothesis of the study was that the structural connectivity of the brain network would determine the prestimulus functional network properties and/or its task-related modulation. This was studied using stepwise multivariate regression models. Since significant correlations between different structural variables were found, to avoid collinearity effects we performed principal component analyses (PCAs) separately with structural (dMRI) and functional (EEG) variables for global and theta bands. This allowed a priori reducing the number of comparisons for further analyses, thus reducing the Type I errors risk. Individual structural and functional network factor scores were introduced respectively as independent and dependent variables in the regression model aimed to predict functional properties from structural network data.

2.6.3 | Clinical and cognitive correlates

Next, we studied the cognitive and clinical correlates of graph-theory parameters for the patients using stepwise multivariate regression models (for structural and functional data). To calculate a global score summarizing cognition, individual cognitive scores were introduced in a PCA. The resulting individual scores were saved and introduced as dependent variables in the model. Possible associations between graph-theory parameters and symptoms were similarly assessed.

To discard major confounders, correlation coefficients were calculated between graph-theory parameters and both illness duration and current treatment doses.

3 | RESULTS

There were no statistically significant differences between patients and controls in age and sex distribution in the whole sample, nor between

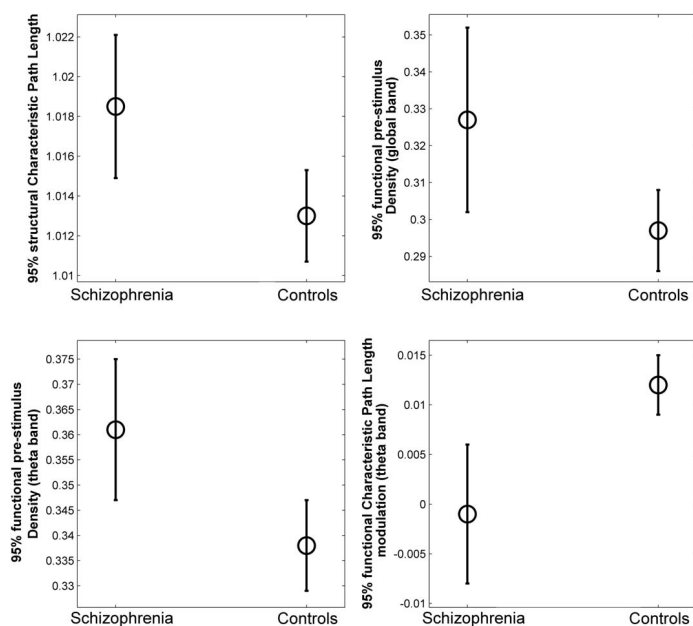


FIGURE 3 Error bars corresponding to the graph-theory parameters with statistically significant differences between patients and controls (from left to right, structural PL, functional prestimulus D at the global and at the theta bands, and functional PL task-related modulation at the theta band). Circles represent the mean value, while bars indicate the interval of confidence (95%)

patients and controls with dMRI data. Patients had fewer study years and a generalized cognitive deficit (Table 1).

3.1 | Comparison of graph-theory parameters

3.1.1 | Structural parameters

Patients showed statistically significant longer mean dMRI-PL values than controls ($t = 2.20$, $df = 58$, unadjusted $p = .03$; Figure 3).

Values of dMRI-PL were inversely associated to FA values in relevant tracts linking PFC with anterior cingulate, superior temporal, insular and superior parietal cortices and hippocampus and caudate. Moreover, dMRI-CLC and dMRI-D values were directly associated to FA values in these tracts (see Section 3.2.3).

3.1.2 | Functional parameters

Both EEG-PL and EEG-CLC in the global band and EEG-D in the theta band showed a significant increase from prestimulus to response within patients and control groups, which remained significant only in the controls after Bonferroni adjustment (Table 2). Controls, but not patients, showed a significant increase in EEG-CLC and EEG-PL values in the theta band from prestimulus to response (Table 2). Therefore, a

significant positive task-related modulation of EEG-CLC and EEG-PL values was found in this band only in controls.

In the global band, prestimulus window EEG-D was significantly higher for patients ($t = 2.52$, $df = 115$, unadjusted $p = .03$; Figure 3; Table 2), without significant differences in the corresponding task-related modulation.

In the theta band, prestimulus EEG-D was higher ($t = 2.637$, $df = 115$, $p = .010$), and EEG-PL task-related modulation was lower ($t = -2.128$, $df = 115$, $p = .035$) for patients (Figure 3; Table 2)

Between-group differences in functional and structural graph-theory parameters had medium effect sizes (Cohen's d ; Table 2), although these differences would not survive after Bonferroni adjustment.

3.1.3 | Comparison between FE and chronic patients

As compared with the FE subgroup, we found larger structural PL in the chronic patients, while no differences were obtained between patient subgroups in global and theta band prestimulus density nor in theta band modulation (Supporting Information Table S3).

TABLE 2 Structural and functional graph-theory parameters for patient and controls

	Structural (dMRI) network			Functional (EEG) network			Cohen's <i>d</i>
	Global band		Theta band	Global band		Theta band	
	Schizophrenia (<i>n</i> = 33)	Controls (<i>n</i> = 27)	Schizophrenia (<i>n</i> = 39)	Controls (<i>n</i> = 78)	Schizophrenia (<i>n</i> = 39)	Controls (<i>n</i> = 78)	
CLC	0.995 (0.002)	0.995 (0.001)	1.006 (0.004)	1.007 (0.005)	1.009 (0.006)	1.008 (0.004)	0.001 (0.004)*
	1.018(0.009)**	1.013 (0.005)	0.001 (0.001)*	0.001 (0.002)**	-8.526E-05 (0.004)	0.001 (0.004)*	
PL	0.329 (0.032)	0.346 (0.030)	1.087 (0.028)	1.088 (0.027)	1.104(0.027)	1.099 (0.022)	-0.432
	0.329 (0.032)	0.346 (0.030)	0.003 (0.008)*	0.004 (0.013)**	-0.001 (0.020)**	0.009 (0.025)*	
D	0.329 (0.032)	0.346 (0.030)	0.326 (0.078)*	0.297 (0.053)	0.361 (0.043)**	0.3381 (0.042)	0.514
	0.329 (0.032)	0.346 (0.030)	0.001 (0.009)	-0.001 (0.013)	0.008 (0.025)*	0.020 (0.032)*	

Mean values are shown with the corresponding SD per group. Task-related modulation is defined as the difference for the corresponding functional parameter between its value at the response and prestimulus windows.

*Statistically significant within-group task-related modulation (response minus prestimulus; $p < .05$); **Statistically significant differences between patients and controls ($p < .05$); *** Item $p < .001$.

3.2 | Association between structural and functional networks

3.2.1 | Correlations among graph-theory parameters: PCA

Correlations were high among graph-theory parameters based on structural (dMRI-CLC vs. dMRI-D $r = .802$, $p < .001$; dMRI-CLC vs. dMRI-PL $r = -.515$, $p < .001$) and functional data in the global (EEG-CLC vs. EEG-PL $r = .791$, EEG-CLC vs. EEG-D $r = .512$, $p < .001$) and in the theta bands (EEG-CLC vs. EEG-PL $r = .919$, $p < .001$; EEG-CLC vs. EEG-D $r = .631$, $p < .001$). Therefore, independent variables for the regression models were calculated from PCAs. Eigenvalues higher than the unit and scree-plots were used to select the number of factors, saving individual factor scores. PCA results are summarized in Supporting Information Table S2.

The PCA for structural parameters yielded one factor explaining 73.07% of variance (eigenvalue 2.192), with positive coefficients for dMRI-CLC and dMRI-D and negative for dMRI-PL. Factor scores were statistically significant lower for patients (mean -0.235 , SD 1.125) than for controls (mean 0.294, SD 0.769; $df = 54$, $t = 2.01$, $p = .049$).

PCA of EEG graph-theory parameters in the global band yielded a three factors solution explaining 88.49% of variance, respectively contributed by EEG-CLC, EEG-PL, and EEG-D task-related modulation (42.40% variance, eigenvalue 2.544), prestimulus EEG-PL and EEG-CLC (25.39% variance, eigenvalue 1.52) and both prestimulus and task-related modulation of EEG-D (20.70% variance, eigenvalue 1.242). Scores for the third factor were significantly larger for patients (mean 0.300, SD 1.138) than for controls (mean -0.134 , SD 0.893, $t = 2.26$, $df = 115$, $p = .026$).

In the theta band, a two-factor solution was found. The first was positively related to task-related modulation of EEG-CLC, EEG-PL and EEG-D (53.07% variance, eigenvalue 3.18), whereas the second factor was positively related to prestimulus EEG-CLC, EEG-PL, and EEG-D (23.55% variance, eigenvalue 1.41). Scores for the first factor were smaller at trend level for patients (mean -0.294 , SD 0.759) than for controls (mean 0.119, SD 1.090, $t = -1.86$, $df = 115$, $p = .065$).

3.2.2 | Prediction of functional scores based on structural scores

For the healthy controls, structural factor scores predicted functional global band prestimulus (EEG-PL and EEG-CLC) scores ($R^2 = 0.222$, $df = 1,24$, $F = 6.86$, $\beta = -0.472$, $p = .015$). This relation was not significant for patients ($R^2 = .008$, $df = 1,29$, $F = 0.23$, $\beta = -0.090$, $p = .606$).

In the patients, structural factor scores inversely predicted values of the first factor in the global band (task-related modulation of EEG-PL and EEG-CLC) ($R^2 = .172$, $df = 1,29$, $F = 6.03$, $\beta = -0.415$, $p = .02$; Figure 4a). Therefore, in the patients, larger dMRI-CLC and dMRI-D values were associated to smaller task-related modulation of EEG-PL and EEG-CLC. Since dMRI-PL contributed negatively to the structural factor, that negative association between structural and functional factors implies that shorter dMRI-PL will predict larger EEG-PL and EEG-CLC task-related modulation.

In the patients structural factor scores did not predict functional parameters that had shown significant differences with controls: task-

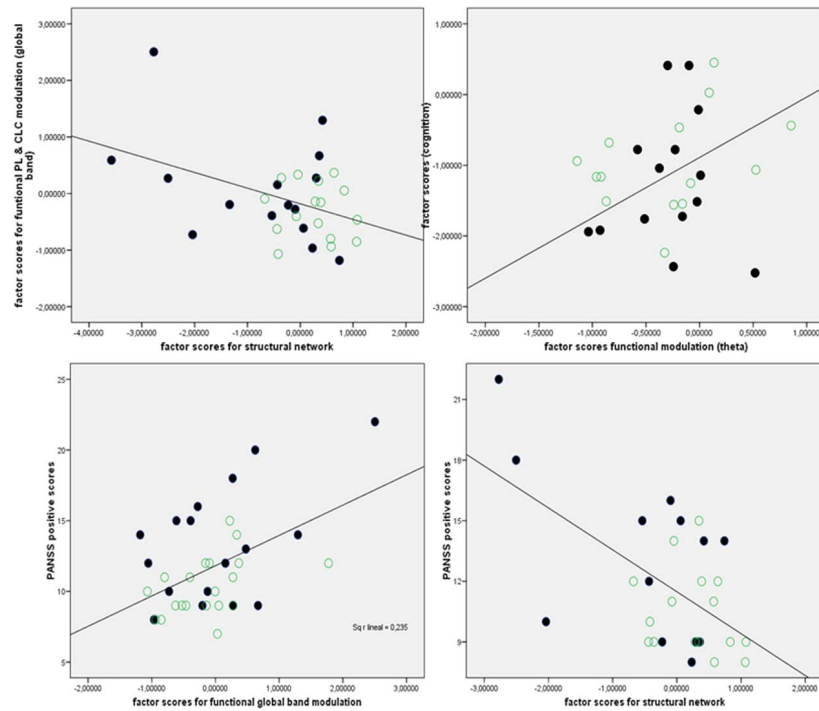


FIGURE 4 Scatterplots showing the association between (a) factor scores resulting from the PCA of structural graph-theory parameters (X axis) and scores of the second factor resulting from the PCA of functional graph-theory parameters in the global band (modulation; Y axis); (b) factor scores for the first factor from the PCA of functional graph-theory parameters at the theta band (modulation) and factor scores from the PCA summarizing cognitive scores; (c) positive PANSS scores and global band PL and CLC task-related modulation and (d) structural network (right) Solid dots represent chronic patients, open dots represent FE patients [Color figure can be viewed at wileyonlinelibrary.com]

related modulation in the theta band ($R^2 = 0.001$, $df = 1,29$, $F = 0.006$, $\beta = 0.015$, $p = .93$), prestimulus EEG-D in the global band ($R^2 = 0.024$, $df = 1,29$, $F = .075$, $\beta = -0.15$, $p = .42$) and prestimulus (EEG-CLC, EEG-PL, and EEG-D) in the theta band ($R^2 = 0.008$, $df = 1,29$, $F = 0.244$, $\beta = 0.091$, $p = .34$).

For the sake of interpretability, we calculated Pearson's correlations between individual d-MRI and EEG graph parameters. dMRI-CLC was negatively associated in the patients to task-related modulation of EEG-PL ($r = -.383$, $p = .03$) and EEG-PL ($r = -.495$, $p = .005$) in the global band. There were no significant correlations between task-related modulation in theta band parameters and individual dMRI-based graph parameters ($-.28 > r > .166$).

3.2.3 | Structural networks and specific tracts

Structural PL was inversely associated to FA ($n = 55$) in the tracts linking homolaterally dorsolateral PFC with right cingulate ($r = -.299$,

$p = .028$), left cingulate ($r = -.357$, $p = .008$), right hippocampus ($r = -.499$, $p < .001$), left caudate ($r = -.446$, $p = .001$), left parietal ($r = -.394$, $p = .003$), left superior temporal ($r = -.359$, $p = .007$), right superior temporal ($r = -.478$, $p < 0.001$), left insula ($r = -.322$, $p = .016$) and right insula ($r = -.359$, $p = .007$). No positive correlations were found between structural PL and FA values.

Structural CLC was directly related to FA in the tracts linking homolaterally dorsolateral PFC with right hippocampus ($r = .508$, $p < .001$), left parietal ($r = .392$, $p = .003$) and right parietal ($r = .273$, $p = .044$). Similarly, structural density was directly related to FA in the tracts linking homolaterally dorsolateral PFC with left hippocampus ($r = .328$, $p = .016$), right hippocampus ($r = .404$, $p = .002$), left thalamus ($r = .337$, $p = .013$), left caudate ($r = .268$, $p = .050$), left parietal ($r = .542$, $p < .001$), right parietal ($r = .435$, $p = .001$), left superior temporal ($r = .331$, $p = .014$), right superior temporal ($r = .475$, $p < .001$), left insula ($r = 0.316$, $p = 0.019$) and right insula ($r = .424$, $p = .001$).

Only associations at $p \leq .001$ were significant after Bonferroni adjustment.

3.3 | Cognitive and clinical correlates

The factor analysis of cognitive scores yielded a single factor (eigenvalue 3.449), with positive coefficients for all but percent of perseverative errors, explaining 54.11% of the total variance.

Scores of the first factor in the theta band (modulation) directly predicted cognitive performance in the patients ($R^2 = 0.312$, $df = 1,28$, $\beta = 0.558$, $F = 12.22$, $p = .002$; Figure 4b). Structural values were not associated to cognition in patients.

Positive symptoms were inversely associated to structural network factor scores ($R^2 = 0.329$, $df = 1,29$, $F = 13.21$, $\beta = -0.573$, $p = .001$; Figure 4c), therefore positively associated to dMRI-CLC and dMRI-D and inversely to dMRI-PL. The first factor in the global band (task-related modulation of EEG-PL and EEG-CLC) positively predicted positive symptoms ($R^2 = 0.235$, $df = 1,35$, $F = 10.74$, $\beta = -1.274$, $p = .002$; Figure 4d). To further clarify this point, we calculated the partial correlation coefficients between positive symptoms and structural factor scores controlling for global band task-related modulation ($r = -.459$, $p = .006$) and between positive symptoms and global band task-related modulation controlling for structural network values ($r = .432$, $p = .01$), supporting the independence of the associations.

3.4 | Confounding factors

Duration of illness was inversely associated to structural factor scores ($r = -.599$, $p = .001$). Thus, larger duration would imply smaller dMRI-CLC and dMRI-D as well as longer dMRI-PL. Current antipsychotic dose was not significantly related to structural ($-.069 < r < .148$, $p = n.s.$) nor functional ($-.040 < r < .183$, $p = n.s.$) graph-theory parameters.

4 | DISCUSSION

Global band network characteristics a baseline in control and its task-related modulation in patients were predicted by structural network parameters. EEG-PL and EEG-CLC in the global band and EEG-D in the theta band showed a significant task-related modulation only in controls after adjustment for multiple comparisons. Although unadjusted, patients showed larger dMRI-PL, higher prestimulus EEG-D at both global and theta bands and reduced functional task-related modulation of EEG-PL at the theta band, without any significant association between these structural and functional alterations. In patients, structural connectivity and theta task-related modulation respectively predicted positive symptoms and cognition.

Network parameters have been calculated from scalp sensors in this work. Therefore, the connectivity estimates are not derived from true sources of the corresponding activity involved in task processing. Volume conduction effects imply that signals from different sources arrive to different sensors, hampering the estimation of the connectivity among the original activity sources (Brunner, Billinger, Seeber, Mullen, & Makeig, 2016; Van de Steen et al., 2016). Our functional

estimates are therefore to be considered just a global outline of the functional network characteristics and their modulation with cognitive activity. However, this outline may contain useful information regarding characteristics such as local clustering, mean PL and density of functional connections. They can be relevant to understand differences between patients and controls in terms of prestimulus network organization and their change with cognition. Source estimates using procedures such as low-resolution tomography might allow identifying activity sources from which PLV values could be calculated and among which structural connectivity could be assessed. This approach would be useful to describe effective connectivity relations among these sources, which can be of interest for the pathophysiology of psychosis. Those procedures, however, are not completely reliable, and the inverse solution problem remains unsolved. Therefore, the functional global outline here describe can hold a significant value, in particular its fast modulation with cognition; although only indirectly reflecting the characteristics of the underlying sources.

We calculated structural connectivity parameters using FA values from white matter tracts linking anatomical regions and functional connectivity using phase similarity of EEG signals between sensors. Both measurements summarized the same properties of the respective networks, and the prediction of global band prestimulus (controls) and task-related modulation (patients) functional values from structural scores supports the relation of both kinds of networks. Caution is necessary when considering these relations, given the above mentioned possible influence of volume conduction effects. Remarkably, abnormalities in structural and functional networks were unrelated in the patients.

The lower factor scores in the patients for structural connectivity (positively loaded for dMRI-CLC and dMRI-D and inversely related to dMRI-PL), suggest a reduced integrity of white matter connectivity in schizophrenia among nearby (reflected in lower CLC) and distant (longer PL) regions. The larger dMRI-PL in our patients is coherent with reports of reduction of global communication paths (Griffa et al., 2015; van den Heuvel et al., 2013) and lower FA in schizophrenia, likely reflecting alterations of long-range tracts (Ellison-Wright & Bullmore, 2009; Patel et al., 2011).

To our notice, no previous study has explored the structural underpinnings of alterations of fast task-related modulation in functional networks in schizophrenia. Odd-ball task performance involves the coordination of different brain regions (Linden et al., 1999). For both groups, EEG-PL and EEG-CLC in the global band increased from prestimulus to response windows, which imply that widespread local task-related activations elongate mean EEG-PL and increase EEG-CLC. In our cases, factor scores summarizing structural network (positively associated to dMRI-CLC and dMRI-D, and negatively to dMRI-PL) inversely predicted EEG-PL and EEG-CLC task-related modulation in the global band in patients. Thus, patients with smaller dMRI-CLC and dMRI-D, and larger dMRI-PL, would show a smaller global band EEG-CLC and EEG-PL modulation. However, as compared with controls, patients did not show a deficit of functional EEG-PL task-related modulation in the global band, raising doubts about the significance for

schizophrenia of that association between structural connectivity and global band modulation.

Instead, we found task-related modulation deficits in patients in the theta band. However, modulation in the global band was not decreased in patients, which may relate to the relatively larger involvement of theta oscillations in P300 performance as shown by relative power and median frequency analysis during this task (Bachiller et al., 2014). Using different methodologies, smaller increases of theta power have been found for schizophrenia patients during P300 tasks (Bachiller et al., 2014; Doege et al., 2009). Taken together, this suggests a higher impact on theta than global band connectivity in schizophrenia. Since theta oscillations have a role in synchronization between distant regions (von Stein, Chiang, & Konig, 2000), the task-related modulation deficit in theta suggests a decreased capacity for integrating activity across cortical regions in schizophrenia, which would be not closely associated to anatomical connectivity deficits according to our results.

Such relative independence of structural and functional connectivity alterations surprised us, but could be explained by data showing that functional connectivity exists between regions without direct anatomical connection (Adachi et al., 2012; Honey et al., 2009). Thus, deficits of functional integration (in the theta band) would not require altered structural substrates. Coordination of activity between distant regions may be established indirectly, since functional connectivity is high among regions with common efferences to third regions, which may convey information to higher regions and may also receive similar afferences (Adachi et al., 2012). Therefore, the alteration in relevant cortical hubs reported in schizophrenia (van den Heuvel et al., 2013) may hamper the synchronization of regions not directly linked via white matter tracts. Although other data using anatomical and functional MRI show a substantial correspondence between the corresponding networks (Hagmann et al., 2008), this relation had not been assessed yet with EEG data. Considering all this, we must underline that structural deficits were found in our patients (larger dMRI-PL and lower factor scores) and were predictive of positive symptoms. This suggests the coexistence of alterations in both structural and functional networks (in the theta band) within schizophrenia, but not necessarily in the same cases. In other words, either both unrelated functional and structural networks alterations are found in schizophrenia or they are characteristics of different schizophrenia subgroups. The latter possibility seems favored by recent reports supporting that structural connectivity values can segregate biologically valid clusters within schizophrenia (Lubeiro et al., 2016; Sun et al., 2015; Wheeler et al., 2015). Using EEG, both no difference (Jhung et al., 2013; Rubinov et al., 2009) and a decrease (Micheloyannis et al., 2006) of CLC at rest were reported in schizophrenia, which may be coherent with that possibility.

Remarkably, prestimulus EEG-D is higher in the patients. The density is the mean network degree (i.e., a measure of the network strength), implying a functional over-connectivity at rest in schizophrenia. This result is in agreement with the increased prefrontal functional connectivity reported in schizophrenia (Anticevic et al., 2015). The different patterns of dMRI-D and EEG-D in patients, and the lack of a significant relation between them, support the independence of the alterations in both networks. Speculatively, the increased EEG-D might

relate to the deficit in GABA function observed in schizophrenia (Gonzalez-Burgos, Fish, & Lewis, 2011; Thakkar et al., 2017), which could lead to hyper-synchronization. In our study, functional connectivity is based on PLV values; thus, larger prestimulus theta EEG-D values suggest and excess of synchronization in the patients in this band, which could have a ceiling effect on task-related synchronization and might hamper theta EEG-D modulation. Therefore, an inhibitory transmission deficit could justify both the increased baseline D values and the lower modulation in the theta band, given its large implication in P300 task performance (Bachiller et al., 2014; Doege et al., 2009). This possible dependence on inhibitory function might also justify the lack of a significant prediction of theta modulation by structural connectivity.

The increase in theta task-related modulation values (i.e., larger functional density, CLC and PL in this band) predicted better cognition in the patients. There was only one cognitive factor, which is not surprising since the assessment instrument (BACS) included the dimensions where performance was previously found decreased in schizophrenia. That predictive relationship suggests that cognitive deficit is secondary to the decreased capacity of modulating the functional network in the theta band, perhaps indicating a lesser capacity to integrate the activity of different areas in a task.

Our study is limited by the sample size of patients with both structural and functional network data available. A larger sample would be needed to test the hypothesis of distinct schizophrenia clusters based on structural connectivity. In addition, the assessment of nodal parameters could be of interest. However, connectivity analysis at the sensor level is very problematic due to effects of field spread (Schoffelen & Gross, 2009). Therefore, future studies should also be focused on increasing the number of EEG electrodes to provide more accurate results. Moreover, we cannot rule out an effect of treatment, although antipsychotic doses were unrelated to structural and functional graph parameters. It must be also noted that all EEG measures are influenced by volume conduction. In order to minimize this effect, a well-known strategy is based on the assumption that volume conduction affects the connectivity estimates in a similar way in two different experimental contrasts, such as prestimulus and response conditions (Bastos & Schoffelen, 2016). With regard to the use of dMRI-based connectivity, the accuracy of the cortical segmentation and the choice of the tractography method influence the obtained connectivity matrices. Although FA is the most usual dMRI descriptor for white matter integrity, it cannot identify the ultimate origin of connectivity alterations.

We may conclude that task-related modulation deficit in the theta band in schizophrenia is independent from deviation from normal structural network properties. This, considered together with the different correlates of functional and structural connectivity alterations, might support different clusters within the schizophrenia syndrome.

ORCID

Vicente Molina  <http://orcid.org/0000-0003-2457-2487>

REFERENCES

- Adachi, Y., Osada, T., Sporns, O., Watanabe, T., Matsui, T., Miyamoto, K., & Miyashita, Y. (2012). Functional connectivity between anatomically unconnected areas is shaped by collective network-level effects in the macaque cortex. *Cerebral Cortex*, 22(7), 1586–1592.
- Anticevic, A., Hu, X., Xiao, Y., Hu, J., Li, F., Bi, F., ... Gong, Q. (2015). Early-course unmedicated schizophrenia patients exhibit elevated prefrontal connectivity associated with longitudinal change. *Journal of Neuroscience*, 35(1), 267–286.
- Bachiller, A., Diez, A., Suazo, V., Dominguez, C., Ayuso, M., Hornero, R., ... Molina, V. (2014). Decreased spectral entropy modulation in patients with schizophrenia during a P300 task. *European Archives of Psychiatry and Clinical Neuroscience*, 264(6), 533–543.
- Bachiller, A., Poza, J., Gomez, C., Molina, V., Suazo, V., & Hornero, R. (2015a). A comparative study of event-related coupling patterns during an auditory oddball task in schizophrenia. *Journal of Neural Engineering*, 12, 016007.
- Bachiller, A., Romero, S., Molina, V., Alonso, J. F., Mananas, M. A., Poza, J., & Hornero, R. (2015b). Auditory P3a and P3b neural generators in schizophrenia: An adaptive sLORETA P300 localization approach. *Schizophrenia Research*, 169, 318–325.
- Bastos, A. M., & Schoffelen, J. M. (2016). A tutorial review of functional connectivity analysis methods and their interpretational pitfalls. *Frontiers in Systems Neuroscience*, 9, 175.
- Bledowski, C., Prvulovic, D., Hoehstetter, K., Scherg, M., Wibral, M., Goebel, R., & Linden, D. E. (2004). Localizing P300 generators in visual target and distractor processing: A combined event-related potential and functional magnetic resonance imaging study. *Journal of Neuroscience*, 24(42), 9353–9360.
- Bob, P., Palus, M., Susta, M., & Glaslova, K. (2008). EEG phase synchronization in patients with paranoid schizophrenia. *Neuroscience Letters*, 447(1), 73–77.
- Bohken, M. M., Brouwer, R. M., Mandl, R. C., Van den Heuvel, M. P., Hedman, A. M., De Hert, M., ... Hulshoff Pol, H. E. (2016). Structural Brain Connectivity as a Genetic Marker for Schizophrenia. *JAMA Psychiatry*, 73(1), 11–19.
- Bressler, S. L., Coppola, R., & Nakamura, R. (1993). Episodic multiregional cortical coherence at multiple frequencies during visual task performance. *Nature*, 366(6451), 153–156.
- Brunner, C., Billinger, M., Seeber, M., Mullen, T. R., & Makeig, S. (2016). Volume conduction influences scalp-based connectivity estimates. *Frontiers in Computational Neuroscience*, 10, 121.
- Bullmore, E., & Sporns, O. (2009). Complex brain networks: Graph theoretical analysis of structural and functional systems. *Nature Reviews Neuroscience*, 10(3), 186–198.
- Collin, G., Scholtens, L. H., Kahn, R. S., Hillegers, M. H. J., & van den Heuvel, M. P. (2017). Affected anatomical rich club and structural-functional coupling in young offspring of schizophrenia and bipolar disorder patients. *Biological Psychiatry*, 82(10), 746–755.
- Dehaene, S., & Changeux, J. P. (2011). Experimental and theoretical approaches to conscious processing. *Neuron*, 70(2), 200–227.
- Desikan, R. S., Segonne, F., Fischl, B., Quinn, B. T., Dickerson, B. C., Blacker, D., ... Killiany, R. J. (2006). An automated labeling system for subdividing the human cerebral cortex on MRI scans into gyral based regions of interest. *Neuroimage*, 31(3), 968–980.
- Dhollander, T., & Connelly, A. (2016). Unsupervised 3-tissue response function estimation from single-shell or multi-shell diffusion mr data without a co-registered t1 image. In *ISMRM Workshop on Breaking the Barriers of Diffusion MRI*. (vol. 5).
- Di Biase, M. A., Cropley, V. L., Baune, B. T., Olver, J., Amminger, G. P., Phassouliotis, C., ... Zalesky, A. (2017). White matter connectivity disruptions in early and chronic schizophrenia. *Psychological Medicine*, 47(16), 2797–2810.
- Doegi, K., Bates, A. T., White, T. P., Das, D., Boks, M. P., & Liddle, P. F. (2009). Reduced event-related low frequency EEG activity in schizophrenia during an auditory oddball task. *Psychophysiology*, 46(3), 566–577.
- Ellison-Wright, I., & Bullmore, E. (2009). Meta-analysis of diffusion tensor imaging studies in schizophrenia. *Schizophrenia Research*, 108(1–3), 3–10.
- Fischl, B., van der, K. A., Destrieux, C., Halgren, E., Segonne, F., Salat, D. H., ... Dale, A. M. (2004). Automatically parcellating the human cerebral cortex. *Cerebral Cortex*, 14, 11–22.
- Gomez-Pilar, J., Lubeiro, A., Poza, J., Hornero, R., Ayuso, M., Valcarcel, C., ... Molina, V. (2017). Functional EEG network analysis in schizophrenia: Evidence of larger segregation and deficit of modulation. *Progress in Neuropsychopharmacology and Biological Psychiatry*, 76, 116–123.
- Gomez-Pilar, J., Poza, J., Bachiller, A., Gomez, C., Nuñez, P., Lubeiro, A., ... Hornero, R. (2018). Quantification of graph complexity based on the edge weight distribution balance: Application to brain networks. *International Journal of Neural Systems*, 28(01), 1750032.
- Gonzalez-Burgos, G., Fish, K. N., & Lewis, D. A. (2011). GABA neuron alterations, cortical circuit dysfunction and cognitive deficits in schizophrenia. *Neural Plastics*, 2011, 1.
- Griffa, A., Baumann, P. S., Ferrari, C., Do, K. Q., Conus, P., Thiran, J. P., & Hagmann, P. (2015). Characterizing the connectome in schizophrenia with diffusion spectrum imaging. *Human Brain Mapping*, 36(1), 354–366.
- Hagmann, P., Cammoun, L., Gigandet, X., Meuli, R., Honey, C. J., Wedeen, V. J., & Sporns, O. (2008). Mapping the structural core of human cerebral cortex. *PLoS Biology*, 6(7), e159.
- Honey, C. J., Sporns, O., Cammoun, L., Gigandet, X., Thiran, J. P., Meuli, R., & Hagmann, P. (2009). Predicting human resting-state functional connectivity from structural connectivity. *Proceedings of the National Academy of Sciences of the United States of America*, 106(6), 2035–2040.
- Honey, C. J., Thivierge, J. P., & Sporns, O. (2010). Can structure predict function in the human brain? *Neuroimage*, 52(3), 766–776.
- Jhung, K., Cho, S. H., Jang, J. H., Park, J. Y., Shin, D., Kim, K. R., ... An, S. K. (2013). Small-world networks in individuals at ultra-high risk for psychosis and first-episode schizophrenia during a working memory task. *Neuroscience Letters*, 535, 35–39.
- Jones, J. T., DiFrancesco, M., Zaal, A. I., Klein-Gitelman, M. S., Gitelman, D., Ying, J., & Brunner, H. I. (2015). Childhood-onset lupus with clinical neurocognitive dysfunction shows lower streamline density and pairwise connectivity on diffusion tensor imaging. *Lupus*, 24(10), 1081–1086.
- Kambeitz, J., Kambeitz-Ilankovic, L., Cabral, C., Dwyer, D. B., Calhoun, V. D., van den Heuvel, M. P., ... Malchow, B. (2016). Aberrant functional whole-brain network architecture in patients with schizophrenia: A meta-analysis. *Schizophrenia Bulletin*, 42(Suppl 1), S13–S21.
- Kay, S. R., Fiszbein, A., & Opler, L. A. (1987). The positive and negative syndrome scale (PANSS) for schizophrenia. *Schizophrenia Bulletin*, 13(2), 261–276.
- Lachaux, J. P., Rodriguez, E., Martinerie, J., & Varela, F. J. (1999). Measuring phase synchrony in brain signals. *Human Brain Mapping*, 8(4), 194–208.
- Linden, D. E., Prvulovic, D., Formisano, E., Vollinger, M., Zanella, F. E., Goebel, R., & Dierks, T. (1999). The functional neuroanatomy of

- target detection: An fMRI study of visual and auditory oddball tasks. *Cerebral Cortex*, 9(8), 815–823.
- Lo, C. Y., Su, T. W., Huang, C. C., Hung, C. C., Chen, W. L., Lan, T. H., ... Bullmore, E. T. (2015). Randomization and resilience of brain functional networks as systems-level endophenotypes of schizophrenia. *Proceedings of the National Academy of Sciences of the United States of America*, 112(29), 9123–9128.
- Lubeiro, A., Rueda, C., Hernandez, J. A., Sanz, J., Sarramea, F., & Molina, V. (2016). Identification of two clusters within schizophrenia with different structural, functional and clinical characteristics. *Progress in Neuropsychopharmacology & Biological Psychiatry*, 64, 79–86.
- Ma, S., Calhoun, V. D., Eichele, T., Du, W., & Adali, T. (2012). Modulations of functional connectivity in the healthy and schizophrenia groups during task and rest. *Neuroimage*, 62(3), 1694–1704.
- Martin-Santiago, O., Gomez-Pilar, J., Lubeiro, A., Ayuso, M., Poza, J., Hornero, R., ... Molina, V. (2016). Modulation of brain network parameters associated with subclinical psychotic symptoms. *Progress in Neuropsychopharmacology & Biological Psychiatry*, 66, 54–62.
- Micheloyannis, S., Pachou, E., Stam, C. J., Breakspear, M., Bitsios, P., Vourkas, M., ... Zervakis, M. (2006). Small-world networks and disturbed functional connectivity in schizophrenia. *Schizophrenia Research*, 87(1–3), 60–66.
- Molina, V., Lubeiro, A., Soto, O., Rodriguez, M., Alvarez, A., Hernandez, R., & de Luis-Garcia, R. (2017). Alterations in prefrontal connectivity in schizophrenia assessed using diffusion magnetic resonance imaging. *Progress in Neuropsychopharmacology & Biology Psychiatry*, 76, 107–115.
- Nunez, P., Poza, J., Bachiller, A., Gomez-Pilar, J., Lubeiro, A., Molina, V., & Hornero, R. (2017). Exploring non-stationarity patterns in schizophrenia: Neural reorganization abnormalities in the alpha band. *Journal of Neural Engineering*, 14(4), 046001.
- Patel, S., Mahon, K., Wellington, R., Zhang, J., Chaplin, W., & Szeszko, P. R. (2011). A meta-analysis of diffusion tensor imaging studies of the corpus callosum in schizophrenia. *Schizophrenia Research*, 129(2–3), 149–155.
- Patenaude, B., Smith, S. M., Kennedy, D. N., & Jenkinson, M. (2011). A Bayesian model of shape and appearance for subcortical brain segmentation. *Neuroimage*, 56(3), 907–922.
- Rubinov, M., Knock, S. A., Stam, C. J., Micheloyannis, S., Harris, A. W., Williams, L. M., & Breakspear, M. (2009). Small-world properties of nonlinear brain activity in schizophrenia. *Human Brain Mapping*, 30(2), 403–416.
- Rubinov, M., & Sporns, O. (2010). Complex network measures of brain connectivity: Uses and interpretations. *Neuroimage*, 52(3), 1059–1069.
- Salvador, R., Pena, A., Menon, D. K., Carpenter, T. A., Pickard, J. D., & Bullmore, E. T. (2005). Formal characterization and extension of the linearized diffusion tensor model. *Human Brain Mapping*, 24(2), 144–155.
- Schoffelen, J. M., & Gross, J. (2009). Source connectivity analysis with MEG and EEG. *Human Brain Mapping*, 30(6), 1857–1865.
- Segarra, N., Bernardo, M., Gutierrez, F., Justicia, A., Fernandez-Egea, E., Allas, M., ... Keefe, R. S. (2011). Spanish validation of the Brief Assessment in Cognition in Schizophrenia (BACS) in patients with schizophrenia and healthy controls. *European Psychiatry*, 26(2), 69–73.
- Shim, M., Kim, D. W., Lee, S. H., & Im, C. H. (2014). Disruptions in small-world cortical functional connectivity network during an auditory oddball paradigm task in patients with schizophrenia. *Schizophrenia Research*, 156(2–3), 197–203.
- Smith, S. M. (2002). Fast robust automated brain extraction. *Human Brain Mapping*, 17(3), 143–155.
- Spencer, K. M., Nestor, P. G., Niznikiewicz, M. A., Salisbury, D. F., Shenton, M. E., & McCarley, R. W. (2003). Abnormal neural synchrony in schizophrenia. *Journal of Neuroscience*, 23, 7407–7411.
- Stam, C. J., de Haan, W., Daffertshofer, A., Jones, B. F., Manshanden, I., van Cappellen van Walsum, A. M., ... Scheltens, P. (2009). Graph theoretical analysis of magnetoencephalographic functional connectivity in Alzheimer's disease. *Brain*, 132(1), 213–224.
- Sui, J., Yu, Q., He, H., Pearson, G. D., & Calhoun, V. D. (2012). A selective review of multimodal fusion methods in schizophrenia. *Frontiers in Human Neuroscience*, 6, 27.
- Sun, H., Lui, S., Yao, L., Deng, W., Xiao, Y., Zhang, W., ... Gong, Q. (2015). Two patterns of white matter abnormalities in medication-naive patients with first-episode schizophrenia revealed by diffusion tensor imaging and cluster analysis. *JAMA Psychiatry*, 72(7), 678–686.
- Thakkar, K. N., Rosler, L., Wijnen, J. P., Boer, V. O., Klomp, D. W., Cahn, W., ... Neggers, S. F. (2017). 7T Proton magnetic resonance spectroscopy of gamma-aminobutyric acid, glutamate, and glutamine reveals altered concentrations in patients with schizophrenia and healthy siblings. *Biological Psychiatry*, 81(6), 525–535.
- Tournier, J. D., Calamante, F., & Connelly, A. (2007). Robust determination of the fibre orientation distribution in diffusion MRI: Non-negativity constrained super-resolved spherical deconvolution. *Neuroimage*, 35(4), 1459–1472.
- Van de Steen, F., Faes, L., Karahan, E., Songirir, J., Valdes-Sosa, P. A., & Marinazzo, D. (2016). Critical comments on EEG sensor space dynamical connectivity analysis. *Brain Topography*, [Epub ahead of print].
- van den Heuvel, M. P., Mandl, R. C., Stam, C. J., Kahn, R. S., & Hulshoff Pol, H. E. (2010). Aberrant frontal and temporal complex network structure in schizophrenia: A graph theoretical analysis. *The Journal of Neuroscience: The Official Journal of the Society for Neuroscience*, 30(47), 15915–15926.
- van den Heuvel, M. P., Sporns, O., Collin, G., Scheewe, T., Mandl, R. C., Cahn, W., ... Kahn, R. S. (2013). Abnormal rich club organization and functional brain dynamics in schizophrenia. *JAMA Psychiatry*, 70(8), 783–792.
- van Diessen, E., Numan, T., van Dellen, E., van der Kooij, A. W., Boersma, M., Hofman, D., ... Stam, C. J. (2015). Opportunities and methodological challenges in EEG and MEG resting state functional brain network research. *Clinical Neurophysiology*, 126(8), 1468–1481.
- Varela, F., Lachaux, J. P., Rodriguez, E., & Martinerie, J. (2001). The brainweb: Phase synchronization and large-scale integration. *Nature Reviews Neuroscience*, 2(4), 229–239.
- von Stein, A., Chiang, C., & Konig, P. (2000). Top-down processing mediated by interareal synchronization. *Proceedings of the National Academy of Sciences of the United States of America*, 97(26), 14748–14753.
- Wheeler, A. L., Wessa, M., Szeszko, P. R., Foussias, G., Chakravarty, M. M., Lerch, J. P., ... Voineskos, A. N. (2015). Further neuroimaging evidence for the deficit subtype of schizophrenia. A cortical connectomics analysis. *JAMA Psychiatry*, 72(5), 446–455.
- Yu, Q., Sui, J., Rachakonda, S., He, H., Gruner, W., Pearson, G., ... Calhoun, V. D. (2011). Altered topological properties of functional network connectivity in schizophrenia during resting state: A small-world brain network study. *PLoS One*, 6(9), e25423.

Zhang, Y., Brady, M., & Smith, S. (2001). Segmentation of brain MR images through a hidden Markov random field model and the expectation-maximization algorithm. *IEEE Transactions on Medical Imaging*, 20(1), 45-57.

SUPPORTING INFORMATION

Additional Supporting Information may be found online in the supporting information tab for this article.

How to cite this article: Gomez-Pilar J, de Luis-García R, Lubeiro A, et al. Relations between structural and EEG-based graph metrics in healthy controls and schizophrenia patients. *Hum Brain Mapp.* 2018;00:1-14. <https://doi.org/10.1002/hbm.24066>

Supplementary material of the paper: “Relations between structural and EEG-based graph metrics in healthy controls and schizophrenia patients”

Table A.2: Factor structure of connectivity networks and cognitive scores. Results of the principal components analyses performed to obtain factor scores for structural and functional (global band and theta band) networks and cognitive performance. The variables included in each component are boldfaced.

	Factor 1
CLC	0.928
PL	-0.725
D	0.897
Structural network	

	Factor 1	Factor 2
CLC pre-stimulus	-0.167	0.935
PL pre-stimulus	-0.088	0.934
D pre-stimulus	-0.229	0.570
CLC modulation	0.889	-0.302
PL modulation	0.870	-0.253
D modulation	0.856	-0.029
Functional theta band		

	Factor 1	Factor 2	Factor 3
CLC pre-stimulus	0.059	0.900	0.388
PL pre-stimulus	0.131	0.960	-0.110
D pre-stimulus	-0.085	0.158	0.923
CLC modulation	0.936	0.163	0.080
PL modulation	0.929	0.037	0.081
D modulation	0.429	-0.014	0.739
Functional global band			

	Factor 1
Verbal memory	0.783
Working memory	0.794
Motor speed	0.505
Verbal fluency	0.710
Performance speed	0.806
Tower of London	0.654
Perseverative errors	-0.608
Cognitive scores	

Table A.3: P300 latency and amplitude at Pz electrode.

	Schizophrenia	Controls	<i>p</i> -value
P300 amplitude (μV)	2.15 ± 1.56	2.9863 ± 1.62	0.0086
P300 latency (ms)	435.38 ± 70.35	454.68 ± 71.89	0.1698

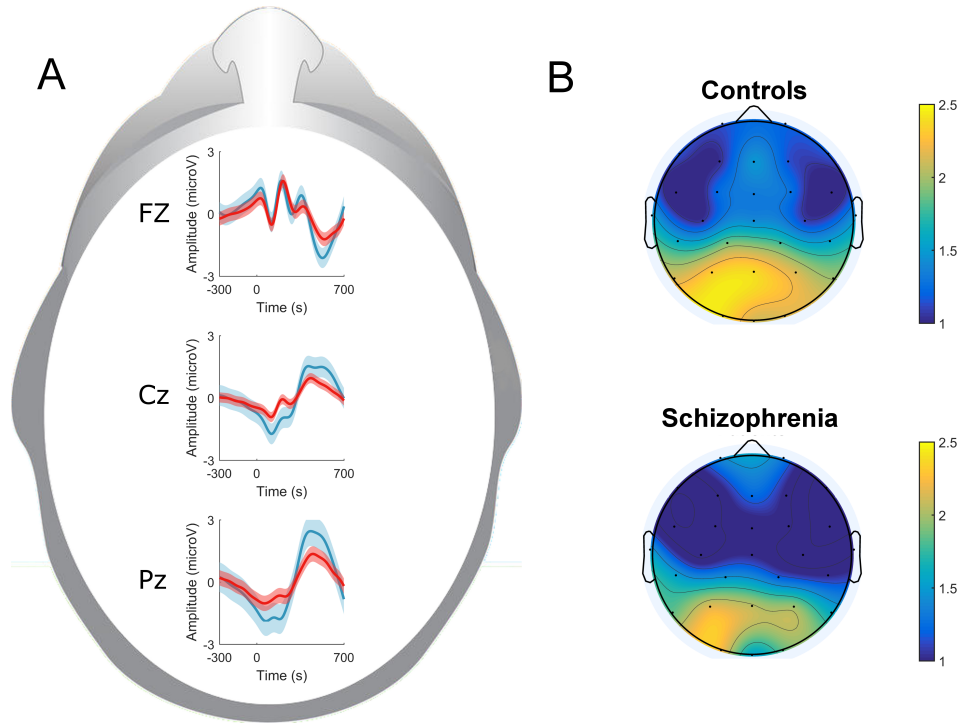


Figure A.1: (A) P300 waveforms in the middle line of the brain scalp (Fz, Cz and Pz electrodes) for controls (blue) and patients (red). (B) Scalp map depicting the P300 peak amplitude at Pz for controls and patients around the latency of both groups (450 ms).

Table A.4: Mean values and comparison between first episode (FE) and chronic (CH) schizophrenia patients for the network variables with significant differences between patients and healthy controls. * Significantly higher in chronic patients (Mann-Whitney U -test, $p = 0.009$)

	Structural PL	Global band D	Theta band D	Theta band modulation
FE	1.014(0.005)	0.313 (0.064)	0.346 (0.029)	0.001 (0.020)
CH	1.023 (0.112)*	0.338 (0.083)	0.373 (0.047)	-0.001 (0.190)

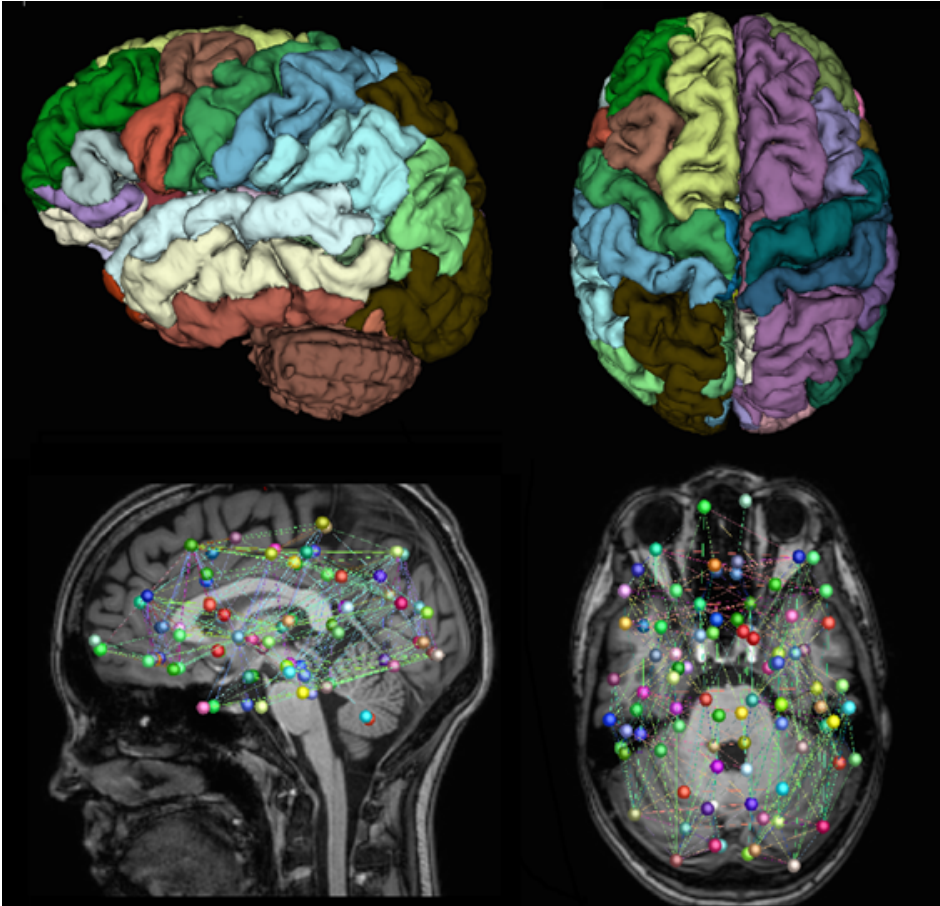


Figure A.2: Upper row: Lateral and superior views of the regions from which the structural connectivity matrix was built. Lower row: Lateral and superior views of hypothetical dMRI network based on segmented regions.

Quantification of Graph Complexity Based on the Edge Weight Distribution Balance: Application to Brain Networks

Javier Gomez-Pilar*, Jesús Poza^{*,†,‡,||}, Alejandro Bachiller*,
Carlos Gómez*, Pablo Núñez*, Alba Lubeiro[§],
Vicente Molina^{‡,§,¶} and Roberto Hornero^{*,†,‡}
^{*}Biomedical Engineering Group, E.T.S. Ingenieros de Telecomunicación
Universidad de Valladolid, Paseo Belén, 15, 47011 Valladolid, Spain
[†]IMUVA, Instituto de Investigación en Matemáticas
Universidad de Valladolid, Valladolid, Spain
[‡]INCYL, Instituto de Neurociencias de Castilla y León
Universidad de Salamanca, Salamanca, Spain
[§]Psychiatry Department, Facultad de Medicina
Universidad de Valladolid, Valladolid, Spain
[¶]Clinical University Hospital of Valladolid, Valladolid, Spain
^{||}jesus.poza@tel.uva.es

Accepted 19 May 2017
Published Online 10 July 2017

The aim of this study was to introduce a novel global measure of graph complexity: Shannon graph complexity (SGC). This measure was specifically developed for weighted graphs, but it can also be applied to binary graphs. The proposed complexity measure was designed to capture the interplay between two properties of a system: the ‘information’ (calculated by means of Shannon entropy) and the ‘order’ of the system (estimated by means of a disequilibrium measure). SGC is based on the concept that complex graphs should maintain an equilibrium between the aforementioned two properties, which can be measured by means of the edge weight distribution. In this study, SGC was assessed using four synthetic graph datasets and a real dataset, formed by electroencephalographic (EEG) recordings from controls and schizophrenia patients. SGC was compared with graph density (GD), a classical measure used to evaluate graph complexity. Our results showed that SGC is invariant with respect to GD and independent of node degree distribution. Furthermore, its variation with graph size (N) is close to zero for $N > 30$. Results from the real dataset showed an increment in the weight distribution balance during the cognitive processing for both controls and schizophrenia patients, although these changes are more relevant for controls. Our findings revealed that SGC does not need a comparison with null-hypothesis networks constructed by a surrogate process. In addition, SGC results on the real dataset suggest that schizophrenia is associated with a deficit in the brain dynamic reorganization related to secondary pathways of the brain network.

Keywords: Graph theory; brain networks; brain complexity; entropy.

1. Introduction

The application of graph-theoretical analyses to study brain networks constitutes an evolving field with a high impact in neuroscience. The characterization of brain networks in terms of integration,

segregation, regularity or complexity has become of paramount importance to identify the underlying processes of the functional neural organization in the brain. In order to understand brain network behavior, previous works conducted resting-state activity

analyses^{1,2} as well as task-related activity ones.³⁻⁵ Both together provide an overall view of brain networks generated under different conditions. Functional complex brain networks are usually depicted by a set of nodes (vertices) and connections (edges or links). These connections represent the statistical dependence between neural activity in different brain areas, obtained by correlations, mutual information or coherence, among others.^{6,7} Most brain graph studies use binary connections between nodes (i.e. a threshold is applied to dichotomize the edge weights).⁸ Although this is an apparently simple model, these graph analyses are interpretable in relation to general principles of complex system organization.⁸ On the other hand, weighted network analysis introduces the concept of connection strength between nodes. It can be considered a more realistic approach of the physiological properties of brain networks.^{8,9} Unfortunately, the use of weighted graphs is not exempt from methodological concerns, which have not been completely solved yet.⁹

A high amount of measures have been proposed to describe the organization and function of brain networks.¹⁰⁻¹² These network measures are usually defined for binary graphs and, when possible, generalized for more complex graphs such as weighted and/or directed graphs. Roughly speaking, network measures can be divided into two classes, depending on the nodes involved: (i) local measures, related to a single node or edge (for the computation other nodes/edges can be involved, even all of them), and (ii) global measures, which describe the properties of the entire network. Usually, global network measures are strongly influenced by basic properties such as network size (N), graph density (GD) and node degree distribution.⁹ For instance, consider a graph **A**, as a complete, binary and undirected graph with $N = 10$ nodes, and a graph **B** with equal basic characteristics (complete, binary and undirected), but with $N = 100$ nodes. Node degree distributions are similar for both cases, and the maximum GD possible for each respective N is reached for these two graphs. Although both graphs have similar topology and their main difference is N , the characteristic path length (i.e. the average shortest path length between all pairs of nodes in the network¹³) of graph **A** is much lower than that of graph **B** because of the network size. Consequently, the statistical significance of the network parameters must be considered by

comparing them with null-hypothesis networks (i.e. networks constructed by surrogate process).¹¹ Null-hypothesis networks can be modeled as networks with the same basic characteristics as the original network (N , GD and node degree distribution), but with different topology.¹¹ Null models are often used as a reference point to determine whether a graph displays a topological feature to a greater extent than expected by chance. To date, the most widespread method to construct null-hypothesis weighted networks is based on applying a random rewiring process.¹ Although there are several ways to generate these null-hypothesis networks, none of them is bias-free for weighted graphs.⁹ There are even graph methodologies that remove nonrelevant connections from the brain graphs by means of techniques based on the percentile¹⁴ or the p -value,¹⁵ making surrogate processes completely necessary, even when the same electrode configuration is used.

It is generally accepted that the brain is a well-designed anatomical network, which exhibits an optimal balance between functional integration and segregation.^{6,16} On the other hand, pathological networks are usually accompanied by diverse alterations and/or deficits in network functions. However, contradictory results have been found after computing measures of integration or segregation when some specific diseases were studied. Discrepancies in brain network properties can occur due to several reasons: the method of edge weight assignment, the thresholding method used to construct binary graphs (when these are considered instead of weighted graphs) or the surrogate process used to compare with null-hypothesis networks, among others. Nevertheless, there is consensus about the high complexity of the brain when compared with other networks, such as regular or random configurations.¹⁷ Although the study of complex networks has provided us with a further understanding of brain coupling dynamics,¹⁸⁻²¹ the underlying concern is that there is not a widely accepted scientific definition of graph complexity. Several complexity measures have attempted to capture the intuitive notion of complexity by emphasizing the idea that complex systems are neither completely regular nor completely random.²² In this context, a number of graph complexity measures have been proposed to assess brain behavior. This is the case of the study of Ahmadlou *et al.*,²³ which proposed the power of

scale-freeness of a graph structure and the maximum eigenvalue of the adjacency matrix of a graph as features to measure graph complexity. For that purpose, they used visibility graph similarity (VGS) a recently introduced concept to accurately quantify the overall synchronization in both identical and nonidentical couplings of time series.²⁴ Machta and Machta²⁵ proposed the computational complexity of a parallel algorithm, to evaluate brain behavior. Meyer-Ortmanns²⁶ associated the complexity of the network with the number of topologically nonequivalent graphs generated by selecting vertices and partitioning the edges of the original vertex among the new vertices. There are even measures that define graph complexity in the context of information theory^{22,27,28} Tononi *et al.*²² reported an elaborate new concept of complexity based on mutual information, which relies on the coexistence of functional specialization and integration. Morabito *et al.*²⁸ used mutual information to construct the connectivity matrix. Claussen²⁷ defined off-diagonal complexity, computed by the entropy of a vertex-vertex edge correlation matrix. Nonetheless, all these measures are influenced by network topology, making surrogate processes necessary. This implies an additional source of possible confusion that it is convenient to avoid. To date, none of them has been generalized for weighted graphs. In our opinion, the weighted graph model is more appropriate than the binary one to analyze brain dynamics, as it provides a realistic framework to address the characterization of the neural substrates of the brain. Thus, a new and complementary graph complexity measure, not influenced by network topology, is pertinent.

The main objective of this study was to introduce Shannon graph complexity (SGC), a novel graph measure based on the assumption that a complex network is a system that can be modeled as a graph that should maintain equilibrium between the ‘order’ and the amount of ‘information’ stored. SGC should meet three requirements: (i) it should be able to measure the aforementioned interplay, (ii) it should be independent of the network topology and (iii) it should not require a comparison with null-hypothesis networks. Our primary hypothesis for the mathematical definition of SGC states that, for a fixed topology, the weight distribution of a complex network is directly related to its reliability and information propagation speed. The second objective of the

present study was to assess the usefulness of SGC in determining the properties of the real brain networks. Specifically, real graphs were obtained from the electroencephalographic (EEG) signals of controls and schizophrenia patients during an auditory oddball task. In this regard, we hypothesize that pathological neural substrates affecting network connectivity²⁹ can be characterized by analyzing the balance of the weight distribution by means of SGC.

This paper is divided into six sections. In Sec. 2, the theoretical ground of SGC is introduced. Section 3 describes the four synthetic and the real EEG datasets used in the study. The simulation results for synthetic data and the results obtained from EEG recordings are shown in Sec. 4. Finally, we discuss the implications of these results and summarize the main conclusions of the study.

2. Complex Network Measures

2.1. Null-hypothesis models and traditional global measures

Several null-hypothesis networks have been proposed to accurately assess brain graphs. The two most used weighted null-hypothesis networks are: (i) null-hypothesis networks that preserve N , GD and edge weight distribution by means of a connection reshuffling process¹ and (ii) null-hypothesis networks that preserve N , GD and the degree of each node.³⁰ It is important to note that none of the two null-hypothesis networks preserves node degree distribution for weighted graphs, especially if the weight distribution is nonhomogeneous.¹¹ Ansmann and Lehnertz⁹ compared these two kinds of surrogate processes and the nonsurrogate model. They concluded that weight-preserving null-hypothesis networks could segregate the influence of basic parameters more accurately than degree-preserving network model and the model performed without any surrogate process. However, all the previous methods are not bias-free.⁹ Even though the bias is always present in any measure, the bias introduced via surrogate data must be reduced as much as possible for preventing inappropriate conclusions.⁹ Specifically, this bias could be the reason of the previously mentioned contradictory results in graph measures when some specific diseases were studied. To overcome this issue, three options can be proposed. The first one is to accept the bias introduced by the weight-preserving

surrogate process; nonetheless, this additional source of bias could yield contradictory results. The second option is to design a new nonbiased method, although some researches claim that an ‘unbiased method for empirical data does not exist’.³¹ Due to the drawbacks of the previously mentioned options, we chose the third one: to define a global graph measure that does not need a surrogate process.

Indeed, there are network measures, such as GD, that do not need a surrogate process, when comparing networks with the same N . GD values are identical in the original network and in the null-hypothesis networks constructed using the weight-preserving approach. Thereby, this measure does not depend on the node degree distribution and normalization is not required. GD is then an appropriate measure to validate SGC, not only because a surrogate process is not needed to compute both measures, but also because GD can be used to estimate network complexity.^{10,12} In fact, Bonchev and Buck renamed GD for binary graphs as ‘normalized edge complexity’.¹² In addition, GD indicates the connectivity of the network, as it provides a measure of the average weight of the graph edges. For undirected, weighted networks without self-loops, GD can be mathematically defined as follows:

$$\text{GD} = \frac{\sum_{i=1}^N \sum_{j>i} w_{ij}}{T}, \quad (1)$$

where w_{ij} represents the edge weight between nodes i and j and $T = N(N - 1)/2$ is the total number of connections in an undirected graph.

2.2. Shannon graph complexity

Most of the complexity definitions proposed in previous studies have different drawbacks: (i) high computational cost; (ii) difficulty to be generalized for weighted graphs and (iii) influence of network topology. This influence is not a problem by itself but, to segregate the influence of the topology, a comparison with null-hypothesis networks becomes necessary, especially for small networks typically derived from the study of functional connectivity using EEG signals.⁹ In order to overcome these limitations, we introduce a novel definition of complexity that is independent of network topology. In our preliminary study,³² we defined a novel graph complexity measure based on information theory; nevertheless, the dependences on basic network parameters were

not assessed. SGC is based on analyzing the weight distribution balance of the network. This statistical complexity measure considers that the weight distribution of a graph can be measured in terms of ‘order’ and ‘information’. To capture this interplay, SGC was defined as the product of the Shannon graph entropy (H) and the statistical disequilibrium (D):

$$\text{SGC} = H \cdot D. \quad (2)$$

First, for the computation of H , we rely on the definition of Shannon entropy,³³ as a measure of the stochastic edge weight distribution. H is given by the following formula¹²:

$$H = \frac{-1}{\log_2 T} \sum_{i=1}^N \sum_{j>i} \frac{w_{ij}}{W} \log_2 \frac{w_{ij}}{W}, \quad (3)$$

where W is the sum of all weights of the graph and $\log_2 T$ is a normalization factor introduced to ensure that $0 \leq H \leq 1$.

Secondly, D is defined as the statistical distance in the probability space between the equilibrium distribution and the weighted distribution of the graph under study.³⁴ It is noteworthy that the distribution with uniform weights (i.e. weights with the same value) is considered as the equilibrium distribution in Gibbs’ statistical mechanics.³⁴ Thereby, a highly balanced weighted graph (such as a graph with all weights equally valued) yields a maximum Shannon graph entropy, $H^{\text{balanced}} = 1$, and a value of D equal to zero. On the contrary, a highly unbalanced weighted graph distribution gives $H^{\text{unbalanced}} \approx 0$ and a high D value. In this study, the Euclidean distance was used to compute D as follows:

$$D = \sqrt{\frac{1}{T-1}} \cdot \frac{\sigma}{\bar{w}}, \quad (4)$$

where \bar{w} is the average of all edge values of the graph and σ is the standard deviation of those values.

In Eq. (4), D was normalized to take values in the 0-1 interval, dividing by its maximum value.³⁴

In a different context, this concept of complexity was defined by López-Ruiz *et al.*³⁵ The authors defined a statistical measure of complexity as a balance between ‘order’ and amount of ‘information’. They proposed that a crystal might have maximum ‘order’ and minimum ‘information’ (the structure can be described using two or three parameters). Conversely, an ideal gas would have minimum ‘order’ and maximum ‘information’. They are examples of

simple models and, therefore, systems with zero complexity.³⁵ The parallelism between a lattice graph and the description of a crystal in terms of ‘information’ and ‘order’ is clear. On the other hand, an ideal gas can be seen as an unbalanced graph. Therefore, it is expected that these two kinds of graphs have complexity values close to zero.

It is noteworthy that, by definition, SGC depends on both N and the weight distribution balance, but it is normalized with respect to GD and is independent of node degree distribution. To illustrate these issues, four synthetic datasets were generated by varying different network properties.

3. Simulated and Real Data

To perform the simulations of synthetic graphs and to analyze the real data, we used Matlab[®] R2013b (MathWorks Inc., USA) by means of custom scripts and the available functions on Statistics and Machine Learning Toolbox and Signal Processing Toolbox. In addition, EEGLAB toolbox was used to carry out the independent component analysis (ICA) over the EEG data in order to remove artifacts.

3.1. Synthetic graphs

In this section, we describe four synthetic graph datasets. Synthetic graphs were generated by varying: (i) N ; (ii) the unbalancing factor, UF (i.e. a measure of the unbalancing strength, which is defined as the number of times the largest graph edge value is greater than the lower one); (iii) GD and (iv) the node degree distribution (i.e. distribution of the sum of the weights reaching to each node). The datasets were constructed in order to study the SGC dependences on the previous variables in terms of weight balance. Figure 1 illustrates the construction process for the four datasets.

DATASET-1: In order to determine the SGC dependence on N and UF , *DATASET-1* was generated as follows:

- (i) Consider a weighted and undirected graph with size N in which all the edges, except one, have a fixed value of 1. The remaining edge was set to the UF value.
- (ii) An edge with a value 1 was randomly chosen and replaced by the UF value, obtaining a new graph.

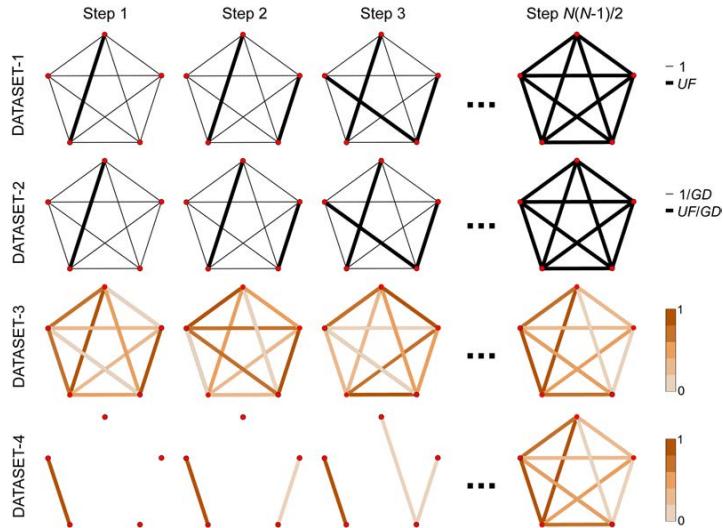


Fig. 1. Dataset construction examples for $N = 5$. Each row exemplifies the construction of one of the datasets.

- (iii) Step (ii) was repeated until all edges were set to the UF value. The last graph is defined as a completely balanced graph.
- (iv) The process was repeated for all combinations of network sizes with $N \in \{2, 3, \dots, 128\}$ and different values of UF $\in \{2, 10, 10^2, 10^3, 10^4, 10^5\}$. The maximum value of N was selected for being the typical value of the number of electrodes in high-density EEG recordings. On the other hand, UF was chosen in order to comprise a range of values large enough to accurately assess SGC dependences.

This dataset is comprised of $6 \sum_{N=2}^{128} N(N-1)/2 = 2,097,024$ adjacency matrices with sizes between 2×2 and 128×128 , 6 different UF values and a single change in each of their connections (there are a total of $N(N-1)/2$ connections in each graph).

DATASET-2: This dataset was used to characterize the graph complexity when N and UF change, but GD remains constant. Construction of DATASET-2 is similar to the generation of DATASET-1, except that all graphs were normalized by their GD. Thus, edge weights in DATASET-2 were proportional to DATASET-1, but their GD was fixed to 1.

DATASET-3: The purpose of this dataset was to determine the dependence of SGC on the node degree distribution. The generation of DATASET-3 can be summarized as follows:

- (i) Consider a weighted and undirected graph with fixed size ($N = 31$), where all the edges values are randomly distributed. The value of N was chosen in order to coincide with the number of EEG electrodes in the DATASET-real (see Sec. 3.2 for details).
- (ii) A new graph was constructed by randomly reshuffling the edge weights. By means of this process, different node degree distributions were obtained, but maintaining the same weight distribution.
- (iii) Step (ii) was repeated 999 times, obtaining a total of 1000 graphs with the same weights, but different node degree distributions.
- (iv) All the previous steps were performed for three different distributions of edge values: a uniform distribution from 0 to 1 edge values, a normal distribution (0.5 ± 0.1 , mean \pm standard

deviation, SD) and a bimodal distribution constructed as the mixture of two normal distributions ($1/3 \pm 0.1$ and $2/3 \pm 0.1$, mean \pm SD).

It is important to note that we ensured that all edge values ranged from 0 to 1. Thus, 3000 (1000 of each type) graph formed this DATASET-3.

DATASET-4: The purpose of this dataset was to study the behavior of SGC for graphs with different number of connections. The DATASET-4 construction is summarized as follows:

- (i) Consider an empty graph (edgeless graph) with size N .
- (ii) An aleatory edge between two disconnected nodes was set to a random value from 0 to 1 (edge values were uniformly distributed between those values).
- (iii) Step (ii) was repeated until all edges were connected. The last graph is defined as a fully connected graph.
- (iv) The process was repeated for all combinations of network sizes with $N \in \{2, 3, \dots, 128\}$. As in DATASET-1 and DATASET-2, the maximum value of N was selected for being a common value of the number of electrodes in high-density EEG recordings.

This dataset comprised $\sum_{N=2}^{128} N(N-1)/2 = 349,504$ adjacency matrices with sizes between 2×2 and 128×128 .

3.2. Real EEG data

As an example of application on real graphs, a real dataset (DATASET-real hereinafter) was included in this study. Connectivity patterns come from the EEG recordings of 51 healthy controls and 28 schizophrenia patients. Diagnosis was made by an expert clinician involved in the treatment of the patients according to Diagnostic and Statistical Manual of Mental Disorders, 5th edition criteria.³⁶ The clinical status of schizophrenia patients was scored using the Positive and Negative Syndrome Scale.³⁷ Demographics and clinical characteristics of schizophrenia patients and controls are summarized in Table 1. In order to avoid medical conditions, which might influence the results, controls and schizophrenia patients were selected using inclusion/exclusion criteria based on clinical history and structured interviews (see Refs. 3 and 4 for a

Table 1. Demographic and clinical characteristics.

Characteristic	SCH patients	Controls
Age (years)	31.19 ± 10.43	29.31 ± 9.74
Gender (M:F)	13 : 15	24 : 27
PANSS-positive	11.39 ± 3.40	NA
PANSS-negative	18.26 ± 8.24	NA
PANSS-total	54.00 ± 21.47	NA

Note: Values are shown as mean ± standard deviation (SD). NA means 'not applicable'. M: male; F: female.

complete description). No significant between-group differences ($p > 0.05$) were found in age (Wilcoxon signed-rank test) or gender (χ^2 test). All participants gave their informed consent prior to their participation in the study. Moreover, the study protocol was approved by the local Ethics Committee of Clinical University Hospital of Valladolid (Spain), according to the code of ethics of the World Medical Association (Declaration of Helsinki).

Data acquisition and preprocessing were performed in an identical way as described by Nakamura *et al.*³⁰ In summary, the acquisition was performed using an EEG system (BrainVision, Brain Products GmbH, Munich, Germany). The electrode placement followed the 10/10 system, with 32 active electrodes. Impedances were kept below 5 k Ω . Event-related potentials (ERPs) were recorded while the participants were sitting with their eyes closed. The auditory oddball task consisted of random series of 600 tones with three different kinds of tones: target (500 Hz tone), distractor (1000 Hz tone) and standard (2000 Hz tone) with probabilities of 0.20, 0.20 and 0.60, respectively. Only attended target tones (i.e. target tones followed by a mouse click from the participants) were considered. ERP signals were recorded at a sampling frequency of 500 Hz during 13 min of an auditory oddball task. After a visual inspection, signals from TP9 and TP10 electrodes were removed because of muscle artifacts. Data were re-referenced to the average activity of all active sensors obtaining 31 channels. Signals were filtered using a band-pass finite impulse response filter between 1 and 70 Hz, as well as a 50 Hz notch filter. Finally, a three-step artifact rejection algorithm was applied to minimize ocular noise and myographic artifacts: (i) ICA was carried out and, after visual inspection, ICA components associated with artifacts were

discarded; (ii) reconstruction and segmentation of the data into trials of 1 s length ranging from 300 ms before to 700 ms after stimulus onset and (iii) automatic and adaptive trial rejection using a statistical-based thresholding method.⁴

In order to study the dynamical changes in the EEG, the single trial approach was used.^{38,39} Each trials of 1 s length was divided into two time windows: baseline window ([-300 0] ms from the stimulus onset) and response window ([150 450] ms after the stimulus onset).^{3,4} The baseline window is related to the resting prior to the stimulus and the response window corresponds to the cognitive response of the P300 task processing. Accordingly, the auditory oddball task is useful to analyze the dynamical neural reorganization during a cognitive processing.^{3,4}

Continuous wavelet transform (CWT) was used in order to generate brain graphs. Wavelet transform is a useful method to accurately assess the changes of electrophysiological signals in the time-frequency plane.⁴⁰ In this study, the complex Morlet wavelet was used as 'mother' function, as it provides a plausible biological fit to EEG data.³⁸ It is characterized by the bandwidth (Ω_b) and the wavelet center frequency (Ω_c) parameters. They were set to 1 to obtain an adequate balance between the temporal and frequency resolution.⁴ Complex Morlet can be defined as follows:

$$\phi(t) = \frac{1}{\sqrt{\pi \cdot \Omega_b}} \cdot e^{-j \frac{2\pi \Omega_c t^2}{\Omega_b}}. \quad (5)$$

To obtain the CWT coefficients, the convolution of each 1 s length EEG trial, $x(t)$, and the complex Morlet function must be calculated as:

$$\text{CWT}(k, s) = \frac{1}{\sqrt{s}} \cdot \int_{-\infty}^{\infty} x(t) \cdot \phi * \left(\frac{t-k}{s} \right) \cdot dt, \quad (6)$$

where s and k denote the dilation and translation factors and $*$ represents the complex conjugation. It is important to note that edge effects are not negligible, as the trials are finite short-length time series.³⁸ Contrary to Fourier analysis, CWT has a variable time-frequency resolution.³⁶ In this regard, a Heisenberg box can be introduced. It is defined as a constant area rectangle whose height and width depend on the frequency (Δf) and the time (Δt) resolution, respectively.³⁶ Following previous studies, the size of the Heisenberg box was chosen to be two times Δt

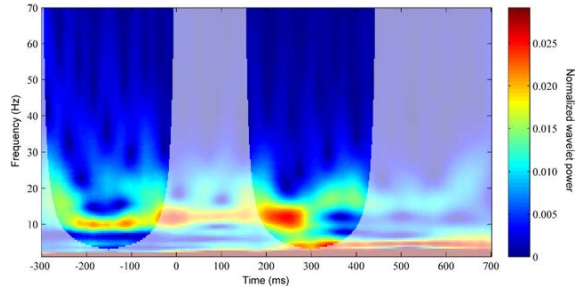


Fig. 2. Example of the normalized wavelet coefficients at Pz electrode averaged across trials in a control subject. The transparency outline represents the limits of the COI in the baseline and response windows, where the spectral content is not affected by edge effects.

and Δf .³⁷ The influence of the edge effect changes across that representation, because Δt and Δf are not constant in the time-frequency plane. Hence, in order to overcome the errors at the beginning and the end of the wavelet power spectrum, zero padding was introduced at the extremes of each EEG trial. Nevertheless, this introduces discontinuities at the edges. Thus, the spectral content must only be considered in the time-frequency regions delimited by their respective cones of influence (COIs), where the edge effect can be ignored (Fig. 2). In this study, target trials of 1 s length were decomposed into the baseline and response windows. Therefore, it is necessary to define one COI for each of the aforementioned time window.

The analysis of the delta band was not performed because it could be affected by a significant bias, resulting in an inaccurate time-frequency estimation. In this regard, some studies recommend six cycles to accurately estimate wavelet coefficients;⁴¹ nevertheless, two cycles can also be used at the expense of frequency resolution.⁴² In this study, this latter approach was used in order to study a maximum range of the spectral content, taking care with the lower frequencies because of the possible bias introduced due to the time-frequency resolution. Thereby, the CWT from 4 to 70 Hz was divided according to the conventional EEG frequency bands: theta (4–8 Hz), alpha (8–13 Hz), beta-1 (13–19 Hz), beta-2 (19–30 Hz) and gamma (30–70 Hz).

Graph edge weights were obtained from the WC without the application of any threshold to obtain

the adjacency matrices. Each node of the graph corresponds to an electrode ($N = 31$) and each edge weight corresponds to the WC between the signals of the considered pair of electrodes. To obtain the WC, the wavelet cross-spectrum (WCS) between two 1 s length ERP trials was computed as follows:

$$WCS_{ij}(k, s) = CWT_i(k, s) \cdot CWT_j^*(k, s), \quad (7)$$

where subscripts i and j identify a pair of electrodes. Once WCS was obtained for all pairwise electrode combinations, it was averaged across trials in two windows of interest: (i) the baseline window and (ii) the response window. Finally, WC between two given electrodes i and j was calculated as follows^{4,43}:

$$WC_{ij}(s) = \frac{|WCS_{ij}(s)|^2}{WCS_{ii}(s) \cdot WCS_{jj}(s)}, \quad (8)$$

WC is a straightforward method, commonly used in previous EEG studies.^{43–45} It represents the linear relationship between the amplitude of two signals in the spectral domain (nonlinear relationships are not considered).⁴⁴ WC was obtained for each frequency (or scale) and then averaged across scales in the previously defined frequency bands. Hence, one adjacency matrix was obtained for each frequency band, subject and time window (i.e. 10 adjacency matrices per subject). As a result, 790 graphs were obtained for the DATASET-real: 79 subjects \times 2 time windows (baseline and response) \times 5 frequency bands. Graph edge weights range from 0 to 1, as a thresholding method was not applied to the WC values.

4. Results

4.1. Results on synthetic graphs

Figure 3 shows the changes in SGC and GD for DATASET-1 and DATASET-2 for different values of UF, N and the number of edges set to UF (ES-UF). The last parameter, ES-UF, reflects the balance of the edge weight distribution. When only one edge value is set to UF (and UF is large enough), the unbalance strength reaches its maximum; on the contrary, when all the edge values are set to UF, the edge weight distribution is completely balanced.

The first row show SGC values for DATASET-1 and DATASET-2. SGC values are exactly the same for both datasets, which implies that SGC is density-invariant (the only difference between DATASET-1 and DATASET-2 is that graphs in DATASET-2 were normalized by their GD). SGC plots show that there is little variation in the complexity values for $N > 30$. Furthermore, there is a strong dependence between UF and the number of ES-UF needed to reach an equilibrium between a completely weight balanced distribution and a strongly weight unbalanced distribution (i.e. the maximum value of SGC when N is fixed).

On the contrary, GD behavior is completely different for these two datasets, as it directly depends on weight values but not on the weight distribution. The two bottom rows in Fig. 3 show the GD dependences for these two datasets. For DATASET-1, GD increases with the number of ES-UF. In addition, GD becomes higher as UF increases (note the logarithmic scale on z -axis). It is important to note that all the GD plots of the DATASET-1 have the same shape, but it is not evident as all plots have the same scale in the axes. On the other hand, GD remains constant and equal to 1 for DATASET-2, as each graph was normalized by their own GD. Therefore, the behavior of GD for DATASET-1 is completely different from that for DATASET-2, contrary to SGC. It is noteworthy that SGC and GD cannot be computed for all N and number of ES-UF, as it is impossible to generate an undirected graph of size N with more than $N(N-1)/2$ ES-UF. That is the reason why some SGC and GD values were not plotted.

The results for DATASET-3 showed that SGC and GD values were constant for each distribution. Therefore, SGC and GD are invariant with respect to the node degree distribution. These measures only

depend on the value of the edge weights, but not on the degree of each node. Additionally, SGC provided complexity values of 0.026 for a uniform distribution, 0.020 for a bimodal distribution and 0.015 for a normal distribution (Table 2). On the contrary, GD was not able to differentiate between these distributions.

The DATASET-4 was constructed to analyze the behavior of SGC for graphs with different numbers of connections. The SGC and GD results are shown in Fig. 4. Similar to DATASET-1 and DATASET-2, SGC showed little variation for $N > 30$. On the other hand, GD showed an important dependence on the number of connections.

Finally, Fig. 5 depicts SGC as a function of H and UF for $N = 31$ (number of nodes in DATASET-real). The graphs used to generate Fig. 5 are the same as those used in DATASET-1, but with several more values of UF in order to obtain a compact representation of SGC. Figure 5(a) is useful to visualize SGC as a function of H and UF, while the maximum and minimum values of SGC are easily observed in Fig. 5(b).

4.2. Results on real brain graphs: Application to schizophrenia

We computed SGC for real ERP signals recorded from healthy controls and schizophrenia patients. Complexity values were compared between time windows (baseline and response) and groups (controls and patients) in the five frequency bands under study. Prior to this, an exploratory analysis was carried out to analyze data distribution. The Kolmogorov-Smirnov and the Levene tests were used to check normality and homoscedasticity of data distributions. Nonparametric tests were applied to assess statistical differences, since parametric assumptions were not met: (i) Wilcoxon signed-rank test was used to compare baseline and response network measures for within-group analyses and (ii) Mann-Whitney U -test was used for between-group analyses. In addition, Bonferroni correction for multiple comparisons was applied. Thus, the significance level was set to $\alpha = 0.01$.

Within-group analyses for SGC values on each group and window are shown in Fig. 6(a). Only the theta band exhibited statistical differences between baseline and response windows ($Z = -5.37, p = 7.83E - 8$, in the control group; $Z = -3.05, p =$

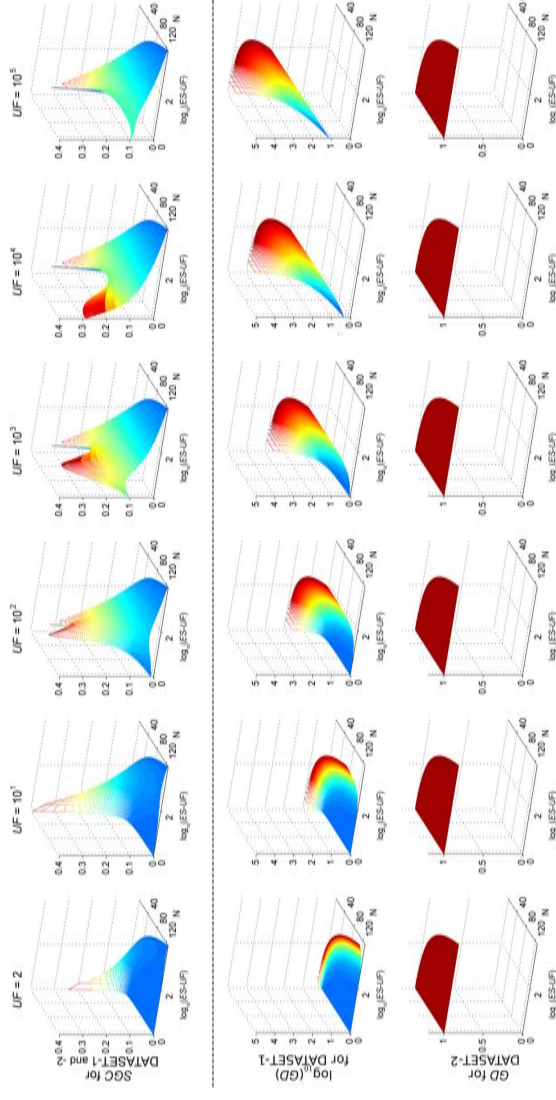


Fig. 3. SGC and GD values for DATASET-1 and DATASET-2. Note that GD results for DATASET-1 (second row) are represented in logarithmic scale, due to the high dependence of GD on N and UF .

Table 2. SGC and GD values for all the graphs of DATASET-3. SGC and GD are independent of node degree distribution.

	Uniform distribution	Normal distribution	Bimodal distribution
GD	0.500	0.500	0.500
SGC	0.026	0.015	0.020

$2.28E - 3$, in the schizophrenia group). On the other hand, GD was computed to validate the performance of SGC (Fig. 6(b)). Within-group analyses showed a statistically significant increase from the baseline to the response window in the theta band for both controls ($Z = 5.75, p = 8.65E - 9$) and schizophrenia patients ($Z = 3.37, p = 7.51E - 4$). No significant differences were found on the other frequency bands. In view of these results, only the theta band was considered for further analyses.

SGC and GD were baseline-corrected (i.e. complexity values during baseline window were subtracted from their values during response window).^{3,38} Between-group analyses showed a marked reduction on SGC values during the response window for both controls and schizophrenia patients. However, no significant differences were found in between-group comparisons using corrected SGC

after Bonferroni correction though ($Z = -1.95, p = 5.01E - 2$). Nevertheless, controls showed a more marked decrease in SGC values during cognitive response than patients. Regarding GD analysis, results indicated that controls exhibited a statistically significant more prominent increase in corrected GD values during the response than schizophrenia patients ($Z = 2.64, p = 8.31E - 3$). Hence, for both networks, changes from baseline to response were more prominent in controls than in schizophrenia patients.

It is interesting to note that H increased during the response window for both controls and schizophrenia patients. This indicates that the reduction of SGC, which is a measure of the equilibrium between balanced and unbalanced edge eight distribution, is due to an increase in the weight balance of the network. To evaluate brain complexity dynamics during the auditory oddball task, the change of SGC as a function of H from baseline to response windows for controls and schizophrenia patients is represented in Fig. 7.

5. Discussion

The main objective of this study was to propose a novel graph complexity measure and to assess its behavior under different conditions using synthetic and real datasets. SGC is essentially normalized

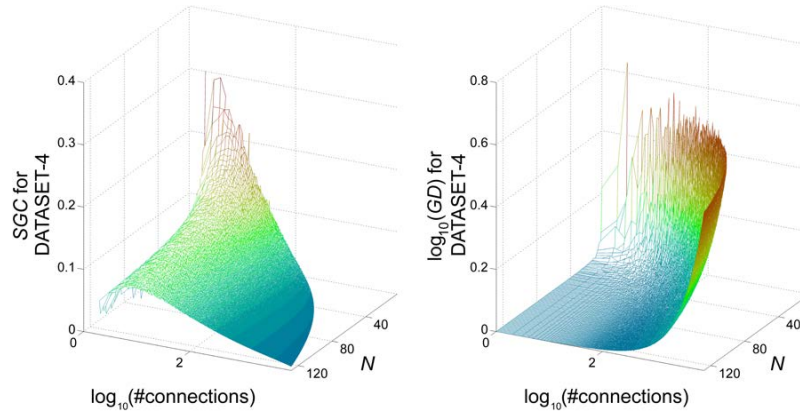


Fig. 4. SGC and GD values for DATASET-4. Note that GD results are represented in logarithmic scale, due to the high dependence of GD on the number of connections.

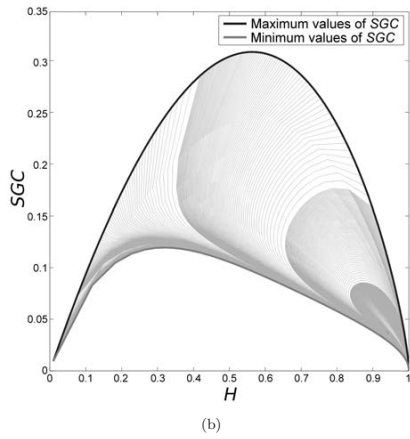
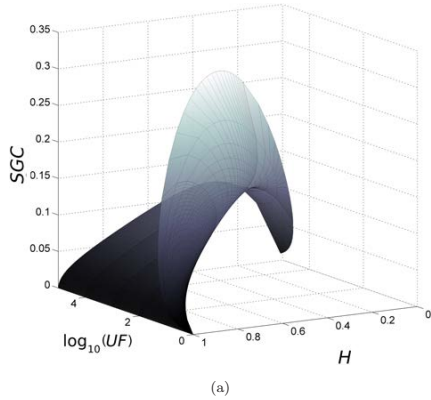


Fig. 5. (a) 3D and (b) 2D plots corresponding to SGC as function of H and UF , when $N = 31$. Maximum and minimum values of SGC are also depicted in (b).

with respect to GD and independent of node degree distribution. Additionally, the influence of network size on SGC seems to be small for $N > 30$ when UF takes small values. Hence, the need to make comparisons with null-hypothesis networks was not required for networks of the same size. On the other hand, statistically significant differences in network reorganization dynamics after an auditory oddball task were

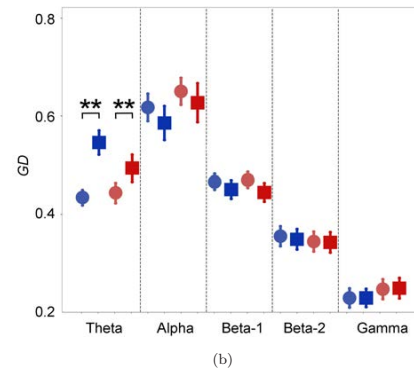
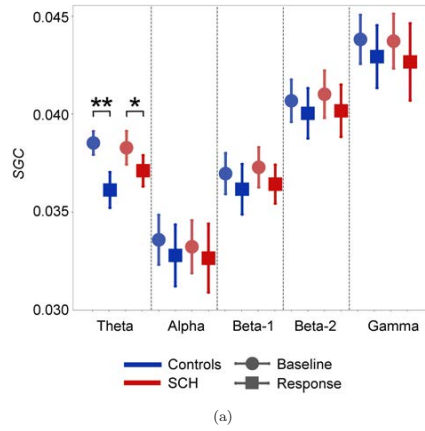


Fig. 6. (a) SGC and (b) GD values for each group, window and frequency band. Values are depicted as mean and standard error. * indicates $p < 0.01$, while whereas ** indicates $p < 0.001$.

found between controls and schizophrenia patients with SGC.

5.1. SGC dependences: Synthetic graphs

Four synthetic datasets were generated by varying basic network characteristics, such as N , UF , GD and node degree distribution. DATASET-1 showed that SGC and GD depend on N and the number of ES- UF . It is important to note that a high UF value

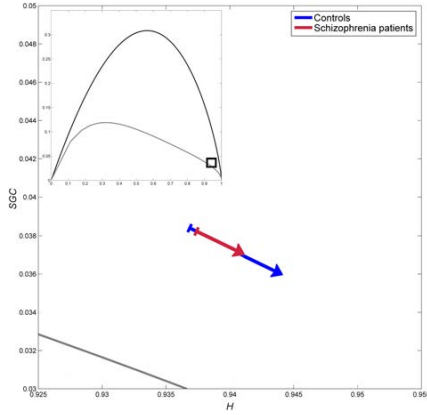


Fig. 7. Detailed plot of the complexity dynamics from baseline to response in the theta frequency band for controls (blue arrow) and schizophrenia patients (red arrow). The small figure represents the maximum and minimum possible SGC values for this network size. The square in the small figure corresponds to the zoomed area in the large figure. H increases and SGC decreases for both groups, but the behavior is more remarkable for controls than for schizophrenia patients.

yields weighted graphs with similar behavior than binary graphs. Binary graphs have some connections set to 1 and others set to 0. Their behavior is similar to weighted graphs with connections set to a high UF value and others set to 1. Therefore, when SGC is applied to binary graphs, the behavior is similar to the previously shown performance. This is a significant advantage with respect to other complexity measures, which cannot always be applied to binary and weighted graphs.²⁵⁻²⁷ On the contrary, SGC can be directly applied to binary and weighted graphs.

Figure 3 shows that the maximum of SGC for each N is always obtained for a number of ES-UF lower than $N(N-1)/2$. This is an important difference compared to GD, where the maximum is reached for $ES-UF = N(N-1)/2$. Therefore, SGC introduces a graph complexity definition more intuitive than GD, as graph complexity is considered as an equilibrium between ‘order’ and ‘information’ stored. If graph complexity is measured by means of GD,¹² a complete graph (i.e. a graph with all their nodes connected) with network connections set to the

maximum value always has the highest complexity. However, this does not correspond to the intuitive notion of graph complexity, where some connections (and thus pathways) are more important than others, creating a tangled mesh of paths.⁴⁶

DATASET-2 was assembled similarly to DATASET-1. The only difference was that the DATASET-2 graphs were normalized by their own density. That is the reason for the constant GD values shown in the bottom row of Fig. 3. Nevertheless, graphs with proportional weights show the same H and D values by construction; therefore, SGC is also the same. In this regard, the same SGC values were reached for DATASET-1 and DATASET-2 (Fig. 3). This is another advantage of SGC in comparison with GD. In addition, it is not necessary to normalize the graphs by their density to compare the complexity among them, enabling the comparability between studies.

Results obtained from DATASET-3 proved that both SGC and GD are independent of node degree distribution. This implies that SGC is independent of network topology, which suggests that this measure provides complementary information to network measures based on topology. Two graphs with different node degree distribution or GD, but with the same set of weights, would have the same SGC value. Therefore, comparisons with null-hypothesis networks become unnecessary for networks with the same N . Furthermore, as we mentioned previously, the change of SGC is small for $N > 30$, when UF takes small values and ES-UF is fixed. Hence, the possible bias introduced when comparing with networks of different sizes is minimized in relation to other topology-based graph measures. DATASET-3 also provides an important difference between the two measures of graph complexity analyzed in this study. GD took the same value for the three different distributions. However, SGC results indicated that a uniform distribution of the edge weights had a higher complexity value than a normal or a bimodal distribution. This advantage of SGC with respect to GD is based on the ‘order’ of each distribution. A graph with maximum ‘order’ (a complete graph with the same value of all edges) corresponds to a delta distribution. In that case, SGC would provide a value equal to zero. The more the distribution under study resembles the distribution of maximum ‘order’, the lower the value of complexity provided

by SGC. For that reason, the minimum complexity value was obtained with the normal distribution, with a value of 0.015 (Table 2). The bimodal distribution achieved a SGC value of 0.020, whereas the uniform one obtained a value of 0.026.

Regarding DATASET-4, our results showed that the SGC behavior with not fully connected graphs is similar to that observed for fully connected ones, since there is little variation of SGC for $N > 30$. On the other hand, GD has an important dependence on the number of connections in the graph.

Finally, it is important to note that graphs with the same size and edge values, but different topology, achieve the same value of SGC. Therefore, from the point of view of ‘order’ and amount of ‘information’ stored by the system, there are no differences between, for example, scale-free and small-world networks (if they have the same size and edge values).

In addition, the computational cost of SGC is significantly lower than other complexity measures based on several iterations of mutual information²² or on generating motifs from the original network.²⁶ SGC is based on Shannon entropy, and it only needs one iteration to be computed. This is another important difference with previously proposed complexity measures.^{22,26}

5.2. Brain dynamics using SGC: Real graphs

The results derived from DATASET-real showed that SGC is a metric that may allow differentiating the brain networks of controls and schizophrenia patients. For both groups, SGC decreased during the response window, which suggests a reduction of the equilibrium between ‘order’ and amount ‘information’ stored by the system. In addition, Fig. 6 showed higher values of H during the response window for both groups. Therefore, the ‘order’ decreased while the amount of ‘information’ stored by the system increased in the subjects’ brain networks during the cognitive task. However, the variation of SGC from the baseline to the response window is more prominent in controls, specifically in the theta band, which could evidence a deficit in the reorganization patterns in schizophrenia. In this regard, results showed that only theta band exhibited statistical differences in within-group analyses. In addition, the changes between baseline and response windows were lower

in schizophrenia patients. Previous studies reported a decrease of the relative power in the alpha frequency band in schizophrenia patients^{47,48} and an increase of power in the theta band.⁴⁹ Furthermore, oscillations in low frequency ranges (such as theta) are related with the modulation of the long-range synchronization,^{50,51} whereas high frequency ranges (such as beta and gamma) reflect synchronization in large-scale networks.⁵² Thus, it can be inferred that impaired activation response of long-range interactions might contribute to the pathological process of schizophrenia, which usually shows an integration deficit among distant brain areas.²⁹ In view of these results, the present study reports similar ideas to previous ones, which suggested that schizophrenia is accompanied by a disrupted network reorganization of neural functions, mainly in long-range interactions.^{3,53,54}

Our results also agree with previous studies that linked impaired network reorganization capacity with the aberrant salience and the disconnection hypotheses.^{55,56} In this regard, Bachiller *et al.*⁴ posed the idea that schizophrenia patients failed to change their coupling dynamics between stimulus response and baseline when performing a stimulus processing. It can be related to a diminished ability to optimize the neural synchronicity leading to a functional disconnection. This idea was clearly shown by GD results. Controls showed a significant increase in GD during the response, which implies a global increment of connectivity patterns. As reported in task-related studies,^{4,57} an increase of ERP synchronicity on the theta frequency band is observed during cognitive processing. Nonetheless, schizophrenia patients usually show a failure to modulate synchronous activity, particularly when asked to attend to target stimuli.^{4,58} This modulation deficit produces lower WC values for schizophrenia patients than for controls. Therefore, it seems reasonable that schizophrenia patients exhibited lower GD values during the response window.

There are important aspects that indicate the complementarity of SGC and GD. On the one hand, SGC (jointly with H) showed that the weight distribution is more balanced during the response compared with baseline (Fig. 6). Taking into account only SGC results, the increased balance could be a consequence of: (i) a prominent increase in the value of weak connections (i.e. secondary neural

pathways); (ii) a decrease in the value of the connections with higher values or (iii) the combined effect of the previous two points. On the other hand, GD showed an increase, on average, of the edge weights during the response window. Therefore, the increase of edge values for the secondary neural pathways should have a higher effect than a possible decrease in the connections with higher values (option (i)). Furthermore, SGC modulation is higher for controls, but statistically significant differences were not found between the baseline windows of both groups. Thus, it is likely that secondary neural pathways can be strengthened in controls compared with schizophrenia patients during cognitive processing. This strengthening balances the weight distribution, which could increase the reliability and the information propagation speed in the brain. Therefore, controls can reorganize their brain network between different areas in a flexible and transient way in order to coordinate the response to the cognitive task. The previous inferences have only been possible due to the complementary information provided by SGC and GD. Although the statistical differences between healthy subjects and schizophrenia patients are more marked for GD than for SGC, it is important to note that the second objective of this study is to assess the usefulness of SGC in determining the properties of the real brain networks. In this regard, SGC provided different and complementary information to that of a classical measure of graph complexity, GD, meeting the second objective of the study.

The idea of classifying brain graph connections in different topological levels (primary and secondary connections) is in line with a recent concept introduced in neuroscience to model the brain network: the minimum spanning tree (MST).^{46,59} MST is an acyclic subgraph that connects all nodes using exactly $N - 1$ edges while minimizing distance between nodes (i.e. maximizing the connection strength).⁶⁰ It represents a critical backbone of information flow in weighted networks, providing information about how the brain structures the information in different topological levels. The nodes involved could be similar to those forming the weighted ‘rich club’ (i.e. a subset of high-degree nodes that are connected by a larger fraction of the most highly weighted edges in the graph than expected by chance).⁶¹ Thus, the brain network is modeled as a two-topological level structure. The

first topological level is formed by the main connections (i.e. the MST backbone and the ‘rich club’ motifs). The second topological level is formed by secondary neural pathways, which are removed in the MST model. Thus, this idea supports our concept of network complexity: the brain is a network halfway between a completely balanced and unbalanced weight distribution, where the higher-level topologies are part of the previously mentioned MST backbone. SGC is useful to evaluate the relationship between primary and secondary pathways in terms of weight balance, which can support the existence of ‘rich club’ assemblies in the brain network. In this regard, it is commonly accepted that the archetypal brain network is sparsely connected between nodes in different modules.⁶² In this study, SGC showed that weak connections increase their strength during the response window, generating new alternative pathways that should work to increment network integration. It is noteworthy that several EEG studies reported an increase in brain network integration during cognitive processing.^{63,64} This integration, usually measured by means of the path length, is reduced in schizophrenia patients compared with controls during an oddball task,⁵ which is again in agreement with the disconnection hypothesis.²⁹ The present results support an altered information processing in schizophrenia, which may not characterize, however, all the patients in this syndrome, given its likely heterogeneous biological substrate.⁶⁵

5.3. *Limitations and future lines of research*

Some methodological issues of this study merit consideration. First, SGC does not provide information about graph topology. Although this is an important advantage because the requirement for a surrogate process is avoided by comparing networks with the same N , the lack of this information requires the use of complementary measures in order to obtain a global vision of the network. Nonetheless, the need for various measures to fully characterize a graph is commonly accepted.^{66,67} Individually, topological features do not provide information on the connectivity balance or the strength of the functional neural connections. In our opinion, this edge weight distribution balance has a very important role in the analysis of the impact of network complexity. Therefore,

the lack of this information could lead to ignoring important aspects of the brain network.

The second methodological issue is related to the intrinsic SGC property as an entropy-based measure. Previous studies suggested that entropy quantifiers might overestimate the irregularity in the brain network.⁶⁸ This could explain why entropy values obtained from brain networks reached values close to 1, as shown in Fig. 7. Different entropy measures could provide different degrees of disorder estimation. Future works should address this concern by quantifying the irregularity by means of other entropy measures. Likewise, different disequilibrium measures based on more complex measures of distance (Euclidean distance was used in this study) could provide complementary results.

Thirdly, the methods used to estimate the connectivity between brain areas could have a high impact on measures that are strongly dependent on edge weights. DATASET-real was obtained by applying WC to EEG recordings. The choice of this connectivity measure was motivated by its widespread use as a method for weight estimation in functional brain graphs.⁴⁴ Coherence is a straightforward method that assesses the linear relation between the amplitude of two signals in the frequency domain. However, it is sensitive to volume conduction,⁴⁴ which could lead to an erroneously high estimation of connectivity between two network nodes.^{44,69} In this regard, a statistical threshold to remove spurious connections could help to clarify the results. Future works should be carried out to evaluate SGC behavior in graphs obtained using metrics that do not overestimate the connectivity between nodes, such as phase-based measures. In addition, it could be interesting to apply multivariate approaches for causal interactions between nodes, as directed edges can be interpreted in a more physiological way. The application of SGC in these conditions would not need any reformulation, as it is applicable to directed graphs. Nonetheless, it is important to note that the proposed measure is an extension of a metric originated in information theory by considering normalized weights as probabilities. For that reason, it is not possible to compute SGC when a graph takes negative edge weights. In this regard, an interesting future line of research could be a more theoretical approach of the interpretation of the proposed metric. It would provide more meaningful and general results.

6. Conclusions

Several pieces of evidence suggest that the edge weight distribution of complex brain networks is directly related to reliability aspects and to its information propagation speed. Therefore, graph measures that evaluate the weight distribution are fully justified. SGC was introduced as a useful alternative to GD and other graph complexity measures. In this study, we proved the independence of SGC with respect to basic graph characteristics, in addition to an almost small dependence on N when UF takes small values.

Our results from real brain graphs indicate that SGC is particularly useful to determine the intrinsic properties of neural dynamics during a cognitive task. Specifically, SGC results suggest that the auditory oddball task elicits an increment of the connection weights, mainly in the edges related to secondary neural links. This provides alternative pathways to the neural backbone. Another important remark is the prominent change in SGC and GD observed in controls compared with schizophrenia patients. These insights are in line with the disconnection and aberrant salience hypotheses. They involve a deficit in neural network reorganization during cognitive processing that could lead to a lower functional integration of the brain network.

Acknowledgments

This research project was supported in part by the ‘Ministerio de Economía y Competitividad’ and FEDER under project TEC2014-53196-R; the ‘Fondo de Investigaciones Sanitarias (Instituto de Salud Carlos III)’ under projects FIS PI11/02203 and PI15/00299 and the ‘Gerencia Regional de Salud de Castilla y León’ under projects GRS 932/A/14 and GRS 1134/A/15. A. Bachiller and J. Gomez-Pilar were in receipt of a PIF-UVA grant from University of Valladolid. A. Lubeiro has a predoctoral scholarship from the ‘Junta de Castilla y León’ and European Social Fund. P. Núñez was in receipt of a ‘Promoción de empleo joven e implantación de la Garantía Juvenil en I + D + i’ grant from ‘Ministerio de Economía y Competitividad’ and the University of Valladolid. We would like to express our gratitude to the Psychiatry Service of the Clinical University Hospital of Valladolid (Spain) for their help and support.

References

1. C. J. Stam *et al.*, Graph theoretical analysis of magnetoencephalographic functional connectivity in Alzheimer's disease, *Brain* **132** (2009) 213–224.
2. D. S. Bassett, B. G. Nelson, B. A. Mueller, J. Camchong and K. O. Lim, Altered resting state complexity in schizophrenia, *Neuroimage* **59** (2012) 2196–2207.
3. J. Gomez-Pilar *et al.*, Neural network reorganization analysis during an auditory oddball task in schizophrenia using wavelet entropy, *Entropy* **17** (2015) 5241–5256.
4. A. Bachiller *et al.*, A comparative study of event-related coupling patterns during an auditory oddball task in schizophrenia, *J. Neural Eng.* **12** (2015) 16007-1–16007-13.
5. M. Shim, D. W. Kim, S. H. Lee and C. H. Im, Disruptions in small-world cortical functional connectivity network during an auditory oddball paradigm task in patients with schizophrenia, *Schizophr. Res.* **156** (2014) 197–203.
6. G. Deco, G. Tononi, M. Boly and M. L. Kringelbach, Rethinking segregation and integration: Contributions of whole-brain modelling, *Nat. Rev. Neurosci.* **16** (2015) 430–439.
7. S. Boccaletti, V. Latora, Y. Moreno, M. Chavez and D. U. Hwang, Complex networks: Structure and dynamics, *Phys. Rep.* **424** (2006) 175–308.
8. E. T. Bullmore and D. S. Bassett, Brain graphs: Graphical models of the human brain connectome, *Annu. Rev. Clin. Psychol.* **7** (2011) 113–140.
9. G. Ansman and K. Lehnertz, Surrogate-assisted analysis of weighted functional brain networks, *J. Neurosci. Methods* **208** (2012) 165–172.
10. L. D. F. Costa, F. A. Rodrigues, G. Travieso and P. R. V. Boas, Characterization of complex networks: A survey of measurements, *Adv. Phys.* **56** (2005) 167–242.
11. M. Rubinov and O. Sporns, Complex network measures of brain connectivity: Uses and interpretations, *Neuroimage* **52** (2010) 1059–1069.
12. D. Bonchev and G. A. Buck, in *Complexity in Chemistry, Biology, and Ecology*, ed. Media, S. S. & B. (Springer, USA, 2007), pp. 191–235. doi:10.1007/0-387-25871-X.
13. D. Watts and S. Strogatz, Collective dynamics of small-world networks, *Nature* **393** (1998) 440–442.
14. L. Astolfi *et al.*, Assessing cortical functional connectivity by linear inverse estimation and directed transfer function: Simulations and application to real data, *Clin. Neurophysiol.* **116** (2005) 920–932.
15. F. D. V. Fallani *et al.*, Extracting information from cortical connectivity patterns estimated from high resolution EEG recordings?: A theoretical graph approach, *Brain Topogr.* **19** (2007) 125–136.
16. M. Ahmadlou, H. Adeli and A. Adeli, Graph theoretical analysis of organization of functional brain networks in ADHD, *Clin. EEG Neurosci.* **43** (2012) 5–13.
17. O. Sporns and J. D. Zwi, The small world of the cerebral cortex, *Neuroinformatics* **2** (2004) 145–162.
18. M. Chiappalone, A. Vato, L. Berdondini, M. Koudelka-Hep and S. Martinoia, Network dynamics and synchronous activity in cultured cortical neurons, *Int. J. Neural Syst.* **17** (2007) 87–103.
19. F. Han, M. Wiercigroch, J.-A. Fang and Z. Wang, Excitement and synchronization of small-world neuronal networks with short-term synaptic plasticity, *Int. J. Neural Syst.* **21** (2011) 415–425.
20. P. J. Neefs, E. Steur and H. Nijmeijer, Network complexity and synchronous behavior — An experimental approach, *Int. J. Neural Syst.* **20** (2010) 233–247.
21. T. Yamanishi, J.-Q. Liu and H. Nishimura, Modeling fluctuations in default-mode brain network using a spiking neural network, *Int. J. Neural Syst.* **22** (2012) 1250016.
22. G. Tononi, G. M. Edelman and O. Sporns, Complexity and coherency: Integrating information in the brain, *Trends Cogn. Sci.* **2** (1998) 474–484.
23. M. Ahmadlou, H. Adeli and A. Adeli, New diagnostic EEG markers of the Alzheimer's disease using visibility graph, *J. Neural Transm.* **117** (2010) 1099–1109.
24. M. Ahmadlou and H. Adeli, Visibility graph similarity: A new measure of generalized synchronization in coupled dynamic systems, *Phys. D Nonlinear Phenom.* **241** (2012) 326–332.
25. B. Machta and J. Machta, Parallel dynamics and computational complexity of network growth models, *Phys. Rev. E Stat. Nonlinear Soft Matter Phys.* **71** (2005) 1–9.
26. H. Meyer-Ortmanns, Functional complexity measure for networks, *Physica A* **337** (2004) 679–690.
27. J. C. Claussen, Offdiagonal complexity: A computationally quick complexity measure for graphs and networks, *Physica A* **375** (2007) 365–373.
28. F. C. Morabito *et al.*, A longitudinal EEG study of Alzheimer's disease progression based on a complex network approach, *Int. J. Neural Syst.* **25** (2015) 1550005.
29. K. J. Friston, The disconnection hypothesis, *Schizophr. Res.* **30** (1998) 115–125.
30. T. Nakamura, F. G. Hillary and B. B. Biswal, Resting network plasticity following brain injury, *PLoS One* **4** (2009) e8220.
31. B. C. M. van Wijk, C. J. Stam and A. Daffertshofer, Comparing brain networks of different size and connectivity density using graph theory, *PLoS One* **5** (2010) e13701.

32. J. Gomez-Pilar *et al.*, Novel measure of the weigh distribution balance on the brain network: Graph complexity applied to schizophrenia, *Proc. 35th Annual International Conference of the IEEE Engineering in Medicine and Biology Society Conference*, IEEE, pp. 700–703 (2016).
33. C. E. Shannon, A mathematical theory of communication, *Bell Syst. Tech. J.* **27** (1948) 379–423.
34. M. T. Martin, A. Plastino and O. A. Rosso, Statistical complexity and disequilibrium, *Phys. Lett. A* **311** (2003) 126–132.
35. R. López-Ruiz, H. L. Mancini and X. Calbet, A statistical measure of complexity, *Phys. Lett. A* **209** (2002) 321–326.
36. American Psychiatric Association, *Diagnostic and Statistical Manual of Mental Disorders, 5th Edition: DSM-5* (American Psychiatric Publishing, Arlington, 2013). doi:10.1176/appi.books.9780890425596.893619, 87–122.
37. S. R. Kay, L. A. Opler and J. P. Lindenmayer, The Positive and Negative Syndrome Scale (PANSS): Rationale and standardisation, *Br. J. Psychiatry* **155** (1989) 59–65.
38. B. J. Roach and D. H. Mathalon, Event-related EEG time-frequency analysis: An overview of measures and an analysis of early gamma band phase locking in schizophrenia, *Schizophr. Bull.* **34** (2008) 907–926.
39. K. Michalopoulos, M. Zervakis, M.-P. Deiber and N. Bourbakis, Classification of EEG single trial microstates using local global graphs and discrete hidden Markov models, *Int. J. Neural Syst.* **26** (2016) 1650036.
40. S. Mallat, *A Wavelet Tour of Signal Processing*, Academic Press, pp. 20–41 (1999). doi:10.1016/B978-012466606-1/50004-0
41. C. S. Herrmann, M. Grigutsch and N. Busch, EEG oscillations and wavelet analysis, in *Event-related potentials: A methods Handbook*, MIT Press, pp. 1–39 (1999).
42. C. Tallon-Baudry, O. Bertrand, C. Delpuech and J. Pernier, Oscillatory gamma-band (30–70 Hz) activity induced by a visual search task in humans, *J. Neurosci.* **17** (1997) 722–734.
43. Z. Sankari, H. Adeli and A. Adeli, Wavelet coherence model for diagnosis of Alzheimer disease, *Clin. EEG Neurosci.* **43** (2016) 268–278.
44. E. van Diessen *et al.*, Opportunities and methodological challenges in EEG and MEG resting state functional brain network research, *Clin. Neurophysiol.* **126** (2015) 1468–1481.
45. Z. Sankari and H. Adeli, Probabilistic neural networks for diagnosis of Alzheimer’s disease using conventional and wavelet coherence, *J. Neurosci. Methods* **197** (2011) 165–170.
46. P. Tewarie, E. van Dellen, A. Hillebrand and C. J. Stam, The minimum spanning tree: An unbiased method for brain network analysis, *Neuroimage* **104** (2015) 177–188.
47. J. M. Ford, B. J. Roach, W. O. Faustman and D. H. Mathalon, Synch before you speak: Auditory hallucinations in schizophrenia, *Am. J. Psychiatry* **164** (2007) 458–466.
48. E. Bramon, S. Rabe-Hesketh, P. Sham, R. M. Murray and S. Frangou, Meta-analysis of the P300 and P50 waveforms in schizophrenia, *Schizophr. Res.* **70** (2004) 315–329.
49. J. Polich, Updating P300: An integrative theory of P3a and P3b, *Clin. Neurophysiol.* **118** (2007) 2128–2148.
50. P. Sauseng *et al.*, Theta coupling in the human electroencephalogram during a working memory task, *Neurosci. Lett.* **354** (2004) 123–126.
51. A. von Stein, C. Chiang and P. König, Top-down processing mediated by interareal synchronization, *Proc. Natl Acad. Sci. USA* **97** (2000) 14748–14753.
52. P. J. Uhlhaas, Dysconnectivity, large-scale networks and neuronal dynamics in schizophrenia. *Curr. Opin. Neurobiol.* **23** (2013) 283–290.
53. J. Gomez-Pilar *et al.*, Association between electroencephalographic modulation, psychotic-like experiences and cognitive performance in the general population, *Psychiatry Clin. Neurosci.* **70** (2016) 286–294.
54. C. Schmiecht, A. Brand, H. Hildebrandt and C. Basar-Eroglu, Event-related theta oscillations during working memory tasks in patients with schizophrenia and healthy controls, *Cogn. Brain Res.* **25** (2005) 936–947.
55. S. Kapur, Psychosis as a state of aberrant salience: A framework linking biology, phenomenology, and pharmacology in schizophrenia, *Am. J. Psychiatry* **160** (2003) 13–23.
56. K. E. Stephan, K. J. Friston and C. D. Frith, Dysfunction in schizophrenia: From abnormal synaptic plasticity to failures of self-monitoring, *Schizophr. Bull.* **35** (2009) 509–527.
57. P. J. Uhlhaas and W. Singer, Abnormal neural oscillations and synchrony in schizophrenia, *Nat. Rev. Neurosci.* **11** (2010) 100–113.
58. P. J. Uhlhaas, C. Haenschel, D. Nikolić and W. Singer, The role of oscillations and synchrony in cortical networks and their putative relevance for the pathophysiology of schizophrenia, *Schizophr. Bull.* **34** (2008) 927–943.
59. G. J. Ortega, R. G. Sola and J. Pastor, Complex network analysis of human ECoG data, *Neurosci. Lett.* **447** (2008) 129–133.
60. R. C. Prim, Shortest connection networks and some generalizations, *Bell Syst. Tech. J.* **36** (1957) 1389–1401.
61. A. Fortino, A. Zalesky and E. Bullmore, *Fundamentals of Brain Network Analysis* (Academic Press, 2016) 430.



ELSEVIER

Contents lists available at ScienceDirect

Schizophrenia Research

journal homepage: www.elsevier.com/locate/schres

Altered predictive capability of the brain network EEG model in schizophrenia during cognition

Javier Gomez-Pilar^{a,*}, Jesús Poza^{a,b,c}, Carlos Gómez^a, Georg Northoff^d, Alba Lubeiro^e, Benjamín B. Cea-Cañas^e, Vicente Molina^{c,e}, Roberto Hornero^{a,b,c}

^a Biomedical Engineering Group, E.T.S. Ingenieros de Telecomunicación, University of Valladolid, Valladolid, Spain

^b IMVA, Instituto de Investigación en Matemáticas, University of Valladolid, Valladolid, Spain

^c INCYL, Instituto de Neurociencias de Castilla y León, University of Salamanca, Salamanca, Spain

^d Institute of Mental Health Research, University of Ottawa, Ottawa, Canada

^e Psychiatry Department, University Hospital of Valladolid, Valladolid, Spain

ARTICLE INFO

Article history:

Received 13 November 2017

Received in revised form 10 April 2018

Accepted 29 April 2018

Available online xxx

Keywords:

Modeling;

Neural pathways

Neural synchronization

Schizophrenia

EEG

ABSTRACT

The study of the mechanisms involved in cognition is of paramount importance for the understanding of the neurobiological substrates in psychiatric disorders. Hence, this research is aimed at exploring the brain network dynamics during a cognitive task. Specifically, we analyze the predictive capability of the pre-stimulus theta activity to ascertain the functional brain dynamics during cognition in both healthy and schizophrenia subjects. Firstly, EEG recordings were acquired during a three-tone oddball task from fifty-one healthy subjects and thirty-five schizophrenia patients. Secondly, phase-based coupling measures were used to generate the time-varying functional network for each subject. Finally, pre-stimulus network connections were iteratively modified according to different models of network reorganization. This adjustment was applied by minimizing the prediction error through recurrent iterations, following the predictive coding approach. Both controls and schizophrenia patients follow a reinforcement of the secondary neural pathways (i.e., pathways between cortical brain regions weakly connected during pre-stimulus) for most of the subjects, though the ratio of controls that exhibited this behavior was statistically significant higher than for patients. These findings suggest that schizophrenia is associated with an impaired ability to modify brain network configuration during cognition. Furthermore, we provide direct evidence that the changes in phase-based brain network parameters from pre-stimulus to cognitive response in the theta band are closely related to the performance in important cognitive domains. Our findings not only contribute to the understanding of healthy brain dynamics, but also shed light on the altered predictive neuronal substrates in schizophrenia.

© 2018 Elsevier B.V. All rights reserved.

1. Introduction

It is well-established that disturbed cognition is a core feature of schizophrenia. Schizophrenia patients often exhibit global IQ deficits (Zanelli et al., 2010) and impairments in several cognitive domains, such as semantic memory (Rossell and Batty, 2008), executive function (Simonsen et al., 2011), and sustained attention (Sánchez-Morla et al., 2009), among others (Sheffield and Barch, 2016; Vöhringer et al., 2013). These impairments are likely related to alterations in prefrontal neural network dynamics in schizophrenia (Mukherjee et al., 2016; Poppe et al., 2016). However, the exact relationship between neural network abnormalities and cognitive impairment remains unclear.

Cognition has not only been exhaustively studied using a neuropsychiatric approach both in healthy individuals (Leech and Sharp, 2014) and in schizophrenia patients (Moustafa and Gluck, 2011; Vöhringer et al., 2013), but also from a neuroscientific perspective (Li et al., 2016; van den Heuvel and Fornito, 2014). In this context, a dynamical causal model of the brain behavior has been previously proposed (Friston et al., 2003). Despite the number of virtues of the model, dynamical causal modeling requires a high computational cost and the adjustment of several parameters (Thai et al., 2009). Additionally, the complexity of this model makes it rather difficult to draw direct relationship to brain networks without a strong a priori hypothesis. For these reasons, intuitive models focused on explaining the observed neurodynamics, could be helpful. In this regard, the framework of the predictive coding could be the basis to provide a Bayesian inference of the observed environment (Kilner et al., 2007). Predictive coding is based on minimizing prediction error through recurrent interactions among cortical hierarchy levels (Kilner et al., 2007). The neural activity

* Corresponding author at: Biomedical Engineering Group (GIB), E.T.S. Ingenieros de Telecomunicación, University of Valladolid, Paseo de Belén 15, 47011 Valladolid, Spain.
E-mail address: javier.gomez@gib.tel.uva.es (J. Gomez-Pilar).
URL: <http://www.gib.tel.uva.es> (J. Gomez-Pilar).

encoding a particular brain state determines where the current dynamics are within the hierarchical sequence (Friston and Kiebel, 2009). Therefore, the encoding of a particular state would have a predictive capability of the subsequent state. Perceptual alterations could be then explained by abnormalities in the dynamic mechanisms of predictive coding (Hohwy et al., 2008).

In this study, we propose an intuitive and reliable model of neural network dynamics during a cognitive task, in which the error between the modeled network and the real brain network is recurrently minimized. Thus, the brain network during the pre-stimulus activity (i.e., prior to stimulus presentation or perception) determines the brain network during the subsequent state. It is necessary, therefore, to characterize the brain network in different moments of the task. One approach being considered would be to directly compare these network parameters, i.e. an arithmetic difference, which would summarize the brain dynamics. This approach can be useful to characterize the network changes, but not the underlying neural mechanisms of such changes. A probabilistic model is, therefore, required in order to identify the neural underpinnings associated with the cognitive task. For that purpose, graph-theoretical analyses combined with EEG can be used to provide a mathematical representation of the functional brain network for studying rapid changes in the coordination and synchronization between different regions. Based on previous evidence about the importance of rapid changes in the cognitive processing (Varela et al., 2001), EEG becomes a suitable tool to analyze brain network changes in the range of milliseconds, unreachable by other neuroimaging techniques, such as fMRI. In addition, it is crucial the use of complementary network measures to obtain a comprehensive characterization of the functional brain network (Rubinov and Sporns, 2010). It is generally accepted that functional brain network is well-connected (Power et al., 2013) and complex (Liu et al., 2008). Furthermore, it exhibits an optimal balance between integration and segregation (Deco et al., 2015), as well as between regularity and irregularity (Tononi et al., 1998). Abnormalities in the previously mentioned brain network features have been reported in schizophrenia (Liu et al., 2008; van den Heuvel and Fornito, 2014; Yeo et al., 2016). Therefore, a combination of the previous network characteristics should be helpful to characterize brain network dynamics related to cognition in schizophrenia.

Dysfunctional interactions between brain areas have been repeatedly suggested as a relevant contribution to explain the mental alterations in schizophrenia (Bjorkquist et al., 2016; Friston and Frith, 1995; Whalley, 2005). Within this framework, disrupted connectivity in long-range interactions plays a central role in this disorder (Dickerson et al., 2010; Friston et al., 2016; Gomez-Pilar et al., 2015; Sigurdsson et al., 2010). It is noteworthy that a relationship between long-range interactions and low frequency bands, such as delta and theta, has been proposed (Uhlhaas and Singer, 2010). Therefore, it is not surprising that noticeable findings have been usually reported in the literature about the strong association between schizophrenia and brain connectivity in the low EEG frequency bands (Ford et al., 2002; Koenig et al., 2001; Uhlhaas and Singer, 2010). Alterations on low frequency bands have been related to a temporal misalignment of working memory function in schizophrenia (Kikuchi et al., 2007). In this regard, it was suggested that the neural activity underlying working memory may be abnormally dominated by slow frequencies in schizophrenia (Northoff and Duncan, 2016). Similarly, theta oscillations were proposed to be the basis for memory integration (Buzsáki, 2005) and top-down processing (Uhlhaas et al., 2008), both impaired in schizophrenia patients (Clare, 1993; Rossell and Batty, 2008). In addition, it has been suggested that cognitive control deficits may contribute to episodic memory deficits in schizophrenia (Barch and Sheffield, 2014), in which hippocampal and prefrontal regions could play an important role. This, jointly with our previous studies (Bachiller et al., 2015; Gomez-Pilar et al., 2018c), lead us to claim the importance of theta band to characterize the dynamical cognitive network. The analysis of the electric brain activity at low frequencies during the performance

of an oddball task (related to working memory function and top-down processing) could then enhance our understanding of memory mechanisms in schizophrenia.

In the last decade, several studies assessed the brain network changes during a cognitive task in schizophrenia and healthy individuals, some of them by means of an oddball task (Bachiller et al., 2015; Reijneveld, 2011; Shim et al., 2014). They reported differences in connectivity and/or network features during the cognitive processing. However, for the sake of comparability, it would be appropriate to go a step further and identify a cognitive network model to explain the observed neural dynamics. In a previous study (Gomez-Pilar et al., 2018c), we suggested that network differences between a healthy and a schizophrenia brain could be related with secondary pathways (i.e., pathways between nodes weakly connected) of the brain network during the pre-stimulus activity. These pathways would be strongly reinforced during the cognitive processing, while other connections would remain almost unchanged. These differences could be specifically linked to frequency bands related to memory and hippocampal activity (i.e. low frequency bands).

Hence, the present study aimed at elucidating the dynamical network model during a cognitive task that better fits the brain network changes in a healthy population, as well as the possible abnormalities in schizophrenia. To avoid inter-subject variability, we performed an individualized approach that provides a specific network model for each subject.

2. Methods and materials

2.1. Study subjects

Thirty-five schizophrenia patients were recruited from the Psychiatry Department at the University Hospital of Valladolid (Spain). Diagnoses were made according to the Diagnostic and Statistical Manual of Mental Disorders, 5th edition (DSM-V) criteria (American Psychiatric Association, 2013). Fifty-one healthy control subjects, keeping a non-statistically significant age and gender ratio, were also included in the study. Inclusion/exclusion criteria were undertaken identically as in our previous studies (Bachiller et al., 2014; Gomez-Pilar et al., 2018c; Gomez-Pilar et al., 2017) (see Supplementary material for details). Cognitive data were collected using the Spanish version of the Brief Assessment in Cognition in Schizophrenia (BACS) (Segarra et al., 2011). Clinical and sociodemographic characteristics, as well as antipsychotic doses equivalents for patients, are summarized in Table 1.

All controls and patients gave their informed consent to be included in the study. The study protocol was approved by the research board of the University Hospital of Valladolid (Spain) and was conducted in accordance with the Declaration of Helsinki guidelines.

2.2. Cognitive EEG task

All participants performed a three-stimulus oddball task. During the 13-minutes of the auditory oddball paradigm, participants heard binaural tones bursts presented in random series of 600 tones with an inter-stimulus interval randomly jittered between 1.16 and 1.44 s. Three different tones were presented: target (500 Hz-tone; probability; 0.2), distractor (1000 Hz-tone; probability; 0.2) and standard (2000 Hz-tone; probability; 0.6). The participants were asked to keep their eyes closed and to press a button with their right hand whenever they detected the target tones. Only attended target tones were considered for further analyses. The behavioral performance of both groups is included in Table 1. After preprocessing, the number of trials for target condition was 97.41 ± 9.98 for controls and 89.26 ± 17.04 for patients.

2.3. EEG network estimation and model reconstruction

2.3.1. Acquisition protocol and network analysis

EEG recordings were acquired at a sampling frequency of 500 Hz in 28 electrodes with a BrainVision® equipment (Brain Products GmbH;

Table 1
Sociodemographic and clinical characteristics of schizophrenia patients and healthy control subjects.

		Controls		Patients		Comparison	
		Mean	SD	Mean	SD	t	p
Demographic data	Age (years)	29.31	9.74	32.68	10.37	−1.510	0.135
	Gender (male:female)	23:28		20:15		$\chi^2 = 0.851$	0.356
Symptom scale scores	PANSS +	–	–	12.63	7.53	–	–
	PANSS –	–	–	18.26	8.24	–	–
	PANSS total	–	–	54	21.47	–	–
BACS scale	Working memory	20.67	4.00	15.79	5.31	4.601	<0.001
	Processing speed	70.00	14.10	42.45	15.42	8.055	<0.001
	Executive function	17.18	2.63	15.57	3.44	2.311	<0.05
	Verbal memory	51.61	8.57	34.76	11.25	7.457	<0.001
	Motor speed	72.16	14.11	47.34	14.69	4.415	<0.001
	Verbal fluently	27.89	5.77	17.44	6.39	7.103	<0.001
Illness	Drug equivalence (mg/d)	–	–	351.29	270.10	–	–
	Duration (months)	–	–	84.45	117.40	–	–
Oddball task	Reaction time (ms)	242.43	33.06	277.23	47.32	−4.018	< 0.001
	Precision (%)	98.70	2.13	89.82	16.11	3.897	< 0.001
	Amplitude Pz (μ V)	3.35	1.48	2.29	0.95	3.725	< 0.001
	Latency Pz (ms)	448.78	86.22	457.49	117.11	−0.397	> 0.05

PANSS: Positive and Negative Syndrome Scale.

BACS: Brief Assessment in Cognition in Schizophrenia.

Munich, Germany) while the participants underwent the previously mentioned oddball task. Electrode impedance was always kept under 5 k Ω and each channel was referenced over Cz electrode. After a preprocessing to reduce the noise in the EEG recordings (see Supplementary material for details), brain networks were estimated.

The connectivity values of the functional brain network were computed using the phase-locking value (PLV) across successive trials in the theta frequency band (4–8 Hz). Once the connectivity matrices were obtained, five complementary network features were assessed: (i) integration, (ii) segregation, (iii) connectivity strength, (iv) complexity, and (v) irregularity. They were quantified by means of the characteristic path length, the clustering coefficient, the graph density, the Shannon graph complexity and the Shannon graph entropy, respectively. Since the last two measures have been recently introduced, they do not have widespread use. In summary, the graph irregularity of the brain network was characterized by the Shannon Graph Entropy, defined as follows (Gomez-Pilar et al., 2018c):

$$H = \frac{-1}{\log_2 T} \sum_{i=1}^N \sum_{j=1}^N \frac{w_{ij}}{W} \log_2 \frac{w_{ij}}{W}, \quad (1)$$

where W is the sum of all weights of the graph and $\log_2 T$ is a normalization factor introduced to ensure that $0 \leq H \leq 1$. On the other hand, graph complexity was estimated using the Shannon Graph Complexity, defined as follows (Gomez-Pilar et al., 2018c):

$$SGC = H \cdot \sqrt{\frac{1}{T-1}} \cdot \frac{\sigma}{\bar{w}}, \quad (2)$$

where \bar{w} is the average of all edge values of the graph and σ is the standard deviation of those values. More details about network matrices generation and network parameter definitions have been included in the Supplementary material.

To evaluate brain network changes during the cognitive task, network measures were computed during the pre-stimulus of each trial (i.e., time interval ranging from 300 ms before to the stimulus onset) and during the subsequent brain response (from the stimulus onset to 700 ms after it), with special attention on the brain response related to P3 potential (i.e., a time window of 300 ms centered on 300 ms) (Gomez-Pilar et al., 2017). This procedure is also useful to avoid confounding factors due to volume conduction effects (Bastos and Schoffelen, 2016).

2.3.2. Dynamical network modeling during cognition

The dynamical network model was individually identified for each subject. We considered six different models of brain dynamics. Among all possible models, the six models explained below were selected for being intuitive and easy to explain in physiological terms. As we will discuss later, we are aware that changes in the brain network are probably more complex. The considered models are the following:

- Reinforcement of primary connections. This model assumes that the primary connections of the brain (i.e. connections with higher values of connectivity measured by PLV) during pre-stimulus will suffer more marked changes during the cognition. Specifically, the connection values are increased during the cognitive processing.
- Reinforcement of secondary connections. This model assumes that the secondary connections of the brain (i.e. connections with lower values of connectivity measured by PLV) during pre-stimulus will suffer a more marked increase during cognition.
- Reinforcement of a connection at random. This model assumes that the increase of the brain connections during the pre-stimulus can randomly occur.

We also took into account three additional models, which are similar to models i), ii) and iii) but considering a decrease in the edge values:

- weakening of primary connections,
- weakening of the secondary connections and
- weakening of a connection at random.

In order to determine the dynamical network model for each subject, an iterative algorithm was used. The schematic overview of the procedure is shown in Fig. 1. In summary, the algorithm modified the connections of the pre-stimulus activity following the models previously described. After repeating the algorithm for each of the six models, the model with the lowest mean square error (MSE) between the real and the modeled response was selected. It ensures that the selected model is the one that better fits the cognitive response. All the steps of the algorithm are detailed in the Supplementary material.

Please cite this article as: Gomez-Pilar, J., et al., Altered predictive capability of the brain network EEG model in schizophrenia during cognition, Schizophr. Res. (2018), <https://doi.org/10.1016/j.schres.2018.04.043>

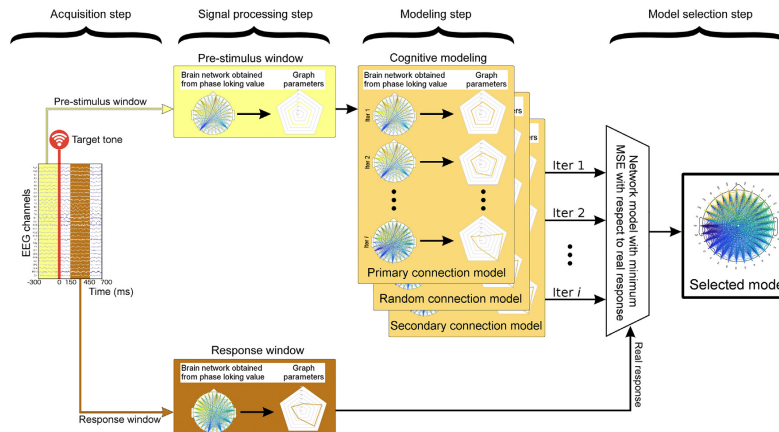


Fig. 1. Cognitive network modeling procedure. After the EEG acquisition, the pre-stimulus window and the response window were segmented. During the signal processing step, graph parameters in each window were computed from the phase-locking value (PLV) connectivity matrix. In the modeling step, the pre-stimulus connectivity matrix was modified by applying the different cognitive models under study. Finally, in the model selection step, the cognitive model and the iteration that obtained the minimum Mean Square Error (MSE) with respect to the network parameters in the response window were selected.

2.4. Statistical analysis

Statistical analysis was done with SPSS (version 19) and Matlab ‘Statistics and Machine Learning’ Toolbox (version 2013b). After checking that parametric assumptions were not met, group differences in gender and age distribution were tested using the Chi-squared test and the Mann-Whitney U test, respectively. Network measures showed a non-Gaussian distribution. Thus, depending on the number of groups, between-group differences were tested using the Mann-Whitney U test or Kruskal-Wallis H test. The effects of age, gender and psychoactive drugs on PLV, network measures and cognitive data were assessed using Spearman’s bivariate correlation test (see “Confounding factors” of the Supplementary material for further details), which is robust against spurious since it deals with monotonic associations in a flexible manner. This test was also used for correlation analyses between graph parameters, cognition and symptoms. Finally, Chi-squared test was used for the between-group comparison of the model distributions.

For all the tests, a significance level of $\alpha = 0.05$ was used. The Bonferroni correction was applied to control the multiple comparisons problem in the correlation analyses between network parameters and cognition. No correction for multiple comparison was performed when comparing graph parameters, since measures were obtained at network level, i.e. one value for each network.

3. Results

3.1. Network dynamics

A visual comparison of the averaged brain networks before and after the stimulus onset (see Fig. 2) shows a global increase of the edge weight values for both groups, though this increase is more noticeable for controls. The brain networks were visualized using the BrainNet Viewer (Xia et al., 2013). To assess network evolution across time, a sliding window approach was used. Windows of 300 ms with an overlap of 90% were selected for network measures computation. Fig. 3A shows the associated dynamics for each network parameter and group. Statistically significant between-group differences for each time window

were marked with black rectangles. The main differences were found around the N2 and P3 event-related potentials.

Fig. 3B depicts violin plots with the distribution of the averaged change of the network parameters from pre-stimulus to cognitive response for both groups. Statistically significant differences between groups for the change from pre-stimulus activity to cognitive response were obtained: integration ($U(84) = 619$; $p < 0.05$), segregation ($U(84) = 553.0$; $p < 0.01$), connectivity strength ($U(84) = 559.5$; $p < 0.01$), complexity ($U(84) = 670.5$; $p < 0.05$) and irregularity ($U(84) = 670.5$; $p < 0.05$). In summary, brain network during pre-stimulus window has lower changes in the response window in schizophrenia patients compared to healthy controls.

3.2. Modeling the network changes

Network modeling with the three different scenarios (primary, secondary and random connection models) was applied to data obtained from the pre-stimulus window. Thus, the model that better predicted the cognitive response network using the pre-stimulus network was selected individually for each subject. The behavior of the modeling is shown in Fig. 4. On average, the MSE between the network parameters in pre-stimulus window and the response window was 10.69% for controls and 2.96% for patients (from yellow to orange lines). Furthermore, the MSE between the predicted model and the cognitive response was 0.21% for controls and 0.07% for patients, which serves to exemplify the accuracy of the model.

The procedure selected a single model for each subject. The distribution of the model for each group is shown in Fig. 5A. Secondary reinforcement model was selected for most of the subjects, especially in the control group. Models based on weakening network connections were selected only in 15% of the subjects (thirteen subjects: seven controls and six schizophrenia patients; more details are indicated in the Supplementary material). Statistically significant differences between groups in the model selection distribution were obtained ($\chi^2(2, N = 73) = 6.6874$, $p < 0.05$; Chi-square test). Likewise, MSE distribution of the network parameters in each cognitive model was also assessed for both groups (Fig. 5B). Within-group comparisons indicate that controls exhibited a statistically significant different MSE

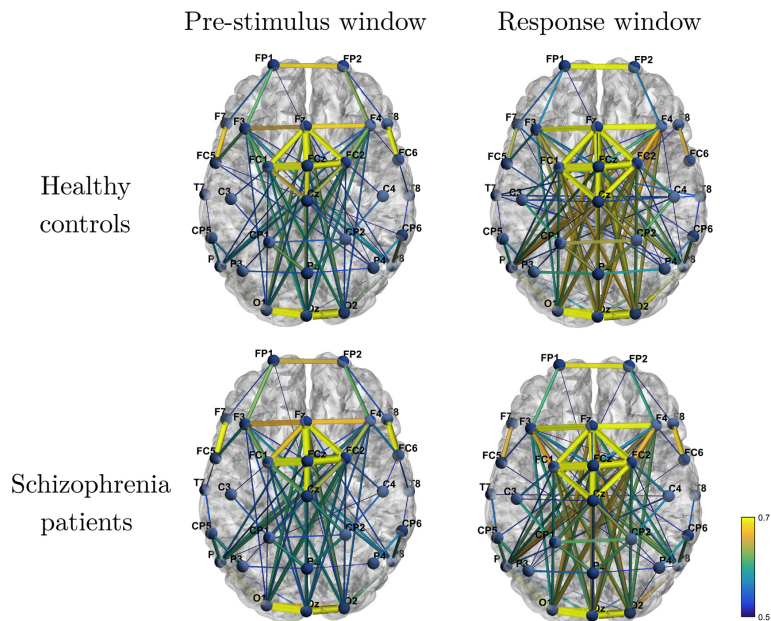


Fig. 2. Averaged brain networks for both groups before and after stimulus onset. Both groups show an increase in the edge weight values from the pre-stimulus (from -300 ms to the stimulus onset) to the response window (from 150 ms to 450 ms after the stimulus), though this increase is more noticeable for controls. To facilitate the visualization of the networks, a threshold was applied: only those connections with phase-locking values higher than 0.5 were depicted. The brain networks were visualized using the BrainNet Viewer (Xia et al., 2013).

distribution ($\chi^2(2, N = 44) = 22.0032, p < 0.001$), but not schizophrenia patients ($\chi^2(2, N = 29) = 2.6302, p > 0.05$). In summary, the higher change from pre-stimulus activity to cognitive response for controls, the higher probability to model their behavior by a reinforcement of the secondary connections. The schizophrenia patients do not follow this tendency, as they do not exhibit a relevant change from pre-stimulus activity to the post-stimulus period during the cognitive response.

3.3. Cognitive correlates

Interest in the assessment of correlations between cognition and brain functioning is growing, as it is becoming increasingly evident that it is a useful way to evaluate the heterogeneity of schizophrenia (Sheffield and Barch, 2016). As shown in Fig. 6, there was a noticeable relationship between connectivity strength modulation (measured as the percent of change from pre-stimulus to cognitive response) and cognitive parameters (z -score corrected).

Specifically, the connectivity strength was statistically significant correlated to processing speed ($r = 0.472, p < 0.001$), verbal fluency ($r = 0.499, p < 0.001$) and verbal memory ($r = 0.423, p < 0.001$) after Bonferroni correction. The positive correlations indicate that the greater susceptibility to change in the pre-stimulus, the better cognitive performance. No other statistically significant correlations were found after Bonferroni correction.

Additionally, we performed correlations between cognition and symptoms, as well as between network parameters and symptoms. All these correlations are shown in the Supplementary material.

4. Discussion

To the best of our knowledge, this is the first study that combine network modeling and EEG recordings to determine a model of network dynamics during cognition for healthy and schizophrenia subjects. The proposed network modeling effectively predicts the functional brain network of the cognitive response from the pre-stimulus activity.

4.1. Disrupted brain dynamics of the phase-based mechanisms in schizophrenia

Schizophrenia has been characterized by abnormal brain network reconfigurations, commonly described in the literature (Gomez-Pilar et al., 2017; Shim et al., 2014). These abnormal dynamics (see Fig. 3) suggest a disrupted phase-based mechanisms during the cognitive processing (Lakatos et al., 2013).

In this study, a significant reduced dynamic capability of the network during the pre-stimulus was observed in patients. This reduction is driven by the phase of the EEG theta band. The lack of change in schizophrenia patients was characterized by complementary network parameters. All of them showed statistically significant reduced changes, which involves an impaired ability to modify the main topological features of the brain network. The reduced flexibility of the network integration and connectivity strength during the task supports an impaired capability of the communication among brain network, which is in agreement with the results obtained by previous studies (Bob et al., 2008; Friston, 1998; Kim et al., 2003). The lower change on segregation in functional brain networks indicates lower local

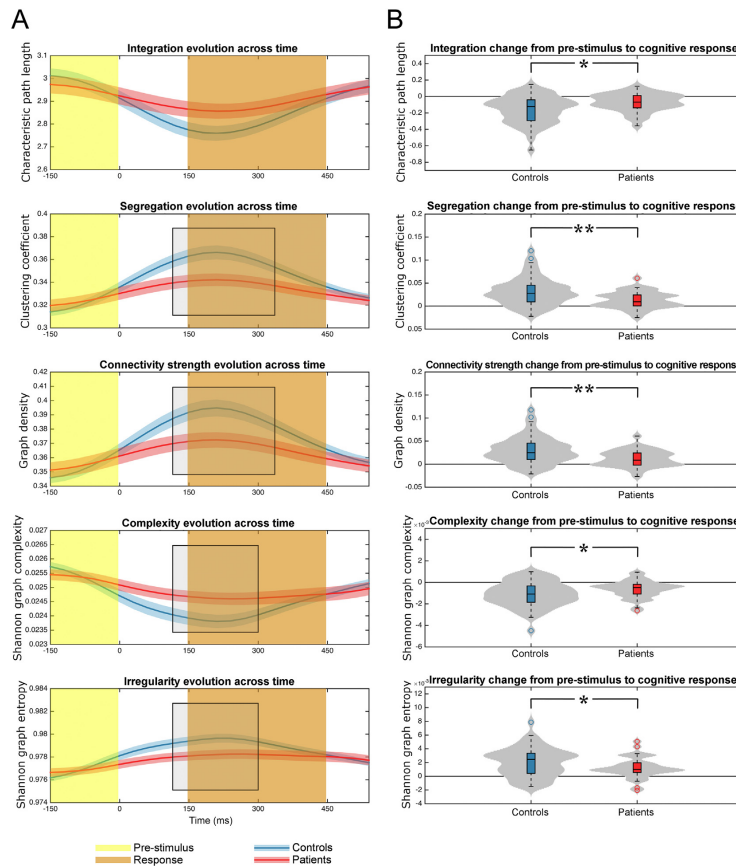


Fig. 3. Time evolution of the network parameters. (A) Mean and standard error of the network parameters for controls (blue) and patients (red). Control subjects exhibit higher changes from pre-stimulus (yellow) to cognitive response (orange) compared to patients. Statistically significant differences between the network parameter evolution across time of both groups are highlighted by a black rectangle ($p < 0.05$, Mann-Whitney U test). The results indicate an impaired ability in patients to modify the functional brain network during an oddball task. (B) Boxplots and violin plots showing the distribution of the averaged change of the network parameters from pre-stimulus (yellow transparency in A) to cognitive response (orange transparency in A) for both groups. Statistically significant differences between groups are indicated with one asterisk ($p < 0.05$, Mann-Whitney U test) or two asterisks ($p < 0.01$, Mann-Whitney U test). (For interpretation of the references to colour in this figure legend, the reader is referred to the web version of this article.)

communication or less segregated neural processing (Rubinov and Sporns, 2010). Finally, a reduced change in graph regularity and graph complexity was also found for patients. The physiological interpretation of this result could be related to abnormalities in small-world structure (Liu et al., 2008; Micheloyannis et al., 2006) and, therefore, a reduced network efficiency (Bassett and Bullmore, 2006; Boccaletti et al., 2006).

The underlying biological mechanisms that influence the abnormal dynamics can have different explanations. From the graph theory point of view, a fMRI study reported a diminished number of hubs during a cognitive task in schizophrenia (Ma et al., 2012). These well-connected nodes typically increase the global integration and connectivity, as well as local segregation. Therefore, the lower the number of hubs in schizophrenia during a cognitive task, the lower the global

integration, connectivity and segregation. From a physiological perspective, this lack of change can be related to the abnormal oscillatory behavior during a cognitive task in schizophrenia, which could elicit a lower synchronization between brain regions in comparison to healthy subjects. It could be explained by an abnormal balance between inhibitory GABAergic interneurons (Lewis et al., 2005; Moghaddam, 2003) and pyramidal neurons producing dysfunctionalities between excitation and inhibition processes, which is reflected in the phase measures. This affects to the neural pathways in long-range synchronization (Dickerson et al., 2010), providing abnormal phase-based network measures. Hence, the result that the diminished EEG response was observable in complementary network parameters (see Figs. 3 and 4) suggests that different brain network domains are significantly affected by schizophrenia.

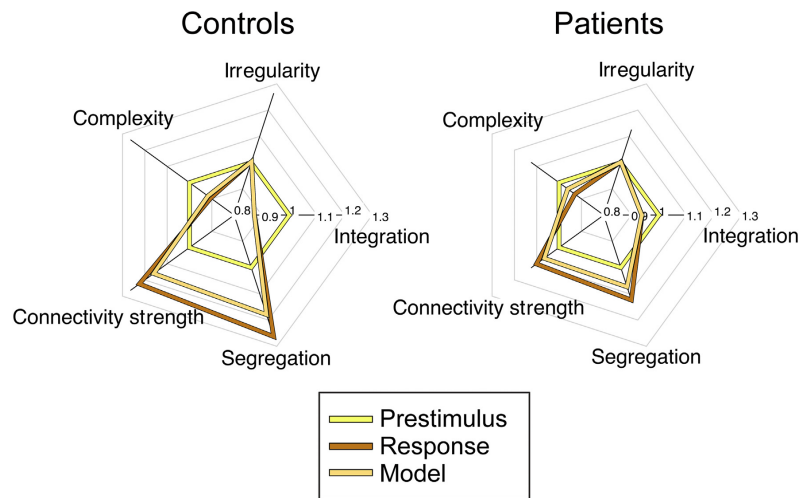


Fig. 4. Prediction capability of the network modeling from the phase information of the theta band during the pre-stimulus window. Grand-average normalized network parameters for the pre-stimulus window (yellow) and the real response window (dark orange). The network measures prediction obtained by the model from the phase information of the pre-stimulus window is also shown (light orange). The model fitting for both the controls and the patient groups is computed by minimizing the mean square error (MSE). (For interpretation of the references to colour in this figure legend, the reader is referred to the web version of this article.)

4.2. Reinforcement of the secondary pathways as a predominant model

The results show (Fig. 5A) that the predominant model of brain network dynamics during cognition in healthy and schizophrenia subjects involves a reinforcement of the secondary pathways of the pre-stimulus network (i.e., connections with lower phase synchronization between brain areas prior to stimulus perception). However, there are statistically significant differences in the model distribution between groups.

In order to provide a reason of these differences, we rely on the predictive coding (Hohwy et al., 2008). In this study, we constructed generative models that minimize the error at each iteration following the main neurocomputational principle for the brain perception of the environment (Hohwy et al., 2008). The recurrent error minimization until the most likely model has been obtained is formally equivalent to empirical Bayesian inference (Kilner et al., 2007). This implies that abnormalities in the dynamical process of the brain reconfiguration would

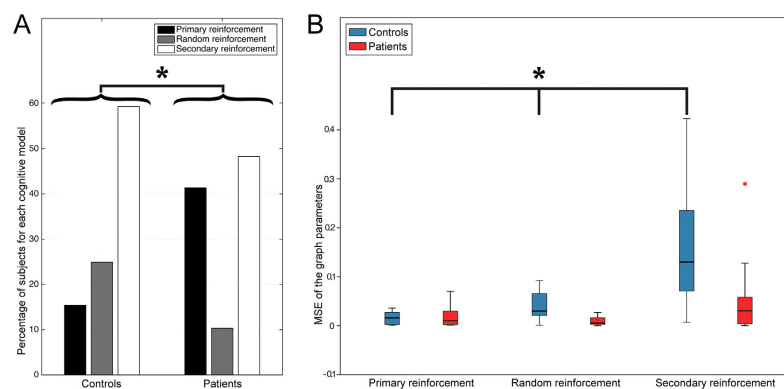


Fig. 5. Histogram of the selected models and mean square error (MSE) distribution for each model. (A) Percentage of subjects that best fit each model for controls and schizophrenia patients. The reinforcement of the secondary connections is the most frequently selected model for both groups; however, statistically significant differences between the histograms of controls and patients were found and marked with an asterisk ($\chi^2 = 6.6874$, $p < 0.05$; Chi-square test). (B) Change from pre-stimulus to cognitive response of the network parameters measured by means of the mean square error (MSE) and grouping by the network model. Differences among models were statistically significant for controls and marked with an asterisk ($\chi^2(2, N = 73) = 22.0032$, $p < 0.001$; Kruskal-Wallis test), but not for patients ($\chi^2(2, N = 73) = 2.6302$, $p > 0.05$; Kruskal-Wallis test).

Please cite this article as: Gomez-Pilar, J., et al., Altered predictive capability of the brain network EEG model in schizophrenia during cognition, Schizophr. Res. (2018), <https://doi.org/10.1016/j.schres.2018.04.043>

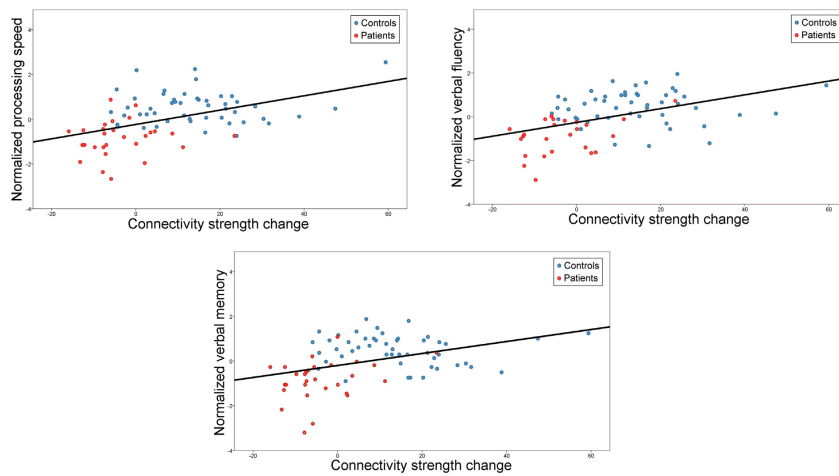


Fig. 6. Correlations between cognition and network parameter. Statistically significant correlations after Bonferroni correction for the comparison between cognition and network parameters: (i) normalized processing speed and change in connectivity strength ($r = 0.472$, $p < 0.001$; Spearman's rank correlation coefficient); (ii) normalized verbal fluency and change in connectivity strength ($r = 0.499$, $p < 0.001$; Spearman's rank correlation coefficient) and; (iii) normalized verbal memory and change in connectivity strength ($r = 0.423$, $p < 0.001$; Spearman's rank correlation coefficient).

have a strong impact on the subsequent state. Following the aberrant salience hypothesis (Kapur, 2003), schizophrenia leads to an aberrant assignment of salience to the elements of one's experience. It suggests that the relevance assignment to the unexpected stimulus in an oddball task would be disrupted in schizophrenia and, as a consequence, would cause an increase in the prediction error. Therefore, the observed disrupted brain dynamics in schizophrenia patients yield a higher prediction error in schizophrenia subjects compared to controls. The abnormalities in the response network in schizophrenia, in turn, account for the cognitive deficits in this disorder.

Additionally, for controls, it was found a statistically significant relationship between the amount of change from pre-stimulus to cognitive response and the model that better predicts the cognitive network. Fig. 5B shows that the secondary pathway reinforcement modeling is linked to a higher network reconfiguration in controls, which could be considered the 'normal behavior'. However, schizophrenia patients did not show that trend. This was observed in the theta band, which supports the concept of the impaired top-down processing in schizophrenia (Uhlhaas et al., 2008). This lack of activation of the connections with low synchronization during pre-stimulus in several schizophrenia patients could be due to several reasons. Thereby, it could be related with abnormal structural connectivity networks (Gomez-Pilar et al., 2018a), with hyperactive functional connectivity in the patients during the pre-stimulus (Gomez-Pilar et al., 2018b), or with deficits in the inhibitory/excitatory circuits, usually linked to glutamate neurotransmission (Moghaddam, 2003), which could elicit abnormalities in the synchronization between brain regions.

Glutamatergic abnormalities could not only be related to the long-range synchronization in the theta band, but also to the way of organizing the connections during a cognitive task. While subjects are waiting for the next relevant stimulus, the brain is in a state of alert related to glutamate resting-state concentration in the perigenual anterior cingulate cortex (PACC) (Bai et al., 2015). This level of glutamatergic activity has a strong relationship with the pre-stimulus oscillations. Therefore, possible abnormalities of glutamatergic concentrations in schizophrenia

would affect to the predisposition to change of the pre-stimulus network (Bai et al., 2015). Furthermore, a special association between pre-stimulus activity levels and stimulus-induced activity has been suggested in previous studies (Bai et al., 2015). We can speculate that the aberrant network dynamics during cognition in schizophrenia may be driven by underlying abnormalities in the glutamate resting-state concentration in the PACC. Could these abnormalities impact on the cognitive network model of schizophrenia patients? Could it be the reason for the almost dichotomous distribution of the selected models in the schizophrenia group?

A plausible hypothesis for explaining the heterogeneity of the selected models could be the extended concept that schizophrenia is a complex and heterogeneous disorder with distinguishable genotypes (Sheffield and Barch, 2016) and network abnormalities (Gomez-Pilar et al., 2018a), which can influence the cognitive traits. Schizophrenia heterogeneity should not be related to the symptoms, but to underlying neural mechanisms, which are maybe phase-related. To address this heterogeneity, we measured the correlation between network topology features and the cognitive variables.

4.3. Relationship between topological network measures and cognitive variables

Our results showed a positive correlation between the modulation (i.e., change from pre-stimulus to cognitive response) of the connectivity strength and three cognitive domains measured by means of the BACS: processing speed, verbal fluency and verbal memory. Consequently, the higher averaged values of change in synchronization between brain regions would involve a better performance in the measured cognitive traits. Due to the novelty of our approach, we only have notice of one study that previously assessed the association between the modulation of network parameters and cognitive data in schizophrenia (Gomez-Pilar et al., 2017). Despite the difficulty to compare the correlations observed in this study with previous findings and for the sake of brevity, we link the present findings with previous works in the Supplementary material.

4.4. Further steps towards a comprehensive neural cognitive model

Despite the clues provided in this study to obtain a reliable model of the brain network dynamics during cognition, a number of questions remain unresolved. First, brain functioning is complex; probably it is more complex than the proposed model. It could result in losing relevant information about brain interactions likely related to the heterogeneity among subjects. For instance, complementary processes could be taking place, such as changes in specific connections or deactivations of a few well-connected pathways during pre-stimulus. Therefore, an almost infinite number of combinations of changes in synchronization could be analyzed to individually improve the model adjustment, but the generalization capability of the model would be likely lost.

Second, the present study was focused on the theta frequency band. Knowing the importance of other frequency bands in the brain functioning, we focused on theta band because of its close relationship with memory processes, top-down control and long-range interactions in the brain, all of them involved in core features of the schizophrenia pathology. Additionally, it was not feasible to simultaneously determine the model for all the frequency bands due to the high computational cost for individually adjusting the more confident model. Future works should investigate network dynamics in other frequency bands to ascertain the predisposition to change of the pre-stimulus activity.

Finally, a hierarchical clustering analysis using both the graph measures and the cognitive/behavioral data could be useful to check the schizophrenia subgroups found by the proposed EEG model. However, a large number of observations would be needed for this kind of analysis, being insufficient the number of subjects of the present study. Future studies with larger number of subjects should address this issue.

5. Conclusions

We provided direct evidence of the predictive capability of the proposed model to ascertain the functional brain behavior during cognition. Our results support the idea that schizophrenia is associated with significant abnormalities in the relation between neural dynamics during the pre-stimulus and cognitive response, which are directly related to cognitive performance. Furthermore, we presented a new model of network organization during cognition based on graph theory measures, which could be used to differentiate behavioral phenotypes of schizophrenia. Our findings not only contribute to a further understanding of healthy neural dynamics during cognition, but also provide new insights for identifying the altered neural underpinnings of schizophrenia.

Role of the funding source

This research project was supported in part by "Ministerio de Economía y Competitividad" and FEDER (TEC2014-53196-R), by "European Commission" (POCTEP 0378.AD.EEGWA_2.P), by "Consejería de Educación de la Junta de Castilla y León" (VA037U16), by "Fondo de Investigaciones Sanitarias (Instituto de Salud Carlos III)" under projects FIS P111.02203 and P115.00299, and by "Gerencia Regional de Salud de Castilla y León" under projects GRS 932/A/14 and GRS 1134/A/15. A. Lubeiro was in receipt of a grant from the Consejería de Educación (Junta de Castilla y León). J. Gomez-Pilar was in receipt of a grant from University of Valladolid.

Contributors

J. Poza, R. Hornero and G. Northoff designed the study. J. Gomez-Pilar, C. Gómez, J. Poza and R. Hornero analyzed the EEGs and undertook the statistical analyses. J. Gomez-Pilar wrote the manuscript and performed the computational modeling. V. Molina recruited the patients and performed clinical assessment. A. Lubeiro and B. Cea-Cañas performed the electroencephalographic recordings and the cognitive assessment. All authors contributed to the article, revised and approved the final manuscript.

Conflict of interest

The authors report no biomedical financial interests or potential conflicts of interest.

Acknowledgement

The authors thank Mr. Martinez-Cagigal for providing the Matlab scripts that significantly enhance the appearance of some figures of the manuscript. We also would like to express our gratitude to the Psychiatry Service of the Clinical University Hospital of Valladolid (Spain), for their help and support and the altruistic volunteers for participation.

Appendix A. Supplementary data

Supplementary data to this article can be found online at <https://doi.org/10.1016/j.schres.2018.04.043>.

References

- American Psychiatric Association. 2013. Diagnostic and Statistical Manual of Mental Disorders. 5th Edition. American Psychiatric Publishing, Arlington DSM-5. <https://doi.org/10.1176/appi.books.9780890425968.893619>.
- Bachiller, A., Díez, A., Suazo, V., Domínguez, C., Ayuso, M., Hornero, R., Poza, J., Molina, V., 2014. Decreased spectral entropy modulation in patients with schizophrenia during a P300 task. *Eur. Arch. Psychiatry Clin. Neurosci.* 264:533–543. <https://doi.org/10.1007/s00406-014-0488-6>.
- Bachiller, A., Poza, J., Gómez, C., Molina, V., Suazo, V., Hornero, R., 2015. A comparative study of event-related coupling patterns during an auditory oddball task in schizophrenia. *J. Neural Eng.* 12:16007. <https://doi.org/10.1088/1741-2560/12/1/016007>.
- Bai, Y., Nakao, T., Xu, J., Qin, P., Chaves, P., Heinzl, A., Duncan, N., Lane, T., Yen, N.-S., Tsai, S.-Y., Northoff, G., 2015. Resting state glutamate predicts elevated pre-stimulus alpha during self-relatedness: a combined EEG-MRS study on "rest-self overlap". *Soc. Neurosci.* 9:1–15. <https://doi.org/10.1080/17470919.2015.1072582>.
- Barch, D.M., Sheffield, J.M., 2014. Cognitive impairments in psychotic disorders: common mechanisms and measurement. *World Psychiatry* 13:224–232. <https://doi.org/10.1002/wps.20145>.
- Bassett, D.S., Bullmore, E., 2006. Small-world brain networks. *Neuroscientist* 12:512–523. <https://doi.org/10.1177/1073858406293182>.
- Bastos, A.M., Schoffelen, J.-M., 2016. A tutorial review of functional connectivity analysis methods and their interpretational pitfalls. *Front. Syst. Neurosci.* 9:175. <https://doi.org/10.3389/fnys.2015.00175>.
- Bjorkquist, O.A., Olsen, E.K., Nelson, B.D., Herbener, E.S., 2016. Altered amygdala-prefrontal connectivity during emotion perception in schizophrenia. *Schizophr. Res.* 175:35–41. <https://doi.org/10.1016/j.schres.2016.04.003>.
- Bob, P., Palus, M., Susta, M., Glaslova, K., 2008. EEG phase synchronization in patients with paranoid schizophrenia. *Neurosci. Lett.* 447:73–77. <https://doi.org/10.1016/j.neulet.2008.09.055>.
- Boccaletti, S., Latora, V., Moreno, Y., Chavez, M., Hwang, D.U., 2006. Complex networks: structure and dynamics. *Phys. Rep.* 424:175–308. <https://doi.org/10.1016/j.physrep.2005.10.009>.
- Buzsáki, G., 2005. Theta rhythm of navigation: link between path integration and landmark navigation, episodic and semantic memory. *Hippocampus* 15:827–840. <https://doi.org/10.1002/hipo.20113>.
- Clare, L., 1993. Memory in schizophrenia: what is impaired and what is preserved? *Neuropsychologia* 31, 1225–1241.
- Deco, G., Tononi, G., Boly, M., Kringelbach, M.L., 2015. Rethinking segregation and integration: contributions of whole-brain modelling. *Nat. Rev. Neurosci.* 16:430–439. <https://doi.org/10.1038/nrn3963>.
- Dickerson, D.D., Wolff, A.R., Bilkey, D.K., 2010. Abnormal long-range neural synchrony in a maternal immune activation animal model of schizophrenia. *J. Neurosci.* 30:12424–12431. <https://doi.org/10.1523/JNEUROSCI.3046-10.2010>.
- Ford, J.M., Mathalon, D.H., Whitfield, S., Faustman, W.O., Roth, W.T., 2002. Reduced communication between frontal and temporal lobes during talking in schizophrenia. *Biol. Psychiatry* 51:485–492. [https://doi.org/10.1016/S0006-3223\(01\)01335-X](https://doi.org/10.1016/S0006-3223(01)01335-X).
- Friston, K.J., 1998. The disconnection hypothesis. *Schizophr. Res.* 30:115–125. [https://doi.org/10.1016/S0920-9964\(97\)00140-0](https://doi.org/10.1016/S0920-9964(97)00140-0).
- Friston, K., Frith, C.D., 1995. Schizophrenia: a disconnection syndrome? *Clin. Neurosci.* 3, 89–97.
- Friston, K., Kiebel, S., 2009. Predictive coding under the free-energy principle. *Philos. Trans. R. Soc. B Biol. Sci.* 364:1211–1221. <https://doi.org/10.1098/rstb.2008.0300>.
- Friston, K.J., Harrison, L., Penny, W., 2003. Dynamic causal modelling. *NeuroImage* 19:1273–1302. [https://doi.org/10.1016/S1053-8119\(03\)00202-7](https://doi.org/10.1016/S1053-8119(03)00202-7).
- Friston, K., Brown, H.R., Siemerkus, J., Stephan, K.E., 2016. The dysconnection hypothesis (2016). *Schizophr. Res.* 176:83–94. <https://doi.org/10.1016/j.schres.2016.07.014>.
- Gomez-Pilar, J., Poza, J., Bachiller, A., Gómez, C., Molina, V., Hornero, R., 2015. Neural network reorganization analysis during an auditory oddball task in schizophrenia using wavelet entropy. *Entropy* 17:5241–5256. <https://doi.org/10.3390/e17085241>.
- Gomez-Pilar, J., Lubeiro, A., Poza, J., Hornero, R., Ayuso, M., Valcárcel, C., Haidar, K., Blanco, J.A., Molina, V., 2017. Functional EEG network analysis in schizophrenia: evidence of larger segregation and deficit of modulation. *Prog. Neuro-Psychopharmacol. Biol. Psychiatry* 76:116–123. <https://doi.org/10.1016/j.pnpbp.2017.03.004>.
- Gomez-Pilar, J., de Luis-García, R., Lubeiro, A., de la Red, H., Poza, J., Núñez, P., Hornero, R., Molina, V., 2018a. Relations between structural and EEG-based graph metrics in healthy controls and schizophrenia patients. *Hum. Brain Mapp.* <https://doi.org/10.1002/hbm.24066>.
- Gomez-Pilar, J., de Luis-García, R., Lubeiro, A., de Urbe, N., Poza, J., Núñez, P., Ayuso, M., Hornero, R., Molina, V., 2018b. Deficits of entropy modulation in schizophrenia are predicted by functional connectivity strength in the theta band and structural clustering. *NeuroImage Clin.* 18:382–389. <https://doi.org/10.1016/j.nicl.2018.02.005>.
- Gomez-Pilar, J., Poza, J., Bachiller, A., Gómez, C., Núñez, P., Lubeiro, A., Molina, V., Hornero, R., 2018c. Quantification of graph complexity based on the edge weight distribution balance: application to brain networks. *Int. J. Neural Syst.* 28:1750032. <https://doi.org/10.1142/S0129065717500320>.
- Hohwy, J., Roepstorff, A., Friston, K., 2008. Predictive coding explains binocular rivalry: an epistemological review. *Cognition* 108:687–701. <https://doi.org/10.1016/j.cognition.2008.05.010>.

Please cite this article as: Gomez-Pilar, J., et al., Altered predictive capability of the brain network EEG model in schizophrenia during cognition, *Schizophr. Res.* (2018), <https://doi.org/10.1016/j.schres.2018.04.043>

ARTICLE IN PRESS

10

J. Gomez-Pilar et al. / Schizophrenia Research xxx (2018) xxx–xxx

- Kapur, S., 2003. Psychosis as a state of aberrant salience: a framework linking biology, phenomenology, and pharmacology in schizophrenia. *Am. J. Psychiatry* 160:13–23. <https://doi.org/10.1176/appi.ajp.160.1.13>.
- Kikuchi, M., Koenig, T., Wada, Y., Higashima, M., 2007. Native EEG and Treatment Effects in Neuroleptic-naïve Schizophrenic patients: Time and Frequency Domain Approaches. 97:pp. 163–172. <https://doi.org/10.1016/j.schres.2007.07.012>.
- Kilner, J.M., Friston, K.J., Frith, C.D., 2007. Predictive coding: an account of the mirror neuron system. *Cogn. Process.* 8:159–166. <https://doi.org/10.1007/s10939-007-0170-2>.
- Kim, J.-J., Kwon, J.S., Park, H.J., Youn, T., Kang, D.H., Kim, M.S., Lee, D.S., Lee, M.C., 2003. Functional disconnection between the prefrontal and parietal cortices during working memory processing in schizophrenia: a [15O]H₂O PET study. *Am. J. Psychiatry* 160:919–923. <https://doi.org/10.1176/appi.ajp.160.5.919>.
- Koenig, T., Lehmann, D., Saito, N., Kuginuki, T., Kinoshita, T., Koukkou, M., 2001. Decreased functional connectivity of EEG theta-frequency activity naïve patients with schizophrenia: preliminary results. *Schizophr. Res.* 50, 55–60.
- Lakatos, P., Musacchia, G., O'Connell, M., Falchier, A., Javitt, D., Schroeder, C., 2013. The spectrotemporal filter mechanism of auditory selective attention. *Neuron* 77:750–761. <https://doi.org/10.1016/j.neuron.2012.11.034>.
- Leech, R., Sharp, D.J., 2014. The role of the posterior cingulate cortex in cognition and disease. *Brain* 137:12–32. <https://doi.org/10.1093/brain/awt162>.
- Lewis, D.A., Hashimoto, T., Volk, D.W., 2005. Cortical inhibitory neurons and schizophrenia. *Nat. Rev. Neurosci.* 6:312–324. <https://doi.org/10.1038/nrn1648>.
- Li, F., Chen, B., Li, H., Zhang, T., Wang, F., Jiang, Y., Li, P., Ma, T., Zhang, R., Tian, Y., Liu, T., Guo, D., Yao, D., Xu, P., 2016. The time-varying networks in P300: a task-evoked EEG study. *IEEE Trans. Neural Syst. Rehabil. Eng.* 24:725–733. <https://doi.org/10.1109/TNSRE.2016.2523678>.
- Liu, Y., Liang, M., Zhou, Y., He, Y., Hao, Y., Song, M., Yu, C., Liu, H., Liu, Z., Jiang, T., 2008. Disrupted small-world networks in schizophrenia. *Brain* 131:945–961. <https://doi.org/10.1093/brain/awn018>.
- Ma, S., Calhoun, V.D., Eichele, T., Du, W., Adali, T., 2012. Modulations of functional connectivity in the healthy and schizophrenia groups during task and rest. *NeuroImage* 62:1694–1704. <https://doi.org/10.1016/j.neuroimage.2012.05.048>.
- Micheliyannis, S., Pachou, E., Stam, C.J., Breakspear, M., Bitsios, P., Vourkas, M., Erimaki, S., Zervakis, M., 2006. Small-world networks and disturbed functional connectivity in schizophrenia. *Schizophr. Res.* 87:60–66. <https://doi.org/10.1016/j.schres.2006.06.028>.
- Moghaddam, B., 2003. Bringing order to the glutamate chaos in schizophrenia. *Neuron* 40:881–884. [https://doi.org/10.1016/S0896-6273\(03\)00757-8](https://doi.org/10.1016/S0896-6273(03)00757-8).
- Moustafa, A.A., Gluck, M.A., 2011. Computational cognitive models of prefrontal-striatal-hippocampal interactions in Parkinson's disease and schizophrenia. *Neural Netw.* 24:575–591. <https://doi.org/10.1016/j.neunet.2011.02.006>.
- Mukherjee, P., Sabharwal, A., Kotov, R., Szekeley, A., Parsey, R., Barch, D.M., Mohanty, A., 2016. Disconnection between amygdala and medial prefrontal cortex in psychotic disorders. *Schizophr. Bull.* 42:1056–1067. <https://doi.org/10.1093/schbul/sbw012>.
- Northoff, G., Duncan, N.W., 2016. How do abnormalities in the brain's spontaneous activity translate into symptoms in schizophrenia? From an overview of resting state activity findings to a proposed spatiotemporal psychopathology. *Prog. Neurobiol.* 145:146–26–45. <https://doi.org/10.1016/j.pneurobio.2016.08.003>.
- Poppe, A.B., Barch, D.M., Carter, C.S., Gold, J.M., Ragland, J.D., Silverstein, S.M., MacDonald, A.W., 2016. Reduced frontoparietal activity in schizophrenia is linked to a specific deficit in goal maintenance: a multisite functional imaging study. *Schizophr. Bull.* 42:1149–1157. <https://doi.org/10.1093/schbul/sbw036>.
- Power, J.D., Schlaggar, B.L., Lessov-schlaggar, C.N., Petersen, S.E., 2013. Article evidence for hubs in human functional brain networks. *Neuron* 79:798–813. <https://doi.org/10.1016/j.neuron.2013.07.035>.
- Reijnenveld, J.C., 2011. Altered small-world brain networks in temporal lobe in patients with schizophrenia performing an auditory oddball task. *Front. Syst. Neurosci.* 5:1–13. <https://doi.org/10.3389/fnys.2011.00007>.
- Rossell, S., Batty, R., 2008. Elucidating semantic disorganisation from a word comprehension task: do patients with schizophrenia and bipolar disorder show differential processing of nouns, verbs and adjectives? *Schizophr. Res.* 102:63–68. <https://doi.org/10.1016/j.schres.2008.04.008>.
- Rubinov, M., Sporns, O., 2010. Complex network measures of brain connectivity: uses and interpretations. *NeuroImage* 52:1059–1069. <https://doi.org/10.1016/j.neuroimage.2009.10.003>.
- Sánchez-Morla, E.M., Barabash, A., Martínez-Vizcaíno, V., Tabarés-Seisdedos, R., Balanzá-Martínez, V., Cabranes-Díaz, J.A., Baca-Baldomero, E., Gómez, J.L.S., 2009. Comparative study of neurocognitive function in euthymic bipolar patients and stabilized schizophrenic patients. *Psychiatry Res.* 169:220–228. <https://doi.org/10.1016/j.psychres.2008.06.032>.
- Segarra, N., Bernardo, M., Gutierrez, F., Justicia, A., Fernandez-Egea, E., Allas, M., Safont, G., Contreras, F., Gascón, J., Soler-lina, P.A., Menchon, J.M., Junque, C., Keefe, R.S.E., 2011. Spanish validation of the Brief Assessment in Cognition in Schizophrenia (BACS) in patients with schizophrenia and healthy controls. *Eur. Psychiatry* 26:69–73. <https://doi.org/10.1016/j.eurpsy.2009.11.001>.
- Sheffield, J.M., Barch, D.M., 2016. Cognition and resting-state functional connectivity in schizophrenia. *Neurosci. Biobehav. Rev.* 61:108–120. <https://doi.org/10.1016/j.neubiorev.2015.12.007>.
- Shim, M., Kim, D.W., Lee, S.H., Im, C.H., 2014. Disruptions in small-world cortical functional connectivity network during an auditory oddball paradigm task in patients with schizophrenia. *Schizophr. Res.* 156:197–203. <https://doi.org/10.1016/j.schres.2014.04.012>.
- Sigurdsson, T., Stark, K.L., Karayiorgou, M., Gogos, J.A., Gordon, J.A., 2010. Impaired hippocampal – prefrontal synchrony in a genetic mouse model of schizophrenia. *Nature* 464:763–767. <https://doi.org/10.1038/nature08855>.
- Simonsen, C., Sundet, K., Vaskinn, A., Birkenaes, A.B., Engh, J.A., Faerden, A., Jonsdottir, H., Ringen, P.A., Opjordsmoen, S., Melle, I., Friis, S., Andreassen, O.A., 2011. Neurocognitive dysfunction in bipolar and schizophrenia spectrum disorders depends on history of psychosis rather than diagnostic group. *Schizophr. Bull.* 37:73–83. <https://doi.org/10.1093/schbul/sbp034>.
- Thai, N.J., Longe, O., Rippon, G., 2009. Disconnected brains: what is the role of fMRI in connectivity research? *Int. J. Psychophysiol.* 73:27–32. <https://doi.org/10.1016/j.ijpsycho.2008.12.015>.
- Tononi, G., Edelman, G.M., Sporns, O., 1998. Complexity and coherency: integrating information in the brain. *Trends Cogn. Sci.* 2, 474–484.
- Uhlhaas, P.J., Singer, W., 2010. Abnormal neural oscillations and synchrony in schizophrenia. *Nat. Rev. Neurosci.* 11:100–113. <https://doi.org/10.1038/nrn2774>.
- Uhlhaas, P.J., Haenschel, C., Nikolić, D., Singer, W., 2008. The role of oscillations and synchrony in cortical networks and their putative relevance for the pathophysiology of schizophrenia. *Schizophr. Bull.* 34:927–943. <https://doi.org/10.1093/schbul/sbn062>.
- van den Heuvel, M.P., Formito, A., 2014. Brain networks in schizophrenia. *Neurospychol. Rev.* 24:32–48. <https://doi.org/10.1007/s11065-014-9248-7>.
- Varela, F., Lachaux, J.P., Rodriguez, E., Martinerie, J., 2001. The brainweb: phase synchronization and large-scale integration. *Nat. Rev. Neurosci.* 2:229–239. <https://doi.org/10.1038/35067550>.
- Vöhringer, P.A., Barroilhet, S.A., Amerio, A., Reale, M.L., Alvear, K., Vergne, D., Ghaemi, S.N., 2013. Cognitive impairment in bipolar disorder and schizophrenia: a systematic review. *Front. Psychiatry* 4:1–11. <https://doi.org/10.3389/fpsy.2013.00087>.
- Whalley, H.C., 2005. Functional disconnection in subjects at high genetic risk of schizophrenia. *Brain* 128:2097–2108. <https://doi.org/10.1093/brain/awh556>.
- Xia, M., Wang, J., He, Y., 2013. BrainNet viewer: a network visualization tool for human brain connectomics. *PLoS One* 8, e68910. <https://doi.org/10.1371/journal.pone.0068910>.
- Yeo, R.A., Ryman, S.G., van den Heuvel, M.P., de Reus, M.A., Jung, R.E., Pommy, J., Mayer, A.R., Ehrlich, S., Schulz, S.C., Morrow, E.M., Manoach, D., Ho, B., Sponheim, S.R., Calhoun, V.D., 2016. Graph metrics of structural brain networks in individuals with schizophrenia and healthy controls: group differences, relationships with intelligence, and genetics. *J. Int. Neuropsychol. Soc.* 22:240–249. <https://doi.org/10.1017/S1355617715000867>.
- Zanelli, J., Reichenberg, A., Morgan, K., Fearon, P., Kravariti, E., Dazzan, P., Morgan, C., Zanelli, C., Demjaha, A., Jones, P.B., Doody, G.A., Kapur, S., Murray, R.M., 2010. Specific and generalized neuropsychological deficits: comparison of patients with various first-episode psychosis presentations. *Am. J. Psychiatry* 167:78–85. <https://doi.org/10.1176/appi.ajp.2009.09010118>.

Please cite this article as: Gomez-Pilar, J., et al., Altered predictive capability of the brain network EEG model in schizophrenia during cognition, *Schizophr. Res.* (2018), <https://doi.org/10.1016/j.schres.2018.04.043>

Supplementary material of the paper: “Altered predictive capability of the brain network EEG model in schizophrenia during cognition”

For the sake of replicability and completeness, additional methodological details and further analyses are included in this Supplementary material.

Inclusion/exclusion criteria

Among all the subject under study, exclusion criteria were: (i) any neurological illness; (ii) history of cranial trauma with loss of consciousness longer than one minute; (iii) past or present substance abuse, except nicotine or caffeine; (iv) total intelligence quotient (IQ) smaller than 70; and (v) for patients, any other psychiatric process, and (vi) for controls, any current psychiatric or neurological diagnosis or treatment.

Preprocessing

Signals were filtered between 1 and 70 Hz by means of a band-pass finite impulse response filter. A 50 Hz notch filter was also used to remove the power line artifact. Lastly, a three-steps artifact rejection algorithm was applied to minimize, mainly, electrooculographic and electromyographic contamination (1): (i) Independent Component Analysis (ICA) was carried out and, after visual inspection of a specialist, ICA components associated with artifacts were discarded (2); (ii) after ICA reconstruction, EEG data were divided into trials of 1 second length ranging from 300 ms before to 700 ms after stimulus onset, which ensures no overlapping with subsequent trials; and (iii) an automatic and adaptive trial rejection was performed by applying a statistical-based thresholding method.

Continuous wavelet transform and edge effects

EEG recordings are non-stationary signals with changing properties over time. Wavelet transform takes into account these changes, providing an appropriate alternative to Fourier transform.

In this study, complex Morlet was used as mother wavelet. It provides a biologically plausible fit to EEG data (3). Complex Morlet wavelet is characterized by its localization in time (Δt) and frequency (Δf). In this study, Δt and Δf were set to 1 to obtain a balanced relationship at low frequencies (1).

The coefficients of the continuous wavelet transform (CWT) are computed as the convolution between the EEG signal in each artifact-free trial, $x(t)$, and scaled and translated versions of the mother wavelet, $\phi(t)$:

$$CWT(k, s) = \frac{1}{\sqrt{s}} \int_{-\infty}^{\infty} x(t) \cdot \phi^* \left(\frac{t-k}{s} \right) dt, \quad (\text{A.5})$$

where s represents the dilation factor ($s = \{s_i, i = 1, \dots, M\}$), k is the translation factor and the asterisk denotes the complex conjugation. The dilation factor was set to include frequencies from 1 Hz (s_1) to 70 Hz (s_M) in equally-spaced intervals of 0.5 Hz (1). Nevertheless, as we explained in the main text, only theta frequency band (4-8 Hz) was considered for the analyses.

EEG trials are finite and short-time recordings. Therefore, edge effects are not negligible (4). In this study, a cone of influence was defined in order to delimitate the time-frequency regions that included the biased wavelet coefficients (4).

Brain network estimation

Connectivity matrices were obtained by means of phase-locking value (PLV). The PLV has become a useful tool to quantify the phase steadiness between pairs of electrodes (5), given its sensitivity to measure the neural synchronization, even between EEG oscillations with relatively small amplitude (6). As previously mentioned, this study was aimed at analyzing cognitive network dynamics. Thereby, the PLV was calculated in the theta frequency band (4-8 Hz).

Being able to use different approaches for computing the PLV, the CWT was used to extract the phase information from each trial (7). First, to calculate PLV between two signals, it is necessary to extract the instantaneous phase of each signal in a narrow bandwidth (8). CWT can be used to perform filtering and phase extraction in a single step (7). Thus, the instantaneous phases $\phi_x(k, s, \tau)$ and $\phi_y(k, s, \tau)$ of two EEG signals, $x(t)$ and $y(t)$, can be used to define the phase differences as follows:

$$\phi_{xy}(k, s, \tau) = \phi_x(k, s, \tau) - \phi_y(k, s, \tau), \quad (\text{A.6})$$

where τ represents each artifact-free trial.

Detailed procedures about the wavelet parameters and the minimization of the edge effects were reported in our previous studies (1, 9, 10).

PLV estimates the variability of the phase differences across successive trials, as follows:

$$PLV_{xy}(k, s) = w_{ij}(k, s) = \frac{1}{N_t} \left| \sum_{\tau=1}^{N_t} e^{\Delta\Phi_{xy}(k, s, \tau)} \right|, \quad (\text{A.7})$$

where N_t is the total number of artifact-free trials.

Functional connectivity matrices based on PLV were obtained by comparing the synchronization between all EEG channels. The values of the connectivity matrix (w_{ij}) ranged between 0 and 1 (weighted network). A value of 1 was obtained with completely synchronized signals and a value of 0 implied an absence of synchronization. It means that no threshold was applied. This has the advantage that all the connections are considered (even the lower ones), but the computational cost increases comparing to a semi-weighted network.

Network parameters

Networks can be described by several parameters. The present study was focused on five complementary features of the brain network: integration, segregation, connectivity strength, complexity and irregularity. The parameters that were used to quantify the previous network features are the following:

- The integration of the network was characterized by means of the characteristic path length. It is defined as the average shortest path length between all pairs of nodes in the network (11):

$$PL = \frac{1}{N} \sum_{i \in n} \frac{\sum_{j \in n, j \neq i} d_{ij}}{n-1}, \quad (\text{A.8})$$

where d_{ij} indicates the minimum distance (i.e. the inverse of PLV) between electrodes i and j . Of note, N represents the number of nodes in the network ($N = 29$).

- The segregation of the network was quantified by the averaged clustering coefficient (11). In the case of weighted networks, the averaged clustering coefficient can be generalized as follows to avoid the influence of the main connection weights:

$$CLC = \binom{n}{3} \sum_{i \in n} \sum_{j, k \in n} (w_{ij} w_{ih} w_{jh})^{\frac{1}{3}}, \quad (\text{A.9})$$

where w_{ij} denotes the connection weight between electrodes i and j .

- The connectivity strength was computed using the network density as follows (10):

$$GD = \frac{\sum_{i=1}^N \sum_{j>i} w_{ij}}{T}, \quad (\text{A.10})$$

where w_{ij} represents the connection weight between nodes i and j , and $T = \frac{N(N-1)}{2}$ is the total number of connections in an undirected graph.

- The irregularity of the brain network was characterized by the Shannon Graph Entropy, defined in our previous work as follows (10):

$$H = \frac{-1}{\log_2 T} \sum_{i=1}^N \sum_{j>i} \frac{w_{ij}}{W} \log_2 \frac{w_{ij}}{W}, \quad (\text{A.11})$$

where W is the sum of all weights of the graph and is a normalization factor introduced to ensure that $0 \leq H \leq 1$.

- The complexity of the brain network was estimated using the Shannon Graph Complexity, defined in our previous work as follows (10):

$$SGC = H \cdot \sqrt{\frac{1}{T-1} \cdot \frac{\sigma}{\bar{w}}}, \quad (\text{A.12})$$

where \bar{w} is the average of all edge values of the graph and σ is the standard deviation of those values.

Importantly, Shannon Graph Entropy and Shannon Graph Complexity do not depend on the connectivity strength. Therefore, changes in these measures ensure that the network changes in the other parameters are not only due to changes in the connectivity strength.

Dynamical network modeling

The steps of the proposed algorithm, individually adjusted for each subject, can be summarized as follows:

1. A specific connection (usually named as w_{ij} in graph theory context) of the pre-stimulus connectivity matrix is randomly selected.
2. The value of the connection, w_{ij} , is eventually modified with a probability P . Both the value of P and how it is modified depend on the specific model being considered, as we explain below.

3. The network features are computed for the modified connectivity matrix.
4. The MSE between the network parameters of the connectivity matrix in 3) and those of the connectivity matrix associated to the cognitive response is computed.
5. The steps 1), 2) 3) and 4) are repeated 5000 times and the MSE is stored for each iteration.
6. The connectivity matrix that minimizes the MSE is selected. The simulations showed that the MSE is a concave function with a minimum that varies for each subject. We checked that the minimum was always achieved before 5000 repetitions. Of note, the number of iterations required for reaching the minimum MSE is different for each subject.

The previous procedure was repeated six times (one for each model). The value of P and how it was modified depend on the model being considered as follows:

1. Reinforcement of primary connections: The value of the connection randomly selected is increased a 1% with probability $P = w_{ij}$ (w_{ij} ranges from 0 to 1).
2. Reinforcement of secondary connections: The value of the connection randomly selected is increased a 1% with probability $P = 1 - w_{ij}$.
3. Reinforcement of a connection at random. The value of the connection randomly selected is increased a 1% with probability $P = 1$.
4. Weakening of primary connections: The value of the connection randomly selected is decreased a 1% with probability $P = w_{ij}$.
5. Weakening of secondary connections: The value of the connection randomly selected is decreased a 1% with probability $P = 1 - w_{ij}$.
6. Weakening of a connection at random. The value of the connection randomly selected is decreased a 1% with probability $P = 1$.

The percentage of change (1%) was heuristically determined as a compromise between goodness of fit and computational cost.

As previously mentioned, the dynamical cognitive network model randomly selected a node in each iteration. In order to minimize the possible bias due to the intrinsic stochastic behavior of the algorithm, all the experiment was repeated 100 times and MSE results were averaged across repetitions in each subject. Nevertheless, we observed that the variability among experiments for each subject was negligible.

Discarding confounding factors

Studies of mental disorders through the EEG are prone to obtain inaccurate results due to the number of confounding factors. In order to avoid misinterpretation and prevent inappropriate conclusions, the influence of potential confounding factors on the clinical and network features was assessed. Thus, we found that the age and gender distributions, as well as the doses of the prescribed medication, did not produce a significant effect on PLV values, network measures or cognitive data ($p > 0.05$; Spearman's bivariate correlation test).

It must be noticed that all EEG measures are influenced by volume conduction. In order to minimize this effect, a well-known strategy is based on the assumption that volume conduction affects the connectivity estimates in a similar way in two different experimental contrasts (12). Spurious estimates can then effectively get rid by comparing both conditions (12). This is the approach followed in our study: comparing pre-stimulus and response during the cognitive task, both acquired during the performance of the oddball task, but in two different moments. In addition, short-scale synchronization is more influenced by volume conduction (5). However, we focused on theta band, which is associated with long-range interactions (13).

In order to discard possible influence of abnormal shape of the event-related potentials (ERPs), they are represented in the Figure A3. In addition, P3b peak and latency for both groups are shown in the Table 1 of the main text. Finally, connectivity matrices are shown in the Figure A4.

Weakening network models

Most of the subjects fitted a reinforcement model; however, in the case of 15% of the subjects (seven controls and six schizophrenia patients), a model based on weakening the connections was selected. For these thirteen subjects, Figure A5 shows the distribution of the selected model for each group. Due to the low number of subjects, statistical analyses were not performed in this case.

The relationship between cognition and network parameters

Relationship between cognition and brain functioning was assessed by means of the correlations between results of the cognitive tests (z -scores corrected) and values of network measures (measured as the percent of change from pre-stimulus to cognitive response). For that purpose, Spearman's bivariate correlation test was

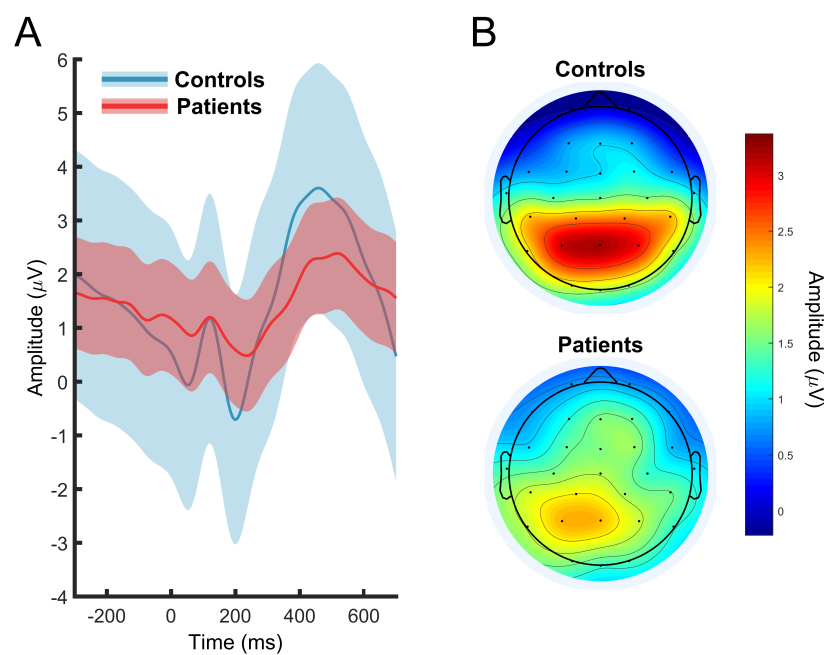


Figure A.3: (A) **P300 waveforms** at Pz electrode for controls (blue) and patients (red). (B) **Scalp maps** depicting the **P3b peak amplitude** (from 300 ms to 550 ms) for controls and patients.

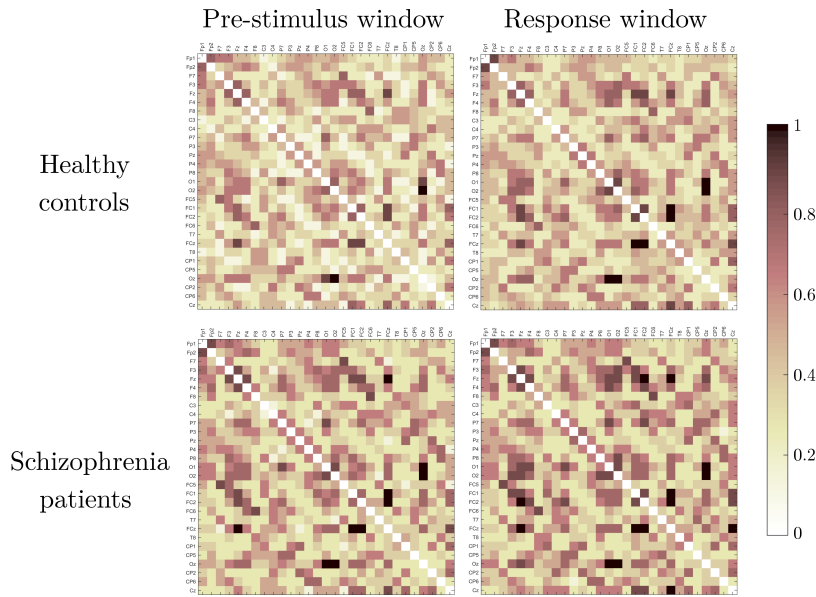


Figure A.4: **Averaged connectivity matrices.** The connectivity matrices are shown for controls and schizophrenia patients before (from -300 to 0 ms) and after (from 150 to 450 ms) stimulus onset.

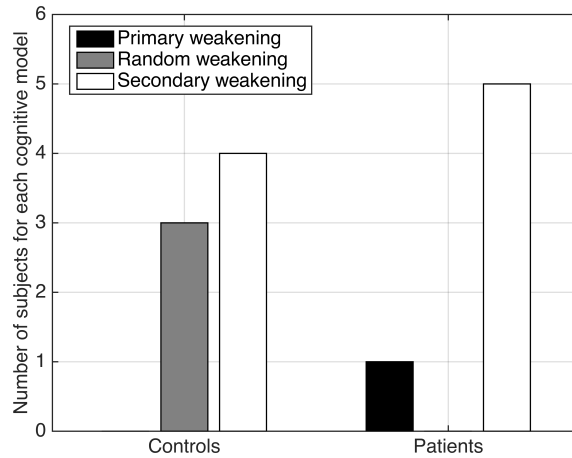


Figure A.5: **Histogram of the selected models and mean square error (MSE) distribution for each model.** Only the subjects that follow a model based on weakening the network connections were depicted in this histogram.

		Integration	Segregation	Connectivity strength	Complexity	Irregularity
Verbal memory	<i>r</i>	-0.196	0.218	0.423	-0.190	0.169
	<i>p</i> -value	0.042	0.027	< 0.001	0.048	0.070
Working memory	<i>r</i>	0.005	0.023	0.199	0.042	-0.034
	<i>p</i> -value	0.484	0.422	0.040	0.357	0.383
Motor speed	<i>r</i>	0.044	-0.017	0.153	0.073	-0.062
	<i>p</i> -value	0.352	0.442	0.090	0.264	0.296
Verbal fluently	<i>r</i>	-0.285	0.331	0.499	-0.160	0.159
	<i>p</i> -value	0.007	0.002	< 0.001	0.087	0.087
Processing speed	<i>r</i>	-0.244	0.261	0.472	-0.178	0.166
	<i>p</i> -value	0.016	0.010	< 0.001	0.060	0.073
Executive function	<i>r</i>	-0.029	-0.012	0.103	0.121	-0.137
	<i>p</i> -value	0.402	0.459	0.186	0.147	0.118

Table A.5: Correlation coefficient and *p*-values for all the possible comparisons between cognition and network parameters. Three correlations remain statistically significant after Bonferroni correction ($p < 0.001$, highlighted in bold).

used. Bonferroni correction was applied to correct for multiple testing (*p*-values were multiplied by 6 cognitive domains x 5 network parameters = 30). All the performed correlations are shown in Table A5. Statistically significant correlations after Bonferroni correction ($p < 0.05$) are highlighted in bold.

The relationship between cognition and symptoms

Symptoms were assessed by means of the PANSS (*z*-scores corrected). Correlation between cognition and symptoms was studied by Spearman's bivariate correlation test. The performed correlations are shown in Table A6. Statistically significant correlations ($p < 0.01$) are highlighted in bold. The symptoms, summarized as the PANSS-total, are negatively correlated to verbal memory and processing speed (i.e., more symptoms are related to poorer cognitive performance).

These findings agree with the intuitive notion that more pronounced symptoms are usually linked to poorer cognitive performance (14). It was suggested that the negative and disorganized symptom dimensions are the reason for the strong correlation between symptoms and cognitive dysfunction in schizophrenia (14).

The relationship between network parameters and symptoms

We also assessed the relationship between symptoms and network measures (as the percent of change from pre-stimulus to cognitive response) by Spearman's bivariate correlation test. The performed correlations are shown in Table A7. Significant

		Verbal memory	Working memory	Motor speed	Verbal fluently	Processing speed	Executive function
PANSS- positive	r	-0.177	-0.224	0.173	-0.106	-0.134	0.171
	p -value	0.193	0.136	0.199	0.319	0.257	0.207
PANSS- negative	r	-0.282	-0.150	-0.03	-0.283	-0.354	0.033
	p -value	0.081	0.233	0.433	0.101	0.038	0.439
PANSS- total	r	-0.459	-0.319	0.061	-0.281	-0.478	0.155
	p -value	< 0.01	0.056	0.384	0.103	< 0.01	0.230

Table A.6: Correlation coefficient and p -values for all the possible comparisons between cognition and symptoms. Two correlations are statistically significant ($p < 0.01$, highlighted in bold).

		Integration	Segregation	Connectivity strength	Complexity	Irregularity
PANSS- positive	r	0.153	-0.273	-0.314	0.413	-0.434
	p -value	0.206	0.068	0.043	0.011	< 0.01
PANSS- negative	r	0.254	-0.331	-0.290	0.215	-0.178
	p -value	0.084	0.035	0.057	0.123	0.170
PANSS- total	r	0.280	-0.4614	-0.413	0.465	-0.445
	p -value	0.064	< 0.01	0.010	< 0.01	< 0.01

Table A.7: Correlation coefficient and p -values for all the possible comparisons between symptoms and network parameters. Four correlations are statistically significant ($p < 0.01$, highlighted in bold).

correlations ($p < 0.01$) are highlighted in bold. The symptoms, summarized as the PANSS-total, are negatively correlated to segregation and irregularity, but positively correlated to complexity. On the other hand, positive symptoms, summarized as PANSS-positive, are negatively correlated to irregularity.

Topological network measures and cognitive variables: comparison with previous findings

Comparisons between network measures and cognitive variables are usually performed using a resting-state approach (15, 16) and sometimes during a cognitive task (17), but it is not usually assessed by analyzing the predisposition to change of the pre-stimulus activity. In our previous study (9), segregation was inversely associated with executive function and directly associated with working memory. Although, the same trend was found in this study, non-significant associations were found between such parameters after Bonferroni correction. This discrepancy can be easily explained due to the number of differences between both studies: (i) connectivity strength was not computed in the previous research; (ii) network parameters were computed using event-related coherence, which is not strictly

a synchronization measure; and (iii) low-density EEG recordings were used (17 channels).

Despite the difficulty to compare the correlations observed in this study with previous findings, it seems natural that a direct correlation between global brain synchronization and cognitive performance exists. In fact, although Pachou et al. (2008) did not evaluate the change from pre-stimulus to cognitive response, they found a correlation in patients between working memory load and global synchronization. This result could indicate that the cognitive effort required higher synchronization of the whole brain. The empirical evidence regarding the association between cognitive functions and network parameters was not so widespread some years ago (18). Nowadays, however, it is well-established that the architecture of functional brain networks is related to cognitive performance (19).

References

1. Bachiller A, Poza J, Gómez C, Molina V, Suazo V, Hornero R (2015): A comparative study of event-related coupling patterns during an auditory oddball task in schizophrenia. *J Neural Eng.* 12: 16007.
2. Flexer A, Bauer H, Pripfl J, Dorffner G (2005): Using ICA for removal of ocular artifacts in EEG recorded from blind subjects. *Neural Networks.* 18: 9981005.
3. Roach BJ, Mathalon DH (2008): Event-Related EEG Time-Frequency Analysis: An Overview of Measures and An Analysis of Early Gamma Band Phase Locking in Schizophrenia. *Schizophr Bull.* 34: 907926.
4. Torrence C, Compo G (1998): A practical guide to wavelet analysis. *Bull Am Meteorol Soc.* 79: 6178.
5. Lachaux JP, Rodriguez E, Martinerie J, Varela FJ (1999): Measuring phase synchrony in brain signals. *Hum Brain Mapp.* 8: 194208.
6. Spencer KM, Nestor PG, Niznikiewicz MA, Salisbury DF, Shenton ME, McCarley RW (2003): Abnormal neural synchrony in schizophrenia. *J Neurosci.* 23: 74077411.
7. Bob P, Palus M, Susta M, Glaslova K (2008): EEG phase synchronization in patients with paranoid schizophrenia. *Neurosci Lett.* 447: 7377.

8. Lachaux JP, Rodriguez E, Martinerie J, Varela FJ (1999): Measuring phase synchrony in brain signals. *Hum Brain Mapp.* 8: 194208.
9. Gomez-Pilar J, Lubeiro A, Poza J, Hornero R, Ayuso M, Valcárcel C, et al. (2017): Functional EEG network analysis in schizophrenia: Evidence of larger segregation and deficit of modulation. *Prog Neuro-Psychopharmacology Biol Psychiatry.* 76: 116123.
10. Gomez-Pilar J, Poza J, Bachiller A, Gómez C, Núñez P, Lubeiro A, et al. (2018): Quantification of graph complexity based on the edge weight distribution balance: Application to brain networks. *Int J Neural Syst.* S0129065717500320.
11. Rubinov M, Sporns O (2010): Complex network measures of brain connectivity: Uses and interpretations. *Neuroimage.* 52: 10591069.
12. Bastos AM, Schoffelen J-M (2015): A tutorial review of functional connectivity analysis methods and their interpretational pitfalls. *Front Syst Neurosci.* 9: 175.
13. Uhlhaas PJ, Roux F, Rodriguez E, Rotarska-Jagiela A, Singer W (2010): Neural synchrony and the development of cortical networks. *Trends Cogn Sci.* 14: 7280.
14. O'Leary DS, Flaum M, Kesler ML, Flashman LA, Arndt S, Andreasen NC (2000): Cognitive correlates of the negative, disorganized, and psychotic symptom dimensions of schizophrenia. *J Neuropsychiatry Clin Neurosci.* 12: 415.
15. Micheloyannis S, Pachou E, Stam CJ, Vourkas M, Erimaki S, Tsirka V (2006): Using graph theoretical analysis of multi channel EEG to evaluate the neural efficiency hypothesis. *Neurosci Lett.* 402: 273277.
16. Smit DJ, Stam CJ, Posthuma D, Boomsma DI, de Geus EJC (2008): Heritability of 'small-world' networks in the brain: A graph theoretical analysis of resting-state EEG functional connectivity. *Hum Brain Mapp.* 29: 13681378.
17. Pachou E, Vourkas M, Simos P, Smit D, Stam CJ, Tsirka V, Micheloyannis S (2008): Working memory in schizophrenia: An EEG study using power spectrum and coherence analysis to estimate cortical activation and network behavior. *Brain Topogr.* 21: 1137.

18. Bullmore E, Sporns O (2009): Complex brain networks: graph theoretical analysis of structural and functional systems. *Nat Rev Neurosci.* 10: 186198.
19. Shine JM, Bissett PG, Bell PT, Koyejo O, Balsters JH, Gorgolewski KJ, et al. (2016): The dynamics of functional brain networks: integrated network states during cognitive task performance. *Neuron.* 92: 544554.

Appendix B

Scientific achievements

B.1 Scientific production

B.1.1 Papers included in this Doctoral Thesis

1. **Javier Gomez-Pilar**, Jesús Poza, Alejandro Bachiller, Carlos Gómez, Vicente Molina, Roberto Hornero, “Neural Network Reorganization Analysis during an Auditory Oddball Task in Schizophrenia using Wavelet Entropy”, *Entropy*, vol. 17, pp. 5241-5256, July, 2015.
2. **Javier Gomez-Pilar**, Alba Lubeiro, Jesús Poza, Roberto Hornero, Marta Ayuso, Cesar Valcarcel, Mahmoud-Karim Haidar, José A. Blanco, Vicente Molina, “Functional EEG network analysis in schizophrenia: Evidence of larger segregation and deficit of modulation”, *Progress in Neuro-Psychopharmacology & Biological Psychiatry*, vol. 76, pp. 116-123, March, 2017.
3. **Javier Gomez-Pilar**, Rodrigo de Luis-García, Alba Lubeiro, Nieves de Uribe, Jesús Poza, Pablo Núñez, Marta Ayuso, Roberto Hornero, Vicente Molina, “Deficits of entropy modulation in schizophrenia are predicted by functional connectivity strength in the theta band and structural clustering”, *Neuroimage-Clinical*, vol. 18, pp. 382-389, February, 2018.
4. **Javier Gomez-Pilar**, Rodrigo de Luis-García, Alba Lubeiro, Henar de la Red, Jesús Poza, Pablo Núñez, Roberto Hornero, Vicente Molina, “Relations between structural and EEG-based graph metrics in healthy controls and schizophrenia patients”, *Human Brain Mapping*, April, 2018.

5. **Javier Gomez-Pilar**, Jesús Poza, Alejandro Bachiller, Carlos Gómez, Pablo Núñez, Alba Lubeiro, Vicente Molina, Roberto Hornero, “Quantification of graph complexity based on the edge weight distribution balance: Application to brain networks”, *International Journal of Neural Systems*, vol. 28 (1), pp. 1750032, February, 2018.
6. **Javier Gomez-Pilar**, Jesús Poza, Carlos Gómez, Georg Northoff, Alba Lubeiro, Benjamín Cea-Cañas, Vicente Molina, Roberto Hornero, Altered predictive capability of the brain network EEG model in schizophrenia during cognition”, *Schizophrenia Research*, April, 2018.

B.1.2 Papers indexed in the Journal Citation Reports

1. Vicente Molina, Alejandro Bachiller, **Javier Gomez-Pilar**, Alba Lubeiro, Roberto Hornero, Benjamín Cea-Cañas, Cesar Valcarcel, Mahmoun-Karim Haidar, Jesús Poza, “Deficit of entropy modulation of the EEG in schizophrenia associated to cognitive performance and symptoms. A replication study”, *Schizophrenia Research*, vol. 195, pp. 334-342, May, 2018.
2. **Javier Gomez-Pilar**, Rodrigo de Luis-García, Alba Lubeiro, Henar de la Red, Jesús Poza, Pablo Núñez, Roberto Hornero, Vicente Molina, “Relations between structural and EEG-based graph metrics in healthy controls and schizophrenia patients”, *Human Brain Mapping*, April, 2018.
3. **Javier Gomez-Pilar**, Jesús Poza, Carlos Gómez, Georg Northoff, Alba Lubeiro, Benjamín Cea-Cañas, Vicente Molina, Roberto Hornero, Altered predictive capability of the brain network EEG model in schizophrenia during cognition”, *Schizophrenia Research*, April, 2018.
4. Nuria Mendoza, Sagrario del Valle Díaz, Natalia Rioja Collado, **Javier Gomez-Pilar**, Roberto Hornero, “Potential benefits of a cognitive training program in MCT”, *Restorative Neurology and Neuroscience*, vol. 36 (2), pp. 207-213, March, 2018.
5. **Javier Gomez-Pilar**, Jesús Poza, Alejandro Bachiller, Carlos Gómez, Pablo Núñez, Alba Lubeiro, Vicente Molina, Roberto Hornero, “Quantification of graph complexity based on the edge weight distribution balance: Application to brain networks”, *International Journal of Neural Systems*, vol. 28 (1), pp. 1750032, February, 2018.

6. **Javier Gomez-Pilar**, Rodrigo de Luis-García, Alba Lubeiro, Nieves de Uribe, Jesús Poza, Pablo Núñez, Marta Ayuso, Roberto Hornero, Vicente Molina, “Deficits of entropy modulation in schizophrenia are predicted by functional connectivity strength in the theta band and structural clustering”, *Neuroimage-Clinical*, vol. 18, pp. 382-389, February, 2018.
7. Víctor Martínez-Cagigal, **Javier Gomez-Pilar**, Daniel Álvarez, Roberto Hornero, “An Asynchronous P300-Based Brain-Computer Interface Web Browser for Severely Disabled People”, *IEEE Transactions on Neural Systems and Rehabilitation Engineering*, vol. 25 (8), pp. 1332-1342, September, 2017.
8. Carlos Gómez, Celia Juan-Cruz, Jesús Poza, Saúl J. Ruiz-Gómez, **Javier Gomez-Pilar**, Pablo Núñez, María García, Alberto Fernández, Roberto Hornero, “Alterations of Effective Connectivity Patterns in Mild Cognitive Impairment: An MEG Study”, *Journal of Alzheimers Disease*, September, 2017.
9. Pablo Núñez, Jesús Poza, Alejandro Bachiller, **Javier Gomez-Pilar**, Alba Lubeiro, Vicente Molina, Roberto Hornero, “Exploring non-stationarity patterns in schizophrenia: neural reorganization abnormalities in the alpha band”, *Journal of Neural Engineering*, vol. 14 (4), pp. 046001, August, 2017.
10. **Javier Gomez-Pilar**, Alba Lubeiro, Jesús Poza, Roberto Hornero, Marta Ayuso, Cesar Valcarcel, Mahmoud-Karim Haidar, José A. Blanco, Vicente Molina, “Functional EEG network analysis in schizophrenia: Evidence of larger segregation and deficit of modulation”, *Progress in Neuro-Psychopharmacology & Biological Psychiatry*, vol. 76, pp. 116-123, March, 2017.
11. Alba Lubeiro, **Javier Gomez-Pilar**, Oscar Martin-Santiago, Aitor Palomino, Myriam Fernandez, Ana González Pinto, Jesús Poza, Roberto Hornero, Vicente Molina, Variation at NRG1 genotype related to modulation of small-world properties of the functional cortical network”, *European Archives of Psychiatry and Clinical Neuroscience*, vol. 267 (1), pp. 25-32, February, 2017.
12. **Javier Gomez-Pilar**, Rebeca Corralejo, Luis F. Nicolás-Alonso, Daniel Álvarez, Roberto Hornero, “Neurofeedback training with a motor imagery-based BCI: neurocognitive improvements and EEG changes in the elderly”,

- Medical & Biological Engineering & Computing*, vol. 54 (11), pp. 1655-1666, October, 2016.
13. **Javier Gomez-Pilar**, Oscar Martin-Santiago, Vanessa Suazo, Sonia Ruiz de Azua, Ricardo Gallardo, Jesús Poza, Roberto Hornero, Vicente Molina, “Association between EEG modulation, psychotic-like experiences and cognitive performance in the general population”, *Psychiatry and Clinical Neurosciences*, vol. 70 (7), pp. 286-294, July, 2016.
 14. Oscar Martin-Santiago, **Javier Gomez-Pilar**, Alba Lubeiro, Marta Ayuso, Jesús Poza, Roberto Hornero, Myriam Fernandez, Sonia Ruiz de Azua, Cesar Valcarcel, Vicente Molina, “Modulation of brain network parameters associated with subclinical psychotic symptoms”, *Progress in Neuro-Psychopharmacology & Biological Psychiatry*, vol. 3 (66), pp. 54-62, April, 2016.
 15. **Javier Gomez-Pilar**, Jesús Poza, Alejandro Bachiller, Carlos Gómez, Vicente Molina, Roberto Hornero, “Neural Network Reorganization Analysis during an Auditory Oddball Task in Schizophrenia using Wavelet Entropy”, *Entropy*, vol. 17, pp. 5241-5256, July, 2015.
 16. Luis F. Nicolás-Alonso, Rebeca Corralejo, **Javier Gomez-Pilar**, Daniel Álvarez, Roberto Hornero, “Adaptive Stacked Generalization for Multiclass Motor Imagery-based Brain Computer Interfaces”, *IEEE Transactions on Neural Systems and Rehabilitation Engineering*, vol. 23 (4), pp. 702-712, July, 2015.
 17. Luis F. Nicolás-Alonso, Rebeca Corralejo, **Javier Gomez-Pilar**, Daniel Álvarez, Roberto Hornero, “Adaptive semi-supervised classification to reduce intersession non-stationarity in multiclass motor imagery-based brain computer interfaces”, *Neurocomputing*, vol. 159 (2), pp. 186-196, July, 2015.
 18. Gonzalo C. Gutiérrez-Tobal, Daniel Álvarez, **Javier Gomez-Pilar**, Félix del Campo, Roberto Hornero, “Assessment of Time and Frequency Domain Entropies to Detect Sleep Apnoea in Heart Rate Variability Recordings from Men and Women”, *Entropy*, vol. 17 (1), pp. 123-141, January, 2015.

B.1.3 Book Chapters

1. **Javier Gomez-Pilar**, Rebeca Corralejo, Daniel Álvarez, Roberto Hornero, *Neurofeedback training with a motor imagery-based BCI improves neurocog-*

nitive functions in elderly people, Brain-Computer Interface Research: A State-of-the-Art Summary 4, pp. 43-55, New York, Springer, Editors: Guger, Christoph, MÄijller-Putz, Gernot, Allison, Brendan. ISBN: 978-3-319-25190-5, 2015.

B.1.4 International Conferences

1. Alba Lubeiro, Vicente Molina, María Guardiola, **Javier Gomez-Pilar**, Mar Fatjó-Vilas, KCNH2 Polymorphism associated to altered EEG functional network modulation in schizophrenia, *6th Biennial Schizophrenia International Research Society Conference*, ISBN: 0586-7614, pp. 397-398, Florencia (Italy), April 4 - April 8, 2018.
2. **Javier Gomez-Pilar**, Víctor Martínez-Cagigal, Roberto Hornero, Neurocognitive Training by means of a Motor Imagery-Based Brain Computer Interface in the Elderly, *6th International Conference on Cognitive Neurodynamics*, pp. 46, Carmona (Spain), August 1 - August 5, 2017.
3. Jesús Poza, Alejandro Bachiller, Carlos Gómez, María García, Pablo Núñez, **Javier Gomez-Pilar**, Miguel A. Tola-Arribas, Mónica Cano, Roberto Hornero, Phase-Amplitude Coupling Analysis of Spontaneous EEG Activity in Alzheimer's Disease, *39th Annual International Conference of the IEEE Engineering in Medicine and Biology Society*, ISBN: 978-1-5090-2809-2, pp. 2259-2262, Jeju (South Korea), July 11 - July 15, 2017.
4. **Javier Gomez-Pilar**, Juan José Navarrete, Claudia Gómez, María Isabel Pedraza, Marina Ruiz, Roberto Hornero, Ángel Luis Guerrero, Spectral analyses of spontaneous electroencephalographic activity in migraine: Preliminary results in a series of 29 patients, *3rd Congress of the European Academy of Neurology*, pp. 23-27, Amsterdam (Netherlands), June 24 - June 27, 2017.
5. Alejandro Bachiller, **Javier Gomez-Pilar**, Jesús Poza, Pablo Núñez, Carlos Gómez, Alba Lubeiro, Vicente Molina, Roberto Hornero, Event-related phase-amplitude coupling: A comparative study, *International Conference on NeuroRehabilitation (ICNR 2016)*, ISBN: 978-3-319-46668-2, pp. 757-761, La Granja (Segovia) (Spain), October 18 - October 21, 2016.
6. Pablo Núñez, Jesús Poza, Alejandro Bachiller, **Javier Gomez-Pilar**, Carlos Gómez, Alba Lubeiro, Vicente Molina, Roberto Hornero, Analysis of functional connectivity during an auditory oddball task in schizophrenia, *Inter-*

- national Conference on NeuroRehabilitation* (ICNR 2016), ISBN: 978-3-319-46668-2, pp. 751-755, La Granja (Segovia) (Spain), October 18 - October 21, 2016.
7. Pablo Núñez, Jesús Poza, **Javier Gomez-Pilar**, Alejandro Bachiller, Carlos Gómez, Alba Lubeiro, Vicente Molina, Roberto Hornero, Analysis of the Non-stationarity of Neural Activity during an Auditory Oddball Task in Schizophrenia, *38th Annual International Conference of the IEEE Engineering in Medicine and Biology Society*, ISBN: 978-1-4577-0220-4, pp. 3724-3727, Orlando (United States), October 16 - October 20, 2016.
 8. Carlos Gómez, Jesús Poza, **Javier Gomez-Pilar**, Alejandro Bachiller, Celia Juan-Cruz, Miguel A. Tola-Arribas, Alicia Carreres, Mónica Cano, Roberto Hornero, Analysis of Spontaneous EEG Activity in Alzheimer's Disease Using Cross-Sample Entropy and Graph Theory, *38th Annual International Conference of the IEEE Engineering in Medicine and Biology Society*, ISBN: 978-1-4577-0220-4, pp. 2830-2833, Orlando (United States), October 16 - October 20, 2016.
 9. **Javier Gomez-Pilar**, Jesús Poza, Alejandro Bachiller, Pablo Núñez, Carlos Gómez, Alba Lubeiro, Vicente Molina, Roberto Hornero, Novel Measure of the Weigh Distribution Balance on the Brain Network: Graph Complexity Applied to Schizophrenia, *38th Annual International Conference of the IEEE Engineering in Medicine and Biology Society*, ISBN: 978-1-4577-0220-4, pp. 700-703, Orlando (United States), October 16 - October 20, 2016.
 10. Víctor Martínez-Cagigal, Rebeca Corralejo, **Javier Gomez-Pilar**, Daniel Álvarez, Roberto Hornero, Diseño, Desarrollo y Evaluación de un Navegador Web basado en Potenciales P300 mediante Brain-Computer Interface Orientado a Personas con Grave Discapacidad, *VI Congreso Internacional de Diseño, Redes de Investigación y Tecnología para todos* (DRT4ALL 2015), ISBN: 978-84-7993-277-0, pp. 343-368, Madrid (Spain), September 23 - September 25, 2015.
 11. Alba Lubeiro, **Javier Gomez-Pilar**, Roberto Hornero, Vicente Molina, Neural dynamic characterization using Small-World measurements in schizophrenia, *Scientific Congress of FEBiotec* (SCIBAC), pp. 1, Salamanca (Spain), July 8 - July 10, 2015.

12. **Javier Gomez-Pilar**, Rebeca Corralejo, Daniel Álvarez, Roberto Hornero, Evaluación del Entrenamiento Neurocognitivo Mediante una Interfaz Cerebro-Ordenador Basada en Ritmos Sensoriomotores: Mejoras en Funciones Cognitivas Relacionadas con el Envejecimiento, *II Encuentro de investigadores. Investigación y envejecimiento: respuestas para dar calidad de vida*, pp. 1, Salamanca (Spain), March 10 - March 10, 2015.
13. **Javier Gomez-Pilar**, Rebeca Corralejo, Luis F. Nicolás-Alonso, Daniel Álvarez, Roberto Hornero, Assessment of Neurofeedback Training by Means of Motor Imagery Based-BCI for Cognitive Rehabilitation, *36th Annual International Conference of the IEEE Engineering in Medicine and Biology Society Conference*, ISBN: 978-1-4244-7928-3, pp. 3630-3633, Chicago (United States), August 27 - August 31, 2014.
14. Andrea Crespo, Félix del Campo, **Javier Gomez-Pilar**, Daniel Álvarez, J. Víctor Marcos, Roberto Hornero, Nonlinear analysis of heart rate variability in patients with sleep apnea hypopnea syndrome (SAHS). A severity study, *5th World Congress on Sleep Medicine*, ISBN: 1389-9457, Valencia (Spain), September 28 - October 2, 2013.
15. Daniel Álvarez, Gonzalo C. Gutiérrez-Tobal, **Javier Gomez-Pilar**, Félix del Campo, Miguel López-Coronado, Roberto Hornero, Applying variable ranking to oximetric recordings in sleep apnea diagnosis, *XIII Mediterranean Conference on Medical and Biological Engineering and Computing*, ISBN: 978-3-319-00845-5, pp. 969-972, Sevilla (Spain), September 25 - September 28, 2013.
16. **Javier Gomez-Pilar**, Gonzalo C. Gutiérrez-Tobal, Daniel Álvarez, Félix del Campo, Roberto Hornero, Classification Methods from Heart Rate Variability to Assist in SAHS Diagnosis, *XIII Mediterranean Conference on Medical and Biological Engineering and Computing*, ISBN: 978-3-319-00845-5, pp. 1825-1828, Sevilla (Spain), September 25 - September 28, 2013.
17. Gonzalo C. Gutiérrez-Tobal, Daniel Álvarez, **Javier Gomez-Pilar**, Félix del Campo, Roberto Hornero, AdaBoost Classification to Detect Sleep Apnea from Airflow Recordings, *XIII Mediterranean Conference on Medical and Biological Engineering and Computing*, ISBN: 978-3-319-00845-5, pp. 1829-1832, Sevilla (Spain), September 25 - September 28, 2013.

18. Gonzalo C. Gutiérrez-Tobal, Daniel Álvarez, **Javier Gomez-Pilar**, Félix del Campo, Roberto Hornero, Assessment of Spectral Bands of Interest in Airflow Signal to Assist in Sleep Apnea-Hypopnea Syndrome Diagnosis, *35th Annual International Conference of the IEEE Engineering in Medicine and Biology Society Conference*, ISBN: 978-1-4577-0214-3, pp. 5021-5024, Osaka (Japan), July 3 - July 7, 2013.
19. Carlos Gómez, Jesús Poza, Alberto Fernández, Alejandro Bachiller, **Javier Gomez-Pilar**, Roberto Hornero, Entropy Analysis of MEG Background Activity in Attention-Deficit/Hyperactivity Disorder, *35th Annual International Conference of the IEEE Engineering in Medicine and Biology Society Conference*, ISBN: 978-1-4577-0214-3, pp. 5057-5060, Osaka (Japan), July 3 - July 7, 2013.

B.1.5 National Conferences

1. Claudia Gómez, **Javier Gomez-Pilar**, Juan José Navarrete, Marina Ruiz, David García Azorín, María Isabel Pedraza, Ángel Luis Guerrero, Roberto Hornero, Análisis espectral de actividad electroencefalográfica basal en pacientes, *LXIX Reunión Anual de la Sociedad Española de Neurología*, pp. 20, Valencia (Spain), November 21 - November 25, 2017.
2. Carlos Gómez, Jesús Poza, **Javier Gomez-Pilar**, Lucía Martín, Pablo Núñez, María Rodríguez, Manuel Figueruelo, Saúl J. Ruiz-Gómez, Roberto Hornero, Caracterización de la actividad neuronal en pacientes con enfermedad de Alzheimer tras una sesión de estimulación multisensorial, *VII Congreso Nacional de Alzheimer 2017*, pp. 1, Málaga (Spain), November 9 - November 11, 2017.
3. Víctor Martínez-Cagigal, **Javier Gomez-Pilar**, Daniel Álvarez, Eduardo Santamaría-Vázquez, Roberto Hornero, Sistema Brain-Computer Interface de Navegación Web Orientado a Personas con Grave Discapacidad, *XXXVIII Jornadas de Automática*, ISBN: 978-84-16664-74-0, pp. 313-319, Gijón (Spain), September 6 - September 8, 2017.
4. Jesús Poza, Carlos Gómez, Alejandro Bachiller, Pablo Núñez, **Javier Gomez-Pilar**, María García, Miguel A. Tola-Arribas, Mónica Cano, Roberto Hornero, Direccionalidad del flujo de información de la actividad electroencefalográfica en la Enfermedad de Alzheimer, *XXXIV Congreso Anual de la Sociedad Es-*

- pañola de Ingeniería Biomédica* (CASEIB 2016), ISBN: 978-84-9048-531-6, pp. 198-201, Valencia (Spain), October 23 - October 25, 2016.
5. Carlos Gómez, Jesús Poza, **Javier Gomez-Pilar**, Lucía Martín, Pablo Núñez, María Rodríguez, Manuel Figueruelo, Saúl J. Ruiz-Gómez, Roberto Hornero, Caracterización de la actividad neuronal en pacientes con la enfermedad de Alzheimer tras una sesión de estimulación multisensorial, *XXXIV Congreso Anual de la Sociedad Española de Ingeniería Biomédica* (CASEIB 2016), ISBN: 978-84-9048-531-6, pp. 400-403, Valencia (Spain), October 23 - October 25, 2016.
 6. Víctor Martínez-Cagigal, **Javier Gomez-Pilar**, Daniel Álvarez, Roberto Hornero, Navegador Web BCI asíncrono controlado mediante potenciales P300, *8 Simposio CEA de Bioingeniería, Interfaces Hombre-Máquina, Cerebro y Periferia, Un camino de ida y vuelta*, ISBN: 2341-4243, pp. 1-8, Madrid (Spain), June 23 - June 24, 2016.
 7. **Javier Gomez-Pilar**, Jesús Poza, Alejandro Bachiller, Carlos Gómez, Vicente Molina, Roberto Hornero, Caracterización de la Dinámica en la Eficiencia de la Red Neuronal en Esquizofrenia en Tarea Cognitiva Auditiva, *XXXIII Congreso Anual de la Sociedad Española de Ingeniería Biomédica* (CASEIB 2015), ISBN: 978-84-608-3354-3, pp. 167-170, Madrid (Spain), November 4 - November 6, 2015.
 8. Carlos Gómez, Jesús Poza, María Rodríguez, Manuel Figueruelo, **Javier Gomez-Pilar**, Roberto Hornero, Caracterización de la actividad neuronal en enfermos de Alzheimer tras su participación en el programa de estimulación Un, Dos, Tres... A recordar esta vez, *XXXIII Congreso Anual de la Sociedad Española de Ingeniería Biomédica* (CASEIB 2015), ISBN: 978-84-608-3354-3, pp. 27-30, Madrid (Spain), November 4 - November 6, 2015.
 9. **Javier Gomez-Pilar**, Rebeca Corralejo, Víctor Martínez-Cagigal, Daniel Álvarez, Roberto Hornero, Análisis de los cambios espectrales del EEG producidos por el entrenamiento neurocognitivo mediante una interfaz cerebroordenador, *7.º Simposio CEA de Bioingeniería 2015, Interfaces Cerebro-Computadora (BCI) y Tecnologías Asistenciales*, ISBN: 2341-4243, pp. 15-21, Málaga (Spain), June 25 - June 26, 2015.
 10. Alejandro Bachiller, Jesús Poza, **Javier Gomez-Pilar**, Carlos Gómez, Vicente Molina, Roberto Hornero, Análisis del acoplamiento cruzado entre

- frecuencias en la esquizofrenia durante la realización de una tarea cognitiva auditiva, *XXXII Congreso Anual de la Sociedad Española de Ingeniería Biomédica* (CASEIB 2014), ISBN: 978-84-617-2446-8, pp. 1-4, Barcelona (Spain), November 26 - November 28, 2014.
11. **Javier Gomez-Pilar**, Alejandro Bachiller, Jesús Poza, Carlos Gómez, Vicente Molina, Roberto Hornero, Caracterización de Potenciales Evocados del EEG en Esquizofrenia mediante Teoría de Redes Complejas, *XXXII Congreso Anual de la Sociedad Española de Ingeniería Biomédica* (CASEIB 2014), ISBN: 978-84-617-2446-8, pp. 1-4, Barcelona (Spain), November 26 - November 28, 2014.
 12. Luis F. Nicolás-Alonso, Rebeca Corralejo, **Javier Gomez-Pilar**, Daniel Álvarez, Roberto Hornero, Ensemble learning for classification of motor imagery tasks in multiclass brain computer interfaces, *6th Computer Science and Electronic Engineering Conference* (CEEC), ISBN: 978-1-4799-6691-2, pp. 79, Colchester (United Kingdom), September 25 - September 26, 2014.
 13. **Javier Gomez-Pilar**, Rebeca Corralejo, Luis F. Nicolás-Alonso, Daniel Álvarez, Roberto Hornero, Diseño y desarrollo de una plataforma de entrenamiento cognitivo basada en BCI para prevenir los efectos del envejecimiento, *6th Simposio CEA de Bioingeniería 2014, Interfaces Mente Computador y Neurotecnologías*, ISBN: 2341-4243, pp. 25-31, Granada (Spain), June 12 - June 12, 2014.
 14. Félix del Campo, Roberto Hornero, **Javier Gomez-Pilar**, Daniel Álvarez, Gonzalo C. Gutiérrez-Tobal, Utilidad diagnóstica de la variabilidad de la frecuencia cardiaca en pacientes con sospecha de SAHS, *46 Congreso Nacional de la Sociedad Española de Neumología y Cirugía Torácica* (SEPAR), Barcelona (Spain), June 14 - June 17, 2013.
 15. **Javier Gomez-Pilar**, Gonzalo C. Gutiérrez-Tobal, Daniel Álvarez, Félix del Campo, Roberto Hornero, Extracción y selección de características de la señal de variabilidad del ritmo cardiaco para la ayuda al diagnóstico del síndrome de la apnea hipopnea del sueño, *XXX Congreso Anual de la Sociedad Española de Ingeniería Biomédica* (CASEIB 2012), ISBN: 978-84-616-2147-7, San Sebastián (Spain), November 19 - November 21, 2012.

16. Gonzalo C. Gutiérrez-Tobal, **Javier Gomez-Pilar**, Daniel Álvarez, Félix del Campo, Roberto Hornero, Evaluación de bandas espectrales de interés en la señal de flujo aéreo para ayudar en el diagnóstico del síndrome de la apnea hipopnea del sueño, *XXX Congreso Anual de la Sociedad Española de Ingeniería Biomédica* (CASEIB 2012), ISBN: 978-84-616-2147-7, San Sebastián (Spain), November 19 - November 21, 2012.

B.2 International research stay during the Doctoral Thesis

- Four-month research stay at the Institute of Mental Health Research, University of Ottawa, Ottawa, Canada

i Purpose of the stay

The main purpose of the stay at the Institute of Mental Health Research was to deepen into advanced methods of processing neuronal activity from the electroencephalogram (EEG) and functional magnetic resonance imaging (fMRI), in order to characterize schizophrenia disorder. To carry out this general objective, the following specific objectives were proposed: i) Multimodal analysis of new biomedical recordings from different signals related to neuroimaging, such as EEG and fMRI; ii) Deepening the automatic characterization of schizophrenia through new methods and techniques of processing; iii) Validation of the methods developed by our research group in new databases; and iv) Application of the knowledge acquired to the study of other schizoaffective pathologies, such as depression and bipolar disorder. Another important purpose of the stay was to promote the collaboration of the University of Valladolid with prestigious Canadian institutions, such as the University of Ottawa. This would not only improve the quality of the research, but also favor future collaborations on international research projects. In addition, this stay would allow the student to opt for the mention of “International Doctor” at the conclusion of the Thesis.

ii Indicators of Quality of the Center

The stay was held at the Institute of Mental Health Research (IMHR) of the University of Ottawa under the supervision of Professor Georg Northoff, MD, PhD, Member of the Royal College of Physicians of Canada (FRCPC) and director of the “Mind, Brain Imaging and Neuroethics Research Unit”. With more than 150 years of history, the University of Ottawa currently has more than 5,000 students and is recognized as one of the most innovative institutions in higher education in Canada. Its education plan has been widely acclaimed in academic circles, leading to a great expansion of the scope of this University. In 2016, according to the ranking of Shanghai, this University was placed between positions 101 and 150, with a marked upward trend in recent

years.

The IMHR is the third largest mental health research center in Canada. In close association with the prestigious Royal Ottawa Health Care Group, the IMHR focuses on innovation in research, patient care and education. It is involved in 107 clinical research projects and 28 basic research projects, generating a total of 180 research articles in first-rate journals in 2017.

The director of the research stay, Professor Georg Northoff, conducts the studies from a multidisciplinary perspective using three complementary points of view of brain behavior: neuroscientific, neuropsychiatric and neurophilosophical. Given its membership in the IMHR and its close collaboration with the Royal Ottawa Health Care Group, the Professor Northoff's research unit is in the possession of vast databases of different brain biological signals. This allows them a deep knowledge of different methodological aspects completely aligned with the area of specialization in which the research stay is framed. Finally, Professor Northoff is the scientific director of the "Mind, Brain Imaging and Neuroethics Research Unit" of the IMHR. Its curriculum accredits more than 280 scientific publications in the field of neuroscience and neuropsychiatry, reaching an h index of 48 (48 publications with 48 or more citations). In 2000 he received the "Senior Research Award on Research on Schizophrenia" for his excellent contribution in the field of characterization of schizophrenia. Likewise, in 2010 he received the special "Arnold Pfeiffer Prize" from the International Society for Neuropsychanalysis of the USA. To date, he has directed more than 30 predoctoral studies.

B.3 Intellectual property protection for computer software

1. Software property registration

Title:	“Domo-BCI”
Authors:	Roberto Hornero Sánchez, Rebeca Corralejo Palacios, Daniel Álvarez González and Javier Gómez Pilar
Code:	VA-99-2015
Date of register:	16/04/2015

2. Software property registration

Title:	“GABA”
Authors:	Javier Gómez Pilar , Jesús Poza Crespo, Carlos Gómez Peña and Roberto Hornero Sánchez
Code:	VA-107-2018
Date of register:	25/04/2018

3. Software property registration

Title:	“Nonlinear C-Tool”
Authors:	Carlos Gómez Peña, Susana Visus Hernández, Jesús Poza Crespo, Javier Gómez Pilar , María García Gadañon and Roberto Hornero Sánchez
Code:	VA-106-2018
Date of register:	25/04/2018

B.4 Awards and honors

- 02/2018: Innovative Solutions for improving the Quality of Life Award in the group ‘Ageing’ modality, organized by the Campus de Excelencia Internacional (CEI) Triangular E-3, for the project: “Plataforma Brain-Computer Interface de Entrenamiento Cognitivo para Atenuar los Efectos del Envejecimiento”, conducted by Víctor Martínez-Cagigal, Javier Gomez-Pilar y Roberto Hornero, 2017.
- 05/2017: Award for the best oral presentation at the 3rd PhD Conference in Information and Communication Technologies for the study “Towards a Brain Connectivity Model and its Relevance in Schizophrenia” (Valladolid, Spain, May 5, 2017).
- 06/2016: Conference support grant from the University of Valladolid to attend at the 38th Annual International Conference of the IEEE-EMBS (Orlando, USA, August 15-20, 2016).
- 11/2015: Second place (“Jose María Ferrero Corral” award) in the XXXIII Congreso Anual de la Sociedad Española de Ingeniería Biomédica (CASEIB 2015) for the study entitled ‘Caracterización de la Dinámica en la Eficiencia de la Red Neuronal en Esquizofrenia en Tarea Cognitiva Auditiva’, Javier Gomez-Pilar, Jesús Poza, Alejandro Bachiller, Carlos Gómez, Vicente Molina and Roberto Hornero, 2015.
- 06/2015: Conference support grant from the University of Valladolid to attend at the 7th Annual National CEA Symposium (Málaga, Spain, June 20-22, 2015).
- 11/2014: Second place (“Jose María Ferrero Corral” award) in the XXXII Congreso Anual de la Sociedad Española de Ingeniería Biomédica (CASEIB 2014) for the study entitled ‘Caracterización de Potenciales Evocados del EEG en Esquizofrenia mediante Teoría de Redes Complejas’, Javier Gomez-Pilar, Alejandro Bachiller, Jesús Poza, Carlos Gómez, Vicente Molina and Roberto Hornero, 2014.

- 09/2014: Finalist in the Annual BCI Research Award 2014 for the project: ‘Neurofeedback training by motor imagery based-BCI improves neurocognitive areas in elderly people’, carried out by Javier Gomez-Pilar, Rebeca Corralejo, Daniel Álvarez and Roberto Hornero, 5th International Brain-Computer Interface Meeting, University of Technology, Graz (Austria), 2014.
- 09/2013: First place in the Young Investigator Competition at the XIII Mediterranean Conference on Medical and Biological Engineering and Computing (MEDICON 2013) for the study entitled ‘AdaBoost Classification to Detect Sleep Apnea from Airflow Recordings’, Gonzalo César Gutiérrez Tobal, Daniel Álvarez González, Javier Gómez Pilar, Félix del Campo Matías and Roberto Hornero Sánchez, 2013.
- 07/2013. Telecommunication Engineering Association (COIT) 2013 Award for the Finalist of best Degree Final Project in Engineering and Medicine (ASISA category) by Javier Gómez-Pilar, entitled ‘Análisis Espectral y No Lineal de la Variabilidad del Ritmo Cardíaco para la Ayuda al Diagnóstico del Síndrome de Apnea-Hipopnea del Sueño’. Advisor: Roberto Hornero and Daniel Álvarez, 2013.

Apéndice C

Resumen en castellano

C.1 Antecedentes

C.1.1 Introducción a la esquizofrenia

La esquizofrenia es un trastorno mental crónico caracterizado por diversos síntomas, entre los que destacan la disociación del pensamiento, alteraciones en la percepción, trastornos afectivos y, usualmente, una deficiencia cognitiva. El curso crónico de esta enfermedad junto con su inicio temprano hace que la esquizofrenia sea un trastorno incapacitante para los pacientes y sus familiares.

Antes de la quinta edición del “Diagnostic and Statistical Manual of Mental Disorders” (DSM-V) en 2013, el diagnóstico de esquizofrenia estaba clasificado en cinco subtipos diferentes: (i) esquizofrenia paranoide, (ii) esquizofrenia desorganizada, (iii) esquizofrenia catatónica, (iv) esquizofrenia indiferenciada y (v) esquizofrenia residual. Sin embargo, de acuerdo con la Asociación Americana de Psiquiatría, debido a la limitada estabilidad diagnóstica, el método de clasificación se modificó para agrupar todas estas categorías bajo un mismo título: esquizofrenia. Con el DSM-V también surgió una nueva forma de diagnóstico de esquizofrenia. Hoy en día, una persona con esquizofrenia debe mostrar al menos dos de los siguientes síntomas:

- Delirios.
- Alucinaciones.
- Habla desorganizada.
- Comportamiento desorganizado o catatónico.
- Síntomas negativos, es decir, indiferencia afectiva, alogia o abulia.

Según este procedimiento diagnóstico, dos personas pueden tener esquizofrenia, pero no compartir ningún síntoma. Esto hace bastante difícil encontrar sustratos neuronales comunes en esta enfermedad, lo que dificulta su tratamiento, siendo ésta la justificación de esta Tesis Doctoral. De hecho, hay una tendencia creciente a considerar la esquizofrenia como una amalgama de diferentes enfermedades. Desde el punto de vista epidemiológico, la tasa de prevalencia de la esquizofrenia depende de una amplia variedad de factores. Dependiendo del estudio, la prevalencia de este trastorno oscila entre 0.26 % - 0.51 %. Además, los pacientes con esquizofrenia tienen una disminución del 20 % de la esperanza de vida en comparación con la población general. No se han encontrado diferencias en la prevalencia en relación con el género. Sin embargo, el bajo nivel socio-económico sí que se ha asociado con una mayor probabilidad de padecer la enfermedad. Esto sugiere que la esquizofrenia tiene una relación importante con el ambiente y no solo con factores genéticos.

La controversia en los factores desencadenantes de la esquizofrenia se extiende también a la fisiopatología de la enfermedad. Aunque existen diversos estudios centrados en comprender los sustratos neuronales alterados en la enfermedad, parece que la comunidad científica aún no ha llegado a un consenso. Hacia donde parecen converger bastantes estudios desde diferentes enfoques es en que la esquizofrenia está asociada a una deficiencia en la actividad cerebral que engloba a varias áreas corticales, así como la interconexión entre ellas. Estos resultados refuerzan la hipótesis de desconexión de la esquizofrenia, la cual asocia a la enfermedad con una reducida capacidad de integrar la información procedente de diferentes regiones cerebrales alejadas. Asimismo, la esquizofrenia se ha asociado con una asignación aberrante de los estímulos externos.

Pese a la identificación de algunos factores fisiopatológicos que parecen ser comunes a una gran mayoría de pacientes con esquizofrenia, aún no se han encontrado marcadores biológicos que permitan caracterizar y comprender en mayor medida este desorden, quedando patente que aún estamos lejos de soluciones globalmente aceptadas. Este hecho ha motivado el estudio de la actividad eléctrica generada en la corteza cerebral con el fin de encontrar anomalías en la red neuronal que nos permitan hacer inferencias fiables, así como caracterizar la enfermedad con propiedad y en profundidad. Puesto que la esquizofrenia es un trastorno cognitivo, cabe esperar que las peculiaridades derivadas de la enfermedad puedan verse reflejadas en la actividad eléctrica cerebral. En concreto, los potenciales eléctricos de la respuesta evocada por estímulos externos puede estar afectada en esquizofrenia. El electroencefalograma (EEG) se convierte entonces en una herramienta útil para caracterizar la dinámica neuronal relativa a la realización de una tarea cognitiva.

C.1.2 Teoría de Redes Complejas en neurociencia

En los últimos años, se ha visto cómo la Teoría de Redes Complejas comienza a desempeñar un papel primordial en los esfuerzos para caracterizar la estructura de la red cerebral. De hecho, la Teoría de Redes Compleja se ha aplicado a diferentes niveles y escalas cerebrales. Los grafos nos facilitan la interpretación de los patrones de conectividad, al tiempo que guardan una estrecha similitud con procesos reales. Todo esto facilita la relación directa de entidades: los nodos de un grafo se corresponden con regiones cerebrales corticales concretas, mientras que la relación entre ellas se representa en un grafo mediante el peso de las conexiones.

Estudios recientes han demostrado mediante teoría de grafos que las redes cerebrales en personas sanas siguen una distribución de “pequeño mundo” (*small-world networks* en inglés, también denominadas estructura de Watts-Strogatz). Estos patrones se encuentran alterados en pacientes con esquizofrenia, lo que podría dar lugar al antes mencionado síndrome de desconexión. Este hallazgo es solo el primer paso hacia una comprensión integral de estas redes, que podrían estar compuestas por otras redes complejas, como redes libres de escala o de Albert-Barabási. Por tanto, renovados esfuerzos son necesarios para modelar la dinámica de las redes cerebrales, así como sus características topológicas. Esta Tesis, por tanto, trata de cuantificar y caracterizar sus propiedades mediante medidas complementarias como complejidad, regularidad, integración, segregación, fuerza o centralidad.

C.2 Hipótesis y objetivos

La esquizofrenia se ha asociado con un déficit en la integración de la información entre regiones cerebrales en interacciones de larga distancia durante la cognición. La Teoría de Redes Complejas proporciona un marco adecuado para caracterizar esta alteración funcional. Por lo tanto, *los análisis de la actividad neuronal basados en la teoría de grafos podrían ser útiles para comprender los procesos cerebrales subyacentes a las funciones cognitivas alteradas en la esquizofrenia*. Se sabe que las tareas cognitivas producen respuestas rápidas en el cerebro en el rango de milisegundos. Además, estudios previos han demostrado que la esquizofrenia está acompañada de una atribución anómala y superlativa de los estímulos relevantes, lo que podría afectar al acoplamiento neuronal entre las áreas cerebrales durante la una tarea cognitiva. Por lo tanto, *técnicas de alta resolución temporal, como el EEG, adquiridas durante una tarea auditiva ‘oddball’, podrían ser utilizadas para caracterizar la dinámica cerebral a nivel de red en la esquizofrenia*.

Los procesos cognitivos dependen de la dinámica global de la red cerebral, lo que implica cambios en el equilibrio de acoplamiento entre regiones. Este equilibrio probablemente se vea alterado en los trastornos mentales. Por lo tanto, es razonable hipotetizar que *el análisis del balance de los pesos de las conexiones cerebrales pueden proporcionar la base para descubrir información relevante acerca de los sustratos neuronales que afectan a los procesos cerebrales patológicos*. Aunque las anomalías descritas en esquizofrenia parecen estar relacionadas en última instancia con una red cerebral alterada, irregularidades en la activación local podrían influir en las interrelaciones entre las regiones funcionales. Por lo tanto, *la activación a nivel de sensor puede estar relacionada con interacciones de largo alcance en las que está involucrada una región concreta del cerebro*. Estas interacciones pueden estar relacionadas no solo con la conectividad funcional, sino también con la conectividad estructural, es decir, las vías “físicas”. De hecho, las alteraciones funcionales de la red pueden tener una relación causal con anomalías estructurales. Por lo tanto, *la evaluación de la relación entre las redes funcionales y estructurales en la esquizofrenia puede ayudar a caracterizar los sustratos neuronales de la disfunción cortical en este trastorno*.

Debido a la cantidad de factores involucrados en la coordinación cerebral, la dificultad para caracterizar la red neuronal de una manera exhaustiva hace que sea difícil modelar el comportamiento dinámico del cerebro. Sin embargo, *el uso de medidas de red complementarias para evaluar la dinámica del cerebro durante una tarea cognitiva puede arrojar luz para desarrollar nuevos modelos de cognición*. Para validar estas hipótesis, esta Tesis Doctoral propone el uso de *la Teoría de Red Compleja aplicada al EEG para proporcionar un entorno de trabajo para evaluar y finalmente modelar la dinámica de las interacciones cerebrales que presumiblemente están alteradas en la esquizofrenia*.

Definidas las hipótesis, el objetivo general de esta Tesis es *estudiar, diseñar y aplicar novedosas medidas derivadas de la Teoría de Redes Complejas, así como nuevos modelos matemáticos de caracterización de redes para identificar los sustratos neuronales alterados en la esquizofrenia*.

Para llevar a cabo este objetivo, se han seguido los siguientes pasos, correspondientes a objetivos específicos en distintas fases de la Tesis:

- 1) Revisar la bibliografía y los últimos avances relacionados con el procesamiento de señales biomédicas útiles para caracterizar el EEG. En particular, este objetivo está enfocado a identificar los métodos apropiados de la teoría de grafos para caracterizar de forma exhaustiva la dinámica neuronal.
- 2) Construir una base de datos que incluya registros EEG, datos socio-demográficos

- y variables clínicas de pacientes adultos con esquizofrenia y controles sanos.
- 3) Seleccionar e implementar los métodos más adecuados para minimizar el ruido de los potenciales relacionados con eventos (*event-related potentials*, ERPs), obtener medidas locales y de la dinámica de la red cerebral (de la literatura o proponer nuevas) y caracterizar el comportamiento de la red cerebral durante la cognición utilizando la señal EEG.
 - 4) Llevar a cabo análisis estadísticos de los resultados para explorar la dinámica neuronal, la relación entre las medidas locales y de red y la asociación entre la conectividad funcional y estructural, así como para identificar los patrones fisiopatológicos en la esquizofrenia. Este objetivo también incluye la construcción de un nuevo modelo probabilístico de la dinámica de la red cerebral durante una tarea cognitiva para explicar los cambios de dicha red en cada individuo.
 - 5) Comparar y discutir los resultados para extraer conclusiones apropiadas. Este objetivo incluye la comparación con los estudios más novedosos de ERP y la comparación de nuestros hallazgos con los resultados obtenidos utilizando otras técnicas, como la magnetoencefalografía (MEG) o la resonancia magnética funcional (*functional magnetic resonance imaging*, fMRI).
 - 6) Difundir los principales resultados y conclusiones de la investigación en revistas de alto impacto, así como en conferencias internacionales y nacionales.

C.3 Materiales

Durante el proceso de realización de la presente Tesis Doctoral, se usaron dos bases de datos cuya potencia estadística fue en incremento. La primera de las bases estaba compuesta por registros de 16 electrodos activos y llegó a constar de 48 pacientes con esquizofrenia (25 crónicos y 23 primeros episodios) y 87 controles. Debido a la conveniencia de realizar análisis de grafos con una alta resolución espacial, se optó por cambiar el equipo de registro a uno más moderno con 32 electrodos activos. Dicha base llegó a estar formada en el último de los estudios de esta Tesis por 39 pacientes con esquizofrenia (19 crónicos y 20 primeros episodios) y 78 controles. Las Tablas C.1 y C.2 muestran los principales datos socio-demográficos, clínicos y cognitivos de los pacientes y controles de las dos bases de datos. Los registros fueron adquiridos con la colaboración de personal clínico perteneciente al grupo de investigación ‘*Sustratos Neuronales de la Psicosis*’ de la Universidad de Valladolid dirigidos por el Dr. Vicente Molina. Todos los registros fueron obtenidos mediante un electroencefalógrafo de electrodos activos (BrainVision, Brain

Tabla C.1: Características socio-demográficas, clínicas y cognitivas de la base de datos completa de 16 electrodos activos. Valores expresados como media(desviación típica). Las diferencias estadísticas significativas entre ambos grupos están marcadas con un asterisco ($p < 0.05$, test t de Student).

	Schizophrenia	Controls
N	48	87
Edad (años)	33.58 (9.27)	30.51 (10.77)
Género (Varón:Mujer)	25:23	44:43
Dosis of CPZ (mg/d)	377.92 (196.94)	NA
Duración de la enfermedad (meses)	97.84 (116.94)	NA
Educación (años)	14.19 (3.60)	16.56 (2.25)
PANSS Síntomas positivos	11.63 (3.39)	NA
PANSS Síntomas negativos	18.03 (7.52)	NA
PANSS Síntomas totales	54.35 (18.56)	NA
IQ *	91.22 (14.19)	111.83 (11.87)
Memoria verbal *	33.92 (12.74)	51.65 (8.26)
Memoria de trabajo *	15.81 (5.01)	21.46 (3.90)
Velocidad motora *	58.14 (14.41)	68.59 (17.84)
Fluencia verbal *	17.99 (5.70)	27.13 (5.33)
Velocidad de procesamiento *	42.83 (15.78)	68.79 (13.25)
Capacidad de resolución de problemas *	15.40 (4.64)	17.54 (2.72)
WCST errores perseverativos *	27.31 (47.43)	10.17 (5.81)
WCST categorías completadas *	4.39 (1.87)	5.79 (0.72)

Products GmbH; Munich, Germany) con una frecuencia de muestreo de 500 Hz, de forma que se aseguraba la compatibilidad entre registros.

Los registros se realizaron bajo un protocolo definido de paradigma auditivo para valorar los potenciales evocados (*event-related potentials*, ERP) asociados al proceso cognitivo de identificación de estímulos novedosos y relevantes. El paradigma consistió en la presentación de 3 estímulos auditivos con distinta probabilidad de aparición: estímulo estándar (2000 Hz; 60 % de probabilidad), estímulo distractor (1500 Hz, 20 % de probabilidad) y estímulo diana (500 Hz, 20 % de probabilidad). Los sujetos debían presionar un botón únicamente al escuchar el estímulo diana, de forma que se producía un potencial evocado P3b.

C.4 Métodos

El EEG es una señal eléctrica cerebral cuyas características varían con el tiempo. Es por ello que su análisis requiere métodos que analicen de forma conjunta

Tabla C.2: Características socio-demográficas, clínicas y cognitivas de la base de datos completa de 32 electrodos activos. Valores expresados como media(desviación típica). Las diferencias estadísticas significativas entre ambos grupos están marcadas con un asterisco ($p < 0.05$, test t de Student).

	Schizophrenia	Controls
N	39	78
Edad (años)	33.05 (8.80)	30.95 (10.84)
Género (Varón:Mujer)	23:16	46:32
Dosis of CPZ (mg/d)	377.90 (196.93)	NA
Duración de la enfermedad (meses)	95.17 (117.39)	NA
Educación (años)	14.19 (3.60)	16.56 (2.25)
PANSS Síntomas positivos	11.70 (3.43)	NA
PANSS Síntomas negativos	17.571 (7.31)	NA
PANSS Síntomas totales	53.810 (18.89)	NA
IQ *	91.061 (14.53)	113.21 (11.09)
Memoria verbal *	34.262 (12.89)	51.11 (8.19)
Memoria de trabajo *	16.151 (5.01)	21.63 (3.62)
Velocidad motora *	58.879 (13.78)	72.61 (16.58)
Fluencia verbal *	18.352 (5.73)	27.86 (5.15)
s Velocidad de procesamiento *	43.700 (15.36)	69.59 (14.38)
Capacidad de resolución de problemas	15.253 (4.62)	17.52 (2.57)
WCST errores perseverativos *	17.92 (10.12)	9.80 (5.14)
WCST categorías completada *	4.42 (1.88)	5.85 (0.61)

las variaciones tiempo-frecuencia. En la presente Tesis Doctoral se ha utilizado la transformada *wavelet* (*Wavelet Transform*, WT), la cual es apropiada para la caracterización de señales pseudo-estacionarias. A partir de esta transformación se han calculado medidas locales (como la entropía), así como medidas de conectividad (como la coherencia) u otras medidas de conectividad basadas en la sincronía dinámica de fase de la señal de EEG, como la medida del acoplamiento de fase (*Phase-Locking Value*, PLV). Una vez obtenidas las medidas de conectividad fue posible obtener las características de la red cerebral. Para ello se realizó un procesado en tres etapas:

- i) Etapa de pre-procesado. Comprende la eliminación de segmentos ruidosos, filtrado de frecuencias no deseadas, descomposición mediante análisis de componentes independientes (*Independent Component Analysis*, ICA) y su posterior reconstrucción, segmentación en épocas relativas a cada estímulo auditivo, así como el rechazo automático y adaptativo de épocas ruidosas.
- ii) Etapa de obtención de las matrices de conectividad. En ella se obtiene la

transformada tiempo-frecuencia de la señal de EEG procedente de la anterior etapa de pre-procesado. Además, se calcula la matriz de conectividad asociada a la fase o a la potencia de la señal mediante medidas como la coherencia y el PLV.

- iii) Etapa de caracterización de red. En esta etapa se calculan los parámetros de grafos que caracterizan la red en su conjunto. Para ello, se seleccionan medidas de grafos que aporten información relevante y complementaria en la caracterización de la red.

Estas etapas son el preámbulo del posterior análisis estadístico en el que se tratan de buscar diferencias entre los grupos de control y de esquizofrenia con el objetivo de identificar anomalías que definan el desorden psiquiátrico de la esquizofrenia.

C.5 Resultados y discusión

Mediante el procesado previamente descrito, fue posible identificar particularidades de la actividad cerebral en la esquizofrenia, tanto a nivel local (mediante la entropía) como a nivel de red (mediante medidas de grafos).

En relación con la caracterización a nivel local, se observó un menor cambio en los patrones de irregularidad en los pacientes con esquizofrenia. Partiendo de valores similares de entropía durante el pre-estímulo, los pacientes con esquizofrenia mostraron una mayor entropía durante la respuesta al estímulo. Esta mayor entropía está relacionada con un espectro más plano, es decir una mayor variedad de oscilaciones neuronales desorganizadas durante la tarea, lo que lleva a una asignación aberrante y disminuida de la relevancia al estímulo, probablemente relacionada con una representación interna desorganizada de dicho estímulo.

En cuanto a las medidas de caracterización de la red cerebral mediante grafos, en primer lugar se observó una capacidad de adaptación al cambio reducida en la esquizofrenia. Este menor cambio entre pre-estímulo y respuesta cognitiva parece venir ligado a una mayor activación/conectividad local estimada mediante el coeficiente de agrupamiento (*Clustering Coefficient*, CIC) durante el intervalo temporal previo al estímulo. En otras palabras, una anormal y elevada conectividad de determinados conjuntos neurales impide la sincronización y comunicación de la red cerebral en relaciones de larga distancia durante el procesamiento cognitivo. En segundo lugar, gracias a la colaboración con el Dr. Rodrigo de Luis del ‘*Laboratorio de Procesado de Imagen*’ de la Universidad de Valladolid, fue posible relacionar

las medidas funcionales de grafos, obtenidas mediante el EEG, con medidas de conectividad estructural procedentes de registros de resonancia magnética por difusión (*diffusion Magnetic Resonance Image*, dMRI). Contrariamente a nuestras primeras expectativas, no se encontró una elevada correlación entre las medidas de conectividad funcional y estructural. Debido a la novedad del estudio (no tenemos constancia de ningún estudio anterior en esquizofrenia en el que se comparen medidas procedentes del EEG y de MRI), no fue posible una comparación directa con anteriores hallazgos de la literatura. Sin embargo, una posible causa podría deberse a la gran heterogeneidad de la esquizofrenia que se ha observado a lo largo de todos los artículos de esta Tesis por compendio. La existencia de *clusters* dentro de la enfermedad enmascararía mutuamente los efectos de los distintos subgrupos, evitando hallar relaciones entre conectividad estructural y funcional.

La propuesta de una nueva medida de complejidad de red (*Shannon Graph Complexity*, SGC) dio lugar a la observación de una reorganización anormal de la red cerebral en la esquizofrenia. Se propuso, por tanto, un nuevo modelo de reorganización dinámica de red durante una tarea cognitiva, lo que mostró diferencias en el comportamiento entre controles y pacientes. En concreto, las conexiones funcionales secundarias (camino neurales débilmente conectados durante el pre-estímulo) se veían fuertemente reforzadas durante el proceso cognitivo en controles sanos. El mismo comportamiento fue observado en un conjunto bien diferenciado de pacientes. Sin embargo, otro conjunto relevante de ellos (42%) veía fuertemente reforzadas principalmente las vías primarias, siguiendo un patrón de comportamiento claramente diferenciado. Esto, junto a los anteriores hallazgos, nos llevan a sugerir la posibilidad de la existencia de subgrupos dentro de la enfermedad de la esquizofrenia. Pese a que esta hipótesis ya ha sido recientemente propuesta en estudios paralelos, no es un concepto aceptado por toda la comunidad científica. Por tanto, estudios adicionales a este respecto serán necesario en el futuro.

C.6 Conclusiones

El análisis de los resultados de esta Tesis Doctoral en su conjunto nos lleva a las siguientes conclusiones:

- La actividad sincronizada de grandes conjuntos neuronales se puede medir utilizando medidas de conectividad basadas en la fase y/o la potencia de la señal de EEG. Esta respuesta coordinada supone la vía principal de inter-

cambio de información entre las áreas cerebrales.

- La regularidad local de la actividad cerebral tiene un papel importante en las características de la red en su conjunto. Así, alteraciones en regiones específicas, como las observadas en la esquizofrenia, podrían afectar a toda la red, produciendo la desconexión entre áreas y contribuyendo a una capacidad anormal de integrar la información en la esquizofrenia.
- Los pacientes con esquizofrenia muestran una red hiper-segregada antes del estímulo, la cual está vinculada a un cambio reducido de la conectividad funcional durante la cognición.
- El uso de diferentes medidas de red complementarias entre sí, en términos de información proporcionada, contribuye a una caracterización completa de la red funcional. Nuestros hallazgos sugieren que un enfoque basado en la teoría de grafos es apropiado para medir las interacciones y la sincronía de la red cerebral funcional durante una tarea cognitiva.
- La esquizofrenia muestra alteraciones en las propiedades de red funcional en la banda de 4 a 8 Hz, así como en la red estructural cerebral. Sin embargo, estas anomalías parecen no estar tan vinculadas como podría suponerse a priori. Las alteraciones halladas podrían estar vinculadas a la existencia de diferentes grupos de pacientes con esquizofrenia.
- Pacientes con el mismo trastorno, esquizofrenia, muestran patrones de respuesta cerebral bien diferenciados ante un estímulo externo. Mientras que un subgrupo de pacientes refuerza las vías neuronales secundarias durante el procesamiento cognitivo (de forma similar a como lo hacen los controles), otro subgrupo sufre un refuerzo de sus conexiones primarias. Los hallazgos ponen de manifiesto la heterogeneidad de este trastorno, así como la posibilidad de la existencia de subgrupos de la enfermedad. Esto abre nuevas líneas futuras de investigación para confirmar este hallazgo.

En resumen, en esta Tesis Doctoral por compendio de publicaciones, el análisis de la actividad cerebral durante una tarea cognitiva se utilizó para obtener información sobre los mecanismos neuronales subyacentes a las disfunciones cognitivas de la esquizofrenia. Los análisis de la teoría de redes complejas basados en la sincronía y el acoplamiento entre las regiones cerebrales proporcionan un marco de trabajo adecuado para describir las alteraciones de la esquizofrenia. Nuestra investigación respalda hallazgos previos, como la hipótesis de respuesta aberrante y la hipótesis de desconexión, a la vez que muestra un déficit en el cambio de la actividad cerebral desde el intervalo pre-estímulo a la respuesta cognitiva. La reorganización de la red cerebral y sus cambios topológicos están claramente di-

ferenciados entre diferentes subgrupos de pacientes. Esto nos proporciona nuevas evidencias sobre la posible existencia de subgrupos dentro de la esquizofrenia.

Bibliography

- American Psychiatric Association (2013). *Diagnostic and Statistical Manual of Mental Disorders, 5th Edition: DSM-5*. Arlington: American Psychiatric Publishing.
- Ansmann, G. and Lehnertz, K. (2012). Surrogate-assisted analysis of weighted functional brain networks. *Journal of Neuroscience Methods*, 208(2):165–172.
- Arieli, A., Sterkin, A., Grinvald, A., and Aertsen, A. (1996). Dynamics of ongoing activity: Explanation of the large variability in evoked cortical responses. *Science*, 273(5283):1868–1871.
- Bachiller, A., Díez, A., Suazo, V., Domínguez, C., Ayuso, M., Hornero, R., Poza, J., and Molina, V. (2014). Decreased spectral entropy modulation in patients with schizophrenia during a P300 task. *European Archives of Psychiatry and Clinical Neuroscience*, 264(6):533–543.
- Bachiller, A., Poza, J., Gómez, C., Molina, V., Suazo, V., and Hornero, R. (2015). A comparative study of event-related coupling patterns during an auditory odd-ball task in schizophrenia. *Journal of Neural Engineering*, 12(1):016007.
- Barabási, A. and Albert, R. (1999). Emergence of scaling in random networks. *Science*, 286(5439):509–512.
- Barch, D. M. and Sheffield, J. M. (2014). Cognitive impairments in psychotic disorders: Common mechanisms and measurement. *World Psychiatry*, 13(October):224–232.
- Bastos, A. M. and Schoffelen, J.-M. (2016). A tutorial review of functional connectivity analysis methods and their interpretational pitfalls. *Frontiers in Systems Neuroscience*, 9(January):175.

- Bhugra, D. (2005). The global prevalence of schizophrenia. *PLoS Medicine*, 2(5):e151.
- Bob, P., Palus, M., Susta, M., and Glaslova, K. (2008). EEG phase synchronization in patients with paranoid schizophrenia. *Neuroscience Letters*, 447:73–77.
- Bronzino, J. (1999). *Biomedical engineering handbook*. CRC press, volume 2 edition.
- Brown, A. S. (2008). The risk for schizophrenia from childhood and adult infections. *American Journal of Psychiatry*, 165(1):7–10.
- Buckley, P. (2008). Update on the etiology and treatment of schizophrenia and bipolar disorder. *CNS Spectrums: The International Journal of Neuropsychiatric Medicine*, 13:1–12 11p.
- Buckner, R. L., Andrews-Hanna, J. R., and Schacter, D. L. (2008). The brain’s default network. *Annals of the New York Academy of Sciences*, 1124(1):1–38.
- Bullmore, E. and Sporns, O. (2009). Complex brain networks: graph theoretical analysis of structural and functional systems. *Nature Reviews Neuroscience*, 10(3):186–198.
- Bullmore, E. T. and Bassett, D. S. (2011). Brain Graphs: Graphical Models of the Human Brain Connectome. *Annual Review of Clinical Psychology*, 7(1):113–140.
- Carlsson, M. L., Carlsson, A., and Nilsson, M. (2004). Schizophrenia: from dopamine to glutamate and back. *Current Medicinal Chemistry*, 11(3):267–277.
- Chatrian, G. E., Lettich, E., and Nelson, P. L. (1985). Ten percent electrode system for topographic studies of spontaneous and evoked EEG activities. *American Journal of EEG Technology*, 25(2):83–92.
- Cohen, M. X. (2014). *Analyzing neural time series data: theory and practice*. MIT press.
- de Haan, W., Pijnenburg, Y. a. L., Strijers, R. L. M., van der Made, Y., van der Flier, W. M., Scheltens, P., and Stam, C. J. (2009). Functional neural network analysis in frontotemporal dementia and Alzheimer’s disease using EEG and graph theory. *BMC Neuroscience*, 10:101.
- Dimitriadis, S. I. and Salis, C. I. (2017). Mining time-resolved functional brain graphs to an EEG-based chronnectomic brain aged index (CBAI). *Frontiers in Human Neuroscience*, 11(August).

- Edwards, S. J. and Smith, C. J. (2009). Tolerability of atypical antipsychotics in the treatment of adults with schizophrenia or bipolar disorder: a mixed treatment comparison of randomized controlled trials. *Clinical Therapeutics*, 31:1345–1359.
- Eguíluz, V. M., Chialvo, D. R., Cecchi, G. A., Baliki, M., and Apkarian, A. V. (2005). Scale-Free brain functional networks. *Physical Review Letters*, 94(1):018102.
- Erdős, P. and Rényi, a. (1959). On random graphs. *Publicationes Mathematicae*, 6:290–297.
- Felleman, D. J. and Van Essen, D. C. (1991). Distributed hierarchical processing in the primate cerebral cortex. *Cerebral Cortex*, 1(1):1–47.
- Friston, K. J. (1998). The disconnection hypothesis. *Schizophrenia Research*, 30:115–125.
- Fuchs, E. C., Zivkovic, A. R., Cunningham, M. O., Middleton, S., LeBeau, F. E., Bannerman, D. M., Rozov, A., Whittington, M. A., Traub, R. D., Rawlins, J. N. P., and Monyer, H. (2007). Recruitment of parvalbumin-positive interneurons determines hippocampal function and associated behavior. *Neuron*, 53(4):591–604.
- Gomez-Pilar, J., de Luis-García, R., Lubeiro, A., de la Red, H., Poza, J., Núñez, P., Hornero, R., and Molina, V. (2018a). Relations between structural and eeg-based graph metrics in healthy controls and schizophrenia patients. *Human Brain Mapping*, in press.
- Gomez-Pilar, J., de Luis-García, R., Lubeiro, A., de Uribe, N., Poza, J., Núñez, P., Ayuso, M., Hornero, R., and Molina, V. (2018b). Deficits of entropy modulation in schizophrenia are predicted by functional connectivity strength in the theta band and structural clustering. *NeuroImage: Clinical*, 18(February):382–389.
- Gomez-Pilar, J., Lubeiro, A., Poza, J., Hornero, R., Ayuso, M., Valcárcel, C., Haidar, K., Blanco, J. A., and Molina, V. (2017). Functional EEG network analysis in schizophrenia: Evidence of larger segregation and deficit of modulation. *Progress in Neuro-Psychopharmacology and Biological Psychiatry*, 76(March):116–123.

- Gomez-Pilar, J., Poza, J., Bachiller, A., Gómez, C., Molina, V., and Hornero, R. (2015). Neural network reorganization analysis during an auditory oddball task in schizophrenia using wavelet entropy. *Entropy*, 17(8):5241–5256.
- Gomez-Pilar, J., Poza, J., Bachiller, A., Gómez, C., Núñez, P., Lubeiro, A., Molina, V., and Hornero, R. (2018c). Quantification of graph complexity based on the edge weight distribution balance: Application to brain networks. *International Journal of Neural Systems*, 28(1):1750032.
- Gomez-Pilar, J., Poza, J., Gómez, C., Northoff, G., Lubeiro, A., Benjamín B., C.-C., Molina, V., and Roberto, H. (2018d). Altered predictive capability of the brain network EEG model in schizophrenia during cognition. *Schizophrenia Research*, in press.
- Harrison, P. J. and Owen, M. J. (2003). Genes for schizophrenia? Recent findings and their pathophysiological implications. *The Lancet*, 361(9355):417–419.
- Huang, Z., Zhang, J., Longtin, A., Dumont, G., Duncan, N. W., Pokorny, J., Qin, P., Dai, R., Ferri, F., Weng, X., et al. (2017). Is there a nonadditive interaction between spontaneous and evoked activity? phase-dependence and its relation to the temporal structure of scale-free brain activity. *Cerebral Cortex*, 27(2):1037–1059.
- Javitt, D. C. and Sweet, R. A. (2015). Auditory dysfunction in schizophrenia: integrating clinical and basic features. *Nature Reviews Neuroscience*, 16(9):535–550.
- Jensen, O. and Mazaheri, A. (2010). Shaping functional architecture by oscillatory alpha activity: gating by inhibition. *Frontiers in Human Neuroscience*, 4:186.
- Jeon, Y.-W. and Polich, J. (2003). Meta-analysis of p300 and schizophrenia: Patients, paradigms, and practical implications. *Psychophysiology*, 40(5):684–701.
- Kapur, S. (2003). Psychosis as a state of aberrant salience: A framework linking biology, phenomenology, and pharmacology in schizophrenia. *American Journal of Psychiatry*, 160:13–23.
- Kapur, S. and Remington, G. (2001). Atypical antipsychotics: new directions and new challenges in the treatment of schizophrenia. *Annual Review of Medicine*, 52:503–517.

- Klosterkotter, J. and Schultze-Lutter, F. (1998). Diagnosing schizophrenia in the prodromal phase. *European Psychiatry*, 13:144s.
- Lachaux, J. P., Rodriguez, E., Martinerie, J., and Varela, F. J. (1999). Measuring phase synchrony in brain signals. *Human Brain Mapping*, 8(4):194–208.
- Laursen, T. M., Nordentoft, M., and Mortensen, P. B. (2014). Excess early mortality in schizophrenia. *Annual Review of Clinical Psychology*, 10(1):425–448.
- Lewis, D. A. and Lieberman, J. A. (2000). Catching up on schizophrenia. *Neuron*, 28(2):325–334.
- Lopes da Silva, F. (2013). EEG and MEG: Relevance to neuroscience. *Neuron*, 80(5):1112–1128.
- Lubeiro, A., Rueda, C., Hernández, J. A., Sanz, J., Sarramea, F., and Molina, V. (2016). Identification of two clusters within schizophrenia with different structural, functional and clinical characteristics. *Progress in Neuro-Psychopharmacology and Biological Psychiatry*, 64:79–86.
- Makeig, S., Debener, S., Onton, J., and Delorme, A. (2004). Mining event-related brain dynamics. *Trends in Cognitive Sciences*, 8(5):204–210.
- Mallat, S. (1999). *A wavelet tour of signal processing*. Academic press.
- Mathalon, D. H., Ford, J. M., and Pfefferbaum, A. (2000). Trait and state aspects of p300 amplitude reduction in schizophrenia: A retrospective longitudinal study. *Biological Psychiatry*, 47(5):434–449.
- Nakamura, T., Hillary, F. G., and Biswal, B. B. (2009). Resting network plasticity following brain injury. *PLoS ONE*, 4(12).
- Niedermeyer, E. and da Silva, F. L. (2005). *Electroencephalography: basic principles, clinical applications, and related fields*. Lippincott Williams & Wilkins.
- Nomi, J. S., Vij, S. G., Dajani, D. R., Steimke, R., Damaraju, E., Rachakonda, S., Calhoun, V. D., and Uddin, L. Q. (2017). Chronnectomic patterns and neural flexibility underlie executive function. *NeuroImage*, 147(August 2016):861–871.
- Núñez, P., Poza, J., Bachiller, A., Gomez-Pilar, J., Lubeiro, A., Molina, V., and Hornero, R. (2017). Exploring non-stationarity patterns in schizophrenia: neural reorganization abnormalities in the alpha band. *Journal of Neural Engineering*, 14(4):046001.

- Nunez, P. L. and Srinivasan, R. (2006a). *Electric fields of the brain: the neurophysics of EEG*. Oxford University Press, USA.
- Nunez, P. L. and Srinivasan, R. (2006b). *Electric fields of the brain: the neurophysics of EEG*. Oxford University Press, USA.
- Nunez, P. L., Srinivasan, R., Westdorp, A. F., Wijesinghe, R. S., Tucker, D. M., Silberstein, R. B., and Cadusch, P. J. (1997). EEG coherency I: Statistics, reference electrode, volume conduction, Laplacians, cortical imaging, and interpretation at multiple scales. *Electroencephalography and Clinical Neurophysiology*, 103(5):499–515.
- O'Donnell, B. F., Vohs, J. L., Hetrick, W. P., Carroll, C. A., and Shekhar, A. (2004). Auditory event-related potential abnormalities in bipolar disorder and schizophrenia. *International Journal of Psychophysiology*, 53(1):45–55.
- Orellana, G. and Slachevsky, A. (2013). Executive functioning in schizophrenia. *Frontiers in Psychiatry*, 4:35.
- Patterson, T. L. and Leeuwenkamp, O. R. (2008). Adjunctive psychosocial therapies for the treatment of schizophrenia. *Schizophrenia Research*, 100(1):108–119.
- Petersen, S. E. and Sporns, O. (2015). Brain networks and cognitive architectures. *Neuron*, 88(1):207–219.
- Polich, J. (2007). Updating P300: An integrative theory of P3a and P3b. *Clinical Neurophysiology*, 118:2128–2148.
- Ramón y Cajal, S. (1995). *Cajal's histology of the nervous system of man and vertebrates (History of Neuroscience)*. OUP USA.
- Roach, B. J. and Mathalon, D. H. (2008). Event-Related EEG Time-Frequency Analysis: An Overview of Measures and An Analysis of Early Gamma Band Phase Locking in Schizophrenia. *Schizophrenia Bulletin*, 34(5):907–926.
- Rubinov, M., Knock, S., Stam, C. J., Micheloyannis, S., Harris, A., Williams, L. M., and Breakspear, M. (2009). Small-world properties of nonlinear brain activity in schizophrenia. *Human Brain Mapping*, 30:403–416.
- Rubinov, M. and Sporns, O. (2010). Complex network measures of brain connectivity: Uses and interpretations. *NeuroImage*, 52(3):1059–1069.

- Scannell, J. W., Burns, G. A., Hilgetag, C. C., O'Neil, M. A., and Young, M. P. (1991). The connectional organization of the cortico-thalamic system of the cat. *Cerebral Cortex*, 9(3):277–99.
- Simeone, J. C., Ward, A. J., Rotella, P., Collins, J., and Windisch, R. (2015). An evaluation of variation in published estimates of schizophrenia prevalence from 1990-2013: a systematic literature review. *BMC Psychiatry*, 15(1):193.
- Spencer, K. M., Nestor, P. G., Niznikiewicz, M. A., Salisbury, D. F., Shenton, M. E., and McCarley, R. W. (2003). Abnormal neural synchrony in schizophrenia. *The Journal of Neuroscience: the Official Journal of the Society for Neuroscience*, 23(19):7407–7411.
- Sporns, O. (2013). Structure and function of complex brain networks. *Dialogues in Clinical Neuroscience*, 15(3):247–262.
- Sporns, O., Tononi, G., and Kötter, R. (2005). The human connectome: A structural description of the human brain. *PLoS Computational Biology*, 1(4):0245–0251.
- Stam, C. J., de Haan, W., Daffertshofer, A., Jones, B. F., Manshanden, I., Van Cappellen Van Walsum, A. M., Montez, T., Verbunt, J. P. A., De Munck, J. C., Van Dijk, B. W., Berendse, H. W., and Scheltens, P. (2009). Graph theoretical analysis of magnetoencephalographic functional connectivity in Alzheimer's disease. *Brain*, 132(2008):213–224.
- Stone, J. M., Morrison, P. D., and Pilowsky, L. S. (2007). Glutamate and dopamine dysregulation in schizophrenia—a synthesis and selective review. *Journal of Psychopharmacology*, 21(4):440–452.
- Swartz, M. S., Wagner, H. R., Swanson, J. W., Stroup, T. S., McEvoy, J. P., Canive, J. M., Miller, D. D., Reimherr, F., McGee, M., Khan, A., Van Dorn, R., Rosenheck, R. A., and Lieberman, J. A. (2006). Substance use in persons with schizophrenia. *The Journal of Nervous and Mental Disease*, 194(3):164–172.
- Uhlhaas, P. J. and Singer, W. (2006). Neural Synchrony in Brain Disorders: Relevance for Cognitive Dysfunctions and Pathophysiology. *Neuron*, 52:155–168.
- Uhlhaas, P. J. and Singer, W. (2010). Abnormal neural oscillations and synchrony in schizophrenia. *Nature Reviews Neuroscience*, 11:100–113.

- van den Heuvel, M. P., Mandl, R. C. W., Stam, C. J., Kahn, R. S., and Hulshoff Pol, H. E. (2010). Aberrant frontal and temporal complex network structure in schizophrenia: a graph theoretical analysis. *The Journal of Neuroscience: the Official Journal of the Society for Neuroscience*, 30(47):15915–15926.
- Von Stein, A. and Sarnthein, J. (2000). Different frequencies for different scales of cortical integration: From local gamma to long range alpha/theta synchronization. *International Journal of Psychophysiology*, 38:301–313.
- Wang, X.-J. (2010). Neurophysiological and computational principles of cortical rhythms in cognition. *Physiological Reviews*, 90(3):1195–1268.
- Watts, D. and Strogatz, S. (1998). Collective dynamics of small-world networks. *Nature*, 393(June):440–442.
- Welham, J., Isohanni, M., Jones, P., and McGrath, J. (2009). The antecedents of schizophrenia: A review of birth cohort studies. *Schizophrenia Bulletin*, 35(3):603–623.
- Whalley, H. C. (2005). Functional disconnectivity in subjects at high genetic risk of schizophrenia. *Brain*, 128(9):2097–2108.
- Womelsdorf, T., Schoffelen, J.-M., Oostenveld, R., Singer, W., Desimone, R., Engel, A. K., and Fries, P. (2007). Modulation of neuronal interactions through neuronal synchronization. *Science*, 316:1609–1612.
- Xia, M., Wang, J., and He, Y. (2013). BrainNet Viewer: A Network Visualization Tool for Human Brain Connectomics. *PLoS ONE*, 8(7):e68910.
- Yener, G. G. and Başar, E. (2013). Brain oscillations in neuropsychiatric disease. *Dialogues in Clinical Neuroscience*, 15(3):291–300.
- Yung, A. R. and McGorry, P. O. (1996). The prodromal phase of first-episode psychosis: Past and current conceptualizations. *Schizophrenia Bulletin*, 22(2):353–370.